FISCHER-TROPSCH IONOMERIC WAXES

by

HENNIE POTGIETER

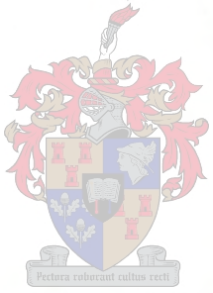

Dissertation presented for the degree of

Doctor of Philosophy (Polymer Science)

at the

University of Stellenbosch

Promoter: Prof R D Sanderson

December 2003

DECLARATION

I, the undersigned, hereby declare that the work contained in this dissertation is my own original work and has not previously in its entirety or in part been submitted at any university for a degree.

ABSTRACT

This dissertation describes work done on Fischer-Tropsch ionomeric waxes. The waxes are characterized with respect to the method of manufacture, the mechanism of the oxidation process, the saponification, the physical properties, the rheological properties, the morphology and the water absorption of the waxes.

Different methods of physical and mechanical analysis are used to prove at which concentration level, for each type of cation tested and for each type of oxidized and grafted wax prepared, the formation of multiplets and clusters within the Fischer-Tropsch ionomeric waxes takes place. An understanding of multiplet and cluster formation in Fischer-Tropsch ionomeric waxes is essential as these morphological phenomena control the mechanical and physical behaviour of the Fischer-Tropsch ionomeric waxes. The ability to be able to analyse the Fischer-Tropsch ionomeric waxes for multiplet and cluster formation should allow one to predict the physical and mechanical behaviour of the Fischer-Tropsch ionomeric waxes in practical applications.

OPSOMMING

Hierdie skripsie beskryf werk gedoen op Fischer-Tropsch ionomeries wasse. Die wasse is gekarakteriseer ten opsigte van die vervaardigingsmetode, die meganisme van oksidasie, die verseping, hulle fisiese en reologiese eienskappe, hulle morfologie en water absorpsie.

Verskillende metodes van fisiese en meganiese analiese is gebruik om te bewys by watter konsentrasie, vir 'n spesifieke katioon en vir 'n spesifieke geoksideerde of entwas, wanneer veelvoud of tros-vorming plaasvind. Die vermoë om te verstaan hoe en wanner veelvoude en trosse in Fischer-Tropsch ionomeries wasse vorm is van kardinale belang, aangesien die fisiese en meganiese eienskappe van die Fischer-Tropsch ionomeries wasse direk beinvloed word deur die vorming van veelvoude en trosse. Die vermoë om Fischer-Tropsch ionomeries wasse te kan analiseer vir veelvoud en tros vorming is voordelig om Fischer-Tropsch ionomeries wasse se meganiese en fisiese eienskappe in praktiese aanwendings te voorspel.

ACKNOWLEDGMENTS

I wish to express my gratitude to:

The Almighty, who guided me and helped me in fulfilling my dreams.

My wife and family for their encouragement and support.

Prof. R.D. Sanderson, Director of the Institute for Polymer Science, University of Stellenbosch, for his part in this project and for his advice, assistance and encouragement during this study and in the preparation of this thesis.

Dr. Margie Hurndall, for invaluable advice during the writing of the final thesis.

My mother and my father, for setting me on the right path in life and laying the foundation for my future.

Schümann Sasol, for the use of their facilities, and the personnel who carried out basic experimentation:

Dr S Strydom, copromoter of this thesis.

Mr. D Johannes, for the work done on the oxidation of waxes.

Mr. K VD Merwe, for the preparation of the oxidized and grafted waxes, the saponification and the physical characterization of the waxes.

Mrs. G Webber, for the fine work done on characterizing the waxes with respect to their rheology.

Mrs. L Michau, for the characterization of the mechanical properties of the waxes.

Last but not least, Mr. John O'Neil, owner of the company Samchem, for his continuous encouragement and financial assistance

LIST OF CONTENTS

LIST OF APPENDICIES

LIST OF TABLES

LIST OF FIGURES

LIST OF SYMBOLS AND ABBREVIATIONS

Å	= Angstrongs, where 10^{10} Å = 1mm
COO^-	= Acid anion
R	= Alkyl group
M^+	= Metal cation
γ	= Gamma
T_g	= Glass transition temperature
β	= Beta
α	= Alfa
τ	= Tau
P	= Phosphorous
WLF	= William, Launders and Ferry
μ	= Micro
ω	= Omega
ΔH_f	= Heat of fusion
ΔS_f	= Entropy of fusion
F-T	= Fischer-Tropsch

CHAPTER 1 : Introduction and objectives

1.1 Introduction

There is a vast array of literature available on ionomeric polymers, covering many facets, but to my knowledge very little has been published on ionomeric waxes and I have not come across any literature published specifically on Fischer-Tropsch (F-T) ionomeric waxes. The ionomeric waxes can however be used in a variety of potential applications where normal waxes [1-8] do not function as well [1-9]. Ionomeric waxes can be any type of low molecular mass hydrocarbon- based polymers where a charge has been imparted on the backbone of the hydrocarbon and the charge neutralised by saponification. F-T ionomeric waxes are waxes which have been produced by the F-T process, and have either been oxidised or grafted onto, and saponified to impart a charge on the backbone of the wax.

Oxidised waxes, which currently form the basis for ionomeric F-T waxes are produced by oxidising saturated hydrocarbons with a stream of air (temperature of ca. 170 °C) in a bubble reactor. The exact structure of the oxidised product is not presently known, but through chemical analysis, one can determine the carboxylic, ester, carbonyl, hydroxyl, etc. content. The oxidation reaction is relatively easy to control and gives relatively consistent results in terms of product understanding. The oxidised wax is then saponified with various cationic hydroxide salts to form the ionomeric wax .

When F-T ionomeric waxes are manufactured and used in various practical applications, the person manufacturing the products is not always aware that morphological changes such as multiplet and cluster formation are taking place. These morphological changes have however a direct impact on the mechanical and physical properties of the ionomeric wax and dictate the behaviour of the wax on exposure to external forces [11-19]. I have not found any literature describing the analysis of F-T waxes based on their morphology and when and how multiplets and clusters are formed.

It is therefore very important to be able to analyse the F-T ionomeric waxes in terms of their morphology so that their mechanical and physical behaviour becomes predictable.

1.2 Objectives

The main objectives of this dissertation were the following:

- To study and investigate the oxidation process of F-T waxes and the corresponding oxidised products formed so that upon saponification , the structure of the ionomeric wax formed is understood.

- To analyse the F-T ionomeric waxes by various analytical techniques so as to determine whether the selected analysis techniques are sensitive enough to detect whether the samples have formed multiplets or clusters.

- To determine at which oxidation concentration and at which percentage saponified (for each type of cation), whether the F-T ionomeric wax has formed multiplets or clusters.

In order to achieve these objectives, the following tasks were envisaged:

1.3 Tasks

1. To carry out a literature study to understand the concept of ionomers, oxidised hydrocarbons and oxidised F-T waxes.

2. To establish a better mechanistic understanding of the oxidation process performed on the F-T waxes and the type of oxidised groups that are formed upon oxidation. The oxidised waxes form the basis for the formation of the ionomeric wax and therefore gives information as to the structure of the oxidised wax which must be understood in order to understand how the ionomeric wax will respond under certain mechanical or physical tests.

3. To describe the synthetic approach followed for the preparation of the F-T ionomeric waxes.

4. To perform various physical, mechanical rheological and absorption tests on the F-T ionomeric waxes in order to determine whether the specific method of analysis tested is sensitive enough to detect whether the samples has formed multiplets or clusters.

5. Overall, to try to determine whether each individual sample tested has formed multiplets or clusters. These results are also compared to that of ionomeric polymers, which have

received more attention in the literature research.

1.4 Layout of thesis

The thesis is divided into eight individual chapters, these being:

CHAPTER 1 : Introduction and objectives

CHAPTER 2 : Historical and theoretical background

CHAPTER 3 : Fischer-Tropsch wax oxidation experimentation

CHAPTER 4 : Fischer-Tropsch wax saponification

CHAPTER 5 : Ionomeric Fischer-Tropsch wax : Physical and mechanical analysis

CHAPTER 6 : Ionomeric Fischer-Tropsch wax : Rheological properties

CHAPTER 7 : Ionomeric Fischer-Tropsch wax : Water sorption and diffusion properties

CHAPTER 8 : Conclusions and recommendations for further research

1.5 References

1. Mehrotha K N, Lata R, Kumar A, **Rev. Roum. Chim.**, 39(5), pp517, 1994
2. **Encyclopaedia of Polymer Science and Technology, Volume 6,** Intersience Publishers, John Wiley and Sons Inc., New York, pp 422, 1964
3. **Encyclopaedia of Polymer Science and Technology, Volume 6,** Intersience Publishers, John Wiley and Sons Inc., New York, pp 421, 1964
4. Mohajer Y, Bagrodia S, Wilkes G L, **J. Appl. Polym. Sci.**, 29, pp1943, 1984
5. Hara M, Jar P, Sauer J A, **Macromolecules**, 23, pp4969, 1990
6. Rees R W, **United States Patent**, No. 3 264 272, Aug. 2 1966
7. Lefelar J A, Weiss R A, **Macromolecules**, 17, pp1145, 1984
8. Bonotto S, Bonner E F, **Macromolecules**, 1, pp514, 1968
9. Makowski H S, Lundberg R D, Westerman L, Bock J, **Advances in Chemistry Series No. 187**, pp3, 1980
10. Broze G, Jerome R, Teyssié P, **Macromolecules**, 15, pp920, 1982
11. http://www.crestchem.co.uk/productsw.html
12. http://www.gujaratwaxes.com
13. http://www.dermochimica.it/inglese/cere/indice-i.html
14. http://www.wax.4mg.com/applications.html
15. http://pa.clariant.com
16. http://www.dermochimica.it/inglese/cere/indice-i.html#4405
17. http://www.luxurylane.com/thelibrary/references/waxes.html
18. http://www.schuemann-sasol-za.com
19 http://www.deurex.de/download/DS_731_Deurex_MM82Micro_1002.pdf

CHAPTER 2 : Historical and theoretical background

2.1 Classifications of ionomeric polymers

Eisenberg and King go into great detail to distinguish between the many types of ion-containing molecules and give a graphical representation of their classification system [1]. This thesis, however, is not going to attempt a detailed explanation of the different definitions for the different classes of ion-containing molecules, but it will rather concentrate on general definitions so that when reference is made to 'ionomers', they are distinguished from other ion-containing molecules.

There are at present several classification methods for ion-containing polymers. As the broad classification as proposed by Eisenberg and King [2] is appropriate for the F-T ionomeric waxes used in this thesis, this thesis has adopted their classification system of ionomers and polyelectrolytes. Ionomers represent polymers of relatively low ion content, while polyelectrolytes represent polymers where most of the repeat units carry ion charges. An example of a commercial ionomer is Surlyn (ethylene-methacrylic acid) copolymers, 10 mole percentage acid units, saponified with zinc or sodium salts. Polyacrylic acid [3] is a typical commercial example of a polyelectrolyte. Both types are shown schematically in Figure 2.1.

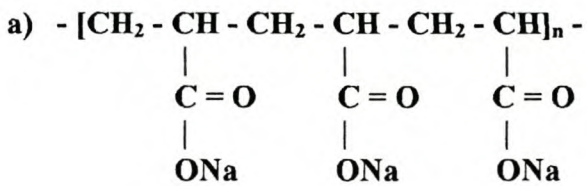

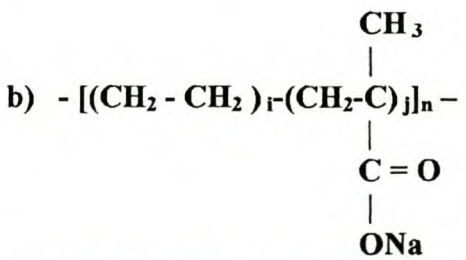

Where subscript i is generally much greater than subscript j

FIGURE 2.1 : Example of a) A polyelectrolyte (b) An ionomer

The above classification does not attempt to contradict or confirm the many other published classifications [4-12] but merely serves as a broad definition for the purpose of this thesis. There are many other types of ion-containing polymers [13] such as:

- Polysalts [14]: A complex formed between oppositely charged polyelectrolytes
- Polycations [15]: Cationic groups on polymers, such as poly-N-alkyl vinylpyridinium chloride
- Ionenes [16-21]: A specific kind of polycation where the cations are situated in the main chain, instead of being pendant to the chain as in polycations
- Telechelics [22-36]: Polymers which have ionic groups on both ends of the polymer
- Polyphosphates [37]: Phosphate containing ionic polymer
- Perfluorinated ionomer membranes [21,38-39]
- Ampholytes [36, 40-43]: Cationic-anionic ionomers containing no inorganic ions
- Ionizable polymer brushes [44]: Polymer brushes grafted with ionizable polymer chains (polyacid or polybase polymers)
- Zwitterionic polymers [45-46]: Polymers where both cationic and anionic charges are situated on the same side branch. These anions and cations can then react with anion-cation salts
- Block Ionomers [47-48]: Ionomers prepared from blocks of different monomers

These particular ion-containing polymers are not of direct interest to this thesis, but only show how varied ion-containing polymers can be.

The above classification is demonstrated for carboxylic acid derivatives (see FIGURE 2.1), but the polar groups could just as well have been sulphonic acid, thioglycolic acid, phosphonic acid or any anion other than carboxylic acids. In fact, according to Lundberg and Makowski , the sulphonic acid ionomers [49-53], when compared to carboxylate ionomers under as similar conditions as possible, possess much stronger ionic association than the corresponding carboxylates. The same reasoning follows for the neutralisation of anions, which is assumed to take place by reacting with a metal salt. This need not be the case and organic bases could also be used [54-58].

The backbone does not need to be constructed of methylene units, as in polyethylene, but could just as well have been constructed of polymers such as polybutadiene [59], polystyrene

[60], polyoxymethylene [61], polypentamer [62] or any other type of backbone, providing the backbone can be classified as essentially non-polar.

2.2 History of ionomeric polymers

Ionomeric polymers have been used for many years but due to a poor understanding of the fundamental aspects of this class of polymers, they have taken a long time to reach their full potential. Patent literature as early as 1933 describes the carboxylation of elastomers [63] (issued to I.G. Farben Industrie) and in 1949 Goodyear introduced HYCAR, which was a butadiene-acrylonitrile-acrylic acid terpolymer. The concept or idea of neutralising the acid groups was apparently largely due to Brown [59]. In the early 1950's, Du Pont introduced Hypalon [64], which was based on sulphonated structures obtained from chlorinated polyethylene (cured with various metal oxides). Du Pont followed Hypalon up in 1960 with their ionomer called Surlyn [6, 8, 65-74]. This is an ethylene-methacrylic acid copolymer containing less than 10 mole percentage acid, which is neutralised mostly with zinc or sodium salts. The unique properties of this polymer, its high melt strength, excellent toughness and optical clarity, made this an ideal material for certain packaging applications and golf ball covers.

Recently, new types of ionomers have been introduced which possess a wide variety of properties, which are utilised in various applications. Du Pont have introduced the Nafion [38, 75] class of perfluorinated sulphonated ionomers, Exxon have described work done on sulphonated ethylene-propylene terpolymers [76-77] and Asahi Glass Company have introduced Flemion [78], a perfluorinated carboxylate ionomer.

Initially the reasons for the improvement in properties of ionomers were not fully understood. A great deal of published literature and patents have been devoted to explaining ionomeric phenomena and the expanded use of these polymers in a practical context. After the initial discoveries described above, there has been an explosion in new materials.

2.3 Typical applications of ion-containing polymers

Ion-containing polymers are currently being used in many commercial applications [79-88] and in novel market areas such as:

- moulded products for housewares, automotive parts, toys
- skin packaging (for high toughness, clarity and good adhesion to paperboard)

- blow-moulded containers (where good oil resistance and transparency are required)
- various types of films (where toughness, good low-temperature properties and ease of opening packages are needed)
- extrusion-coated substrates for good grease resistance
- waterless cement [89] (by mixing zinc oxide powders with polyacrylic acid)
- other applications such as: tubing, electrical insulation, pharmaceutical parts, cosmetic containers, business machine parts and safety gear
- as an additive to cattle feed to increase the yield of milk [81].

2.4 Preparation of ionomers

Since there are many types of ion-containing polymers (see point 1.1. for list of possible types), there have been many methods used to prepare these polymers [35-36, 90-101]. I am not going to describe the many processes in detail but would like to mention a few typical methods, including the formation of ionomeric waxes.

Oxidised waxes, which form the basis for the ionomeric waxes, were produced by oxidising saturated hydrocarbons with a stream of air (temperature of ca. 170 °C) in a bubble reactor (see CHAPTER 3 for more detail). The exact structure of the oxidised product is not presently known, but through chemical analysis, one can determine the carboxylic, ester, carbonyl, hydroxyl, etc content. The reaction is relatively easy to control and gives relatively consistent results. The oxidised wax is then saponified with various cationic hydroxide salts to form the ionomeric wax (see CHAPTER 4, for more detail).

Another example of ionomer preparation is the description given by Broze, Jerome and Teyssie [102] for the preparation of halato-telechelic polymers, by first preparing the telechelic polymer anionically and then neutralising the anionic polymer with metal pivalates or metal methoxides. These ionomers were used as "model ionomers" to investigate the morphology of ionomers.

Ionomers were initially only prepared as copolymers from either methacrylic acid or acrylic acid monomers together with either ethylene [72, 103-107] or styrene [108-110] as co-component. Later there are specific examples of other types of polymers, such as those prepared by Phillips and MacKnight [111] where a polyethylene-phosphonic acid copolymer was prepared by treating polyethylene with phosphorus trichloride.

The compositions of the different copolymers and oxidised waxes vary greatly in structure, resulting in these differences in the physical characteristics. Regardless of the differences in structure, the ionomers all seem to have the same mechanism of formation of multiplets and clusters for a specific ionisation degree and anion percentage (see section 1.5 below for a more detailed explanation).

2.5 Morphological models for ionomeric polymers

2.5.1 Introduction

During the past two decades a large amount of research and development has been done on ionomers, due to their unusual physical characteristics. There are many papers which describe the work done on the morphology of polymers [39, 112-120]. This section describes the different morphological models and their conclusions.

Brown [59] observed that when carboxylated elastomers were saponified with cations such as zinc, the product acted like vulcanised rubber. The natural conclusion was that ionic cross linking was the reason for the properties observed. It was thus assumed that a bond such as:

$$-COO^{-}\ Zn^{2+}\ {}^{-}OOC-$$

would be predominant. This assumption did not take into consideration the coordination tendencies of zinc ions, the influence that the hydrocarbon environment of the backbone would have, or the influence of polar impurities. Initially this explanation for ionomers was widely accepted, even when complicating factors, such as crystallinity in modified polyethylene ionomers, were encountered. The proposed structure for ionomers had to be modified however to explain the structure of monovalent cations. Otocka, Hellmann and Bleyler [68] proposed a dipole-dipole interaction between salt pairs as shown below:

$$\begin{array}{ll} K^{+}\ {}^{-}OOC-R \\ \Updownarrow \quad \Updownarrow \\ R-COO^{-}\ K^{+} \end{array}$$

This proposal recognised the fact that salt groups in the presence of hydrocarbon backbones would be present as contact ion pairs.

The ionic cross-link hypothesis did not however account for all the physical characteristics encountered in ionomers, and other proposed models were developed to explain their structures. Eisenberg [69] gave a comprehensive theoretical attempt at explaining the structure of ionomers. This proposed model assumes that a distance corresponding to their ionic radii separates cations and anions from each other. One thus obtains a contact ion pair. In this proposal there are two considerations: 1). Ionic volumes or radii are used to calculate the largest number of ion pairs which can group together (multiplets), taking into account the effect of intervening hydrocarbon backbones. 2). Energetic considerations are used to explain the formation of larger entities (aggregates or clusters) which are composed of groups of ion pairs separated from each other by a layer of hydrocarbon backbones. A single ion pair can thus be seen as the smallest multiplet that can be formed, while the largest multiplet size will be limited by the size of the ions (ionic radii) and the corresponding backbone attached to it. Clusters can be formed when multiplets associate due to electrostatic interactions between multiplets and overcome opposed forces due to the elastic nature of the hydrocarbon backbone.

Models other than those discussed above were also developed. These are now discussed individually.

2.5.2 The model of Bonotto and Bonner

X-ray [121] and electron microscopy [122-123] experimentation on ionomers has shown that structural reorganisation occurs upon neutralisation. The structural reorganisation then supports the theory of cluster or aggregate formation. Bonotto apparently was the first to propose the idea that association into ionic clusters occurs in ionomers. Bonotto and Bonner [124] later proposed a model for the formation of ionic aggregates which can be seen in FIGURE 2.2.

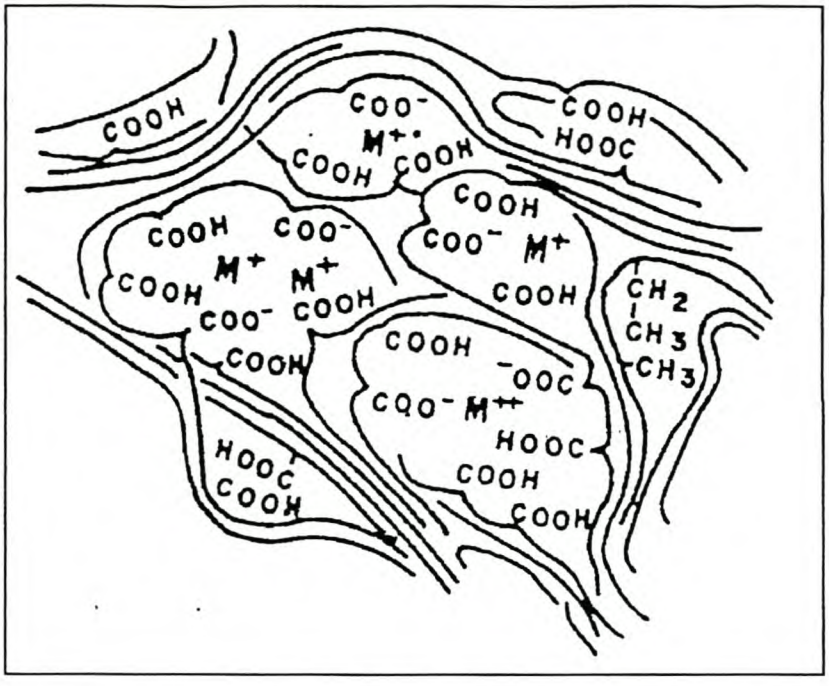

FIGURE 2.2 : Schematic diagram of Bonotto and Bonner[124] model for ionic aggregates

The model is not discussed quantitatively but the concept seems to hinge on the fact that small clusters are formed, which can act as multi functional cross-links. The proposed model does not clarify whether micro-phase separation takes place or whether the domains are multiplets or clusters as defined by Eisenberg [69].

2.5.3 The model of Longworth and Vaughan

Longworth and Vaughan[125] proposed a model, which assumes micro-phase separation between the ionic carboxylic salts and the hydrocarbon backbone of an ethylene carboxylic acid ionomer. This model is based on the analysis of the above ionomer by ionic X-ray scattering peaks. According to the results, there exists an ionic peak, which gives an ionic domain of lower limit 100 Å. This figure is calculated from the fact that for a diffraction peak to occur, at least five repeat units of approximately 20 Å must be present (based on the assumption that the ionic peak observed is a diffraction maximum in the Bragg sense). The absence of higher-order diffraction maxima indicates imperfect periodicity. Ordered hydrocarbon chains are assumed to be the nature of the repeat units within the ionic domains and not the ordered arrangement of the ions themselves. The proposed model of Longworth and Vaughan is shown in FIGURE 2.3.

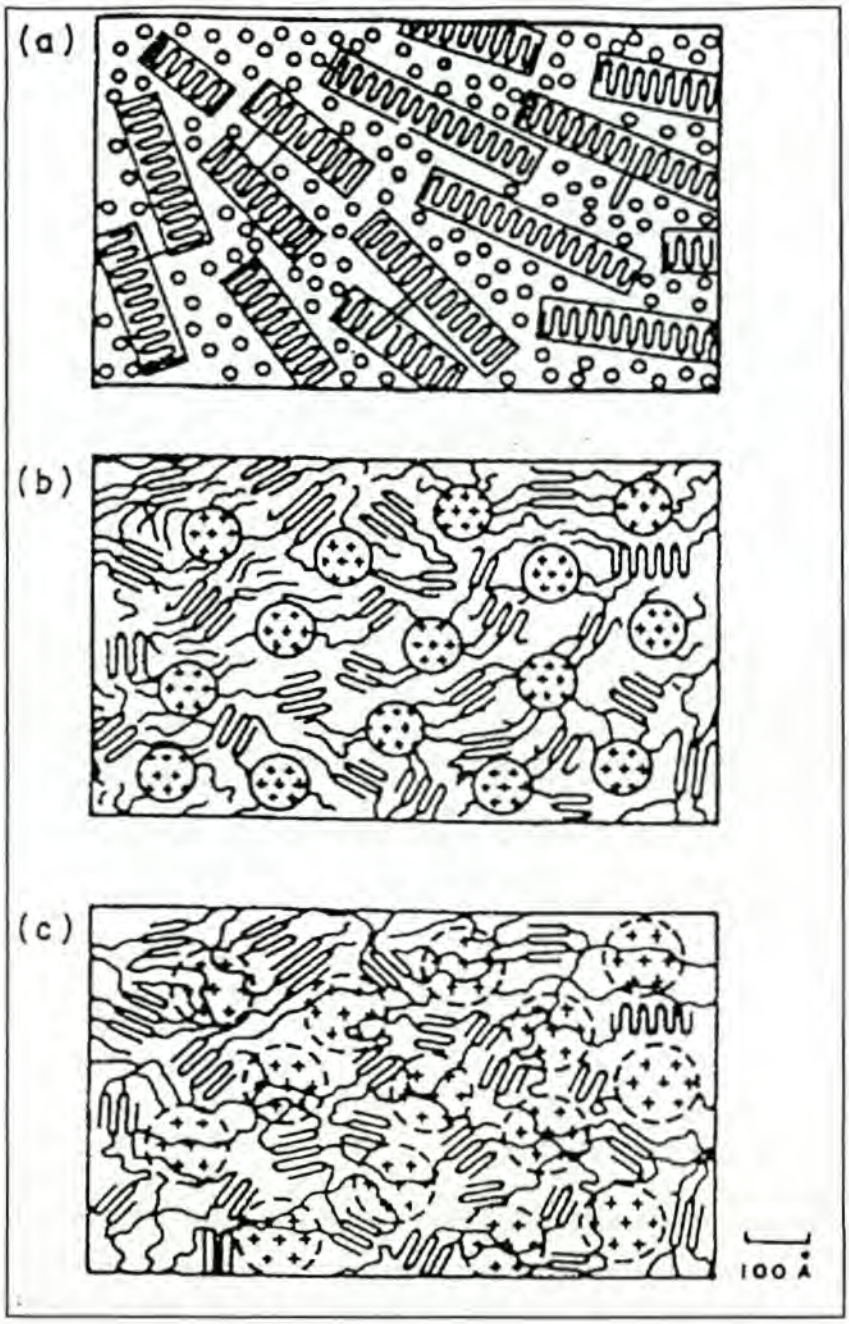

FIGURE 2.3 : Schematic diagram of Longworth-Vaughan[125] model for ionic aggregates (a) acid copolymer (b) dry ionomer (c) wet ionomer

The Longworth-Vaughan model does not explain all the phenomena occurring in ionomers, such as the intensity differences in ionic peaks for different cations. If the intensity in ionic peaks is not cation related, then why does a metal such as cesium show a scattering intensity approximately a thousand times greater than a metal such as lithium [125]? Secondly, a cluster of approximately 100 A should influence the degree of crystallinity, which is not experienced experimentally. There are thus still some unanswered questions.

2.5.4 The model of Marx, Caulfield and Cooper

Marx, Caulfield and Cooper [126] interpreted the ionic peak differently from Longworth and Vaughan [125]. In their interpretation, they assume that there is no micro-phase separation and that the acid groups are arranged as aggregates, homogeneously in the amorphous phase. An aggregate should then contain two or more carboxyl groups, depending on the type of copolymer and the amount of water present. The ionic peak, in this model, is assumed to arise from an electron density difference between the metal ion in the aggregate and the hydrocarbon backbone. The cations are in fact taken as point scatterers on a paracrystalline lattice. Marx et al[126] then conclude, by mathematical formulae and experimental results, that the number of ionic groups that aggregate is in fact very low, amounting to no more than septimers, even at the highest concentration. This then implies that according to Eisenberg's [69] definitions, in actual fact only multiplets are formed and no clusters are formed.

There are some objections to the model of Marx et al[126]. Firstly, the interpretation of the ionic peak as being due to the presence of a paracrystalline lattice of scattering sites implies a considerable degree of regularity in the distance between scattering sites. It is difficult to believe that in the amorphous zone of a random copolymer this can be possible. Secondly, lithium cation ionic peaks are difficult to explain on the basis that the peak originates from electron density differences between the cation and the hydrocarbon backbone. According to the model of Marx et al[126], it is difficult to understand why a peak should be absent for an acid, but present for the lithium salt, when it is considered that this model proposed that the difference in electron density of the lithium carboxylate and corresponding carboxylic acid is very small. Thirdly, as in the Longworth-Vaughan [125] model, such regular scattering sites should affect crystallinity when acids are saponified. The model does not account for the alteration of the crystalline morphology when going from the acid to the corresponding salt form.

2.5.5 The model of MacKnight, Taggart and Stein [127]

The models of Longworth et al.[125] and Marx et al[126], were all based on analyses of the ionic peak, which were based on the assumption that the origin of the ionic peak lies in some structural regularity in the system imposed by the presence of salt groups. The interpretation of diffraction data is by no means unique and the random packing of spheres will also give a peak similar to the ionic peak if the volume fraction of spheres is sufficiently

high. The peak maximum thus obtained in the case of sufficiently large volume spheres is therefore related to the radius of the sphere and not to the distance between spheres [128].

MacKnight, Taggart and Stein [127] used both RDF (radial distribution function) analysis and low-angle x-ray scattering, as well as the theories of Guinier-Fornet [128] and Porod [129], to show that the peak maxima were indeed due to the radius of ionic-spheres and not to the distance between ionic-spheres. The application of the Porod[129] and Guinier-Fornet[128] data treatments to the ionomer experimental results could however only produce fairly crude approximations to the real situation, due to the idealised models on which they had based their assumptions. The idealised model does not take into account particle size disparity, non-uniformity of electron density in phases and interference effects, especially those arising from the presence of ionic peaks. The interference arising from the presence of ionic peaks is especially pronounced in the Guinier-Fornet[128] analysis of the dry salts since the nature of the interference function giving rise to the ionic peak is not known.

Notwithstanding, the combined results of the Porod[129] and Guinier-Fornet[128] analysis and the RDF analysis indicate the presence of ionic clusters 8-10 A in radius, randomly dispersed in the amorphous hydrocarbon matrix. A schematic representation of the MacKnight Taggart and Stein[127] hard sphere model for ionic aggregates is shown in FIGURE 2.4 below.

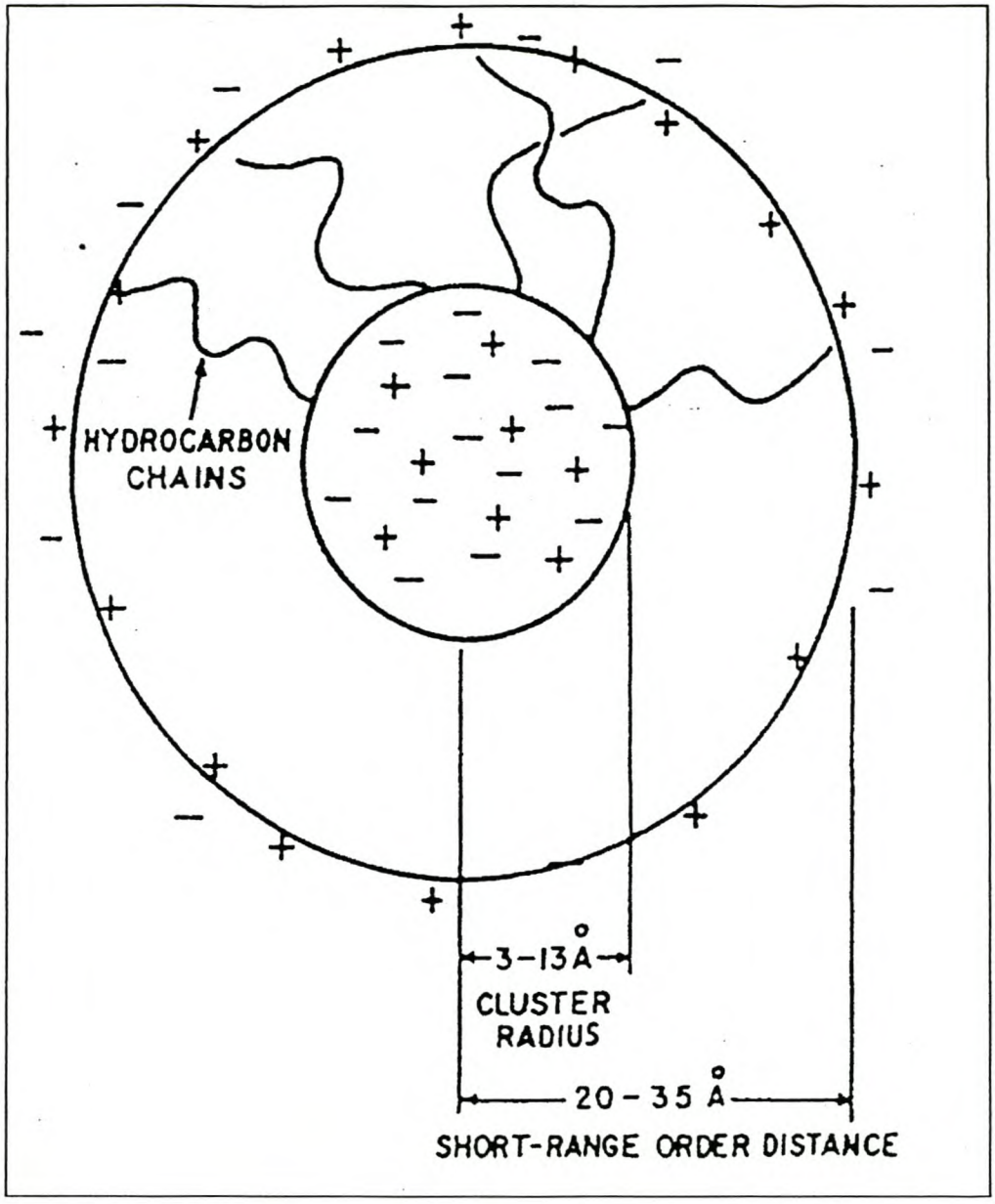

FIGURE 2.4: Schematic diagram of MacKnight, Taggart and Stein[127] model for ionic aggregates

2.5.6 The model of Pineri and co-workers.

Pineri et al, [110, 130] and Meyer and Pineri [131-132] used other methods than those used before to study the morphology of ionomers. They used transition metal cations on which electron spin resonance (ESR) and Mössbauer (γ- ray) spectroscopy could be carried out. They also used small-angle neutron scattering, x-ray scattering and electron microscopy to analyse the ionomers. The type of ionomers studied included:

- copper salts of low-molecular-weight polybutadiene with terminal carboxylic groups (Hycar CTB from B.F. Goodrich Co.)

- copper, manganese and nickel salts of high-molecular-weight butadiene-methacrylic acid copolymers
- iron [Fe(II)] complexes of butadiene-vinyl pyridine copolymers or butadiene-styrene-vinyl pyridine terpolymers

Mathematical models were applied to the experimental neutron and x-ray scattering analysis data to obtain the best fit. The mathematical analysis showed that more than 82 % of the clusters formed were less than 30 Å in radius and that the average cluster radius was ca. 10 Å. These results are in agreement with the results found by MacKnight, Taggart and Stein[127] as discussed in Section 2.5.5.

Mössbauer spectroscopy involves the recoilless resonance absorption of γ-rays by a particular nucleus, usually iron, to give an absorption spectrum which supplies more information about the electronic environment of the specific nucleus. Pineri's study on vinyl pyridine complexes revealed three types of structures:

- dimers which account for 20 % of the iron content
- quasi-isolated complexes which account for less than 20 % of the iron content. These complexes have a weak ferromagnetic coupling and may be present in very small multiplets or preferentially located in the vicinity of clusters
- clusters which account for 40 % to 60 % of the iron content. 90 % of these clusters are less than 30 Å in radius and contain an average number of 30 complexes.

The quasi-isolated complexes and the clusters discussed above are identical to the shell-core model as suggested by MacKnight, Taggart and Stein[127] although the models were developed for different cations. Considering that different cations were used in the respective models, it is remarkable that the estimated sizes of the clusters for both models are more or less the same.

2.5.7 The model of Eisenberg, Hird and Moore[112]

Eisenberg, Hird and Moore [112], proposed a different model to those already proposed. Their model is based on the formation of multiplets. It differs from other cluster models however in that they propose that a cluster is formed when there are enough multiplets for there to be areas of overlap between multiplets. Only the regions of restricted mobility overlap; the multiplets stay intact. As the overlaps become more frequent, large regions of restricted

mobility are formed until the regions are large enough to have their own T_g's. Their model does not require that the clusters be of any geometry, and highly irregular shapes are possible. The clusters also have no upper limit on the number of ion pairs or multiplets that they may contain.

The model also accounts for other experimentally observed phenomena, such as the weak dependence of the Braggs distance on the ion content, phase inversion at a relatively low ion content, the inability to see clusters using electron microscopy, the absence of two-phase behaviour in stiff chain ionomers and the effect of plasticisers.

Tsagaropoulos, Kim and Eisenberg [133], used electron spin resonance spectroscopy to obtain information on the chain mobility in spin-doped poly(styrene-co-(sodium methacrylate)) random ionomers. Based on this and earlier work done on filled systems, DSC and NMR experimental analysis on ionomers[133], they concluded that they had solid proof that the Eisenberg, Hird and Moore [112] model explains the morphology of random ionomers.

2.5.8 Comparison with filler-filled polymers

Tsagaropoulos and Eisenberg [134] showed that there is an interesting comparison between the glass transition properties of ionomers and filled polymers. They proposed that the process of clustering and its effect on ionomer properties should be similar to that of the incorporation of filler particles into polymers, where regions are created at the polymer-filler particle interface, which have restricted mobility. For filled polymer systems with nano-sized filler particles, there should thus be two glass transitions, as for ionomers: one transition for the polymer matrix and a second transition at a higher temperature, which correlates to an interfacial region of restricted mobility. Tsagaropoulos and Eisenberg[134] used several polymers such as poly(vinyl acetate) (PVAc), polystyrene (PS), poly(methyl methacrylate) (PMMA) and poly(4-vinyl pyridine) (P(4VP)) homopolymers filled with nano-particle size silica fillers and used dynamic mechanical thermal analysis (DMTA) measurements to observe the low temperature transitions. In the graph depicted below (FIGURE 2.5) the first and second order transitions for both polymer-filled systems and an ionomer can be seen. The $T-T_g$ values are inconsistent and appear to be derived from the Tan δ peaks and not the extrapolated onsets.

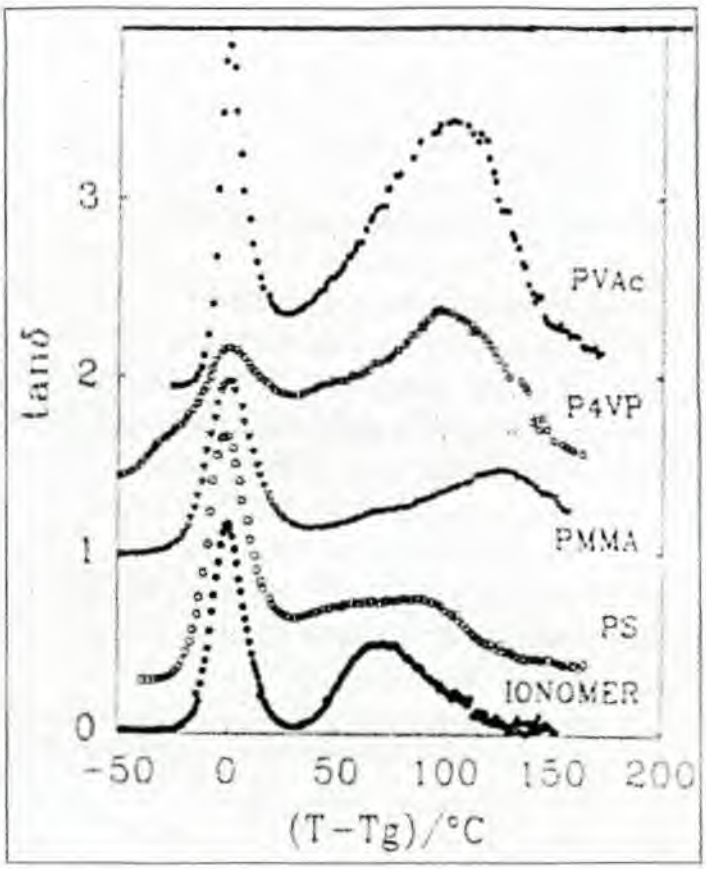

FIGURE 2.5 : Tan δ versus T - T_g curves for a poly(styrene-co-4.5 mol % sodium methacrylate) ionomer (●) and the following polymers filled with 10 wt % of 7 nm silica particles: PS (○), PMMA (▼), P(4VP) (□), and PVAc (■). The curves of the filled polymers have been shifted for clarity by 0.2, 0.9, 1.4 and 1.9 respectively [134].

The authors do not go into a detailed explanation of the morphology of the filler-filled system, but conclude by saying that both types of systems behave in a similar way with respect to their glass transition, implying that they must have similar morphologies. It is easy to envisage the filler-filled system, which could be another way of describing ionomer morphology.

2.5.9 Summary

The preceding sections describe how clusters and multiplet models began and how the different models were developed in trying to describe the experimental findings. Many types of analytical techniques [135-136] were used to analyse the ionomers in an attempt to elucidate their structure. The model according to Eisenberg, Hird and Moore[112], seems to account for most of the experimental observations observed so far with respect to random ionomers. Their approach is different to the previous models and contradicts the so called "hard sphere" model. The experimentation for the morphological understanding of an ionomeric

wax does not form part of this thesis, but it is important to attempt to understand the physical phenomena encountered in ionomeric waxes in relation to their possible morphology.

2.6 Physical properties of ionomeric polymers

2.6.1 Introduction

There are many physical properties of ion-containing polymers, which can be discussed to illustrate the difference between an ionomeric polymer and its non-ionised counterpart. I have only identified a few physical properties, which are of relevance to this thesis. These properties are described to give an idea of how ionomeric polymers perform physically and in order for the ionomeric waxes to be compared to the ionomeric polymers to see how far they differ from each other. The comparison that I am drawing is obviously only a relative comparison since there are already distinct chemical and mechanical differences between different types of ionomers and the ionomeric waxes can therefore be expected to have their own characteristics.

2.6.2 Glass transition in ionomeric polymers

2.6.2.1 Introduction

The glass transition (T_g), implying a transition from a glassy substance to a rubbery consistency, is characteristic of many polymeric solids. During T_g-tests, as the temperature is increased, the segmental mobility increases to the point where rubber-like deformation under applied stress becomes possible. The segmental mobility will be dependent upon the intermolecular forces. In the case of ion-containing polymers, the degree of ionisation, the type of anion and the cation should play a role in the retardation of the segmental motion.

There are a few analytical methods for determining the glass transition temperatures of ionomers. These could include differential scanning calorimetry (DSC) [85, 137-138], dynamic mechanical thermal analysis (DMTA) [85,137-140,141], rheometry [142] and dynamic dielectric spectroscopy [143-144]. These analytical methods show that if the modulus temperature curves were practically obtained, they would verify that the salt form of the original acid polymer is dramatically different from the original non-ionised acid polymer.

2.6.2.2 Specific examples

An example of the difference between the non-ionised polymer and the corresponding salt form of the same polymer, is a comparison between sulphonated ethylene-propylene ionomers and poly(ethylene-propylene) from which the ionomer was produced [95]. The sulphonated-EPDM (ethylene-propylene diene monomer) has an elastic modulus that is virtually constant up to 200 °C, even at very low ionic concentrations (in the multiplet regions), whereas the EPDM polymer displays viscous flow above 50 °C.

Eisenberg and co-workers [71, 106, 145-146] had done extensive studies on the relaxation behaviour of styrene ionomers. They had measured the T_g's by DSC and had found that there is a linear relationship between the observed T_g and the increase in salt concentration of the styrene ionomer. This behaviour is illustrated in FIGURE 2.6 [71] shown below.

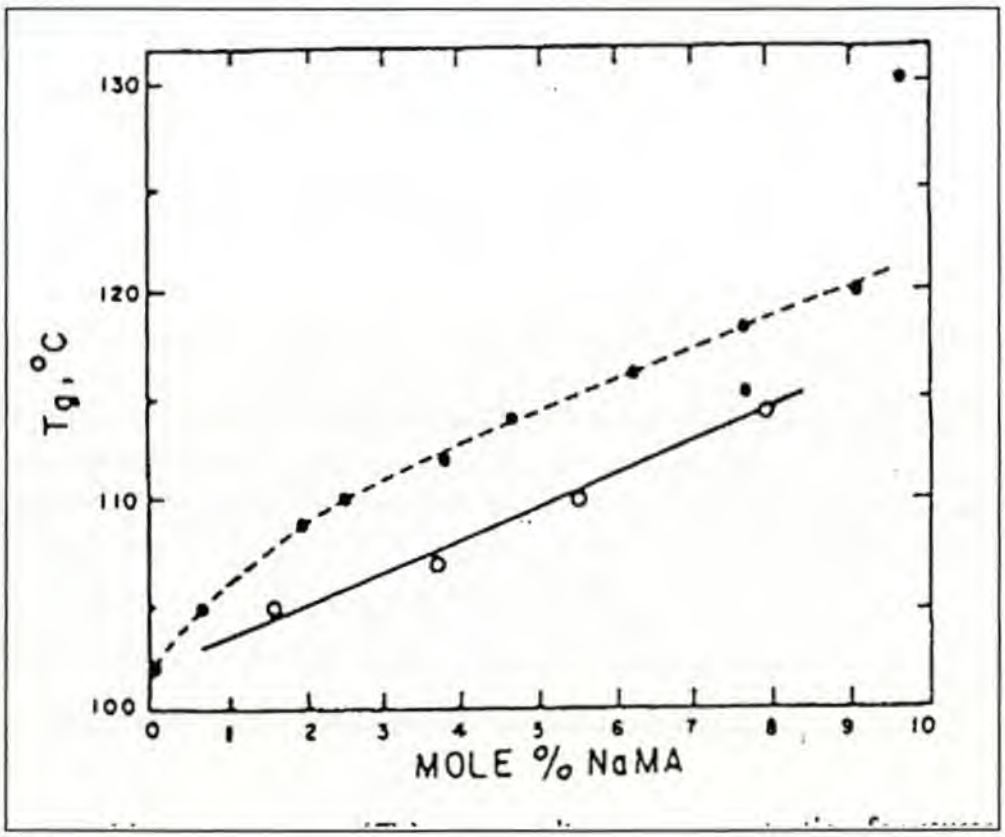

FIGURE 2.6 : Glass transition temperature (T_g) versus salt group concentration for styrene-sodium methacrylate copolymers: (○) low molecular weight, (●) high molecular weight [71]

The T_g of the high-molecular weight polymer increases initially by 8°C for the first 2 mole % of salt groups whereafter the increase in T_g is ca. 2°C/mole % up to 9 mole % of the ionomer. It is interesting to note that there is no change in slope at 6 mole %, which is where ionic clustering starts to form (according to x-ray evidence)[71]. The regular increase in T_g thus implies that a constant fraction of the salt groups remains mixed in the hydrocarbon phase, increasing the T_g by a combination of cross linking and copolymer effects. The above analytical measurements were done by DSC, which is in fact not very sensitive towards transitions versus temperature. Dynamic mechanical analytical measurements would show the transitions much more clearly. In work done by Eisenberg and Navratil [107], two loss peaks are observed for ionomers with less than 6 mole % sodium methacrylate. The two loss peaks are shown graphically in FIGURE 2.7 [107].

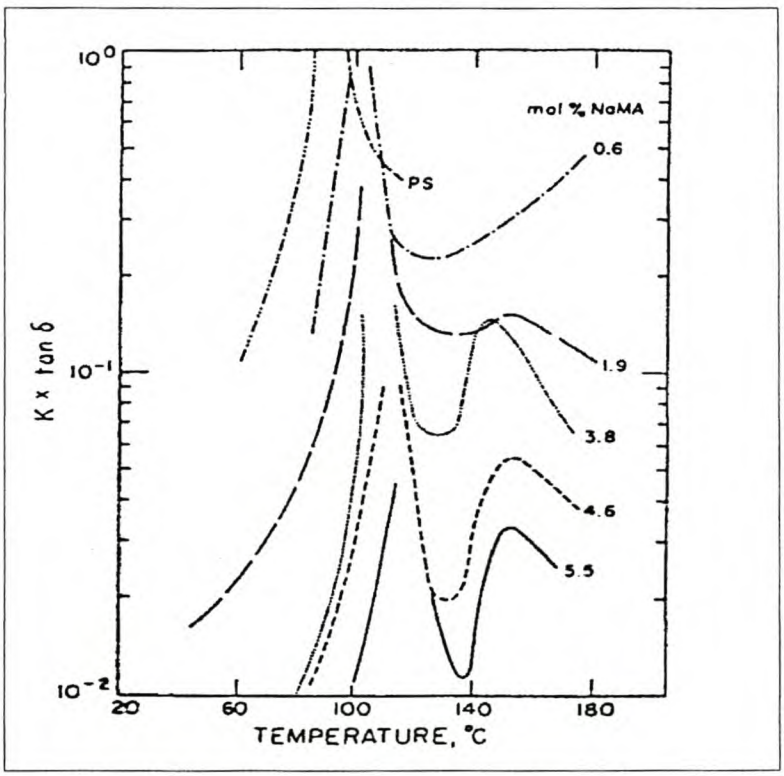

FIGURE 2.7 : Loss tangent (tan δ) versus temperature for styrene ionomers containing less than 6 mole % salt groups[107]

The graph shows that for a molar percentage sodium methacrylate above 0.6 % the first transition (T_β) increases with increasing salt content, while the peak of the second transition (T_α) remains relatively constant at ca. 150°C. For concentrations above 6 mole % however, a continuous increase of the T_α (Tan δ of the 150°C peak), is observed. The broadening of the T_β peak at higher mole % salt groups is depicted graphically in FIGURE 2.8 [107].

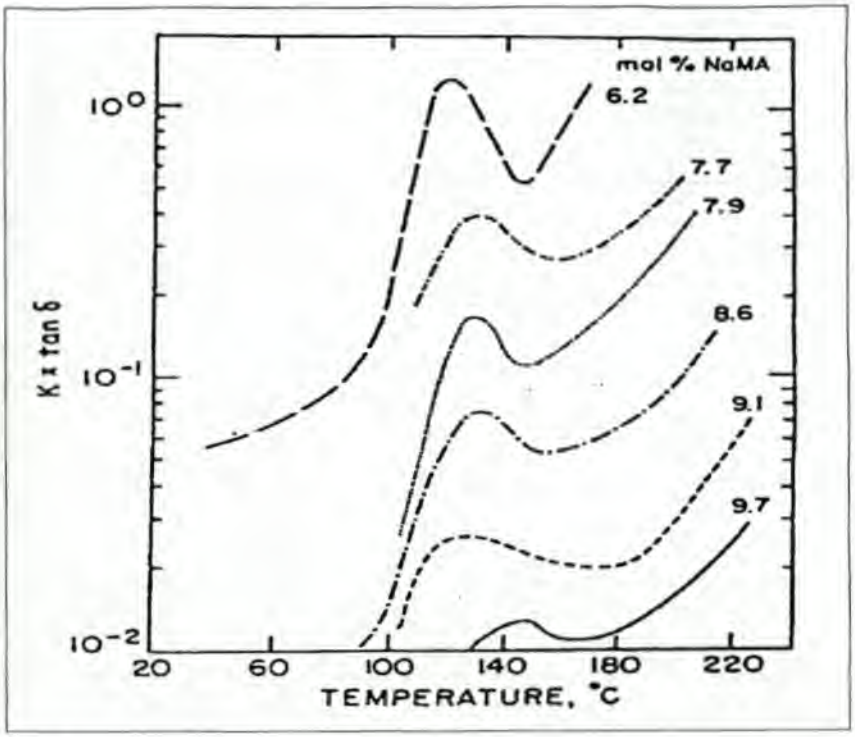

FIGURE 2.8 : Loss tangent (tan δ) versus temperature for styrene ionomers containing more than 6 mole % salt groups[107]

From the above graphs, it is postulated that at low concentrations of salts (where phase separation has not taken place yet), the T_α relaxation would be associated with multiplets. At higher concentrations, where phase separation is more complete and cluster formation is evident, the broader tan δ peak occurs due to the motion of salt groups in large clusters, which themselves have a distribution in size.

Investigations into the dynamic mechanical properties of ethylene-based ionomers have been reported by many scientists [125, 140, 147-152]. Generally, the dynamic mechanical response for both the acid copolymer and the corresponding salt resembles that of low-density polyethylene (LDPE). At ca. -120 °C there is a large loss peak, called the α-relaxation, which is best described as due to a crankshaft motion of short hydrocarbon segments in the amorphous phase. LDPE normally has a transition at ca. - 20 °C, called β-relaxation, which is associated with branching. The acid copolymer however shows a relaxation at between 0°C and 50°C, called β', which is attributed to micro-Brownian segmental motion accompanying restricted motion inbetween crystallites, while the increase in β-relaxation is attributed to the cross linking effect of dimerised carboxyl groups. FIGURE 2.9 [125], shows the effect of an increase in percentage neutralisation of the original annealed acid copolymer. As the acid groups are increasingly neutralised, the β'-relaxation disappears and

the β-relaxation shifts to lower temperatures. The β-relaxation is thus assigned to a relaxation occurring in the branched amorphous polyethylene phase, from which most of the ionic material is excluded.

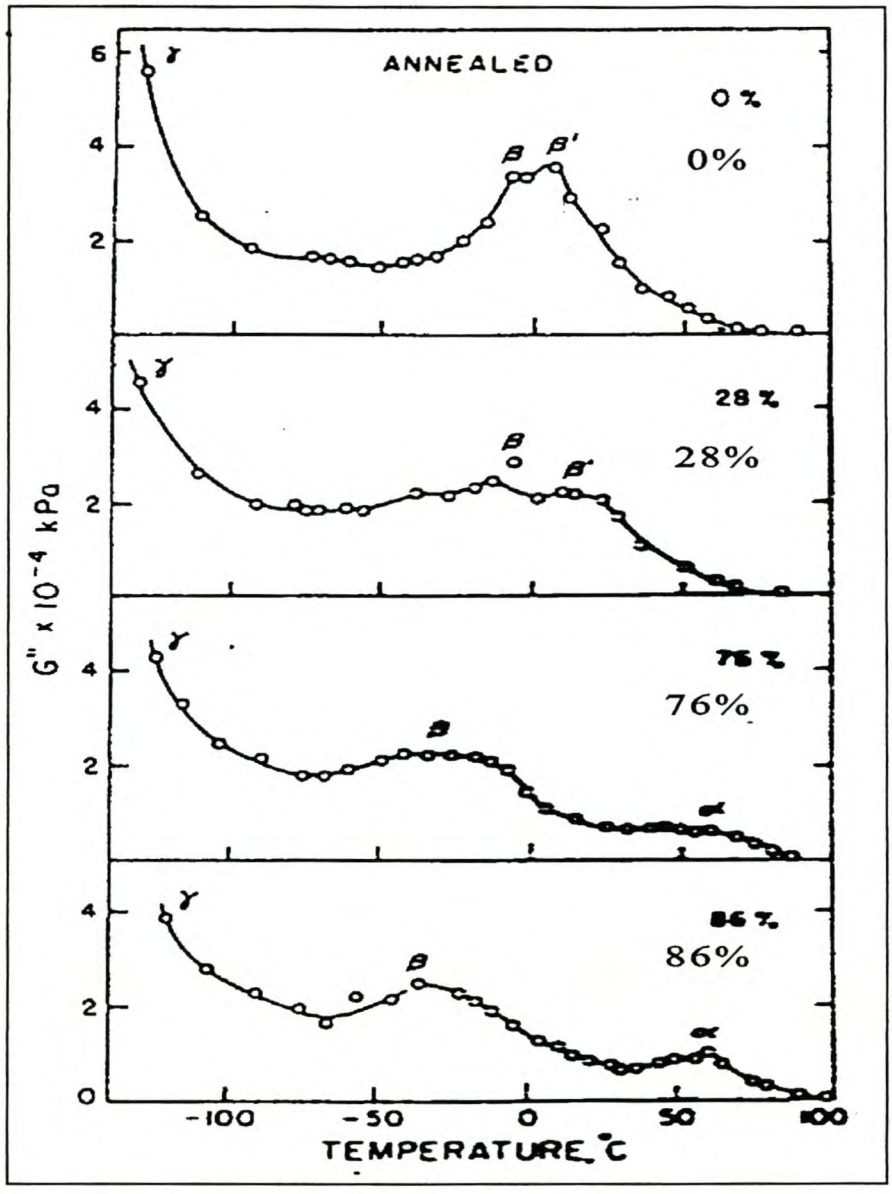

FIGURE 2.9 : Temperature dependence of G" for annealed ethylene methacrylic acid copolymers (4.1 mole % acid) neutralised to various degrees with sodium[125]

Yang, Sun and Risen [153] investigated linear sulphonated polystyrenes in the 3.4 mole % to 20.1 mole % sulphonation range. They used DSC analysis to look at the change in T_g with changes in sulphonation level and type of cation employed. They found that there was no correlation between the cation charge or size and the change in T_g. It appeared that the level of sulphonation was the most important factor influencing the T_g.

The above examples of T_g's for different polymers were used to illustrate the following important conclusions, which form a basis for the investigation into ionomeric waxes:

- the change in peaks associated with ionic clustering will be at different minimum salt concentrations of the parent copolymer, thus implying that the type of anion and parent copolymer backbone all play a role in cluster formation
- it would be difficult to predict onset of cluster formation of an ionomeric wax, based on the above knowledge of shifts in T_g with onset of cluster formation
- DSC analysis is too insensitive to describe the relaxation peak associated with cluster formation alone. The DSC peaks are attributed to T_g's for the amorphous zones as well as for cluster formation.

2.6.3 Rheological properties

2.6.3.1 Introduction

The difference in rheology between the properties of an ionomeric compound and a non-ionised starting compound is a very good and sensitive method to indicate the effect of the chemical changes taking place when an ionomer in neutralised. There are many ways of measuring the rheology of an ionomer (below and above the melt temperature), where all the methods will still show the effect of neutralisation on the physical properties of the ionomer. Rheology does not explain the structure or morphology of a particular ionomer, but the rheological responses are used in conjunction with other techniques to corroborate theories.

The rheology is discussed separately from T_g measurements, as it forms a large part of this thesis. T_g measurements are based on rheological responses to mechanically induced stresses, but only describe a certain transition, and thus do not give a picture of an ionomer's response to time-temperature tests. These time-temperature tests give more information concerning the formation of multiplets and clusters.

The number of ionic groups existing in clusters is strongly dependent on the polarity of the polymer matrix, ionic functionality, and temperature [8-9, 72, 139, 154]. At low neutralisation percentages of an ionomer with a low polarity matrix, only multiplets are favoured, whereas with an increasing degree of neutralisation, cluster formation is favoured. When an ionomer is used with a higher degree of matrix polarity, then a progressively higher content of ionic groups is required in order to favour cluster formation. As the polarity of the matrix

increases, the degree of ionic functionality required for cluster formation increases substantially. TABLE 2.1 shows how the difference in the polarity of the matrix influences the onset of cluster formation[155].

TABLE 2.1
Critical ion concentration for onset of cluster formation [155]

Type of System	Mole % [a]
Polyethylene	1
Polystyrene	4-6
Poly(ethyl acrylate)	10-15
Poly(acrylic acid) with 20 wt % formamide	10-20
Na_2O-xSiO_2	ca. 20
Na_2O-xP_2O_5	Unclustered

[a] Approximate value

The rheological behaviour of ionomers offers convincing evidence that cluster formation or micro-phase separation has a significant impact on physical properties.

2.6.3.2 Specific examples below the melt temperature

An example to illustrate above statement ("the rheological behaviour of ionomers offers convincing evidence that cluster formation or micro-phase separation has a significant impact on physical properties"), is the superimposed time-temperature curves for poly(styrene-co-methacrylic acid) ionomers with a low ionic content (less than 6 mole percent) [156]. The implication is that there is no cluster formation below 6 mole % but only multiplet formation. Similar stress-relaxation data for samples with higher ion concentrations, greater than 6 mole %, could not be superimposed and a master curve describing the viscoelastic response over the entire region of time and temperature could not be constructed. The explanation given was that superposition could not be applied because at higher ionic contents a second relaxation mechanism occurs due to a change in structure.

The above non-conformance of ionomeric polymers with the WLF-equation (William, Landers and Ferry equation) is confirmed by work that was done by Broze et al [157]. They used a α,ω-dicarboxylato polybutadiene saponified with a magnesium salt, and investigated the dynamic mechanical behaviour of this halato telechelic polymer. The resulting master curve for the storage moduli was plotted and it was found that the shift factors (a_t) did not fit the WLF-equation. There was thus no linear relationship found when plotting $(T_0-T)/\log a_t$ versus $(T-T_0)$ where $T_0 = 302$ °K. The authors did however find that the shift factors correspond very well to an Arrhenius-type of temperature dependence. This dependence is shown in FIGURE 2.10 [157] below.

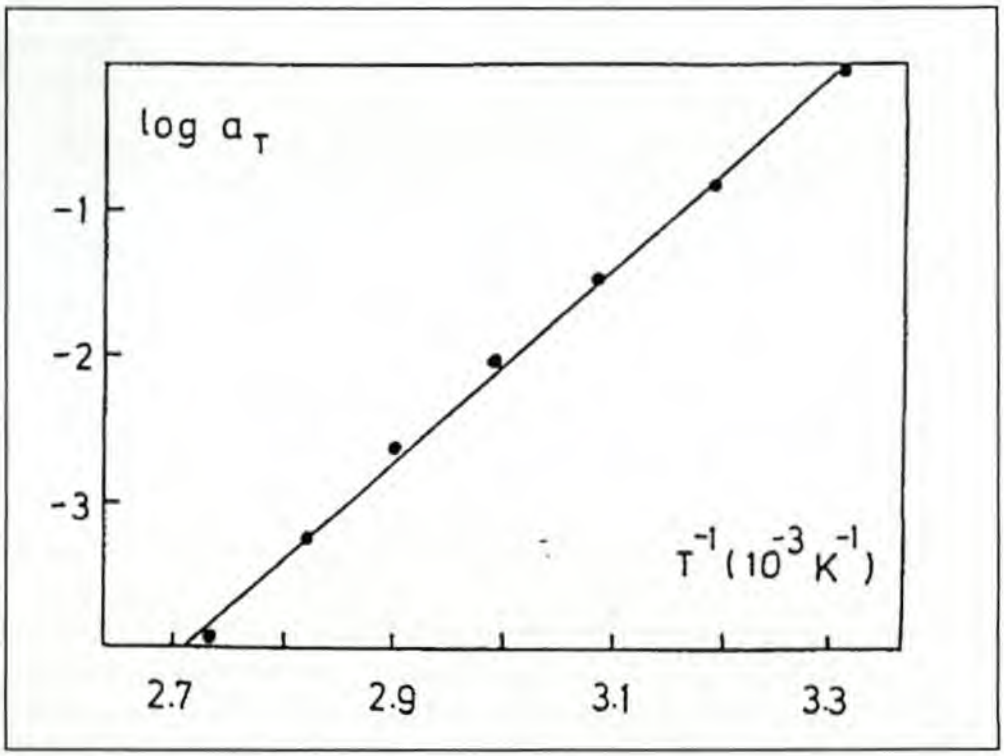

FIGURE 2.10 : Shift factors (a_T) versus 1/T for Mg-α,ω-dicarboxylato polybutadiene (ion content: 2 mole %)[157]

2.6.3.3 Specific examples for above the melt temperature

The viscosity of an ionomer decreases with an increase in shear stress. This is true for all high polymers. An example of an ionomer's viscosity response to an increase in the degree of neutralisation (for change in shear rate), is shown below in FIGURE 2.11 [158].

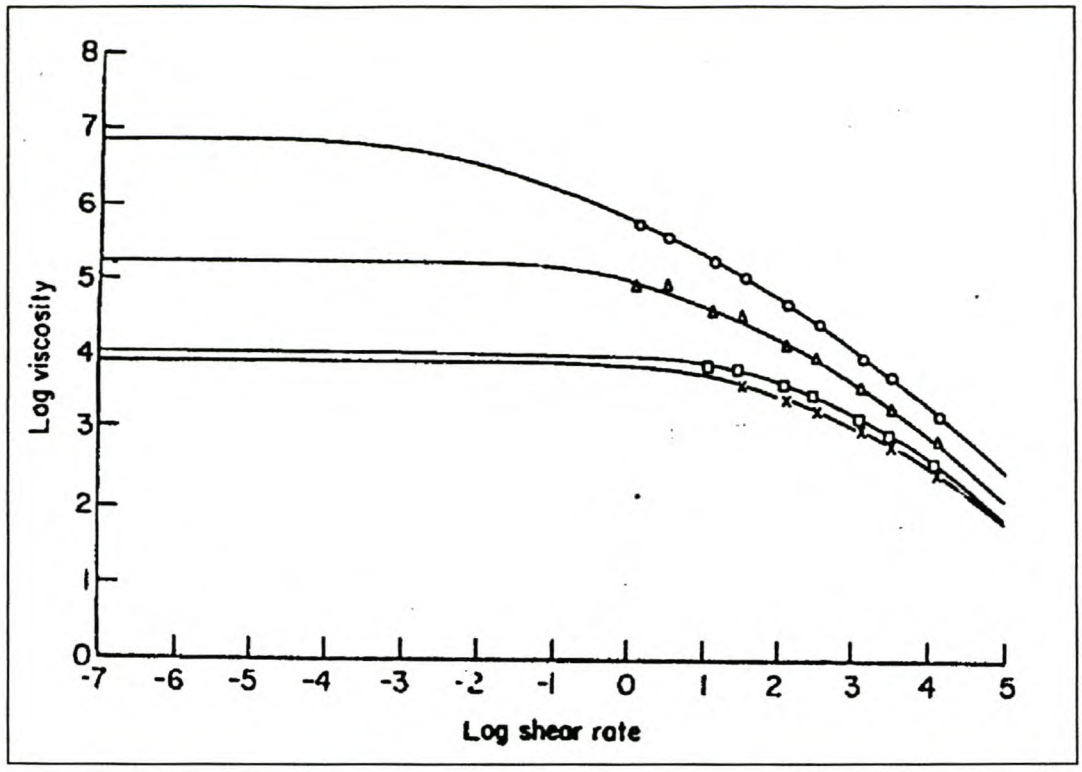

FIGURE 2.11 : Shear rate dependent viscosities of an ethylene-methacrylic acid copolymer (3.5 mole % acid) at various degrees of neutralisation, 160 °C. % Neutralisation: (×) 0; (□)10;(Δ)50;(○)100[158]

The data points used in the graph shown above were used to calculate the parameters of the following empirical equation **(1)** [158] :

$$\log(\eta_{(\gamma)}/\eta_0) = Q(\log \gamma\tau)^2 \quad (\gamma \geq 1/\tau) \qquad (1)$$

where :

η_0 = zero stress or Newtonian viscosity

$\eta_{(\gamma)}$ = shear rate dependent non-Newtonian viscosity at shear rate γ

τ has dimension of time

and for $\gamma < 1/\tau$, $\eta_{(\gamma)} = \eta_0$

The parameters were calculated by linear multiple regression analysis. The value for η_0 was obtained by differentiation. The parameter values were used to calculate the curves shown in the above figure. The above graph shows that there is a large increase in the low shear rate viscosity with an increasing degree of neutralisation, but that the effect is much less at higher shear rates [72]. We can therefore conclude that there is a breakdown in some flow unit in the ionomer at a high shear rate so that the behaviour corresponds more closely to that of the non-ionised copolymer.

It can be seen from the above that rheology is an important parameter for quantifying the onset of multiplet and cluster formation.

2.6.4 Strength of ionomeric polymers

The strength of ionomers is mostly expressed in terms of their tensile strength and strain, although there are obviously many other ways of expressing strength such as toughness, modulus, flexibility, deformation modes [83] etc., depending on the typical end use or one's perspective of what is the most important change occurring during and after reactions with different cations. Some observations follow concerning the effect of ionomerisation on polymers with respect to the change in their strength.

The neutralisation of acid copolymers has the effect of increasing the viscosity and the ultimate tensile strength and of decreasing the elongation at break. This is illustrated in TABLE 2.2[159].

TABLE 2.2
Properties of ionomers and polyethylenes [159]

Properties	ASTM tests	Ionomers		Polyethylenes	
		Surlyn A[a]	HXQD-2137[b]	Low-density	High-density
Melt Index, 44 psi (190°C)	D 1238-52T	0.3-10.0	1.6	1.5	5.0
Density, 23°C/4°C, g/cm^3	D 1505-57T	0.93-0.94	0.955	0.920	0.960
Secant modulus of elasticity at 1% strain, psi	D 882-61T	28 000-40 000	50 000	23 000	150 000
Tensile strength, psi	D 882-61T	3 500-5 500	3 600	1 800	4 600
Yield strength, psi	D 882-61T	2 000-2 500	1 925	1 200	4 200
Elongation, %	D 882-61T	300-400	425	600	15% at yield
Brittleness temperature, 20% failure	D 746-55T	< -160°C	-105°C	-80°C	-70°C
Tensile impact (23°C), ft-lb/in.^{3}	D 1822-61T	150-400	413	388	54
Stress-crack resistance (50°C, Igepal)	D 1693-60T		no failure, 500 h	50 % failures, 24 h	

[a] Dupont, [b] Union Carbide

The above table shows that the tensile strength is increased by neutralisation of the ionomer, and the melt index is reduced.

A graphical representation of how typical ionomers perform during stress strain tests is shown below in FIGURE 2.12 [160].

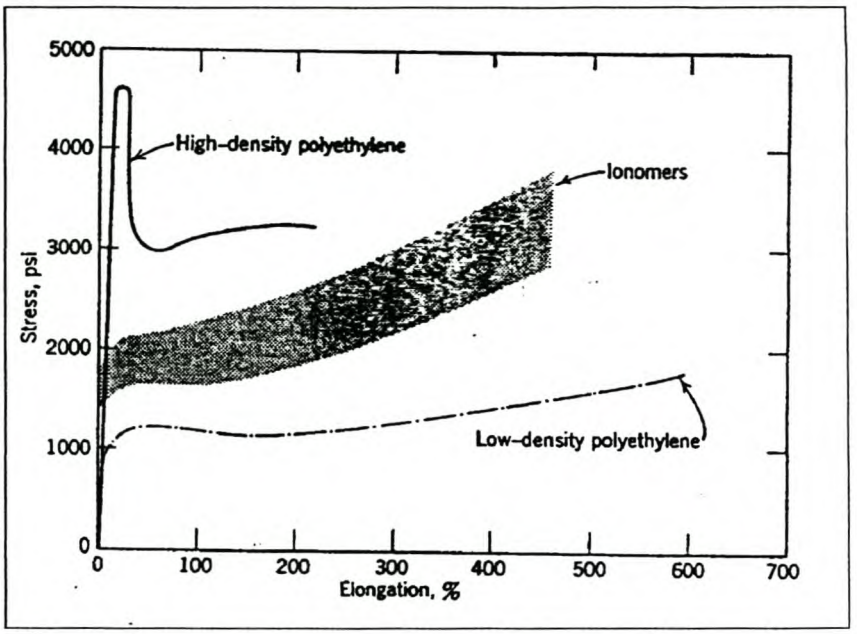

FIGURE 2.12 : Stress-strain curves of ionomers and polyethylene at 23 °C [160]

Mohajer, et al. [161] looked at the influence of excess neutralising agent on the mechanical properties of three-arm star polyisobutylene-based model ionomers. They found that excess neutralising agent increased the tensile strength and postulated that the excess neutralising agents are retained within the multiplets/clusters formed, up to a certain concentration, after which the salts will show phase separation and crystallise out to act as fillers.

Hara, et al. [162] also looked at the effect of excess neutralising agent in a sulphonated polystyrene ionomer with respect to fatigue behaviour. They found that the fatigue behaviour of an ionomer with excess neutralising agent was better than the same ionomer with no excess neutralising agent. They postulated that the better fatigue properties were due to the presence of small particles (1 μm to 5 μm in size), which enhanced resistance to crack propagation.

2.6.5 Effect of cation

2.6.5.1 Introduction

The role that the independent cations, used to neutralise the ionomers, play in the physical and chemical characteristics of ionomers, is described in this section.

2.6.5.2 Mechanical properties

The role that the cation plays with respect to physical properties of the ionomer is varied, as illustrated by TABLE 2.3 [124].

TABLE 2.3
Flow behavior of ethylene-acrylic acid copolymer salts [124]

	Control	Low conversion to salt				
		Na^+	K^+	Li^+	Ca^{2+}	Mg^{2+}
% Ionised	0	30	25	28	30	37
Melt Index[a]	67	3.8	4.5	5.2	3.1	2.5
		High conversion to salt				
		Na^+	K^+	Li^+	Ca^{2+}	Mg^{2+}
% Ionised	0	66	63	67	63	64
Melt Index[a]	67	0.3	0.6	0.2	0.1	0.2

[a] ASTM D1238 @ 190 °C

The above values for melt index show that there is actually not much difference between the different salts tested, especially at high salt conversions. It thus appears from the above results that either the melt index is not sensitive enough to show differences in physical properties or there are no differences, irrespective of the cation, between these particular copolymers.

The effect of cations on the viscosities and physical properties of metal sulphonated EPDM (ethylene-propylene diene-monomers) is shown in TABLE 2.4 [76]. Only zinc and lead decrease the apparent viscosity at 200 °C significantly. The other cations, both monovalent and divalent, cause very high apparent viscosities.

TABLE 2.4 [a]
Effect of cation on flow and physical properties of sulphonated EPDM [76]

Metal	Apparent viscosity [b], mPa.s [c]	Melt fracture at shear rate, Hz	Melt Index @ 190°C, 3.3 MPa [d], 10g/min.	Tensile strength, MPa [d,e]	Elongation [d,e]
Hg	Disintegrated				
Mg	55	< 0.88	0	2.2	70
Ca	53.2	< 0.88	0	2.8	90
Co	52.3	< 0.88	0	8.1	290
Li	51.5	< 0.88	0	5.2	320
Ba	50.8	< 0.88	0	2.3	70
Na	50.6	< 0.88	0	6.6	350
Pb	32.8	88	0.1	11.6	480
Zn	12	147	0.75	10.2	400

[a] Sulphonate content : 32 meq/100 EPDM; [b] At 200°C and 0.88 s^{-1}; [c] To convert mPa.s to centipoise, divide by 1000; [d] To convert MPa to psi, multiply by 145; [e] At 25°C

The effect of various cations on an ethylene-methacrylic acid ionomer's physical properties is shown in TABLE 2.5 [163]. Monovalent, divalent and trivalent cations enhance the physical properties when compared to the original starting copolymer.

TABLE 2.5.
Influence of cation on ethylene-methacrylic acid ionomer properties [163]

	Methacrylic acid	Na^+	Li^+	Ba^{2+}	Mg^{2+}	Zn^{2+}	Al^{3+}
Anion		CH_3O^-	OH^-	OH^-	CH_3COO^-	CH_3COO^-	CH_3COO^-
% Ionised		4.8	2.8	9.6	8.4	12.8	14.0
Properties							
Melt Index, 10 g/min.	5.80	0.03	0.12	0.19	0.12	0.09	0.25
Yield point, MPa[b]	6.1	13.2	13.1	13.4	15.0	13.2	7.1
Elongation, %	553	330	317	370	326	313	347
Ultimate tensile strength, MPa[b]	23.4	35.8	33.9	33.9	40.4	29.7	22.0
Stiffness, MPa[b]	68.9	190.3	206.8	223.4	164.1	208	103.4
Visual transparency	Hazy	Clear	Clear	Clear	Clear	Clear	Clear

[a] 10 wt % methacrylic acid; [b] To convert MPa to psi, multiply by 145

Broze, Jerome and Teyssie [29] used a halato-telechelic polymer as a model compound to try and determine what effect the various variables such as cations, percentage neutralised, etc., would have on the physical characteristics of these model ionomers. A carboxy-telechelic polybutadiene (CTPBD) polymer commercially available from BF Goodrich as Hycar CTB, was neutralised with various cations. FIGURE 2.13 [29] shows that if one keeps the η_{rel} value constant at 3 ($\log \eta_{rel} = 0.48$), then for Mg (ionic radius = 0.65 Å) a concentration of 1.12 g/dL was observed, for Ca (ionic radius = 0.99 Å) a concentration of 1.25 g/dL was observed and for Ba (ionic radius = 1.35 Å) a concentration of 1.48 g/dL was observed. These results are in agreement with equation (**2**).

$$f = (e_A e_C)/(\varepsilon r^2) \qquad (2)$$

where f (the attractive force) between anion (e_A) and cation (e_C), varies inversely with both the dielectric constant (ε) and the square of their distance (r). For the above values, f does thus increase as r decreases. The non-correlation of Cu (ionic radius = 0.69 Å) and Mn (ionic radius = 0.8 Å) to equation (**2**) is ascribed to the less ionic and more coordinating character of these cations.

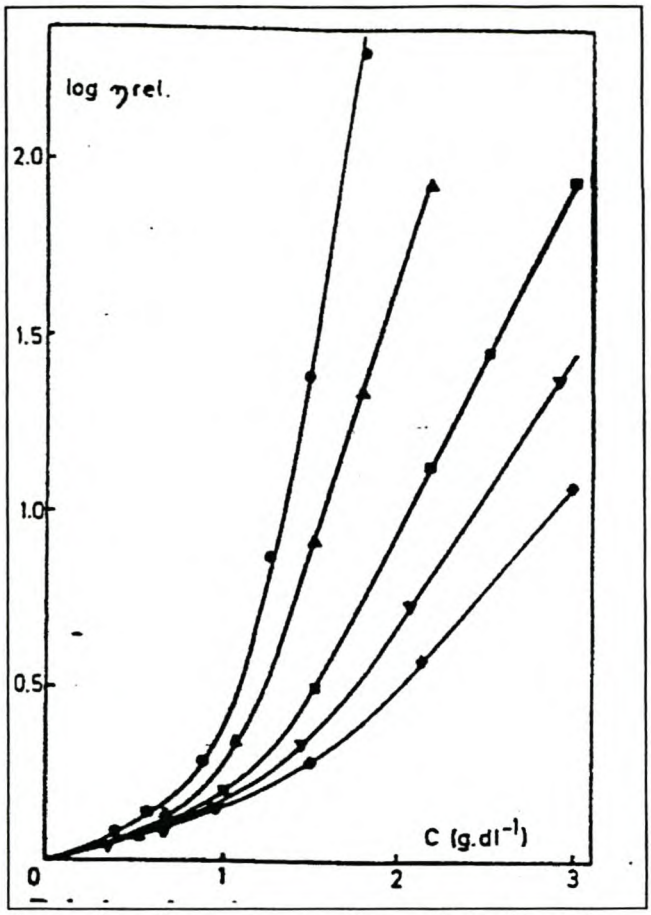

FIGURE 2.13 : Relative viscosity-concentration plots in toluene at 25°C for α,ω–carboxylated-polybutadiene containing different metal ions: (●) Mg ; (▲) Ca ; (■) Ba ; (▼) Cu ; (◆) Mn[29]

The above results show that the effect of the type of cation varies depending on the property measured. Lefelar and Weiss [164] found that with carboxylated ionomers, the packing within anion layers is determined by the cation. Small divalent cations give denser packing. In sulphonated ionomers, the anion packing is independent of the counterion.

To understand the influence of the cations, it is necessary first to look at the complete system and the properties measured. Only then can conclusions be drawn.

2.6.6 Melting point

2.6.6.1 Introduction

The melting point of ionomers is an important physical characteristic, in that this parameter really distinguishes this class of molecules from the normal covalently cross-linked polymers. The ionomers appear to exert a reversible cross linking effect, although this cross linking effect cannot morphologically be directly associated with the normal covalently-

cross-linked polymers (see Section 2.5 Morphological models). The melting point of an ionomer is obviously not only dependent on the ionomeric character of the polymer but also dependent on such factors as hydrogen bonding, molecular mass, van der Waals' bonds and crystallinity. When ionomers do melt, the melting point (T_f) will be dependent upon the ratio of the heat of fusion (ΔH_f) to the entropy of fusion (ΔS_f) ($T_f = \Delta H_f/\Delta S_f$) and the melting point may vary over a wide range.

Disrupting crystallinity in crystallised ionomers results in, over a limited range, lowering of the melting point. The crystalline character of the starting material is thus an important factor to consider before the possible melting point after ionisation can be predicted. This would be especially true for F-T ionomeric waxes, which exhibit a high degree of crystallinity before oxidation. Examples of the influence of crystallinity and ionisation percentage on melting points are shown in TABLE 2.6[148].

TABLE 2.6
Melting points and crystallinities of ethylene-metal acrylate copolymers [148]

COOH/ 100 CH_2	Molar % acid	Acid copolymer melting point (°C)	Na salt		Mg salt	
			Melting point (°C)	Crystallinity	Melting point (°C)	Crystallinity
0.66	1.32	107	99	24	95	18
1.57	3.14	101	95	18	92	< 5
2.26	4.52	98	93	11	Infusible	
2.78	5.56	96	91	< 5	Infusible	

The melting points of the sodium and magnesium salts are lower than the acid copolymer and the original starting material polyethylene. Both the crystallinity and the melting points are lowered with increasing cation concentration. The effect of magnesium on lowering the melting point is greater than that of sodium, although at higher magnesium concentrations the ionomers become infusible, while at the same concentration the sodium salts still melt. The above data can be represented by Flory's copolymer crystallisation equation **(3)**:

$$1/T_m - 1/T^\circ_m = - R/\Delta H_0 \ln N \qquad \textbf{(3)}$$

where:

T_m is the melting point of the copolymer

T°_m is the melting point of the homopolymer

ΔH_0 is the heat of fusion of the homopolymer crystals

N is the fraction of crystallised units.

2.6.7 The effect of plasticisers on ionomers

There have been many articles published on the effect of plasticisers on ionomers [46,52, 120, 143, 165-168]. Properties such as mechanical properties and rheological properties are compared with and without plasticisers, firstly to see the influence of the plasticiser, and secondly to try and deduce the morphology of the ionomers. Many types of ionomers and plasticisers have been tested. I will describe a few of these articles concentrating on the effect of moisture as I later examine the influence of water on ionomers, specifically with regard to diffusion and sorption.

2.6.7.1 The effect of water on ionomers

The effect of moisture on the T_g of poly(styrene-co-methacrylic acid) is described by Kim and Eisenberg [169]. They found that for a polymer containing 3.6 mole % ions, neutralised with sodium, even very small amounts of moisture change the tan δ peak associated with the clusters formed while the matrix peak (polymer backbone peak) is unchanged. They also showed however that the activation energies of the cluster phase are independent of the moisture content. A summary of their results is given in TABLE 2.7 [169]. Kim and Eisenberg's results agree with the findings of Tong and Bazuin [166] where for a poly(ethyl acrylate)-based ionomer plasticised with various amounts of 4-decylaniline, the activation energies for the two glass transitions remained constant. Kim et al. [170] also noted that for a sodium-sulphonated polystyrene ionomer mixed with sodium dodecylbenzene sulphonate, the activation energies for the two T_g's remained constant.

TABLE 2.7
Moisture effect on the matrix peak and cluster peak T_g's and apparent activation energies [169]

Moisture content (%)	Matrix peak			Cluster peak			E_a (kJ/mol)	
	$T_{g,m}$ (°C)	Width @ ½ height (°C)	Area (°C)	$T_{g,c}$ (°C)	Width @ ½ height (°C)	Area (°C)	Matrix phase	Cluster phase
0	128	16	22	184	40	17	530 ± 16	220 ± 15
0.04	127	15	23	173	37	11	520 ± 4	240 ± 7
0.16	129	16	22	181	29	7	500 ± 27	230 ± 10

Villeneuve and Bazuin [171] and Tachino, et al. [172] looked at the influence of plasticisers on various ionomers. Tachino, et al. aged the ionomers, saponified with various cations, at 50% relative humidity for two years, before immersing them in water for a week. They then analysed the different ionomers for stiffness and changes in their respective DSC thermograms. A summary of their results is given in TABLE 2.8 [172].

TABLE 2.8
Changes of DSC thermograms and stiffness upon water immersion [172]

Ionomer	Water content (Wt %)	Stiffness (MPa)	ΔH_i (J/g)	ΔH_M (J/g)
EMAA-0.6Na	0.69[a]/2.24[b]	477[a]/246[b]	16[a]/9[b]	44[a]/38[b]
EMAA-0.6K	1.27/3.47	331/152	17/8	54/43
EMAA-0.6Mg	0.23/0.45	399/391	20/20	19/20
EMAA-0.6Zn	0.09/0.16	404/399	15/14	54/59

[a] before and [b] after water immersion at 293 K for a week.
EEMAA-0.6 Na refers to poly(ethylene-co-methacrylic acid) neutralised with a cation (Na, K, Mg, Zn) to 60% of its acid value.
ΔH_i and ΔH_m refer to the heat of fusion for the ionomeric clusters and the crystallisation region respectively.

The table indicates that the sodium and potassium neutralised samples show a relatively large increase in water content and a corresponding change in stiffness and ΔH_i. The ΔH_m values do not change significantly, irrespective of the cation used for neutralisation (the slight reductions of the ΔH_m for Na and K neutralised samples are ascribed to erratic readings caused by peaks around 380 Kelvin which are due to the release of water). The

authors conclude that certain salts are more prone to water absorption and that the water only affects the ionic aggregates, leaving the crystalline regions unchanged.

Makowski, et al. [173] prepared various metal sulphonated ethylene-propylene-diene terpolymers (EPDM) and tested these ionomers for melt viscosities, physical characteristics and water absorption. They found that if the same base polymer is used and only the type of cation is varied, barium absorbed the most water and lead the least. The graph for water absorption versus immersion time is shown in FIGURE 2.14 [173].

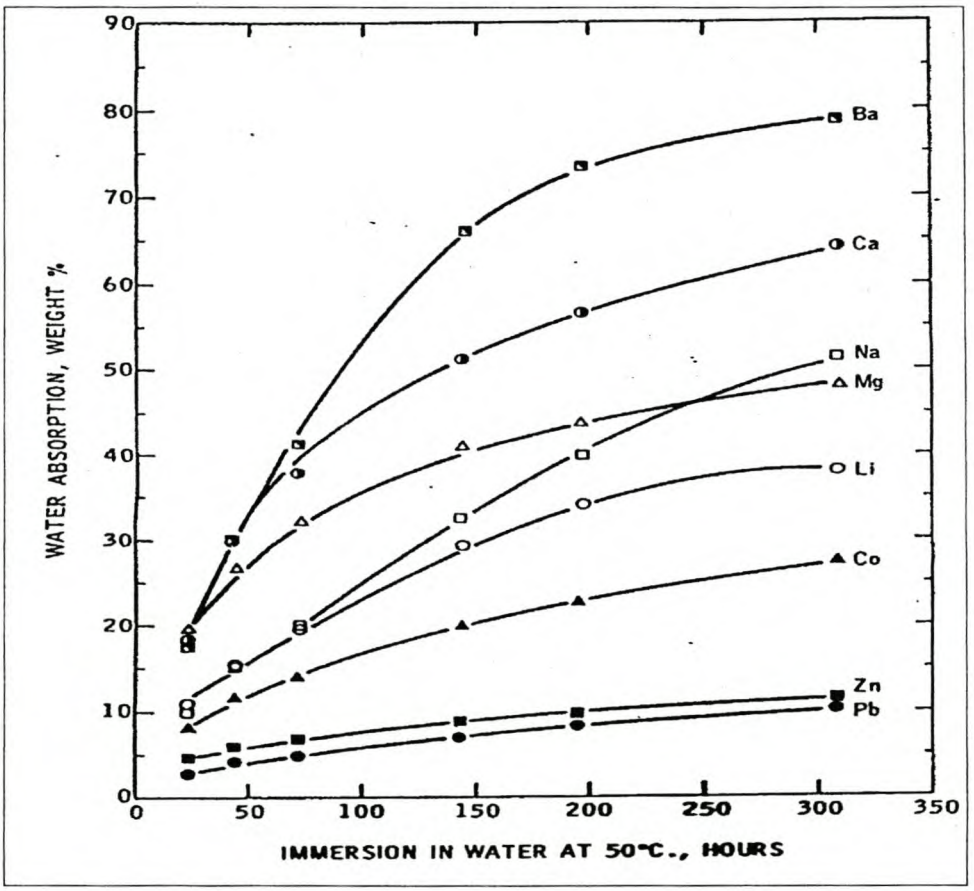

FIGURE 2.14 : Effect of cation on water absorption of sulphonated EPDM terpolymers [173]

Bagrodia, et al. [174], prepared a sulphonated polyisobutylene telechelic ionomer [81] and neutralised the ionomer with calcium, potassium and zinc. They found that the polyisobutylene structure was not very susceptible to water absorption, but that there was still a difference between the different cations used in the sense that the water absorption increased from zinc to calcium to potassium. The relative rate of absorption for the cations tested by Bagrodia et al., agrees with the other authors stated above.

2.7 Fischer-Tropsch wax oxidation

2.7.1 Introduction

This part of the thesis examines literature describing the F-T wax as well as the mechanism of oxidation for hydrocarbons.

2.7.2 Definition of waxes

The word or term 'wax' has evolved from the Anglo-Saxon word 'weax'. Weax was the name given to the material obtained from the honeycomb of the bee. For many years there was no general definition, which could categorise waxes. In 1953, a definition was formulated by the Deutsche Gesellschaft für Fettwissenschaft [175], based on the physical properties of waxes. The definition is given as:

"Wax is a collective technological term for a series of natural or synthetic substances that as a rule have the following properties:

> Can be solid, pliable to hard, brittle at 20°C, coarse to fine crystalline, translucent to opaque but not glassy; melt above 40°C without decomposition, having a relatively low viscosity just above its melting point, cannot be drawn to threads; consistency and solubility strongly dependent upon temperature; can be polished under slight pressure".

The above definition is quite a broad definition and certainly describes most waxes, but I prefer to stick to my own definition of waxes, that is:

> Waxes are generally classified as low molecular mass polymers, which have a higher molecular mass than oligomers and a lower molecular mass than polymers.

2.7.3 History of Fischer-Tropsch waxes

Waxes have also been classified as natural, mineral and synthetic waxes. Natural waxes can be waxes such as beeswax, spermaceti wax (obtained from the head cavities and the bladder of the sperm whale), wool wax, vegetable waxes, candelilla wax, carnauba wax, etc. Mineral waxes are waxes derived from coal in various stages of development. One of these is montan wax, which is obtained by solvent extraction of lignite of brown coal. Other

mineral waxes include paraffin wax, ozocerite wax, ceresin wax, utah wax and peat wax. The main synthetic waxes in commercial use today are F-T and polyethylene waxes.

F Fischer and H Tropsch did research at the Kaiser-Wilhelm Institute (for coal research), later named the Max-Planck Institute, in Muehlheim/Ruhr, in the 1920's. The process, which is named after the two researchers, utilises coke or brown coal and steam to form water gas. The water gas contains, among other things, 6% carbon dioxide, 40% carbon monoxide and 50% hydrogen. The refined water gas is used at elevated temperatures and, with a suitable catalyst, forms aliphatic hydrocarbons. Initially Fischer and Tropsch worked at atmospheric pressure and ca. 200°C to produce the full spectrum of hydrocarbons from methane to hard waxes (waxes with melting points above 100°C). The catalysts used consisted initially of nickel and later mostly of cobalt.

In the years after 1950, the F-T plants operating in Germany and the plants in the USA were shut down due to the high cost of coal. In South Africa though, where no oil could be found and large coal resources were available, the construction of a plant utilising the F-T process, was started in 1953. The fixed bed process is still in operation today.

2.7.4 Products produced at Schümann Sasol through Fischer-Tropsch synthesis

Three main groups of hydrocarbon waxes are produced at Schümann Sasol through the F-T synthesis:

- Hard waxes with melting points above 70°C
- Medium waxes with melting points in the region of 40°C to 60°C
- Liquid paraffins or waxes with melting points below 40°C

This thesis focuses on the hard waxes and I will thus concentrate on these waxes. The Schümann Sasol hard waxes are the bottom distillates from reactor wax where the lighter material is removed by distillation. The wax Paraflint H2 (further referred to as H2), forms the basis of the hard waxes. H2 is further distilled to give products with narrower molecular mass distributions. These products are called Paraflint C105 and Paraflint C80 (further referred to as C105 and C80). The physical properties of H2, C105 and C80 are given below in TABLE 2.9

TABLE 2.9

Physical properties of waxes H2, C105 and C80

Properties	Test method	H2	C105	C80
M_n (Average molecular mass, g/mole)	High temperature GPC [176]	656	1008	541
M_w (Average molecular weight, g/mole)	High temperature GPC [176]	785	1180	564
M_z (g/mole)	High temperature GPC [176]	1003	1458	589
P_d (polydispersity)	High temperature GPC [176]	1.2	1.1	1.0
Iso content (%)	HTGC [177]	2.80	1.19	3.02
Congealing point (°C)	ASTM D 938	98	103	82
Needle penetration @ 65°C (10^{-1} mm)	ASTM D 1231	21	6	44
Viscosity @ 120°C (cPs)	Brookfield, no.1 spindle	12	20	5

The C105 wax is a harder wax than H2 wax, with a higher average molecular mass. The waxes oxidised from C105 for this thesis were, WAX 6 (acid value of ca. 6 mg KOH/g), WAX 16 (acid value of ca. 16 mg KOH/g) and WAX 28 (acid value of ca. 28 mg KOH/g). WAX 6 and WAX 16 were manufactured in the laboratory for use in this thesis, while WAX 28 is manufactured commercially. I used only C105 based oxidised waxes to saponify as these waxes have not been well documented and the narrower cut C105 would possibly give a more consistent product. I will elaborate on the oxidation procedure later in this chapter.

2.7.5 Hard wax uses

The H2, C80 and C105 waxes are used in polishes, in plastics to enhance gloss, in colour dispersions, in candles to improve hardness and finish, in insulation, in can coatings, in carton coatings, in anti-blocking agents, in PVC lubricants, in components for electrical cables, in paper conversion, in chewing gums, in carbon paper backing, in printing inks, in paints, in wax crayons, in hot melt adhesives and as lubricants in the rubber industry, in washing machines and in plastic mouldings.

2.7.6 Structure of Fischer-Tropsch waxes

It is necessary to understand the structure of the non-oxidised F-T waxes before it is possible to understand what happens when these waxes are oxidised. A description of the possible structure of F-T waxes follows.

The production methods of F-T waxes had been well documented before 1960 [178-185] but there was very little work that had been done to explain the structure of the waxes formed from F-T synthesis. Le Roux [186] described the structure of waxy material to be a type I or a type II wax, where a type I wax is a highly crystalline wax and a type II wax is essentially an amorphous material. The two classes described, type I and type II, are seen as extreme cases. Many waxes however would fall into an intermediate class between these two extreme classes. Le Roux utilised IR (infra red) spectrometric analysis, average molecular mass measurements, needle point hardness tests, density measurements, melting points and X-ray diffraction analysis and concluded that a type I wax consists of crystallites which are thick plates. Disorder regions occur, called defects, within the plates. The so-called defects occur due to ends of chains, end of branches and kinks. The amount or volume of these defects has a pronounced effect on the properties of the wax. Waxes are of type I if their molecules do not differ too much from each other, so that they can crystallise out together. Type I waxes are defined as waxes [187-188] where the differences between molecules are so small that three dimensional crystal growth is not hindered. There is no experimental evidence[187-188] of the existence of an amorphous matrix in type I waxes. Plastic deformations in type I waxes are due to the following factors:

- molecular movement within crystallites
- boundary migration helped by the existence of defects
- slip promoted by the presence of crystallites of different sizes

The above third type of mechanism is further promoted by the presence of a liquid layer (very low molecular mass wax) absorbed to the crystallites. All the above factors are probably influenced by molecular mass distribution.

Type II waxes and intermediate waxes are waxes where the crystal structure has been disrupted by either extensive branching (microcrystalline waxes) or where atoms other than carbon and hydrogen are present (oxidised waxes). The viscosity of the matrix, the thickness of the crystallised plates, and the relative amount of the two phases present would determine the properties of a type II wax. The differences between the molecules in type II waxes severely limit crystal growth. Due to the inhibition of new molecular layers to crystallites, the crystallites tend to be thin plates. There is also experimental evidence [187-188] of a highly viscous amorphous matrix. Type II plastic deformations are based on the viscous flow of the amorphous matrix and bending of crystallites.

The waxes used in this thesis are typical type I waxes with a high degree of linearity and low percentage branching. H2 waxes have ca. 98 % linear content and ca. 2 % iso content. C105 has ca. 99 % linear content and ca. 1 % iso content, while C80 has ca. 96 % linear content and ca. 4 % iso content. Thus, due to the high linearity, one would expect essentially linear by-products on oxidation, as there is a very low degree of branching. The oxidation of waxes is more fully discussed in the next section.

2.8 Oxidation of hydrocarbons

2.8.1 Introduction

This section gives a review of the oxidation of hydrocarbons in general. There is not much literature available on the oxidation of F-T waxes [189-190], and the basic chemical mechanisms, which would explain non-F-T hydrocarbon oxidation, should in theory be the same for F-T reactions. Although hydrocarbon reactions have been studied for well over a hundred years, the mechanisms have only been understood for less than 50 years [191-197].

The oxidation of straight chain hydrocarbons containing 20 to 25 carbon atoms (C20-C25), leads to the formation of fatty acids of various molecular weights, beginning in practice from formic acid and ending with the same number of carbon atoms as the initial paraffin. This mixture of acids can be distilled to obtain the "soap fatty acids" with 12 to 18 carbons (C12-C18) and then used in the manufacture of synthetic soaps, which are practically equivalent in detergent action to soaps from animals and vegetable fats and oils [198].

There are obviously two methods of oxidising hydrocarbons, that is, in the vapour phase and the liquid phase. As the oxidation of F-T waxes takes place in the liquid phase, I will only be discussing the liquid phase oxidation of hydrocarbons. The history of hydrocarbon oxidation will be discussed first.

2.8.2 The history of oxidation of hydrocarbons

Approximately twenty five years after the discovery of paraffin wax, Hofstädter [199] was the first to study the oxidation of paraffin wax with nitric acid. Hofstädter obtained reaction products such as butyric acid, valeric acid and succinic acid using the above oxidation method. Gill and Meusel [200] obtained larger oxidation fragments by oxidation with chromic acid.

Engler and Boch [201], established the formation of water soluble fatty acids while studying the oxidation of paraffin wax in air. Schaal [202], was the first to realise the commercial importance of the oxidation reactions and he was granted a patent on the "Process for the oxidation of petroleum and similar hydrocarbons to acids and for the manufacture of soaps and esters of these acids". Schaal [202] was already utilising accelerators such as alkali, but the process was not fully optimised, giving products of low quality.

The company, D Fanto at Pardubitz [203] was the first company to industrialise the process for the oxidation of paraffin wax. At first the oxidation at 130°C to 135°C took weeks to complete, but the process was refined by adding mercury oxide, which shortened the oxidation process to days.

The research of Grün and Ulbrich [204] showed the important influence of the oxidation temperature and the airflow rate on the reaction products of air oxidation. The products prepared on a technical scale were still dark in colour and had an unpleasant smell, but upon saponification, soaps were produced which had a satisfactory foaming action and a considerable detergent activity.

In 1921 the Badische Anilin-und Sodafabrik produced several tons of synthetic fatty acids in an experimental plant in Oppau [205]. In 1931 I.G. Farbenindustrie together with Standard Oil Co. of New Jersey constructed a large experimental plant at Baton Rouge to oxidise petroleum paraffin wax. In 1934, the companies Henkel und Co. of Dusseldorf and Märkishe Seifenindustrie of Witten, later combined in the Deutsche-Fettsäure-Werke, began their investigations on the oxidation of F-T-Rurhchemie synthesised slack paraffin wax.

In America and the former Soviet Union, paraffin wax from crude distilled oil had been the main starting material for oxidation, while in Germany, lignite paraffin wax was mainly used until the slack wax from the F-T-Ruhrchemie synthesis became available.

2.8.3 Mechanism of oxidation

The chemistry of the mechanism of oxidation has been described in many articles [206-229]. The oxidation of hydrocarbons is very complex and there are several sequences of reactions taking place simultaneously, which can affect one another.

Zerner [230] found that two different peroxides are formed during oxidation. One of the peroxides reacts with potassium iodide and sulphuric acid with the liberation of iodine while

the other decolourises indigo sulphuric acid and, only after hydrolysis, liberates iodine immediately with potassium iodide because of the formation of hydrogen peroxide [231-233].

Rieche [234] gave the first clearly acceptable mechanism for the liquid oxidation of hydrocarbons. He assumed the initial reaction to be the formation of an alkyl hydroperoxide produced by the insertion of molecular oxygen between a carbon atom and hydrogen atom, shown below in equation **(4)**.

$$R_1CH_2\text{-}\underset{\displaystyle H}{\underset{|}{CH}}\text{-}CH_2R_2 + O_2 \Rightarrow R_1CH_2\text{-}\underset{\displaystyle OOH}{\underset{|}{CH}}\text{-}CH_2R_2 \qquad \textbf{(4)}$$

Rieche at that stage was not sure how the alkyl hydroperoxide was formed, but Emanual [214] describes the initial reactions during autoxidation of hydrocarbons as (equation **5** to **13**):

$$RH + O_2 \Rightarrow R^{\cdot} + HO^{\cdot}{}_2 \qquad \textbf{(5)}$$

$$2RH + O_2 \Rightarrow 2R^{\cdot} + H_2O_2 \qquad \textbf{(6)}$$

$$R\cdot + O_2 \Rightarrow RO^{\cdot}{}_2 \qquad \textbf{(7)}$$

$$RO\cdot_2 + RH \Rightarrow ROOH + R^{\cdot} \qquad \textbf{(8)}$$

The alkyl hydroperoxide can now rearrange into a semi-acetal, which then decomposes into aldehydes and ketones. The reaction products formed can now also take part in further reactions.

$$RO^{\cdot}{}_2 \Rightarrow RCOH + RO^{\cdot} \qquad \textbf{(9)}$$

$$RO^{\cdot}{}_2 + ROOH, ROH, RCOR \Rightarrow R^{\cdot} + \text{products} \qquad \textbf{(10)}$$

$$R^{\cdot}, RO^{\cdot}, O^{\cdot}H + RH \Rightarrow RH, ROH, H_2O + R^{\cdot} \qquad \textbf{(11)}$$

$$ROOH \Rightarrow \text{products (molecular decomposition)} \qquad \textbf{(12)}$$

$RO^{\cdot}_2 + RO^{\cdot}_2 \Rightarrow$ products **(13)**

A summary of the reactions is shown schematically below in FIGURE 2.15.

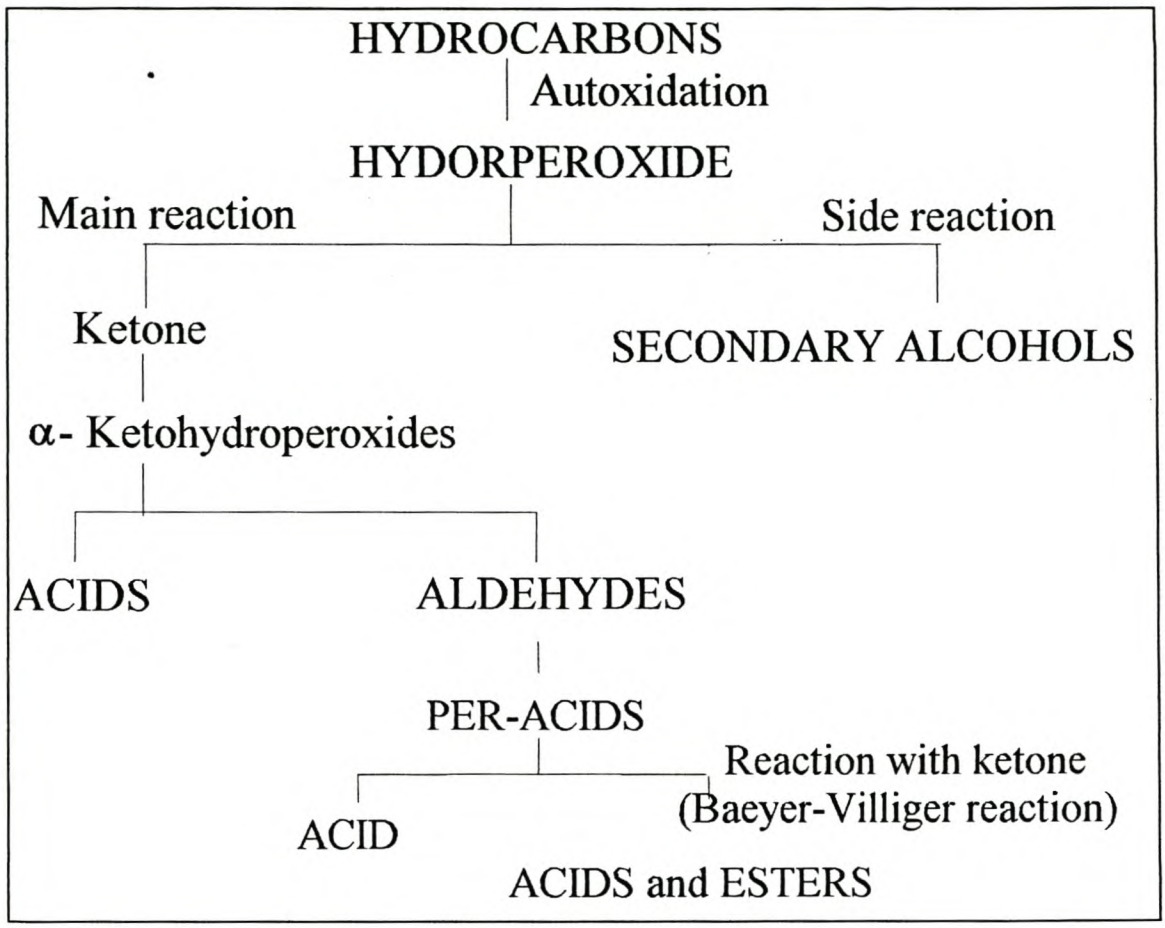

FIGURE 2.15 : Schematic diagram of oxidation reactions of hydrocarbons

It is evident from the above that various end products are formed where equations **4** to **8** are seen as initiation reactions, equations **9** to **11** as propagation reactions and equations **12** to **13** as termination reactions.

Oxidation of hydrocarbons thus produces substances such as acids, esters, lactones, alcohols, ketones and aldehydes, of which the acid groups and to a lesser extent the esters can be saponified, to be utilised in the formation of ionomeric waxes.

2.9 References

1. Eisenberg A, King M, **Ion-Containing Polymers, Physical Properties and Structures, Polymer Physics**, Volume 2, Academic Press, New York, pp5, 1977
2. Eisenberg A, King M, **Ion-Containing Polymers, Physical Properties and Structures, Polymer Physics**, Volume 2, Academic Press, New York, pp7, 1977
3. Allan J R, Wood I J, **Plast. Rubber Compos. Process. Appl.**, 23(5), pp339, 1995
4. Holliday L, **Ionic Polymers,** Applied Science Publishers LTD, Essex, England, pp5, 1975
5. Hoover M F, **Polymer Preprints**, 10, pp908, 1969
6. Otocka E P, **J. Macromol. Sci. Revs. Macromol. Chem.**, C5(2), pp275, 1971
7. Holliday L, **Chemistry and Industry**, 23, pp921, 1972
8. MacKnight W J, Earnest T R, **J. Macromol. Sci. Polym. Technol. Rev.**, 16, pp41, 1981
9. Bazuin C G, Eisenberg A, **Ind. Eng. Chem. Prod. Res. Dev.**, 20, pp271, 1981
10. Longworth R, **Developments in Ionic Polymer I,** Applied Science Publishers Ltd., Chapter 3, 1983
11. MacKnight W J, Lundberg R D, **Rubber Chem. Technol**, 57(3), pp652, 1984
12. MacKnight W J, Earnest T R, **J. Macromol. Sci. Polym. Technol. Rev.**, 16, pp42, 1981
13. Eisenberg A, **Inorg. Macro. Rev.**, 1, pp75, 1970
14. Michaels A S, **Ind. Eng. Chem.**, 57, pp32, 1965Dolezal T, Edwards D C, Wunder R H, **Rubber World**, 158, pp46, 1968
15. Rembaum A, Baumgartner W, Eisenberg A, **J. Polym. Sci.**, B66, pp159, 1968
16. Noguchi H, Rembaum A, **Polymer Preprints**, 10, pp718, 1969
17. Hadek V, Noguchi H, Rembaum A, **Polymer Preprints**, 12, pp90, 1971
18. Gibbs C F, Marvel C S, **JACS**, 56, pp725, 1934
19. Kern W, Brenneissen E, **J. Prakt. Chem.**, 159, pp193, 1941
20. DesMarteau D D, **J. Flourine Chem.**, 72(2), pp203, 1995
21. Ravodski Y F, Neksavov A K, YenikoloPyan N S, **Polym. Sci., USSR**, 13, pp2226, 1971
22. Kennedy J P, Storey R F, Mohajer Y, Wilkes G L, **Proc. IUPAC, Macro 82**, Amherst, Massachusetts, pp905, 1982
23. Kennedy J P, Ross L R, Lackey J E, Nuyken O, **Polym. Bull.**, 4, pp67, 1981
24. Kennedy J P, Storey R F, **Am. Chem. Soc., Prepr. Div. Org. Coat. Appl. Polym. Sci.**, 46, pp182, 1982
25. Bagrodia S, Mohajer Y, Wilkes G L, Storey R F, Kennedy J P, **Polym. Bull.**, 9, pp174, 1983
26. Bagrodia S, Mohajer Y, Wilkes G L, **Polym. Bull.**, 8, pp281, pp1982
27. Broze G, Jerome R, Teyssié P, **Macromolecules**, 14, pp224, 1981
28. Broze G, Jerome R, Teyssié P, **Macromolecules**, 15, pp920, 1982

29. Bagrodia S, Pisipati R, Wilkes G L, Storey R F, Kennedy J P, **J. Appl. Polym. Sci.**, 29, pp3065, 1984
30. Broze G, Jerome R, Teyssié P, Gallot B, **J. Polym. Sci. Polym. Lett. Ed.**, 19, pp415, 1981
31. Reed S E, **J. Polym. Sci.**, Pt. A-1 9, pp2147, 1971
32. Schultz D N, Sandra J C, Willoughby B G, **ACS Symposium Series 166,** American Chemical Society, Washington D.C., 27, pp427, 1981
33. Broze G, Jerome R, Teyssié P, Marco C, **Polym. Bull. Berlin**, 4, pp241, 1981
34. Fitzgerald J J, Weiss R A, J. **Macromolecules, Sci., Rev. Macromol. Chem. Phys.**, C28, pp100, 1988
35. Velichkova R S, Christova D C, **Prog. Polym. Sci.**, 20(5), pp819, 1995
36. Holliday L, **Ionic Polymers,** Applied Science Publishers LTD, Essex, England, Chap. 1, pp8, 1975
37. Yeager H L, Eisenberg A, Eds., **Perflourinated Ionomer Membranes,** ACS Symp. Ser., (American Chemical Society, Washington), pp187, 1982
38. Fujimura M, Hashimoto T, Kawai H, **Macromolecules**, 15, pp136, 1981
39. Salamone J C, Tsai C C, Olson A P, Watterson A C, **J. Polym. Sci.**, A1, 18, pp2983, 1982
40. Salamone J C, Watterson A C, Hsu T D, Tsai C C, Mahmud M U, **J. Polym. Sci., Lett. Ed.**, 15, pp487, 1977
41. Salamone J C, Watterson A C, Hsu T D, Tsai C C, Mahmud A W, Wisniewski A W, Israel S C, **J. Polym. Sci. Polym. Symp.**, 64, pp229, 1978
42. Salamone J C, Tsai C C, Olson A P, Watterson A C, **Am. Chem. Soc. Polym. Div. Polym. Prepr.**, 19(2), pp261, 1978
43. Zhulina E B, Birshtein T M, Borisov O V, **Macromolecules**, 28, pp1491, 1995
44. Köberle P, Laschewsky A, **Macromol. Symp.**, 88, pp165, 1994
45. Galin M, Mathis A, Galin J, **Macromolecules**, 26, pp4919, 1993
46. Eisenberg A, Lennox R B, Desjardins, Zhu J, **Macromolecular Reports**, A31 (Suppls. 6&7), pp755, 1994
47. Lu X, Steckle W P Jr., Hsiao B, Weiss R A, **Macromolecules**, 28, pp2831 1995
48. Lundberg R D, Makowski H S, **Am. Chem. Soc.**, pp 21, 1980
49. Hird B, Eisenberg A, **Macromolecules**, 25, pp6466, 1992
50. Pfeiffer D G, Weiss R A, Lundberg R D, **J. Polym. Sci., Polym. Phys. Ed.**, 20, pp1503, 1982
51. Bazuin C G, Eisenberg A, **J. Polym. Sci., Part B, Polym. Phys.**, 24, pp1151, 1986
52. Lundberg R D, Makowski H S, **Advances in Chemistry Series**, 187(2), pp21, 1980
53. Rees R W, **Polym. Prepr. Am. Chem. Soc. Div. Polym. Chem.**, 14, pp796, 1973

54. Rees R W, **United States Patent,** No. 3 404 134, 1968

55. Rees R W, **United States Patent**, No. 3 471 460, 1996

56. Fan X-D, Bazuin C G, **Macromolecules**, 28, pp8216, 1995

57. Fan X-D, Bazuin C G, **Macromolecules**, 28, pp8209, 1995

58. Brown H P, **Rubber Chem. Technol. 30**, pp 1347, 1957

59. Longworth R, Morawetz H, **J. Polym. Sci.**, 29, pp307, 1958

60. Wisbrun K F, **Macromol. Chem.**, 118, pp211, 1968

61. Sanui K, Lenz R W, MacKnight W J, **J. Polym. Sci. Polym. Chem. Ed.**, 12, pp1965, 1974

62. Holliday L, **Ionic Polymers,** Applied Science Publishers LTD, Essex, England, Chap. 3, pp173, 1975

63. Warner R R, **Rubber Age**, 71, 2, pp205, 1952

64. Delf B W, MacKnight W J, **Macromolecules**, 2, pp309, 1969

65. MacKnight W J, **Polym. Prepr. Am. Chem. Soc. Div. Polym. Chem.**, 11, pp504, 1970

66. Otocka E P, Eirich F R, **J. Polym. Sci.**, Part A-2, 6, pp921, 1968

67. Otocka E P, Hellmann M Y, Bleyler L L, **J. Appl. Phys.**, 40, pp4221, 1969

68. Eisenberg A, **Macromolecule**, 3, pp147, 1970

69. Eisenberg A, **J. Polym. Sci. Polym. Symp.**, 45, pp99, 1974

70. Eisenberg A, Navratil M, **Macromolecules**, 6, pp604, 1973

71. Rees R W, Vaughn D J, **Polym. Prepr. Am. Chem. Soc. Div. Polym. Chem.**, 6, pp296, 1965

72. Ward T C, Tobolsky A V J, **Appl. Polym. Sci.**, 11, pp2403, 1967

73. Rees R W, **Mod. Plastics**, 42, pp209, 1964

74. Gierke T D, **"Perflourinated Ionomer Membranes", ACS Symposium Series, No. 180**, American Chemical Society, Washington, D.C., 1982

75. Makowski H S, Lundberg R D, Westerman L, Bock J, **Advances in Chemistry Series No. 187**, pp3, 1980

76. Makowski H S, Lundberg R D, Singhal G S, **United States Patent**, No. 3 870 841, 1975

77. Ukihashi H, Hamabe M, **"Perflourinated Ionomer Membranes", ACS Symposium Series, No. 180,** American Chemical Society, Washington, D.C., 17, pp427, 1982

78. Zutty N L, Faucher J A, Bonotto S, **Encyclop. of Polym. Science and Engineering,** Second Edition, Vol. 6, pp 429, 1983

79. Lachaise J, Mendiboure B, Dicharry C, Marion G, Bourrel M, Cheneviere P, Salager J L, **Colloids and Surfaces**, A, pp190, 1995

80. Metha V P, Heda L C, Dass D, **Tenside Surfactants Detergents**, 32(1), pp61, 1995

81. Maynard J T, Johnson P R, **Rubber Chem. Technol.**, 36, pp882, 1963

82. Mehrotha K N, Lata R, Kumar A, **Rev. Roum. Chim.**, 39(5), pp517, 1994

83. Sugihara E, Yokote S, Hoshino M, Iwata I, Todoroki H, Sasaki M, Ogawa C, Masuda K, **Eur. Pat. Appl.** EP 661 341, 1995

84. Kuhne H, Düren H B, **Kunststoffe - German Plastics**, 75(1), pp18, 1985

85. Kim Y, Ha C-S, Cho W-J, **Pollimo**, 18(5), pp737, 1994

86. Cooper W, **J. Polym. Sci.**, 28, pp195, 1958

87. Mandal U K, Tripathy D K, De S K, **Polym. Eng. Sci.**, 36(2), pp283, 1996

88. Padilla A, Vasquez A, **J. Mater. Res.**, Vol. 6, No. 11, pp2452, 1991

89. Kennedy J P, Ross L R, Lackey J E, Nuyken O, **Polym. Bull.**, 4, pp67, 1981

90. Ma X, Sauer J A, Hara M, **Macromolecules**, 28, pp3954, 1995

91. Bagrodia S, Tant M R, Wilkes G L, Kennedy J P, **Polymer**, 28, pp2210, 1987

92. Fetters L J, Balsara N P, Huang J S, Jeon H S, Almdal K, Lin M Y, **Macromolecules**, 28, pp4996, 1995

93. Galo C T, Elizabeth S C, Luis H T D, Int. **J. Polym. Mater.**, 26, pp62, 1994

94. Xie H-Q, Ao Z-P, Guo J-S, **J. Macromol. Sci. Phys.**, B34(3), pp249, 1995

95. Weiss R A, **ASTM Spec. Tech. Publ.**, STP 1249(Assignment of the Glass Transition), pp214, 1994

96. Yoshikawa K, Desjardins A, Dealy J M, Eisenberg A, **Macromolecules**, 29, pp1235, 1996

97. Carraher C E Jr, He F, Sterling D, **Polym. Mater Sci. Eng.**, 72, pp114, 1995

98. Rajagopalan P, Tsatsas A T, Risen W M Jr, **J. Polym. Sci., Polym. Phys. Ed.**, 34(1), pp151, 1996

99. Ng C-W A, Lindway M J, MacKnight M J, **Macromolecules**, 27, pp3027, 1994

100. Loveday D, Wilkes G L, Deporter C D, McGrath J E, **Macromolecules**, 28, pp7822, 1995

101. Broze G, Jerome R, Teyssié P, **Macromolecules**, 15, pp920, 1982

102. Watkins J M, Spangler R D, McKannan E C, **J. Applied Phys.**, 27, pp685, 1956

103. MacKnight W J, Kajiyama T, McKenna, L W, **Polym. Eng. Sci.**, 8, pp267, 1968

104. Agarwal P K, Makowski H S, Lundberg R D, **Macromolecules**, 13, pp1679, 1980

105. Eisenberg A, King M, Navratil M, **Macromolecules**, 6, pp734, 1973

106. Eisenberg A, King M, Navratil M, **Macromolecules**, 7, pp90, 1974

107. Fitzgerald W E, Nielsen L E, **Proc. Roy. Soc.**, A282, pp137, 1962

108. Ogura K, Sabue H, Nakamura S, **J. Polym. Sci., Polymer Physics**, 11, pp2079, 1973

109. Pineri M, Meyer C T, Levelut A M, Lambert M, **J. Polym. Sci. Polym. Phys. Ed.**, 12, pp115, 1974

110. Phillips P J, MacKnight W J, **Polymer Letters**, 8, pp87, 1970

111. Eisenberg A, Hird B, Moore B, **Macromolecules**, 23, pp4098, 1990

112. Mauritz K A, **Macromol. Sci. Rev. Macromol. Chem. Phys.**, C28, pp99, 1988

113. Ma X, Sauer J A, Hara M, **Macromolecules**, 28, pp3961, 1995

114. Forsman W C, **Macromolecules**, 7, pp1032, 1982

115. Dreyfus B, **Macromolecules**, 18, pp284, 1985

116. Datye V-K, Taylor P L, **Macromolecules**, 7, pp90, 1974

117. O'Connell E M, Root T W, Cooper S L, **Macromolecules**, 28, pp4000, 1995

118. Yamauchi J, Narita H, Kutsumizu S, Yano S, **Macromol. Chem. Phys.**, 196(2), pp3919, 1995

119. Van Alsten J G, **Macromolecules**, 29, pp2163, 1996

120. MacKnight W J, Taggart W P, Stein R S, **J. Polym. Sci. Polym. Symp.**, 45, pp113, 1974

121. Davis H A, Longworth R, Vaughn D J, **Am. Chem. Soc. Polym. Prepr.**, 9, pp515

122. Holliday L, **Ionic Polymers,** Applied Science Publishers LTD, Essex, England, Chap. 2, pp79, 1975

123. Bonotto S, Bonner E F, **Macromolecules**, 1, pp514, 1968

124. Longworth R, Vaughan D J, **Am. Chem. Soc. Polym. Prepr.**, 9, pp525, 1968

125. Marx C L, Caulfield D F, Cooper S L, **Macromolecules**, 6, pp344, 1973

126. MacKnight W J, Taggart W P, Stein R S, **J. Polym. Sci. Polym. Sym.**, 45, pp 113, 1974

128 Guinier A, Fornet G, **Small Angle Scattering of X-Rays,** Wiley, New York, Chapter 2, 1955

129. Porod G, **Colloid Z**, 124, pp83, 1951

130. Pineri M, Meyer C T, Bourret A, **J. Polym. Sci. Polym. Phys. Ed.**, 13, pp1881, 1975

131. Meyer C T, Pineri M, **J. Polym. Sci. Polym. Phys. Ed.**, 13, pp1057, 1975

132. Meyer C T, Pineri M, **J. Polym. Sci. Polym. Phys. Ed.**, 16, pp569, 1978

133. Tsagaropoulos G, Kim J-S, Eisenberg A, **Macromolecules**, 29, pp2222, 1996

134. Tsagaropoulos G, Eisenberg A, **Macromolecules**, 28, pp396, 1995

135. Visser S A, Cooper S L, **Polymer**, 33 (22), pp4705, 1992

136. Visser S A, Cooper S L, **Polymer**, 33 (18), pp3790, 1992

137. Eisenberg A, **Polymer Preprints**, 14, pp871, 1973

138. Ma X, Sauer J A, Hara M, **Macromolecules**, 28, pp3953, 1995

139. Nishida M, Eisenberg A, **Macromolecules**, 29, pp1507, 1996

140. Otocka E P, Kwei T K, **Macromolecules**, 1, pp401, 1968

141. Loveday D, Wilkes G L, Deporter C D, McGrath J E, **Macromolecules**, 28, pp7822, 1995

142. Takahashi T, Watanabe J, Minagawa K, Koyama K, **Polymer**, 35(26), pp5722, 1994

143. Nengu-Plesu R, Bazuin C G, **J. Polym. Sci., Part B, Polym. Phys.**, 29, pp1305, 1991

144. Boiteux G, **Structure and Properties of Ionomers**, Pineri M, Eisenberg A, Editors, NATO ASI Series, D Riedel Publishing Co., Dortrecht, pp227, 1987

145. Eisenberg A, Navratil M, **J. Polym. Sci.**, B10(7), pp537, 1972

146. Navratil M, Eisenberg A, **Macromolecules**, 7, pp84, 1974

147. Rees R W, Vaughn D J, **J. Am. Chem. Soc. Polym. Prepr.**, 6, pp287, 1965

148. Otocka E P, Kwei T K, **Macromolecules**, 1, pp244, 1968

149. Otocka E P, Kwei T K, **Macromolecules**, 2, pp110, 1969

150. MacKnight W J, McKenna L W, Read B E, **J. Appl. Phys.**, 38, pp4208, 1967

151. MacKnight W J, McKenna L W, Read B E, Stein R S, **J. Phys. Chem.**, 72, pp1122, 1968

152. McKenna L W, Kajiyama T, MacKnight W J, **Macromolecules**, 2, pp58, 1969

153. Yang S, Sun K, Risen W M Jr., **J. Polym. Sci., Part B: Polym. Phys.**, 28, pp1685, 1990

154. Shohamy E, Eisenberg A, **J. Polym. Sci. Polym. Phys.**, 14, pp1211, 1976

155. Eisenberg A, King M, **Ion-Containing Polymers,** Academic Press Inc., New York, pp16, 1977

156. Eisenberg A, King M, **Ion-Containing Polymers,** Academic Press Inc., New York, pp141, 1977

157. Broze G, Jerome R, Teyssié P, **Marco C, Polym. Bull. Berlin**, 4, pp243, 1981

158. Holliday L, **Ionic Polymers,** Applied Science Publishers LTD, Essex, England, Chap. 2, pp101, 1975

159. **Encyclopaedia of Polymer Science and Technology, Volume 6,** Intersience Publishers, John Wiley and Sons Inc., New York, pp 422, 1964

160. **Encyclopaedia of Polymer Science and Technology, Volume 6,** Intersience Publishers, John Wiley and Sons Inc., New York, pp 421, 1964

161. Mohajer Y, Bagrodia S, Wilkes G L, **J. Appl. Polym. Sci.**, 29, pp1943, 1984

162. Hara M, Jar P, Sauer J A, **Macromolecules**, 23, pp4969, 1990

163. Rees R W, **United States Patent**, No. 3 264 272, Aug. 2 1966

164. Lefelar J A, Weiss R A, **Macromolecules**, 17, pp1145, 1984

165. Vinci A, Cummings K, Lajoie M S, **International Patent,** No. 94/29256, 1994

166. Tong X, Bazuin C G, **J. Polym. Sci., Part B, Polym. Phys. Ed.**, 30, pp389, 1992

167. Weiss R A, Fitzgerald J J, Kim D, **Macromolecules**, 24, pp1064, 1991

168. Makowski H S, Lundberg R D, Singhal G H, **United States Patent**, No. 3870841, 1975

169. Kim J, Eisenberg A, **J. Polym. Sci., Part B, Polym. Phys.**, 33, pp200, 1995

170. Kim J, Roberts R J, Eisenberg A, Moore R B, **Macromolecules**, 26, pp5256, 1993

171. Villeneuve S, Bazuin C G, **Polymer**, 32, pp2811, 1991

172. Tachino H, Hara H, Hirasawa E, Kutsumizu S, Yano S, **J. Appl. Polym. Sci.**, 55(1), pp136, 1995

173. Makowski H S, Lundberg R D, Westerman L, Bock J, **Advances in Chemistry Series**, 187(1), pp17, 1980

174. Bagrodia S, Tant M R, Wilkes G L, Kennedy J P, **Polymer**, 28, pp2223, 1987

175. Lüdeke C, Gieser F, **Fette-Seifen-Anstrichm**, 56(3), pp153, 1954

176. The high temperature GPC method is summarised as follows:

Instrument	:	Waters 150C GPC
Columns	:	2 x Waters μ-Styragel 4E, molecular weight separation range 50 - 100 000 g/mole
Temperature	:	Pump compartment: 55 °C, Injector compartment: 100 °C, Column compartment:100 °C
Solvent	:	mobile phase, Xylene
Flow rate	:	1 mL/min
Detector	:	DRI
Sample concentration:		0.050% (m/m)
Injection volume:		200 μl
Analysis results:		Average of three analyses, standard deviation is ca. 28 g/mole
Data handling	:	Millennium 2010 Chromatography Manager Version 2.1
Calibration	:	Relative to n-alkane standards

177 The high temperature GC method is summarised as follows:

Scope and application

This method can analyse for hydrocarbons in the range C12 to C100 (C denotes carbon number). The separation of n-paraffins (n denotes normal) and i-paraffins (i denotes iso) up to C50 is possible, whereafter co-elution of the two species occurs.

Apparatus and requirements

Instrumentation	:	Varian gas chromatograph model 3410
Injector	:	Septum equipped, programmable
Detector	:	FID
Standard	:	Internal, n-C36

Column specifications

Length	:	12 m
Type	:	Bonded phase
Material	:	Aluminium clad
Phase	:	HTS (non-polar)

Film thickness	:	0.15 µm
Maximum temperature	:	460 °C
Inner diameter	:	0.53 mm
Outer diameter	:	0.78 mm

Instrumental conditions

Initial column temperature	:	60 °C
Hold time	:	5 minutes
Column ramp temperature	:	10 °C/minute
Final temperature	:	440 °C
Initial injector temperature	:	40 °C
Hold time	:	0 minutes
Injector ramp rate	:	70 °C/minute
Carrier gas	:	Hydrogen
Detector temperature	:	450 °C
Run time	:	54 minutes

Sample preparation

Dilution	:	0.1 g wax per 50 mL xylene with 1 g n-C36
Injection volume	:	1 µlitre

Calculations and reporting

The relevant concentration of each carbon number, expressed as normalised area percentage, is calculated from: $\% C_i = (A_i * 100) /$ total area

Where A_i = area of i-th hydrocarbon and C_i = i-th carbon number

178 Fischer F, Tropsch H, **German patent** 484337, 1929

179 Bridgewater R M, **Petroleum,** Lond., 8, No. 6, pp109, 1945

180 Fischer F, Tropsch H, **German patent** 411216, 1925

181 Fischer F, Tropsch H, **Ber. Deutsche. chem. Ges.**, 59, pp 832, 1926

182 Fischer F, Tropsch H, **German patent** 531004, 1931

183 Fischer F, Tropsch H, **German patent** 524468, 1931

184 Fischer F, **German patent** 571898, 1933

185 Alberts L, **French patent** 836273, 1939

186 Le Roux J H, Oranje S, **Fischer-Tropsch waxes,** Published by -SASOL one (PTY) LTD, P O Box 1, Sasolburg, 9570, Republic of South Africa, pp12, 1984

187 Le Roux J H, **S. Afr. J. Sci.**, 75, pp356, 1979

188 Le Roux J H, Loubscher N H, **S. Afr. J. Sci.**, 76, pp157, 1980

189 Breet E L J, Luyt A S, Oranje S, **S. Afr. J. Chem.**, 43 (3/4), pp 83, 1990

190 Breet E L J, Luyt A S, **S. Afr. J. Chem.**, 44 (4), pp 101, 1991

191 Semenov N, **Chemical Kinetics and Chain Reactions**, Oxford University Press, London, Eng., pp68, 1935

192 Bolland J L, **Q. Rev.** (London), 3, pp1, 1949

193 Bolland J L, Gee G, **Trans. Faraday Soc.**, 46, pp358, 1950

194 Bolland J L, Koch H P, **J. Chem. Soc.**, pp445, 1945

195 Bateman L, **Q. Rev.** (London), 8, pp147, 1954

196 Bateman L, Gee G, **Proc. R. Soc.** (London), A 195, pp376, 1948

197 Robertson A, Cooley S D, **Adv. Pet. Chem. Ref. III**, 42, pp201, 1946

198 Gensler W I, **Chem. Rev.**, 57, pp191-280, 1957

199 Hofstädter P G, **Liebigs Ann.**, 91, pp326, 1954

200 Gill C H, Meusel E, **J. Chem. Soc.** (London), 6 (2), pp466, 1868

201 Engler , Bock, **Ber. Deutsch. Chem. Ges.**, 12, pp2186, 1879

202 Schaal E, **German Patent** 32 705, 1884

203 Fanto D, **Swiss Patent** 82057, 1916

204 Grün A, Ulbrich E, **Z. Angew. Chem.**, 36, pp125, 1923

205 Wietzel G, **Z. angew. Chem.**, 51, pp531, 1938

206 Semenov N N, **Chim. et Industr.**, 79, pp 3-10, 1958

207 Knox J H, **Petroleum** (London), pp 435-438, Dec. 1958

208 Tripper C F H, **Ind. Chemist**, pp 335, 1959

209 Arndt R, Horn D H S, **South Afr. Industr. Chem.**, pp 136, 1957

210 Morton F, Bell R T T, **J. Inst. Petroleum**, 44, pp 260-272, 1958

211 Emanuel N M, **Oxidation Communications 2**, 3-4, pp 221-238, 1982

212 Kirk-Othmer, **Encyclopaedia of Chem. Tech.**, 2nd edition, Vol 11, pp 224-241, 1966

213 Artemiev R A, Spivac S I, **Rect. Kinet. Catal. Lett.**, Vol. 19, No. 1-2, pp 197-200, 1982

214 Emanual N M, Translated from Izvestiya Akademii Nauk USSR, **Seriya Khimicheskaya**, 5, pp 1056-1072, May 1974

215 Emanual N M, **World Petrol. Congr. Proc. 8th**, 4, pp 407-421, 1971

216 Nemes I, Danczy É, Vidczy T, Vasvári G, Gál D, **Symposium on the Mechanisms of Hydrocarbon Reactions**, Sifok, Hungary, pp 703-719, 5-7 June 1973

217 Howard J A, Ingold K U, **Can. J. Chem.**, 47(20), pp 3797-3801, 1969

218 Baldwin R R, Bennett J P, Walker R W, **Symp. Int. Combust. Proc.**, 16, pp 1041-1051, 1977

219 Turovskii A A, Kucher R V, Translated from Reaktsionnaya Sposobnost **Organicheskikh Soedinenii**, Vol. 5, No. 2, pp 288-296, April-June 1968

220 Howard J A, Ingold K U, **Can. J. Chem.**, 46(16), pp 2544-2660, 1968

221 Howard J A, Adamic K, Ingold K U, **Can. J. Chem.**, 46(20), pp 3739-3795, 1968

222 Howard J A, Chenier J H B, Holden D A, **Can. J. Chem.**, 56(2), pp 170-175, 1978

223 Howard J A, Chenier J H B, **Can. J. Chem.**, 58(24), pp 2808-2812, 1980

224 Adamic K, Howard J A, Ingold K U, **Can. J. Chem.**, 47(20), pp 3803-3808, 1969

225 Korcek S, Chenier J H B, Howard J A, Ingold K U, **Can. J. Chem.**, 50(14), pp 2285-2297, 1972

226 Zaikov G E, Howard J A, Ingold K U, **Can. J. Chem.**, 47(16), pp 3017-3029, 1969

227 Howard J A, Ingold K U, **Can. J. Chem.**, 46(16), pp 2661-2666, 1968

228 Howard J A, Schwalm W J, Ingold K U, **Advan. Chem. Ser.**, 75, pp 6-23, 1968

229 Howard J A, Ingold K U, **Can. J. Chem.**, 45(8), pp 785-792, 1967

230 Zerner, **Österr. Seifenfachbl.**, 2, pp141, 1930

231 Plissoff A K, Maleefa E, **Bull. Soc. Chim. France**, 3(5), pp 1281, 1936

232 Plissoff A K, **Bull. Soc. Chim. France**, 3(5), pp 1274, 1936

233 Plissoff A K, **Khim. Zh. Ser. A, Zh. Obshch. Khim.**, 9, pp 104, 1939

234 Rieche A, **Z. Angew. Chem.**, 50, pp520, 1937

CHAPTER 3: Fischer-Tropsch wax oxidation experimentation

This chapter describes the experimental work done at Schümann Sasol on oxidised wax, to gain a better understanding of the oxidised F-T wax, as well as the experimental waxes prepared for this thesis.

3.1 Oxidation of Fischer-Tropsch waxes

3.1.1 Introduction

This chapter is divided into three sections. The first section describes work done to see how the oxidation of F-T wax proceeds and to obtain a more fundamental understanding of the oxidation process. The second section describes the production of the three oxidised waxes used for the synthesis of ionomeric F-T waxes. The manufacture of grafted waxes is described in the third section.

3.1.2 Experimentation on the effect of oxidation temperature on the functionality of oxidised F-T waxes

This section describes the work done to identify the type of oxidised groups formed during uncatalysed oxidation of F-T waxes, and to determine the influence of oxidation temperature on the formation of the various groups. The results are then correlated with respect to the oxidation mechanism mentioned in the previous Chapter 2 and assumptions are made concerning the structure and reaction mechanism of the waxes used for further saponification and the formation of ionomeric waxes.

3.1.2.1 Experimentation

Two F-T hydrocarbon products produced at Schümann Sasol were oxidised and the formation of functional groups was monitored over a period of time to get a more fundamental understanding of the oxidation process. The two hydrocarbons were a liquid paraffin (C14-C17) and a hard wax called C80. The specifications of the unoxidised C14-C17 are given in APPENDIX 3.1.

The two products were oxidised in laboratory bubble reactors with a capacity of ca. 800 grams. A drawing of a typical reactor is shown below in Figure 3.1 [1].

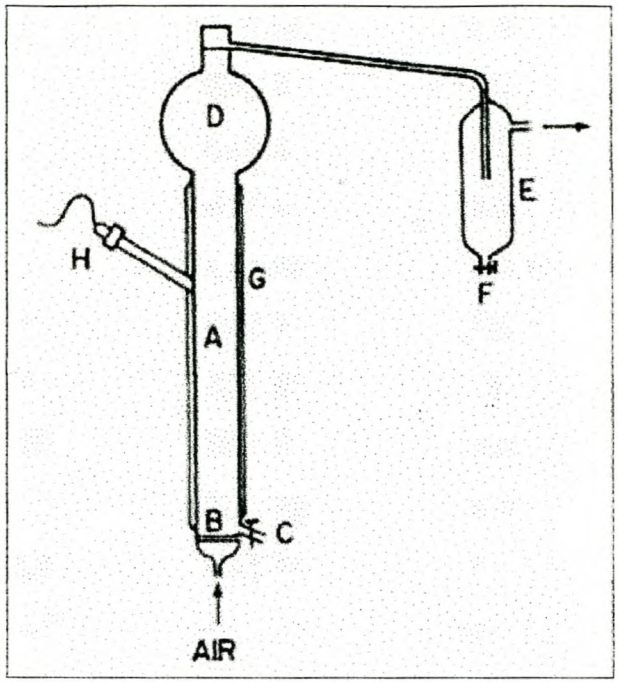

FIGURE 3.1 : Example of a bubble reactor. A. Glass reactor. B. Glass frit. C. Tap for withdrawing wax. D. Glass bulb to prevent mechanical loss of wax. E. Vessel to prevent pressure build up and trap of volatile components. F. Tap. G. Heated reactor. H. Thermocouple coupled to G to regulate temperature [1].

3.1.2.2 Results

The oxidation results for C14-C17 are shown in APPENDIX 3.2 and for C80 in APPENDIX 3.3. The oxidations were conducted at constant temperatures with no catalysts present and the flow rate of the air was kept constant at 2.3 litres/minute.

3.1.2.3 Discussion

The results of APPENDIX 3.2 are depicted graphically in FIGURES 3.2 to 3.4 shown below.

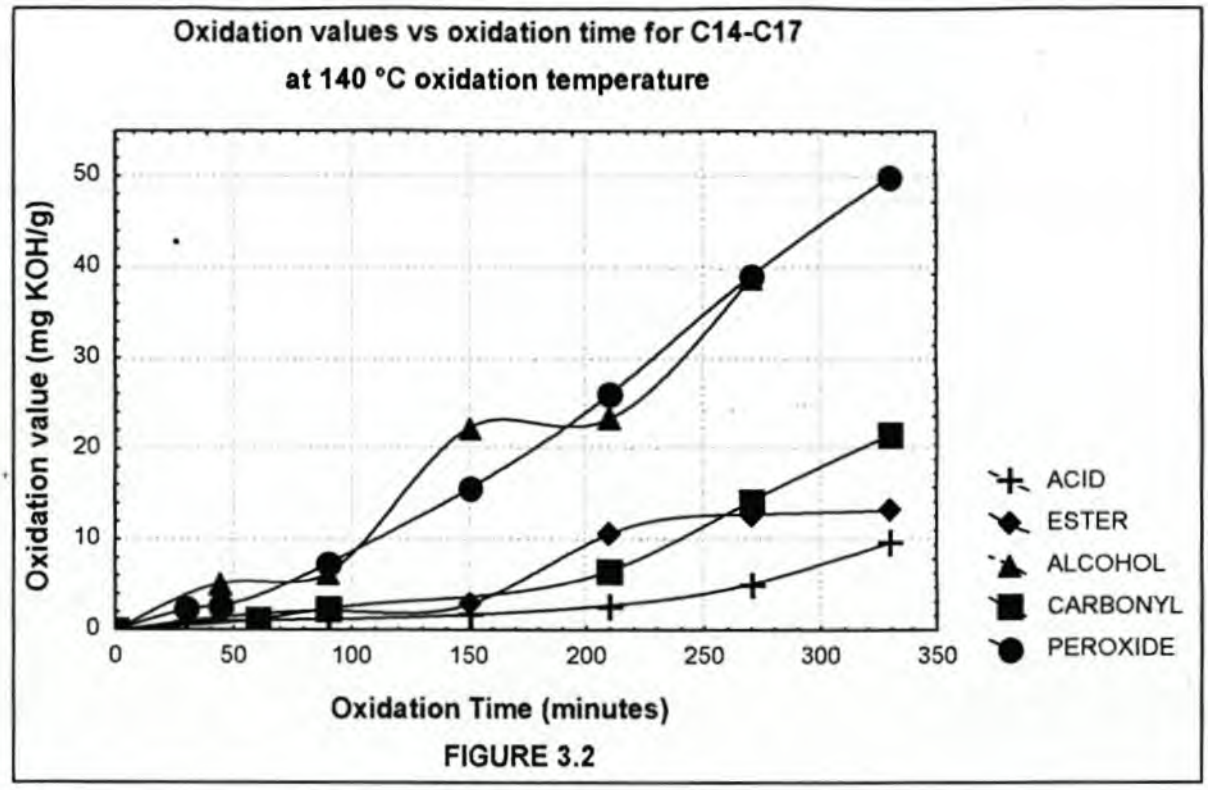

FIGURE 3.2

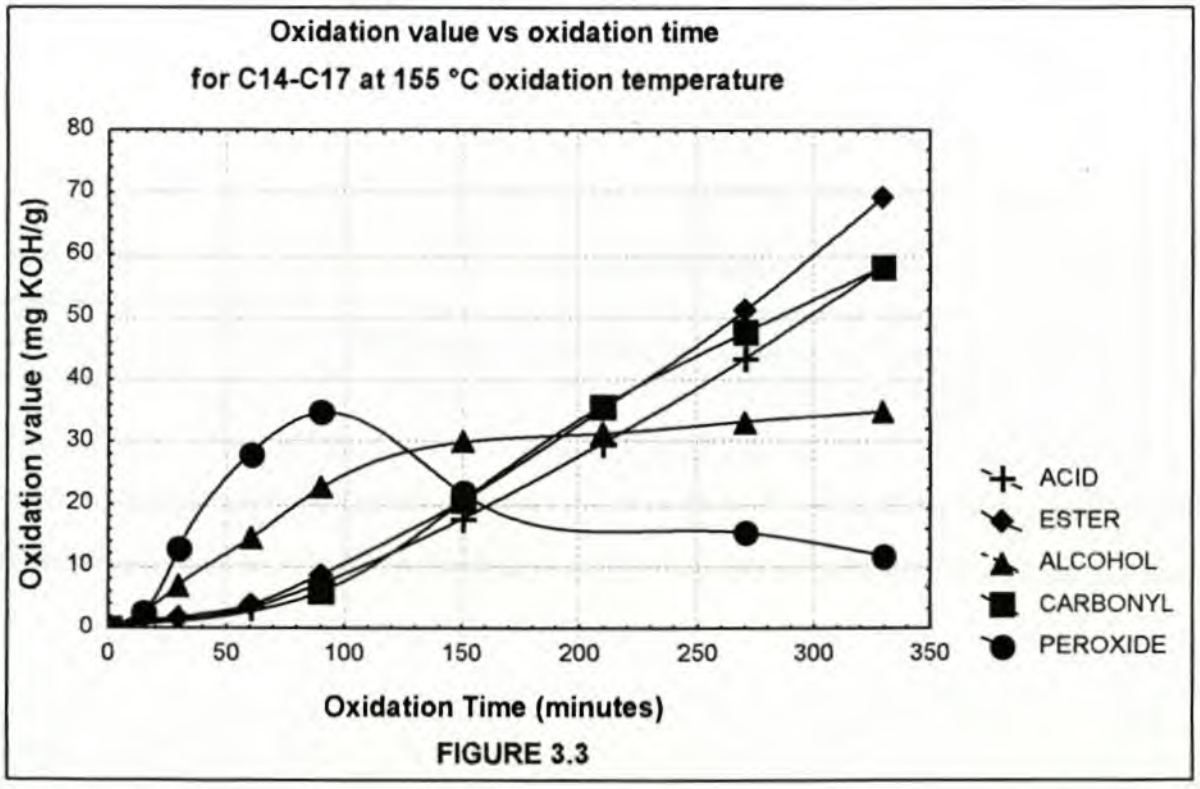

FIGURE 3.3

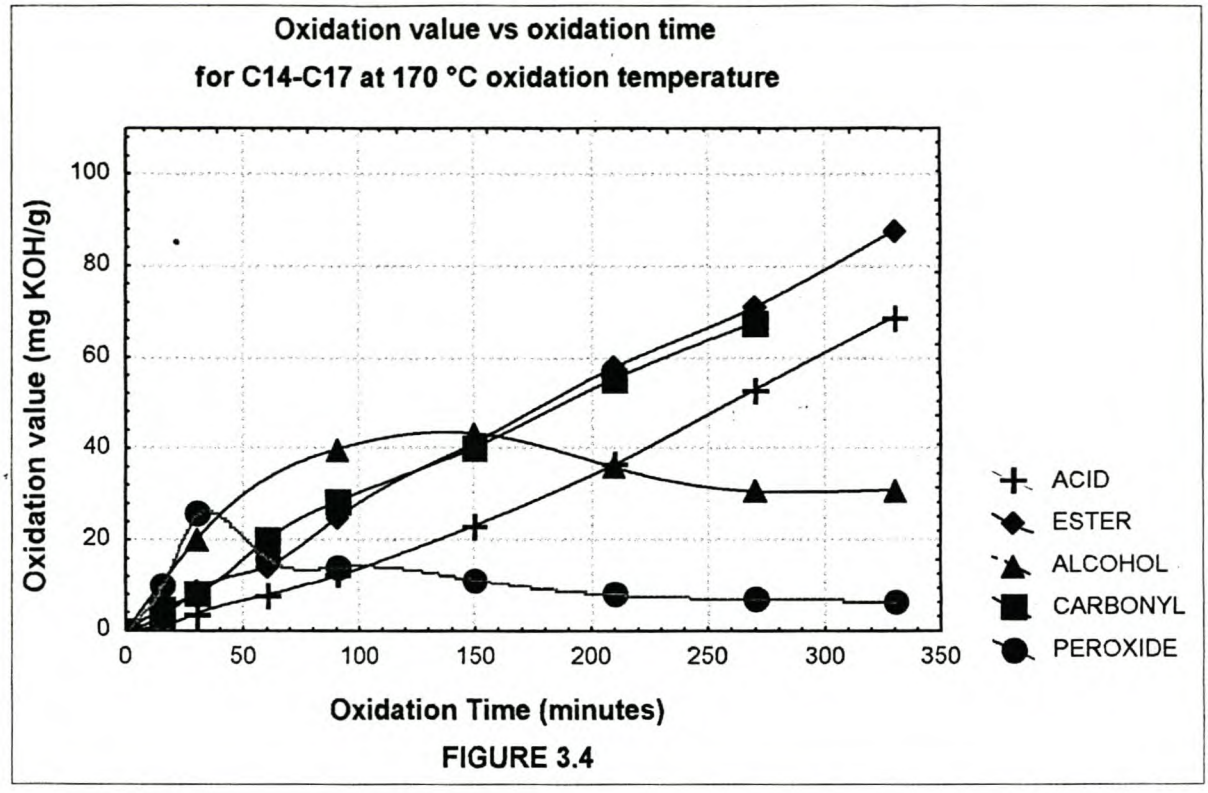

FIGURE 3.4

The three graphs above all show the same trends:

- The formation of alcohol groups and peroxide groups are initially dominant at low temperatures, but as the oxidation temperature increases, the alcohol and peroxide groups are still formed initially, but the conversion to carbonyls, esters and acid groups takes place much faster.
- There are always more ester groups formed than acid groups.
- The carbonyl group formation seems to be more or less on a par with the formation of ester groups.
- The higher the oxidation temperature, the lower the peroxide value.
- The higher the oxidation temperature, the higher the ratio of alcohol value to peroxide value.
- The alcohols formed seem to reach a maximum value after which the alcohol value seems to taper off.

The results of APPENDIX 3.3 are depicted graphically in FIGURES 3.5 to 3.7, which are shown below.

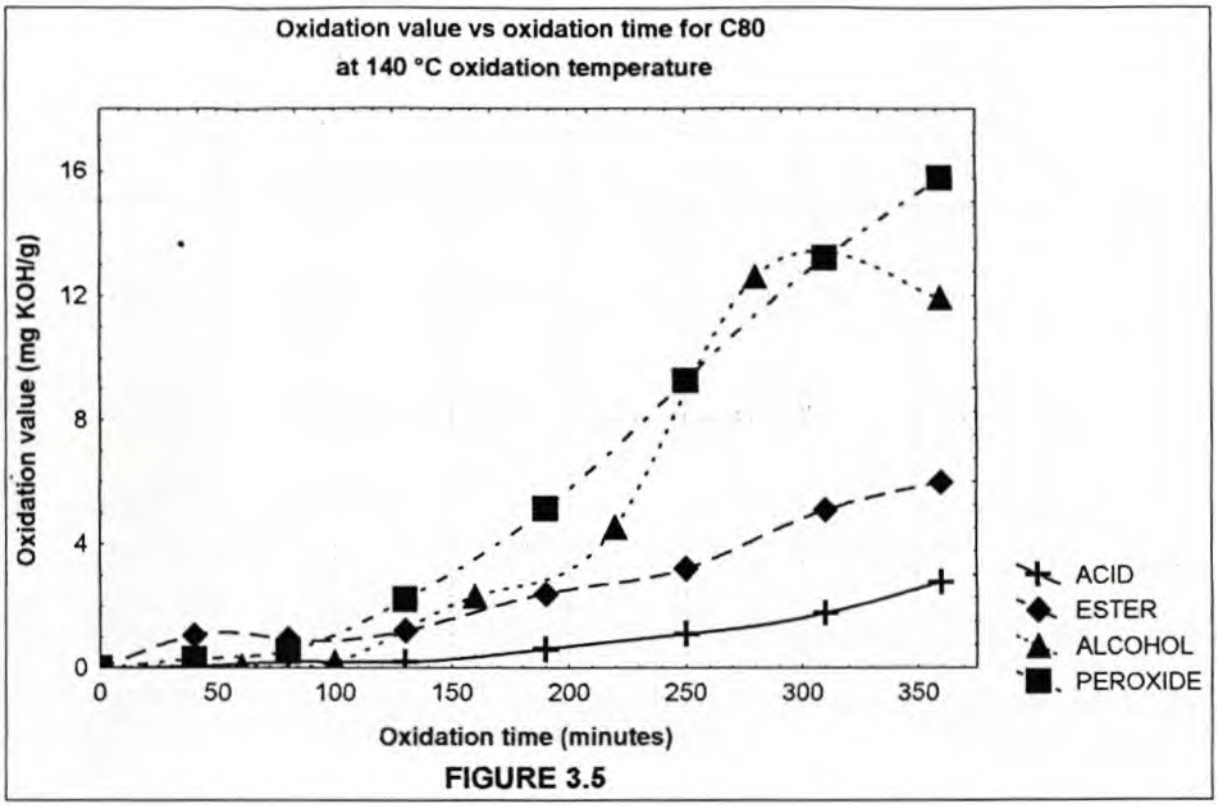

FIGURE 3.5

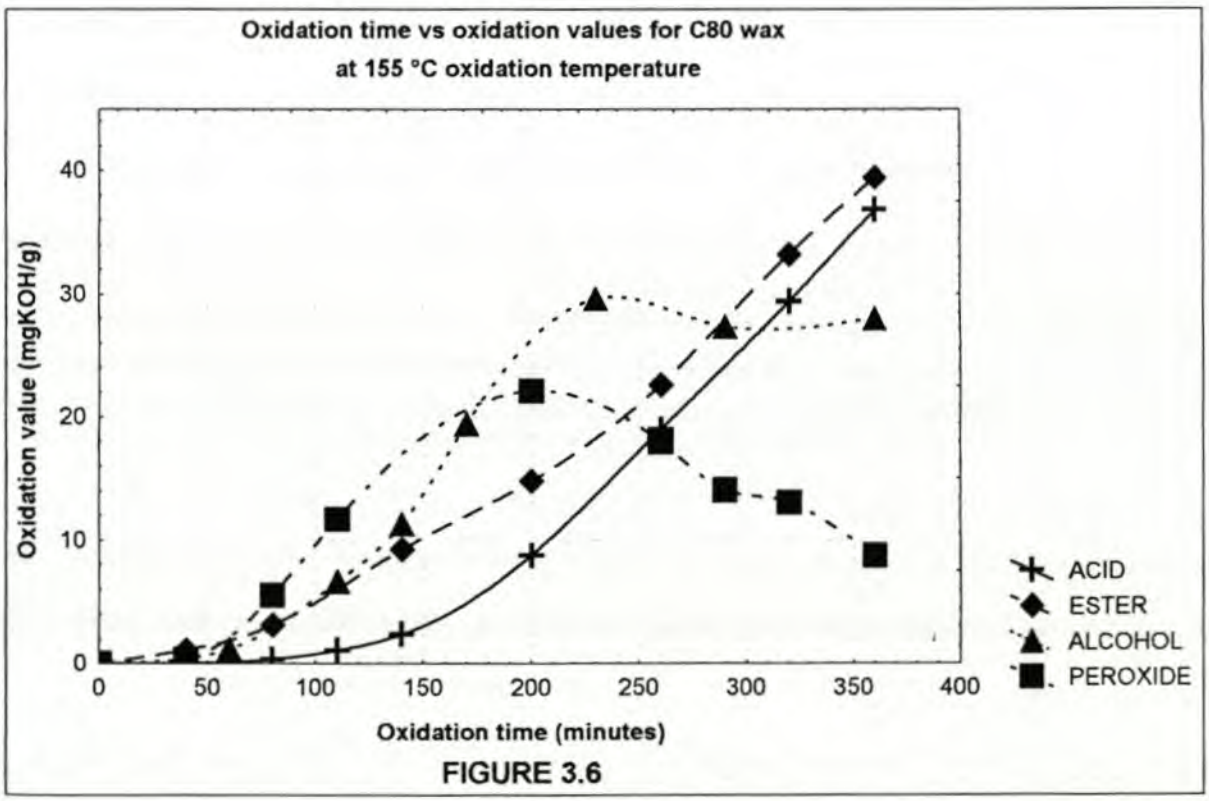

FIGURE 3.6

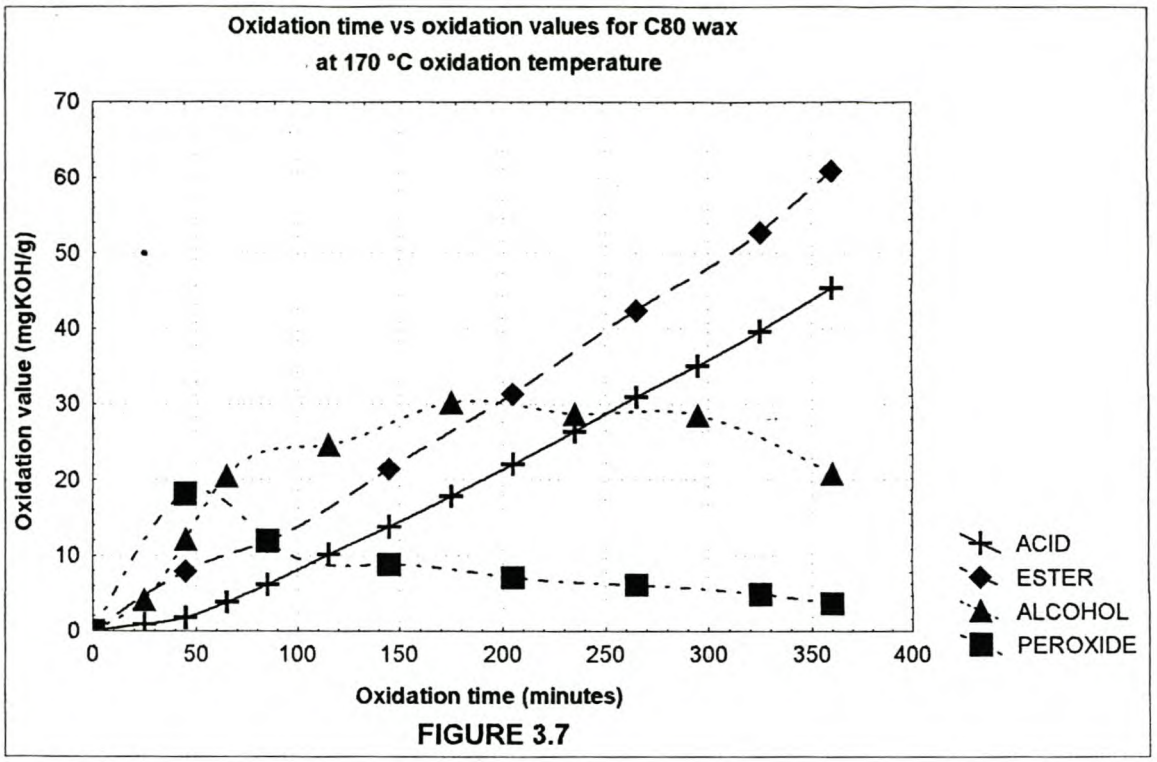

FIGURE 3.7

Please note that the carbonyls were not analysed for the above three graphs. The trends in the above three graphs (excluding the carbonyls, as no results are available for the last three graphs) are identical to the trends described for FIGURES 3.2 to 3.4. The reaction mechanism is therefore assumed to be the same for both types of hydrocarbons, irrespective of the starting molecular mass difference.

If we try and correlate the mechanism of reaction to the equations described in CHAPTER 2, we would see that the initiating equations **4** to **8** describe the formation of the peroxides and equation **9** the formation of the alcohols. As the reaction proceeds however, the peroxides and alcohols formed are converted to acids, esters and carbonyls, with the formation of esters and carbonyls taking preference. In fact, it seems that the carbonyl groups, according to equation **10** and FIGURE 2.15, CHAPTER 2, are the feeding material for the formation of acids and esters.

3.1.3 Oxidation of model compounds

Work had been done at Schümann Sasol [2] on the oxidation of model compounds to further understand the mechanism of reaction in the formation of oxidised F-T waxes.

The study of oxidised F-T waxes and liquids, ranging in carbon numbers from two to one hundred, cannot be analysed meaningfully utilising standard analytical techniques. Model compounds were thus oxidised to try and understand what products are formed during the oxidation process and to try to deduce a mechanism in order to understand more fully the reaction products formed during hard wax oxidation. The three model compounds used were n-hexadecane (n-C16), n-tetracosane (n-C24) and n-dotriacontane (n-C32). Samples were drawn during the reaction of the three model compounds and analysed by GC-MS (Gas Chromotography-Mass Spectroscopy).

Johannes [2] oxidised the n-C16, n-C24 and n-C32 model compounds at various temperatures to try and elucidate the process of oxidation. TABLE 3.1 gives a summary of the results obtained.

TABLE 3.1
Summary of experimental results [2]

Experiments	Results
1.Identification of products formed during oxidation of n-C16 and n-C24	1.1 Products are very similar for both model compounds 1.2 The oxidation products form according to a set pattern 1.3 A substantial amount of the parent alkane remains unaffected by the oxidation process. This is in agreement with the literature [3] 1.4 The alkanes formed have carbon numbers starting at carbon 2 and going up to one less than the parent hydrocarbon 1.5 The aldehydes and ketones range from carbon 2 to the oxygenate with the same number of carbon atoms as the parent molecule. The methyl ketones are predominantly formed during the oxidation and only small amounts of di-ketones are formed 1.6 The γ-lactones formed range from carbon 6 to two carbons less than the parent model compound 1.7 Acids range from carbon 2 to two less carbons than the parent model compound
2.Products formed during the oxidation of n-C16	2.1 The full range of oxygenates is present very early in the oxidation 2.2 The products present in the reaction mixtures at different times during the reaction are similar to those that are present at the start of the reaction 2.3 The major differences between the samples taken at different time intervals concerned were the relative concentration of the products
3.n-C16 oxidised at various temperatures	3.1 The oxidation products formed are similar, irrespective of the temperature of oxidation
4.Molecular mass influence on the oxidation of model compounds (constant temperature)	4.1 The oxidation products are similar although n-C32 could possibly show more isomers of oxidation products than n-C16 4.2 The higher the molecular mass, the higher the concentration will be of the initial oxidation products. That is, the first products formed, before these products are themselves reacted, to form other scission products and derivatives of the first product. 4.3 Experimental results confirm Pope et al.'s [4] theory that oxidation takes place at the end of the molecule
5.Oxidation of a blend of n-C16, n-C24 and n-C32 at a constant temperature	5.1 The higher the molecular mass the faster the molecule is oxidised, within the range examined. 5.2 The products formed for the blended model compounds are the same as for the individual model compounds

3.1.4 Analysis of oxidised Fischer-Tropsch wax

Johannes [2] also took a wax (WAX 28 as used in this thesis, see Section 3.4) that was oxidised for production purposes and analysed the wax to determine its structure.

The oxidised wax was fractionated on a silica column by eluting the wax with different polarity solvents and then analysing the wax elutions using infrared spectroscopy (IR), differential scanning calorimetry (DSC) and high temperature gas chromatography (HTGC). Attempts were made to conduct mass spectroscopy and nuclear magnetic resonance spectroscopy (NMR, both proton and carbon 13 NMR), on the eluted portions, but the spectra were too complex to interpret.

The results and conclusions of Johannes [2] are summarised as follows:

- There is assumed to be an unoxidised portion of the wax ranging in carbon numbers from C20 to C100. This is not really representative of the carbon distribution of the original unoxidised wax, see Table 1.9, Chapter I. The results must thus be due to both the starting material and possible scission products.
- A portion of long chain esters was detected.
- Ketones, alcohols and esters were detected, ranging in molecular mass from high to low with an average carbon distribution of C36.
- Lactones, carbonyls and acids were detected with molecular masses ranging from C20 to C100.
- IR spectra showed the presence of normal esters, which were not detected in the GC-MS of the model compounds, due to the normal ester peaks not being resolved in the spectra.

3.1.5 Summary and conclusions

Through the work of Johannes on oxidised F-T wax and the work done on oxidised hydrocarbons, the following can be concluded with respect to the possible products formed when oxidising F-T waxes:

- Alkanes can be formed or be left unoxidised from the original starting material, which will have a carbon distribution ranging from C2 to the carbon number equal to the original starting material.
- Ketones and aldehydes will be formed ranging up to the carbon number equal to the highest parent hydrocarbon.
- Lactones ranging from C6 to two carbons less than the highest carbon number from the starting material will be formed.

- Acids having carbon numbers ranging from C2 to two carbons less than the highest carbon number from the starting material will be formed.
- Long chain esters will be formed.
- Alcohols will be present.

A myriad of oxidised products will thus be present, of which the acid groups, the ester groups and lactones will be utilised in the formation of the ionomeric waxes.

3.2 Production of grafted Fischer-Tropsch waxes

The possible changing of a wax structure by grafting on acidic groups is an interesting method of producing a wax, which may be saponified, but which does not have the large variation in oxidation groups as when oxidised using the conventional method. The idea behind the grafted waxes is that a more predictable wax will be produced with only specific types of groups added to the wax. The grafting of polymers has been known for many years [5-12] and was the basis of the idea of grafting functional groups onto waxes. In this thesis, the main idea behind the inclusion of grafted waxes was to see how oxidised ionomeric waxes would differ from grafted ionomeric waxes.

3.2.1 Preparation of grafted Fischer-Tropsch waxes

Many types of monomers can be grafted onto F-T waxes. In this thesis study, it was decided to use maleic anhydride as a monomer. The maleic anhydride monomer is not so reactive, that it would rather react with itself to form homopolymer, but in combination with di-tertiary-butyl peroxide (DTBP), it grafts quite readily onto the wax backbone.

The reaction was conducted in a closed Buchi reactor system utilising a high pressure dosing unit to add the DTBP/maleic anhydride mixture. The DTBP/maleic anhydride mixture was dissolved in acetone. DTBP only starts forming radicals at temperatures above ca. 120 °C so that one would be assured that the DTBP/maleic anhydride mixture would not react at room temperature, but only when it entered the reactor. The reaction temperature was 180 °C and the reaction was allowed to proceed for ca. 80 minutes after the addition of the maleic-anhydride and DTBP mixture. The wax was then hydrolysed in the reactor with distilled water at 140°C, by stirring for ca. 30 minutes, after the water addition. This wax was called WAX G11.

3.3 Analysis results of oxidised Fischer-Tropsch waxes

The analysis results of the oxidised waxes, which form the basis of this thesis, are shown below in TABLE 3.2

TABLE 3.2
Analysis results of the oxidised and grafted Fischer-Tropsch waxes

ANALYSIS	METHOD	WAX 6	WAX 16	WAX 28	WAX G11
M_n (g/mole)	Ref. 176 Chapter 2	904	832	821	913
M_w (g/mole)	Ref. 176 Chapter 2	996	983	930	976
Acid value (mg KOH/g)	ASTM D 3242-79a	6.5	16.0	29.0	10.9
Saponification value (mg KOH/g)	Ref. 13 Chapter 3	9.8	30.7	50.5	12.5
Ester value (mg KOH/g	Saponification value - Acid value	4.3	14.7	21.5	1.6

The ester value is obtained by subtracting the acid value from the saponification value. One can see by the decrease in the M_n (molecular mass) value that the wax is lower in molecular mass as the oxidation value increases. This implies that the wax is degraded to lower molecular mass with higher oxidation values. For the acid values observed, the ester value is always less than the acid value. This contradicts the findings for oxidised C80 wax and oxidised C14-C17 liquid wax. I can only assume that the temperature of oxidation is the difference. Figures 3.5 and 3.8 show that the difference in acid and ester values at 170 °C is not as great compared with the differences shown in Figures 3.3 and 3.6 (oxidation at 140 °C). The difference in findings can thus be attributed to temperature of oxidation.

The above waxes were used in the following chapters for saponification purposes.

3.4 References

1. Breet E L J, Luyt A S, Oranja S, **S. Afr. J. Chem.**, 43(3/4), pp83, 1990
2. Johannes D R, **MSc. Thesis, Studies on the composition of thermally oxidised Fischer-Tropsch wax**, University of Cape Town, 1998
3. Hendry D G, Gould C W, Schuetzle D, Suz M G, Mayo F R, **J. Org. Chem.**, 38, pp4435, 1973
4. Pope J C, Dykstra F J, Edgar G, **J. Amer. Chem. Soc.**, 51, pp1875, 1929
5. Yang J, Hsiue G, **J. Appl. Polym. Sci.**, 55, pp653, 1995
6. Ames W A, **USA Patent** 4376855, 1981
7. Roberts T D, Muhlestein K D, Slemons G T, **USA Patent** 5420303, 1995
8. Ames W A, **USA Patent** 4358564, 1982
9. Heintzelman W J, Naaiman M J, **USA Patent** 3437623, 1969
10. Song Z, Baker W E, **Die Angew. Macromd. Chemie**, 181, pp1, 1990
11. Brink A, Dressler F, **Br. Polym. J.**, 1, pp37, 1969
12. Hsiue G, Huang W K, **J. Appl. Polym. Sci.**, 30, pp1023, 1985
13. Boss B D, Hazlett R N, Shephard R L, **Anal. Chem.**, 45, pp2388, 1973

CHAPTER 4 : Fischer-Tropsch wax saponification

4.1 Introduction

The saponification of polymeric acids to form ionomers has been done for many years. In fact, the saponification of acids has been known since the first soap was produced from animal fats. Although soaps do not form exactly the same structures as ionomeric polymers after saponification of the starting chemical, the saponification process remains the same. This chapter is devoted to the description of the saponification process of specific waxes, which were described in CHAPTER 3, as well as a description of the block experimentation process used and a discussion of the results of the chemical analysis.

4.2 Block experimentation design

Because of the many possible variations in the degree of oxidation of the F-T waxes the degree of saponification, and the type of cation used, I decided to use a statistical block experimental approach to reduce the possible number of samples needed to describe the chemical and physical properties of ionomeric F-T waxes. Since this thesis is to my knowledge the first work conducted on F-T ionomeric waxes, I will try, in this thesis, to correlate the physical and mechanical tests results with the unique morphological structure found in ionomeric waxes

I used a computer program called CSS Statistica (windows version 5), which enables one to design a block experiment, and interpret the test results. The experimental approach used was a central composite and non-factorial response surface design. This design is used for the analysis and interpretation of results where the dependence of chemical or physical test results on the initial chemical composition is unknown. The program allows one to do three-dimensional graphic interpretations so that at least two variables can be changed simultaneously and the results of a test be graphically shown, measured against these variable changes. Below, a typical graph shows how the block experiment results can be represented graphically. In the graph, the x-axis shows the % saponified vs. the acid value change on the y-axis, vs. the experimental response on the z-axis (thus a three-dimensional graph) for a typical ionomeric wax.

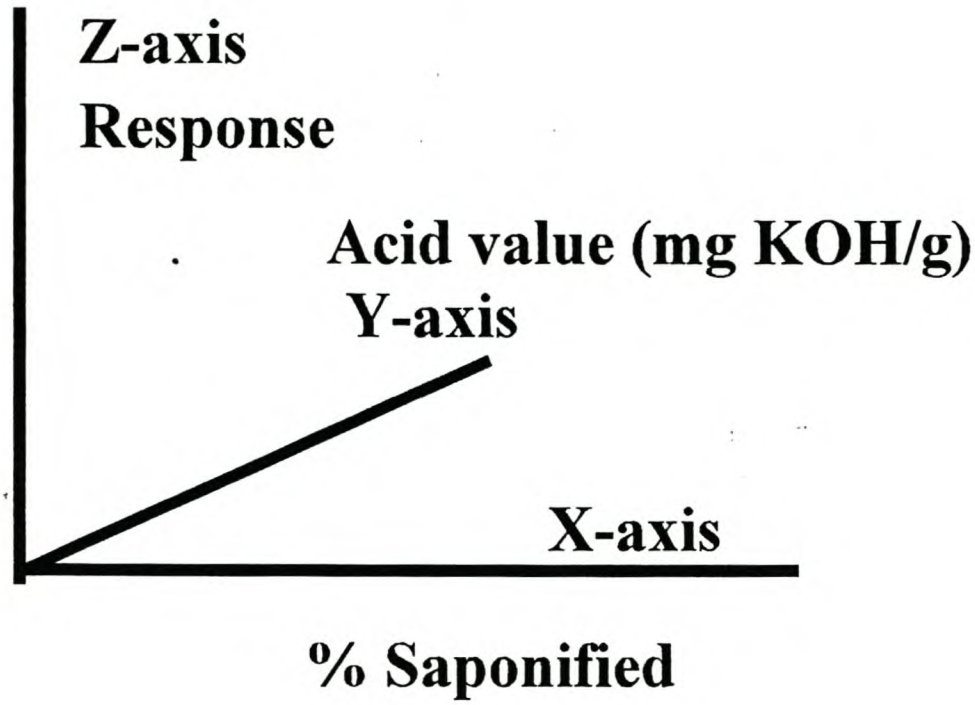

4.3 Type of waxes saponified and types of cations used

Four types of waxes were saponified. The waxes were WAX 6, WAX 16, WAX 28 and WAX G11. The acid numbers of the waxes were 6.5 mg KOH/g, 16.0 mg KOH/g, 29.0 mg KOH/g and 10.9 mg KOH/g as shown in TABLE 3.2, CHAPTER 3. These waxes were saponified to ca. 50 % (m/m) and ca. 100 % (m/m) relative to their acid numbers, with the corresponding cation salts. Cations used for saponification were lithium (Li), sodium (Na), potassium (K), calcium (Ca) and barium (Ba). The cations were used as the hydroxides, which are commercially available in chemically pure grades. WAX G11, the grafted wax, was only saponified with potassium and calcium, as I only wanted to see if one could detect differences between grafted and oxidised waxes saponified with specific cations.

4.4 Saponification method

Polymers are saponified in a very different way from waxes [1-25]. They are normally saponified at much higher temperatures than waxes. Waxes could degrade as oxidation takes place, if it is not run in an inert atmosphere, and concurrently if the temperatures are too high.

The first stage in the saponification process was to melt the waxes while stirring, ensuring that the wax temperature was kept below 140 °C and keeping a nitrogen blanket above the molten wax to avoid oxidation of the wax. A slurry or solution (depending on the type of

hydroxide) of the cationic hydroxide (chemically pure grade) was then added slowly (over a 30 minute period) to the molten wax, ensuring that the temperature remained above 100 °C. If the temperature drops below 100 °C, the wax starts to solidify.

The waxes were kept molten at a temperature of between 130 °C to 140 °C for 20 minutes to 30 minutes before samples were taken for acid value determination. If the acid values were not found to be equivalent to the desired acid value, then additional cationic hydroxide was added to lower the acid value to the desired value. After the desired acid value was obtained, the wax was poured into a shallow metal pan and left to solidify for further use.

4.5 Experimentation

The block experiments were designed as shown below in Table 4.1:

TABLE 4.1
Block experimental design for the ionomeric waxes

Oxidised wax	Cation	% Saponified	Mole % of cation	Mass % of cation
WAX 6 (acid value = 6.5 mg KOH/g)	Li	0	0	0
		50.0	5.2	0.04
		100.0	10.5	0.08
	Na	0	0	0
		59.3	6.2	0.16
		115.0	12.0	0.31
	K	0	0	0
		62.3	6.5	0.28
		125.0	13.1	0.57
	Ca	0	0	0
		57.0	6.0	0.27
		115.8	12.1	0.54
	Ba	0	0	0
		50.0	5.2	0.80
		126.0	13.2	2.01
WAX 16 (acid value = 16.0 mg KOH/g)	Li	0	0	0
		58.7	13.9	0.12
		100.0	23.7	0.20
	Na	0	0	0
		59.9	14.2	0.39
		100.0	23.7	0.66
	K	0	0	0
		70.2	16.7	0.78
		131.9	31.3	1.47
	Ca	0	0	0
		58.8	14.0	0.67
		119.4	28.3	1.37

TABLE 4.1 (continued)
Block experimental design for the ionomeric waxes

Oxidised wax	Cation	% Saponified	Mole % of cation	Mass % of cation
WAX 16 (acid value = 16.0 mg KOH/g)	Ba	0	0	0
		63.3	15.0	2.48
		117.9	28.0	4.62
WAX 28 (acid value = 29.0 mg KOH/g)	Li	0	0	0
		50.0	21.2	0.18
		72.5	30.8	0.26
	Na	0	0	0
		51.4	21.8	0.61
		100.0	42.4	1.19
	K	0	0	0
		59.0	25.0	1.19
		119.9	50.9	2.42
	Ca	0	0	0
		58.2	24.7	1.21
		119.3	50.6	2.47
	Ba	0	0	0
		58.8	25.0	4.17
		129.1	54.8	9.16
WAX G11 (grafted wax, acid value = 10.9 mg KOH/g)	K	0	0	0
		50.0	9.0	0.38
		110.7	19.8	0.85
	Ca	0	0	0
		50.0	9.0	0.39
		129.1	23.1	1.01

NOTE: The molecular masses for WAX 6, WAX 16, WAX 28 and WAX G11 were taken from TABLE 3.2 in CHAPTER 3. These values were used to determine the mole percentage of the cation in the wax. For the above results, the % saponified is an expression of actual amount of salt added with respect to available acid groups and not a percentage of the actual acid groups saponified.

The reaction temperatures of between 130 °C to 140 °C were increased for the samples shown below in TABLE 4.2, as these samples started to gel when the temperatures were below 130 °C, during the cationic hydroxide addition.

TABLE 4.2
Deviations from normal reaction temperatures

WAX TYPE	CATION TYPE	% SAPONIFIED	TEMPERATURE OF SAPONIFICATION (° C)
WAX 16	Li	100.0	135 to 155
	Na	100.0	130 to 150
WAX 28	Li	72.5	130 to 160
	Na	51.4	130 to 150
		100.0	130 to 160
	Ba	118.8	130 to 150

The WAX 28 batch saponified with $LiOH.H_2O$ was only saponified to 72.5 % of the acid value, as the samples started to gel (even running the saponification at higher temperatures did not help) and further addition of the cation hydroxide could not take place.

In TABLE 2.1, CHAPTER 2, the onset of clustering for different polymers is shown. It is very difficult to predict the onset of clustering for the F-T ionomeric waxes, based on the results shown in TABLE 2.1. In the preparation of the waxes, I tried to cover a wide scope of waxes to try and ensure that I might be able to see where multiplet and cluster formation takes place in the oxidised and grafted F-T waxes prepared.

4.5.1 Results

The analyses results for the waxes are shown below in TABLE 4.3 :

TABLE 4.3
Analysis results of saponified oxidised waxes

Oxidised wax	Cation	% Saponified	Acid value (mg KOH/g)	Saponification value (mg KOH/g)	Ester value (mg KOH/g)
WAX 6 (acid value = 6.5 mg KOH/g)	Li	0	6.5	10.8	4.3
		50.0	3.5	7.6	4.1
		100.0	0.6	4.6	4.0
	Na	0	6.5	10.8	4.3
		59.3	3.3	7.1	3.8
		115.0	0.1	3.9	3.8
	K	0	6.5	10.8	4.3
		62.3	3.4	7.7	4.3
		125.0	0.1	3.9	3.8
	Ca	0	6.5	10.8	4.3
		57.0	3.3	7.3	4.0
		115.8	0.2	4.2	4.0

TABLE 4.3 (continued)
Analysis results of saponified oxidised waxes

Oxidised wax	Cation	% Saponified	Acid value (mg KOH/g)	Saponification value (mg KOH/g)	Ester value (mg KOH/g)
WAX 6 (acid value = 6.5 • mg KOH/g)	Ba	0	6.5	10.8	4.3
		50.0	3.6	7.5	3.9
		126.0	0.7	4.6	3.9
WAX 16 (acid value = 16.0 mg KOH/g)	Li	0	16.0	30.8	14.8
		58.7	7.5	19.6	12.1
		100.0	1.3	13.6	12.3
	Na	0	16.0	30.8	14.8
		59.9	7.7	20.2	12.5
		100.0	1.7	13.0	11.3
	K	0	16.0	30.8	14.8
		70.2	7.6	18.7	11.1
		131.9	0.9	9.2	8.3
	Ca	0	16.0	30.8	14.8
		58.8	8.5	23.3	14.8
		117.9	1.4	16.1	14.7
	Ba	0	16.0	30.8	14.8
		63.3	8.2	23.0	14.8
		117.9	1.3	16.0	14.7
WAX 28 (acid value = 29.0 mg KOH/g)	Li	0	29.0	50.5	21.5
		50	15.3	36.9	21.6
		72.5	7.4	28.8	21.4
	Na	0	29.0	50.5	21.5
		51.4	15.0	34.0	19.0
		100.0	2.2	21.4	19.2
	K	0	29.0	50.5	21.5
		59.9	15.0	35.6	20.6
		119.9	2.5	19.9	17.4
	Ca	0	29.0	50.5	21.5
		58.2	16.9	38.5	21.6
		119.3	2.6	24.4	21.8
	Ba	0	29.0	50.5	21.5
		58.8	16.5	37.1	20.6
		118.8	0.5	15.7	15.2
WAX G11 (grafted wax, acid value = 10.9 mg KOH/g)	K	0	10.9	12.7	1.8
		50.0	5.1	6.6	1.5
		110.7	0.9	2.5	1.6
	Ca	0	10.9	12.7	1.8
		50.0	5.3	7.0	1.7
		129.1	3.1	4.6	1.5

The original analysis results for the acid and saponification values as well as the standard deviations are shown in APPENDIX 4.1 and APPENDIX 4.2. The graphical representations of the values are shown in APPENDIX 4.3

4.5.2 Discussion and conclusions

Some of the saponified waxes had to be treated with more than the theoretical amount of cation hydroxides to reach the required acid values. TABLE 4.4 below shows the amount of excess cation hydroxide that was added by taking the drop in actual saponification value versus the amount of cation hydroxide added. The excess cation hydroxide may play a role in the physical and mechanical properties of the waxes. Mohajer, et al.[26] and Hara et al.[27] both conducted work in which they used excess neutralising agent in the ionomers. They concluded that the excess neutralising agent increases the tensile strength of the ionomer up to a point, after which the salts show phase separation and crystallise out, to act as fillers. Before phase separation takes place, the excess neutralising agent is retained within the multiplets/clusters.

TABLE 4.4 below shows that there are some waxes that have excess cations which are not accounted for in the analyses implying that the extra cation hydroxides will be present as unbound cation hydroxides. In the next chapter where the mechanical and physical analyses are discussed, the extra cations may play a role in the response of a wax to the physical or mechanical test that it is subjected to and make the interpretation of the data more understandable.

TABLE 4.4
Excess % cation after saponification

Oxidised wax	Cation	% Saponified	Mole % excess cation	Mass % excess cation
WAX 6 (acid value = 6.5 mg KOH/g)	Li	0	0.0	0.00
		50.0	0.0	0.00
		100.0	0.5	0.00
	Na	0	0.0	0.00
		59.3	0.2	0.00
		115.0	1.1	0.03
	K	0	0.0	0.00
		62.3	1.0	0.04
		125.0	2.5	0.11
	Ca	0	0.0	0.00
		57.0	0.2	0.01
		115.8	1.7	0.08

TABLE 4.4 (continued) Excess % cation after saponification				
Oxidised wax	**Cation**	**% Saponified**	**Mole % excess cation**	**Mass % excess cation**
WAX 6 (acid value = 6.5 mg KOH/g)	Ba	0	0.0	0.00
		50.0	-0.1	-0.01
		126.0	4.0	0.61
WAX 16 (acid value = 16.0 mg KOH/g)	Li	0	0.0	0.00
		58.7	-1.6	-0.01
		100.0	-1.8	-0.02
	Na	0	0.0	0.00
		59.9	-0.9	-0.03
		100.0	-2.7	-0.07
	K	0	0.0	0.00
		70.2	-0.9	-0.04
		131.9	-1.0	-0.05
	Ca	0	0.0	0.00
		58.8	1.7	0.08
		117.9	7.3	0.35
	Ba	0	0.0	0.00
		63.3	2.2	0.36
		117.9	7.1	1.17
WAX 28 (acid value = 29.0 mg KOH/g)	Li	0	0.0	0.00
		50	0.7	0.01
		72.5	-0.7	-0.01
	Na	0	0.0	0.00
		51.4	-1.2	-0.03
		100.0	-0.2	-0.00
	K	0	0.0	0.00
		59.9	5.7	0.27
		119.9	7.3	0.35
	Ca	0	0.0	0.00
		58.2	4.2	0.20
		119.3	14.8	0.72
	Ba	0	0.0	0.00
		58.8	3.1	0.53
		118.8	-0.6	-0.10
WAX G11 (grafted wax, acid value = 10.9 mg KOH/g)	K	0	0.0	0.00
		50.0	-0.5	-0.02
		110.7	3.6	0.15
	Ca	0	0.0	0.00
		50.0	-0.2	-0.01
		129.1	12.8	0.56

A summary of the information of above table is contained in TABLE 4.5, below.

TABLE 4.5
Summary of tabled saponification results

Oxidised wax	Cation	COMMENTS
WAX 6 (acid value = 6.5 mg KOH/g)	Li	A slight excess of LiOH was needed to achieve the desired acid value. Hardly any drop in ester value was seen. There is a slight excess of LiOH in the saponified samples (see TABLE 3.4), but the 50 % sample would most probably be due to experimental errors (see APPENDIX 3.2).
	Na, K	An excess of NaOH and KOH were needed to achieve the desired acid value. Hardly any drop in ester value was seen. There is a significant amount of excess salt, which will most likely be accumulated in the multiplets/clusters [26,27] formed during saponification.
	Ca	An excess of $Ca(OH)_2$ was needed to achieve the desired acid value. Hardly any drop in ester value was seen. There is a significant amount of excess salt, which will most likely be accumulated in the multiplets/clusters [26,27] formed during saponification.
	Ba	An excess of $Ba(OH)_2$ was needed for 100 % saponification to achieve the desired acid value. The 50 % saponification sample needed no excess $Ba(OH)_2$ to reach the desired acid value. Hardly any drop in ester value was seen.
WAX 16 (acid value = 16.0 mg KOH/g)	Li, Na	Although an excess of LiOH and NaOH was used for the 50 % saponified sample to achieve the desired acid value, the excess was used to react with the ester and give a negative excess as shown in TABLE 4.4. A more significant drop in ester value was found due to a more significant reaction of the ester with the hydroxide, when compared to WAX 6. The change in ester results could also be within the repeatability of the analysis method.
	K	Although an excess of KOH was used for the saponification of the samples to achieve the desired acid value, the excess was used to react with the ester and give a negative excess as shown in TABLE 3.4. A more significant drop in ester value was found due to a more significant reaction of the ester with the hydroxide, when compared to WAX 6.
	Ca, Ba	The ester values did not decrease after the divalent salt additions, with the result that the excess salt, as shown in TABLE 3.5, must be taken up in the multiplets/clusters [26,27]
WAX 28 (acid value = 29.0 mg KOH/g)	Li	The ester values did not decrease after LiOH additions. The 100 % sample could only be saponified to 72.5 % of the desired acid value as the sample gelled up and no further salt could be added. The 50 % sample showed a slight excess in salt, TABLE 4.4, due to experimental error (see APPENDIX 4.2).

TABLE 4.5 (continued)
Summary of tabled saponification results

Oxidised wax	Cation	COMMENTS
WAX 28 (acid value = 29.0 mg KOH/g)	Na	The ester values decreased slightly after NaOH additions, which could also be due to experimental errors, see APPENDIX 3.2. No excess of salt was found for the 59 % sample, although an excess of salt was added. The excess must have been consumed by the esters in the sample.
	K	An excess of KOH was added, which was not consumed entirely by the esters in the sample. This is shown in TABLE 4.4 as a significant amount of excess salt, which will most likely be found in the multiplets/clusters formed.
	Ca	An excess of $Ca(OH)_2$ was added, which was not consumed by the esters in the sample and is shown in TABLE 3.4 as a significant amount of excess salt, which will most likely be found in the multiplets/clusters formed.
	Ba	Although an excess of $Ba(OH)_2$ was added to the samples during saponification, only the 58.8 % sample shows an excess salt content, which will most likely be found in the multiplets/clusters formed.
WAX G11 (grafted wax, acid value = 10.9 mg KOH/g)	K, Ca	No significant drop in ester value was seen with the greater than 100 % saponified samples. Both cations showed an excess of salt after saponification.

If one looks at the deviations from normal reaction temperature results in TABLE 4.2, and one correlates these results to the results in Table 4.4 (excess % cation after saponification), then there is a correlation between the samples gelling up (needing a higher temperature to get the sample to flow) and the lack of excess salt. This is true for all the samples in TABLE 4.2, except for the WAX 16, K, 131.9 % saponified sample. This sample did not gel up at normal reaction temperatures and yet it did not have an excess of salts as indicated in TABLE 4.4. I can only deduce from this trend that if there are excess salts present in a highly oxidised sample and the sample is highly saponified (see WAX 16, 100 % saponified samples and WAX 28, 100 % saponified samples), the excess salts help the samples to flow when exposed to heat and shear forces. This concurs with the findings of Mohajer, et al.[26] and Hara et al.[27]; if there are excess salts, the salts will be retained within the multiplets and clusters up to a point where phase separation can occur and the salts act as fillers. The anomaly of the WAX 16, K, 131.9 % sample, I cannot explain. The most likely explanation

is possibly to do with the larger volume that the K cation occupies, relative to the other cations. It was not the intent of this thesis to investigate this anomaly.

4.6 References

1. Shomany E, Eisenberg A, **J. Polym. Science, Polym. Phys. Edition**, 14, pp1213, 1976
2. Eisenberg A, Navratil M, **Polym. Letters,** 10, pp537, 1975
3. Eisenberg A, Navratil M, **Macromolecules**, 6, pp604, 1973
4. Delf B W, MacKnight W J, **Macromolecules**, 2, pp310, 1969
5. Padilla A, Vasquez A, Castano V M, **J. Mater. Res.**, 6, 11, pp2452, 1991
6. Salamone J C, Tsai C C, Olson A P, Watterson A C, **J. Polym. Sci.**, A1, 18, pp2983, 1980
7. Earnest T R Jr., Higgins J S, MacKnight W J, **J. Polym. Sci., Polym. Phys.**, 16, pp144, 1978
8. Broze G, Jerome R, Teyssie P, **Macromolecules**, 15, pp921, 1982
9. Broze G, Jerome R, Teyssie P, Gallot B, **J. Polym. Sci., Polym. Lett. Ed.**, 19, pp415, 1981
10. Plante M, Bazuin C G, Jerome R, **Macromolecules**, 28, pp1567, 1995
11. MacKnight W J, Lundberg R D, **Rubber Chem. Technol.**, 57(3), pp655, 1984
12. Makowski H S, Lundberg R D, Singhal, **USA Patent**, 3 870 841, 1975
13. Lundberg R D, Makowski H S, **Adv. Chem. Ser.**, 187, pp21, 1980
14. Rees R W, **USA Patent**, 3 404 134, 1968
15. Rees R W, **USA Patent**, 3 264 272, 1966
16. Rees R W, Reinhardt H-G, **USA Patent**, 3 997 487, 1976
17. Ehrmann M, Mathis A, Meurer B, Scheer M, Galin J C, **Macromolecules**, 25, pp2253, 1992
18. Bazuin C G, Eisenberg A, **J. Polym. Sci., Part B: Polym. Phys.**, 24, pp1140, 1986
19. Nengu-Plesu R, Bazuin C G, **J. Polym. Sci., Part B: Polym. Phys.**, 29, pp1305, 1991
20. Tong X, Bazuin C G, **J. Polym. Sci., Part B: Polym. Phys.**, 30, pp390, 1992
21. Villeneuve S, Bazuin C G, **Polymer**, 32, pp2811, 1991
22. Lu X, Steckle W P Jr., Hsiao B, Weiss R A, **Macromolecules**, 28, pp2832, 1995
23. Hirasawa E, Yamamoto Y, Tadano K, Yano S, **J. Appl. Polym. Sci.**, 42, pp351, 1991
24. Kim J-S, Eisenberg A, **J. Polym. Sci., Part B: Polym. Phys.**, 33, pp199, 1995
25. Mahmoud F, Qadeer R, **J. Therm. Anal.**, 42, pp 1168, 1994
26. Mohajer Y, Bagrodia S, Wilkes G L, **J. Appl. Polym. Sci.**, 29, pp1943, 1984
27. Hara M, Jar P, Sauer J A, **Macromolecules**, 23, pp4969, 1990

CHAPTER 5 : Ionomeric Fischer-Tropsch waxes : Physical and mechanical properties

5.1 Introduction

The ionomeric waxes prepared in CHAPTER 4 were analysed with respect to their physical and mechanical characteristics. The tests completed included : analysis for penetration, impact strength, softening point, stress, strain, modulus and toughness.

5.2 Wax penetration tests

A wax penetration test is a standard test used for waxes to quantifying their hardness (ASTM D 1231). The penetration test works on the principle that a needle with a certain design is loaded with a certain mass at a certain temperature, to see how far the needle will penetrate the wax within a certain time unit.

The reason behind including this test was to see whether the saponification process alters the structure of the wax significantly enough to identify trends as the wax is saponified and the wax cations are varied.

The penetration tests can be conducted at temperatures ranging from 25 °C to ca. 90 °C, i.e. water temperatures, as the instrument is equipped with a thermostatically controlled water bath. The higher the water temperature, the softer the wax becomes and the more sensitive the test method becomes towards structural changes. The problem with the saponified waxes is that some of the ionomeric waxes tend to be sensitive to water absorption and thus the test could be conducted only at 25 °C (room temperature). The penetration instrument used was not designed to be used within an oven environment, so that there was no practical way to heat the waxes to higher temperatures for an elevated temperature test.

5.2.1 Sample preparation

The waxes were heated to their melting point and cast in a special mould. The moulded samples were left overnight in a vacuum oven at 25 °C to eliminate any moisture that may be present on the surface as well as to ensure that the waxes were treated similarly. The wax moulds were removed from the vacuum oven individually and tested on the penetrometer. Three samples of each wax were tested to assure a more accurate and representative result.

5.2.2 Results and discussion

The results for the tests are shown below in Table 5.1.

TABLE 5.1
Penetration test results of the Fischer-Tropsch ionomeric waxes at 25 °C

Oxidised wax	Cation	% Saponified	Average penetration value (dmm)	Standard deviation (dmm)
WAX 16		0	0.9	0.2
	Li	58.7	0.2	0.1
		100.0	0.2	0.1
	Na	59.9	0.2	0.1
		100.0	0.2	0.1
	K	70.2	0.2	0.1
		131.9	0.2	0.1
	Ca	58.8	0.3	0.1
		119.4	0.2	0.1
	Ba	63.3	0.2	0.1
		117.9	0.2	0.1
WAX 28		0	1.8	0.2
	Li	50.0	0.2	0.1
		72.5	0.3	0.1
	Na	51.4	0.1	0.1
		100.0	0.3	0.1
	K	59.0	0.5	0.2
		119.9	***	***
	Ca	58.2	0.5	0.2
		119.3	0.1	0.1
	Ba	58.8	0.4	0.2
		118.8	0.2	0.1

Note : Only WAX 16 and WAX 28 were tested initially to see if there were any trends. If trends did appear, the rest of the samples were to be tested.

The WAX 28 potassium saponified wax (119.9 %) could not be moulded properly, as the wax viscosity was too high.

A graphical representation of the results of TABLE 5.1 can be seen below in FIGURES 5.1 and 5.2. The mole % for each cation was taken from TABLE 4.1, CHAPTER 4.

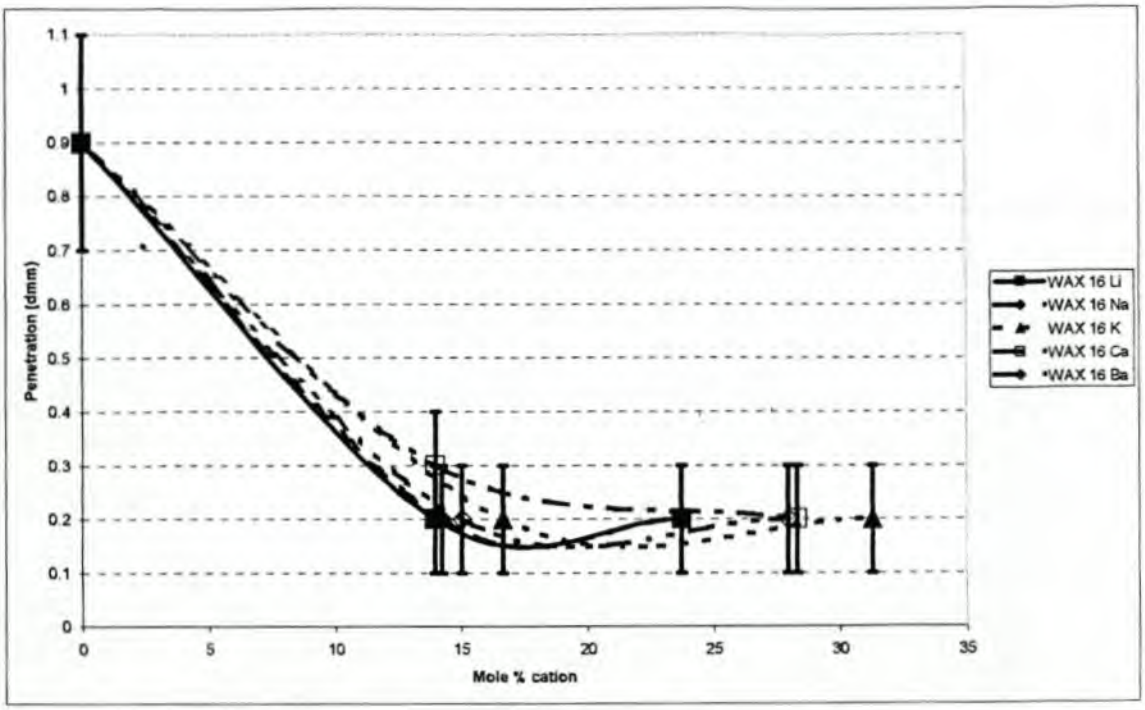

FIGURE 5.1 : WAX 16: Penetration value vs. Mole % cation

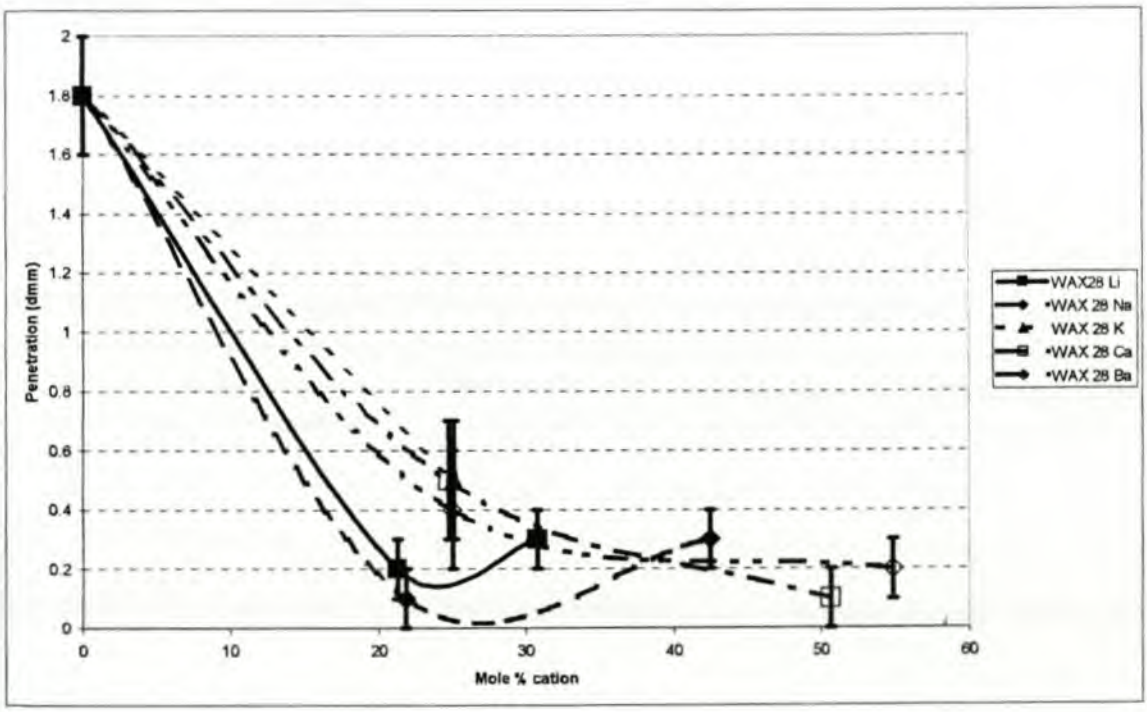

FIGURE 5.2 : WAX 28: Penetration value vs. Mole % cation

A summation of the results from TABLE 5.1, FIGURES 5.1 and 5.2 are shown below in TABLE 5.2.

TABLE 5.2
Summary of penetration test results of the Fischer-Tropsch ionomeric waxes at 25 °C

Oxidised wax	Cation	Comments
WAX 16	Li, Na, K	There is a definite decrease in penetration value at about 50 % saponification when compared to the oxidised wax, and a slight increase in penetration value at 100 % saponification when compared to the 50 % saponified samples. If one looks at the standard deviations of the individual samples however, one cannot conclude an increase, but rather a flattening out trend in hardness.
	Ca	The 50 % saponified sample does not harden to the same values as the saponified samples of the monovalent cations and there seems to be a continued decrease in hardness for the 100 % saponified sample. Even when one takes the standard deviations into account, the assumption that I am making of a continued decrease seems to be reasonable.
	Ba	This cation seems to show the same trend as the monovalent cations.
WAX 28	Li	The 50 % saponified sample shows a much larger percentage decrease than the oxidised wax penetration values than the corresponding WAX 16 sample, but the penetration values for the saponified samples are in the same order as for the WAX 16 samples.
	Na	The trend of the monovalent cation for WAX 28 and WAX 16 to decrease in penetration value from the original oxidised wax and then to increase in penetration value on 100 % saponification is more pronounced for this cation sample. Taking the standard deviations into account however, it could still be a flattening out effect.
	K	No trend could be seen, as the 100 % saponified sample was too viscous to be moulded. The 50 % saponified sample did not show the same percentage penetration decrease as the corresponding lithium and sodium cation samples.
	Ca, Ba	The 50 % saponified samples do not show the same percentage decrease in penetration value as the monovalent cations, but the decreasing trends in penetration value (from 0 to 100 % saponification samples) seem to be the same for WAX 28 and WAX 16.

FIGURES 5.3 to 5.7 show the same results shown in FIGURES 5.1 and 5.2, but the data is arranged according to cations. From these graphs, the summation given above in TABLE 5.2, is more apparent.

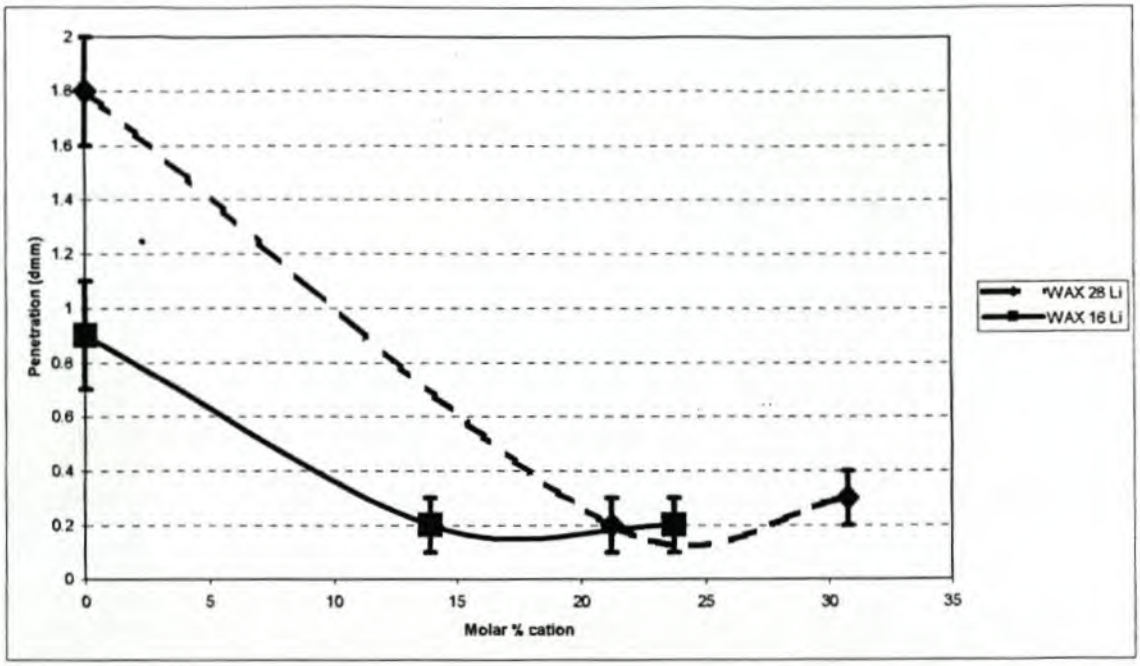

FIGURE 5.3 : Li cation waxes : Penetration value vs. Mole % cation

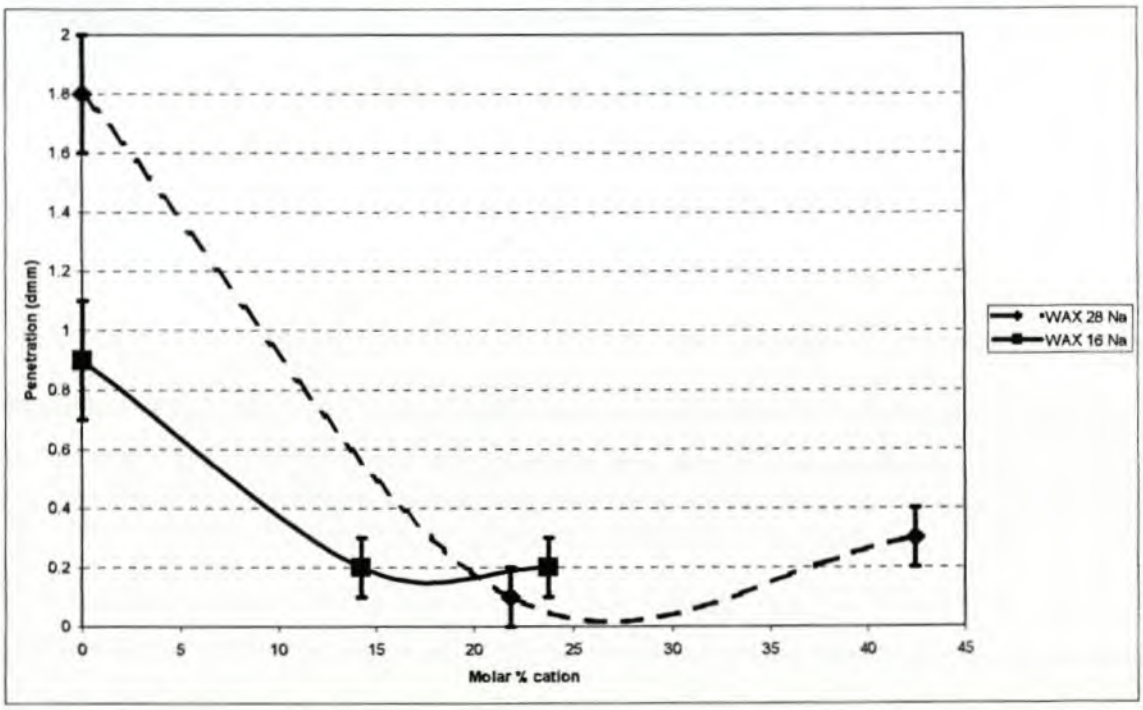

FIGURE 5.4 : Na cation waxes : Penetration value vs. Mole % cation

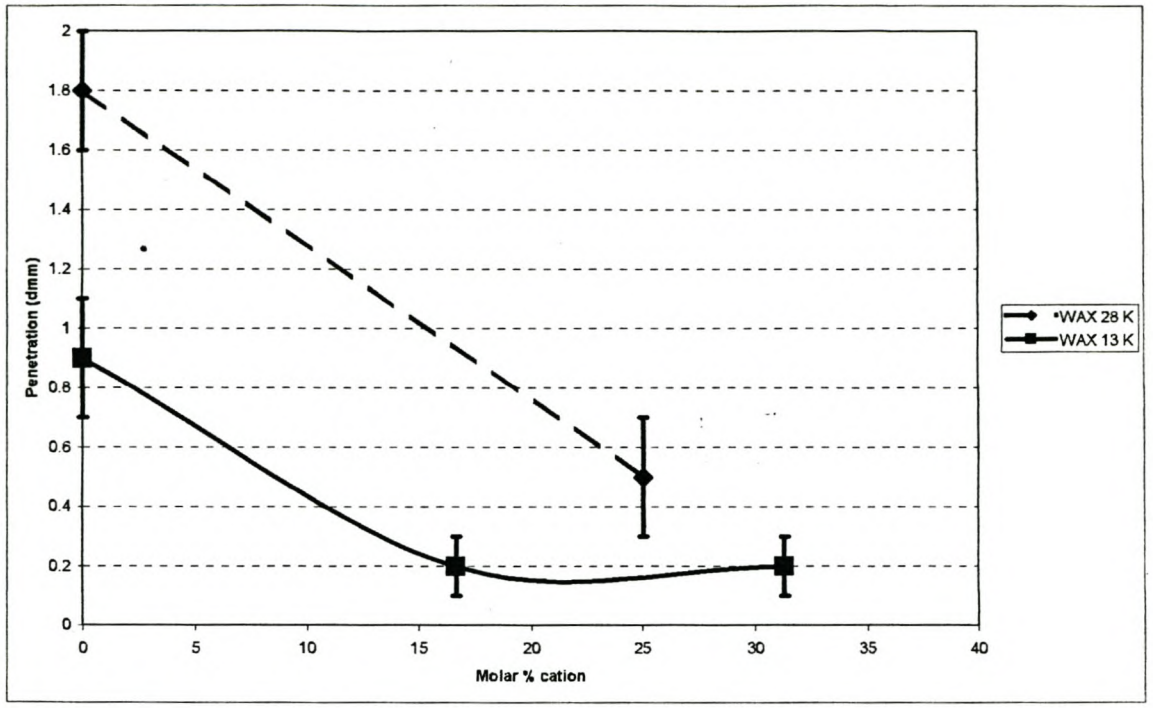

FIGURE 5.5 : K cation waxes : Penetration value vs. Mole % cation

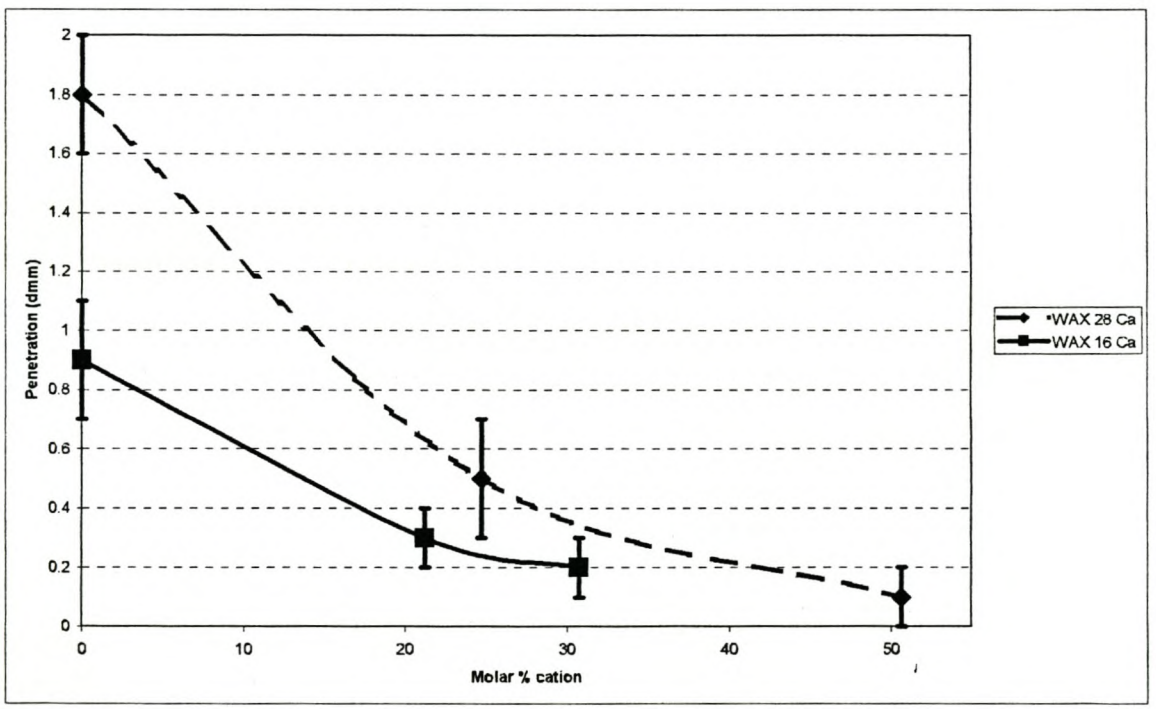

FIGURE 5.6 : Ca cation waxes : Penetration value vs. Mole % cation

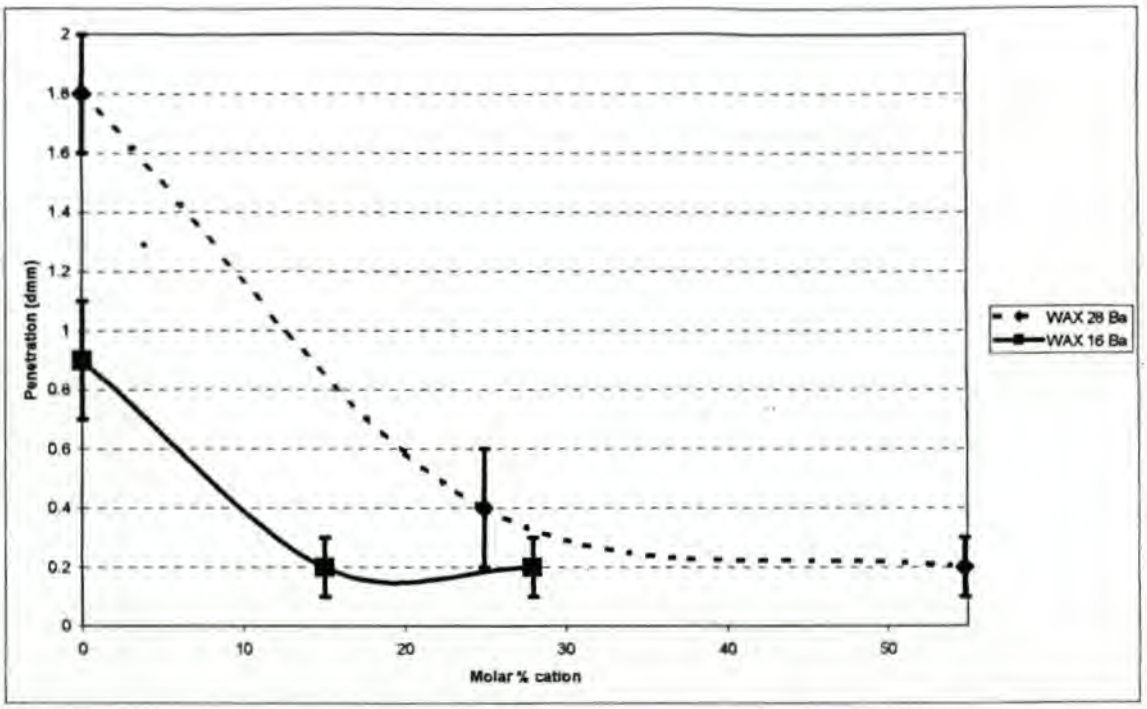

FIGURE 5.7 : Ba cation waxes : Penetration value vs. Mole % cation

It thus appears that the monovalent cation-saponified samples react differently from the divalent-cation saponified samples. From a morphological viewpoint, it might be that the monovalent cations have already formed clusters or multiplets at about 50 % saponification values. This can be deduced from the fact that the wax does not really become harder after 50 % saponification value and seems to flatten out in hardness. The calcium and barium samples (especially WAX 28 samples for barium) show a definite decrease in penetration value from the oxidised wax to the 100 % saponified samples. This test does not show clear changes on the saponified samples to give conclusive proof that the saponified samples are either in a state of multiplet formation or cluster formation. If it were possible to do the penetration tests at higher temperatures one might be able to see more clearly whether multiplet formation or cluster formation is dominant. In isolation, this test is not conclusive as to whether multiplet formation or cluster formation is dominant on the saponified samples, but in conjunction with the other tests performed one might be able to come to a more firm conclusion (see at the end of this Chapter).

5.3 Impact tests

The next test conducted was an impact test. In this test I was looking at whether the frequency of a test, in other words, in this case a high frequency impact test, would reveal any differences between the samples.

5.3.1 Sample preparation

The samples were heated to melting point and moulded in a silicone rubber mould. The samples were left in a vacuum oven overnight to remove any surface moisture and to make sure that the samples were all treated in the same way before the test.

The sample dimensions, after de-moulding, were measured to determine the surface area exposed to the hammer. A reading was taken and the energy required to break the sample was calculated.

5.3.2 Results and discussions

The results for the tests are shown below in Table 5.3.

TABLE 5.3
Impact test results of the Fischer-Tropsch ionomeric waxes at 25 °C

Oxidised wax	Cation	% Saponified	Surface area (mm^2)	Impact reading (J)	Energy to break (kJ/m^2)	Average energy readings (kJ/m^2)	Standard deviation (kJ/m^2)
WAX 16		0	137.76	0.143	1038	1056	26
		0	137.75	0.148	1074		
	Ba	63.3	136.00	0.104	765	792	38
		63.3	134.24	0.110	819		
		117.9	136.60	0.071	520	537	23
		117.9	139.24	0.077	553		
WAX 28		0	136.00	0.126	927	883	62
		0	137.14	0.115	839		
	Li	50.0	135.72	0.099	729	688	59
		50.0	136.30	0.088	646		
		72.5	140.67	0.088	626	590	51
		72.5	138.92	0.077	554		
	Na	51.4	143.40	0.099	690	958	378
		51.4	143.67	0.176	1225		
WAX 28	K	59.0	136.6	0.121	886	920	58
		59.0	138.36	0.136	954		
	Ca	58.2	148.20	0.088	594	671	109
		58.2	147.01	0.110	748		
		119.3	138.94	0.088	633	675	59
		119.3	138.06	0.099	717		
	Ba	58.8	137.76	0.132	958	879	112
		58.8	137.44	0.110	800		

Note : Only a few samples were tested to see if this test would show any trends.

The above results are shown below graphically in FIGURE 5.8.

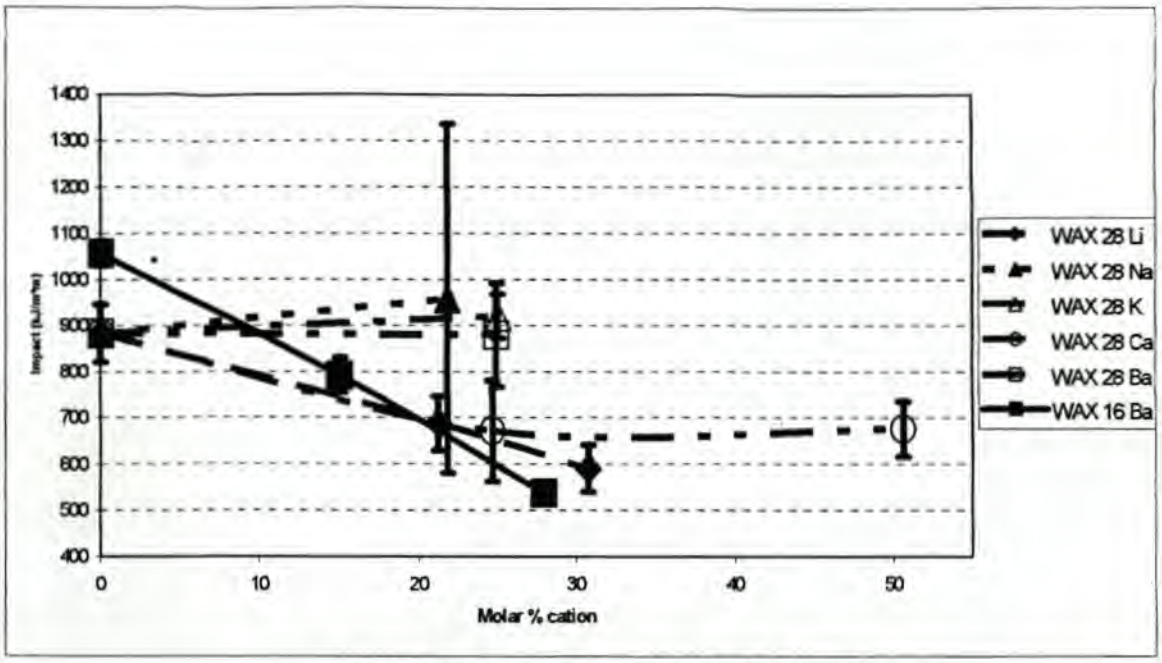

FIGURE 5.8 : Impact vs. Mole % cation

Reproducibility of the impact tests as shown in the above graph and Table 5.3, is rather suspect, especially with respect to samples WAX 28, Na 51.4 % saponified and WAX 28, Ca 58.4 % saponified. Due to the poor reproducibility, only a limited amount of samples were tested. The poor reproducibility could be due to sample preparation.

The structural changes that take place during the formation of ionomeric waxes are a decrease in crystallinity, due to straight chain disrupture and the formation of multiplets and clusters [1-10]. We know from literature references [1, 3, 5-7, 10, 11-19] that multiplets and clusters within an ionomeric polymer take much more energy to deform or flow than the corresponding non-ionised polymer does. The impact test works on the premise that if a sample becomes harder and more brittle, then the sample will show a lower energy value to break. The fact that a sample becomes more brittle as it becomes harder is not always true. Some of the crosslinked polymers become harder with crosslinking but they do not necessarily become more brittle, so that on impact tests they show high impact value on breaking. In the case of the above ionomeric wax samples, I would expect the samples to become more brittle and harder with an increased degree of oxidation in combination with increased % saponification.

The WAX 28 and WAX 16 oxidised wax samples show that the impact value for WAX 28 is in fact lower than the impact value for WAX 16. This is not what I would expect. I would expect that as the crystallinity decreases (acid value increases, hardness decreases and

brittleness decreases), the wax would show a higher impact value. Does this thus imply that a wax with a lower acid value would give you a higher impact value? Would WAX 6 then give a higher impact value than WAX 16 and would the un-oxidised C105 wax give you an even higher impact value? Would this also imply that crystallinity acts as a type of crosslinking? There are too few results from the above analysis to answer my questions, but the tensile analysis test results described later in this chapter could give an answer to the above questions.

The WAX 28 ca. 50 % sodium, potassium and barium samples do not show a trend. The impact values for these samples are, within experimental error, more or less the same value of the oxidised sample value.

The WAX 28 lithium samples and WAX 16 barium samples do show a trend. These samples show lower impact values with increase in saponification value. This implies that the samples became more brittle as the saponification value increased. WAX 28 calcium samples also showed a decrease in impact value with an increase in saponification value, up to the ca. 50 % saponified sample, whereafter the ca. 100 % sample seems to have more or less the same impact value as the ca. 50 % sample.

The above results in isolation are not conclusive enough to state that the WAX 28 lithium and calcium samples and the WAX 16 barium samples have formed multiplets or clusters. In conjunction with the penetration results, one can conclude that for the three sets of samples (WAX 28 lithium and calcium and WAX 16 barium) multiplet or cluster formation must have taken place. Both tests showed that the samples either increased in hardness or brittleness, which implies that only multiplet or cluster formation could have been responsible.

5.4 Softening point test

This test is done according to ASTM 7893. In this test, the waxes are heated and poured molten into a special cup with a certain size aperture. After the wax has solidified, the cup is placed in an instrument where the cup and wax are heated up at a rate of 1 °C/minute. When the wax reaches the softening point, the wax flows out of the cup and falls by gravitational forces. The wax drop falls past a light beam, which then records the temperature. Due to this method being very accurate (inherent standard deviation of 1.3 °C, according to the ASTM method, but in practice it has been found that this method of

analysis is much more accurate). Only single analyses were done and the error bars are therefore not included on the graphs of results. A standard wax is used as a reference to ensure that the instrument is calibrated correctly.

5.4.1 Results and discussion

The results of the softening point tests are shown in Table 5.4.

TABLE 5.4
Softening point results of the Fischer-Tropsch ionomeric waxes

Oxidised wax	Cation	% Saponified	Mole % cation	Softening point (°C)
WAX 6	Li	0	0.00	109.0
		50.0	5.23	109.3
		100.0	10.47	109.4
	Na	0	0.00	109.0
		59.3	6.21	107.8
		115.0	12.04	115.5
	K	0	0.00	109.0
		62.3	6.52	108.9
		125.0	13.08	109.4
	Ca	0	0.00	109.0
		57.0	5.97	109.4
		115.8	12.12	109.5
	Ba	0	0.00	109.0
		50.0	5.23	109.3
		126.0	13.19	108.8
WAX 16	Li	0	0.00	108.1
		58.7	13.92	108.3
		100.0	23.71	112.0
	Na	0	0.00	108.1
		59.9	14.20	104.1
		100.0	23.71	141.0
	K	0	0.00	108.1
		70.2	16.65	108.4
		131.9	31.28	114.6
	Ca	0	0.00	108.1
		58.8	13.94	107.9
		119.4	28.31	107.9
	Ba	0	0.00	108.1
		63.3	15.01	107.0
		117.9	27.96	107.9
WAX 28	Li	0	0.00	104.1
		50.0	21.21	104.5
		72.5	30.75	129.2
	Na	0	0.00	104.1
		51.4	21.80	107.6
		100.0	42.41	129.0
	K	0	0.00	104.1
		59	25.02	105.2
		119.9	50.85	120.3
	Ca	0	0.00	104.1
		58.2	24.68	105.6
		119.3	50.60	107.9
	Ba	0	0.00	104.1
		58.8	24.94	109.0
		118.8	54.75	116.7
WAX G11	K	0	0.00	114.3
		50.0	8.86	112.5
		110.7	19.62	112.2
	Ca	0	0.00	114.3
		50.0	8.86	113.8
		129.1	22.89	113.6

The results from TABLE 5.4 are shown graphically in FIGURES 5.9 to 5.13.

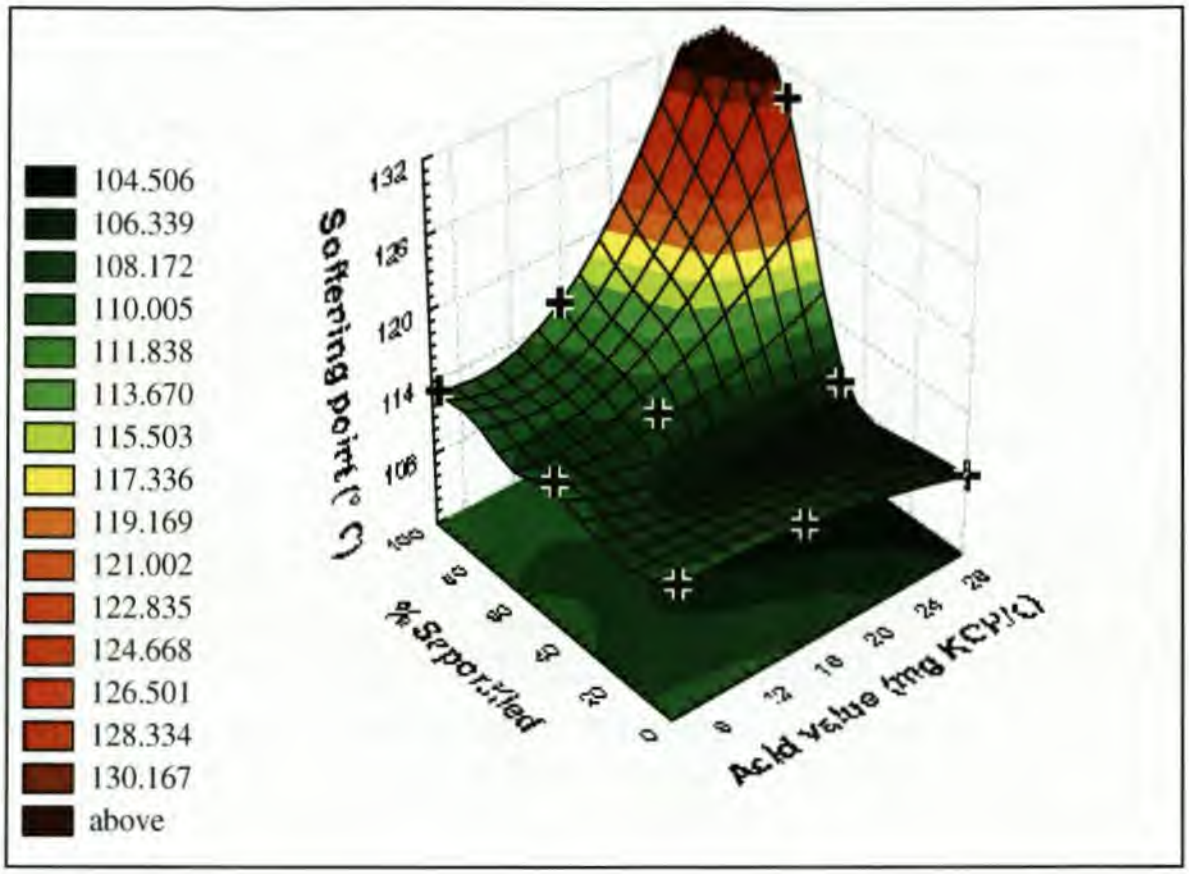

FIGURE 5.9 : Li cation : Acid value vs. % Saponified vs. Softening point

The softening point of a wax is dependent on both the melting point of the wax as well as the flow characteristics of the wax, as the wax droplet will flow under gravitational forces at a certain temperature.

The above graph for lithium cation of the ionomeric F-T waxes show that:

1. For the 0 % saponified waxes, as the acid value increases, so the softening point decreases. This is to be expected, as the more the wax is oxidised, the more the crystallinity is decreased, the amount of chain scissions are increased and oxidative groups are increased so that the softening point is decreased.

2. At ca. 50 % saponification, WAX 16 (acid value 16.0 mg KOH/g) has more or less the same softening point as WAX 6 (acid value 6.5 mg KOH/g), which implies that although the crystallinity has been disrupted by oxidation, the formation of multiplets may have counteracted the lowering of the softening point, resulting in the net effect of the softening point staying the same as for WAX 6. WAX 28 (acid value 29.0 mg KOH/g) has a lower softening point than either WAX 6 or WAX 16,

which implies that the possible formation of multiplets could not counteract the disruption of the crystallinity. There does not seem to be any formation of clusters for any of the ca. 50 % saponified samples, as the change in softening points is not pronounced.

3. For the ca. 100 % saponified samples, the increase in softening point from WAX 6 to WAX 16 is more pronounced. This implies that the formation of multiplets and/or possible clusters is much more pronounced when the softening point is increased, than when the crystallinity is disrupted (lowering of softening point). Wax 28 shows a large increase in softening point compared with WAX 16 and it may therefore be concluded that cluster formation is possible.

4. If one looks at WAX 28, ca. 100 % saponified compared to ca. 50 % saponified, there is a dramatic increase in the softening point, which gives more validity to the statement I made in point 3. For WAX 6 and WAX 16, the increase in softening point versus the increase in % saponified is not that great and I assume that only multiplet formation is seen.

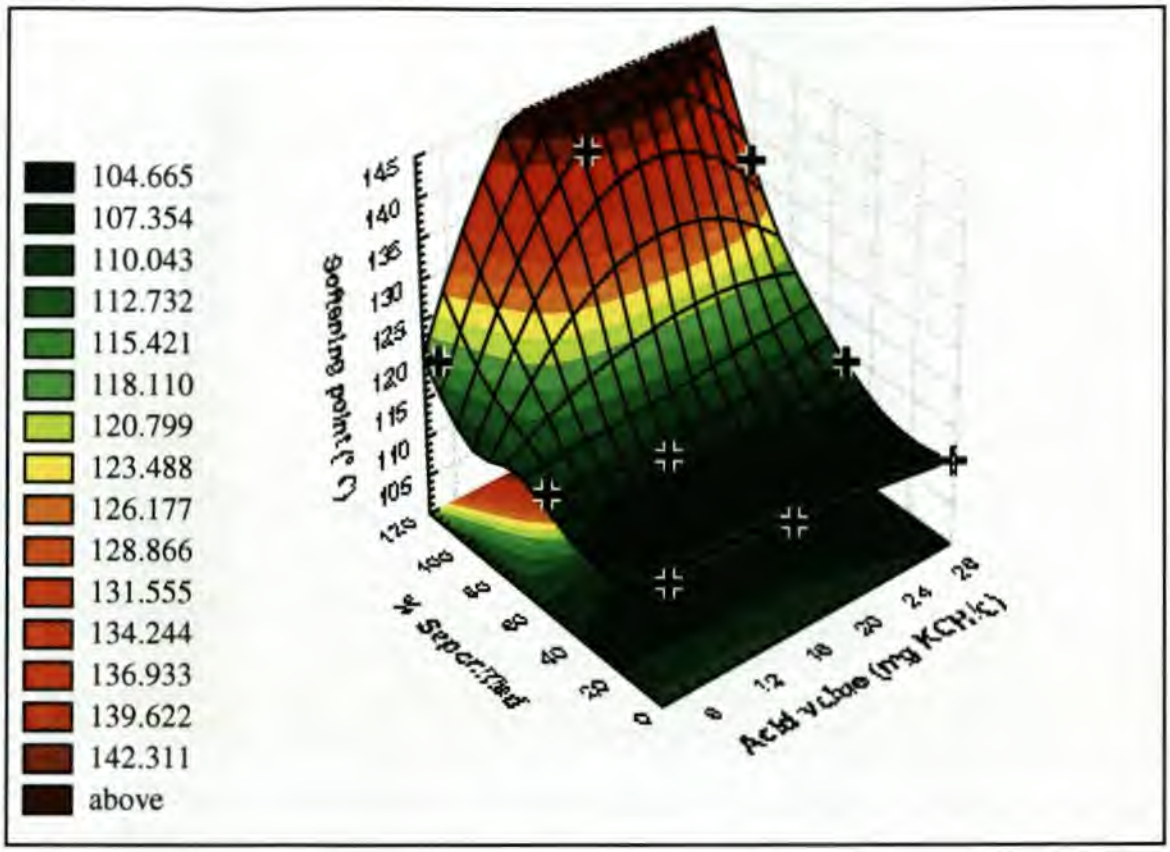

FIGURE 5.10 : Na cation : Acid value vs. % Saponified vs. Softening point

The above graph for the sodium cation of the ionomeric Fisher-Tropsch waxes shows that:

1. For the ca. 50 % saponified samples, the possible decrease in crystallinity is counteracted by the formation of most probably multiplets, giving a net result that the softening point remains more or less the same, irrespective of the acid value.

2. For the ca. 100 % saponified waxes, WAX 16 and WAX 28 show a remarkable increase in softening point versus WAX 6, which could possibly be due to the formation of clusters.

3. If one compares WAX 16 and WAX 28, relative to WAX 6, the increase in softening point from ca. 50 % saponified to ca. 100 % saponification, then one would conclude that cluster formation must be evident.

4. A phenomenon which I cannot explain at this stage, is that WAX 28 at ca. 100 % saponification has a lower softening point than WAX 16 at ca. 100 % saponification. One would expect that WAX 28 (100 % saponification) should have a higher softening point than WAX 16 (100 % saponification) has, due to the larger mole

percentage concentration of Na cation in WAX 28 (100 % saponification) than for the WAX 16 (100 % saponification). As I progress further with the thesis, I will look for patterns regarding this wax sample.

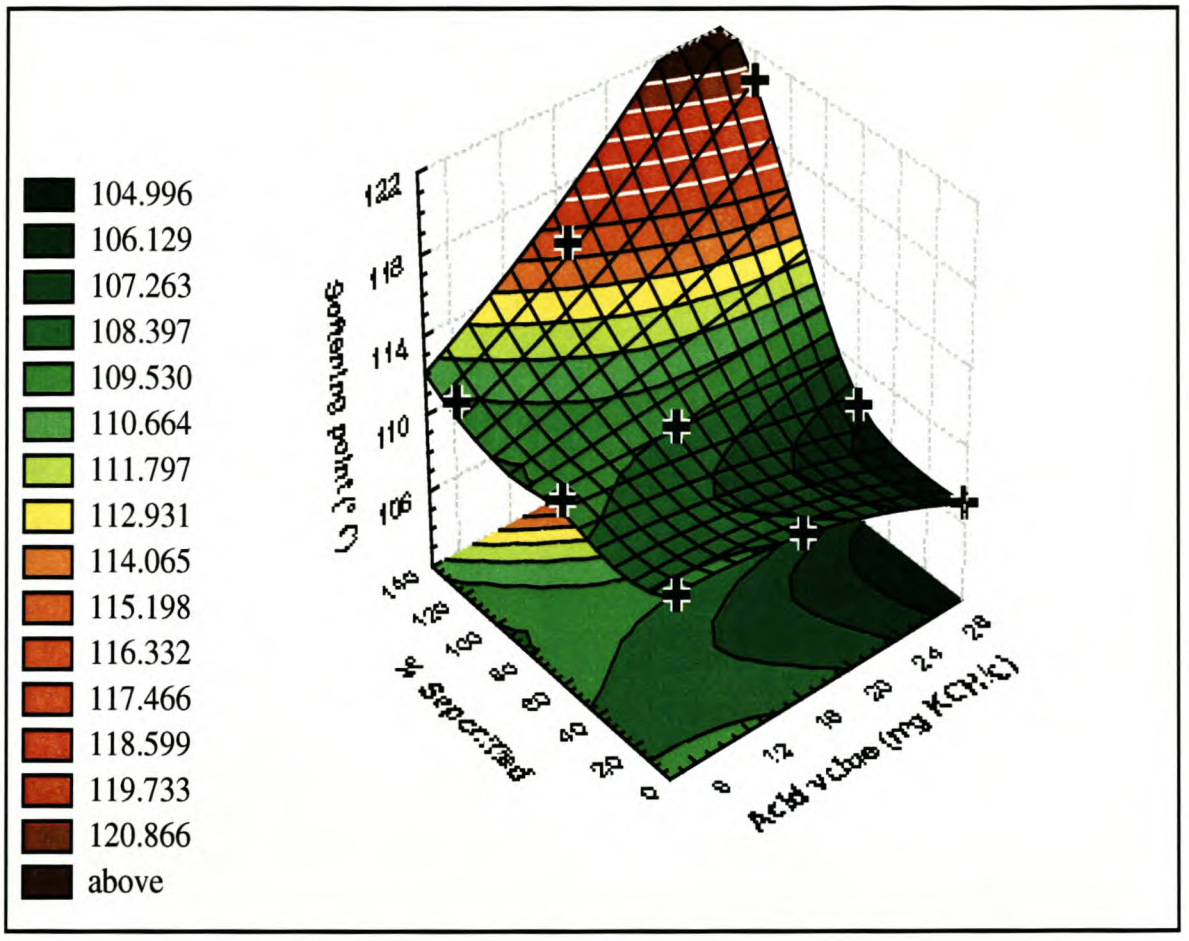

FIGURE 5.11 : K cation : Acid value vs. % Saponified vs. Softening point

The above graph for potassium cation of the ionomeric Fisher-Tropsch waxes shows that:

1. Results are similar to those seen for the lithium cation. That is, the ca. 50 % saponified samples show a decrease in softening point with an increase in acid value and for the 100 % saponified samples there is a dramatic increase in softening point with an increase in acid value. For Wax 28, 100 % saponified, the increase in softening point is most likely due to cluster formation.

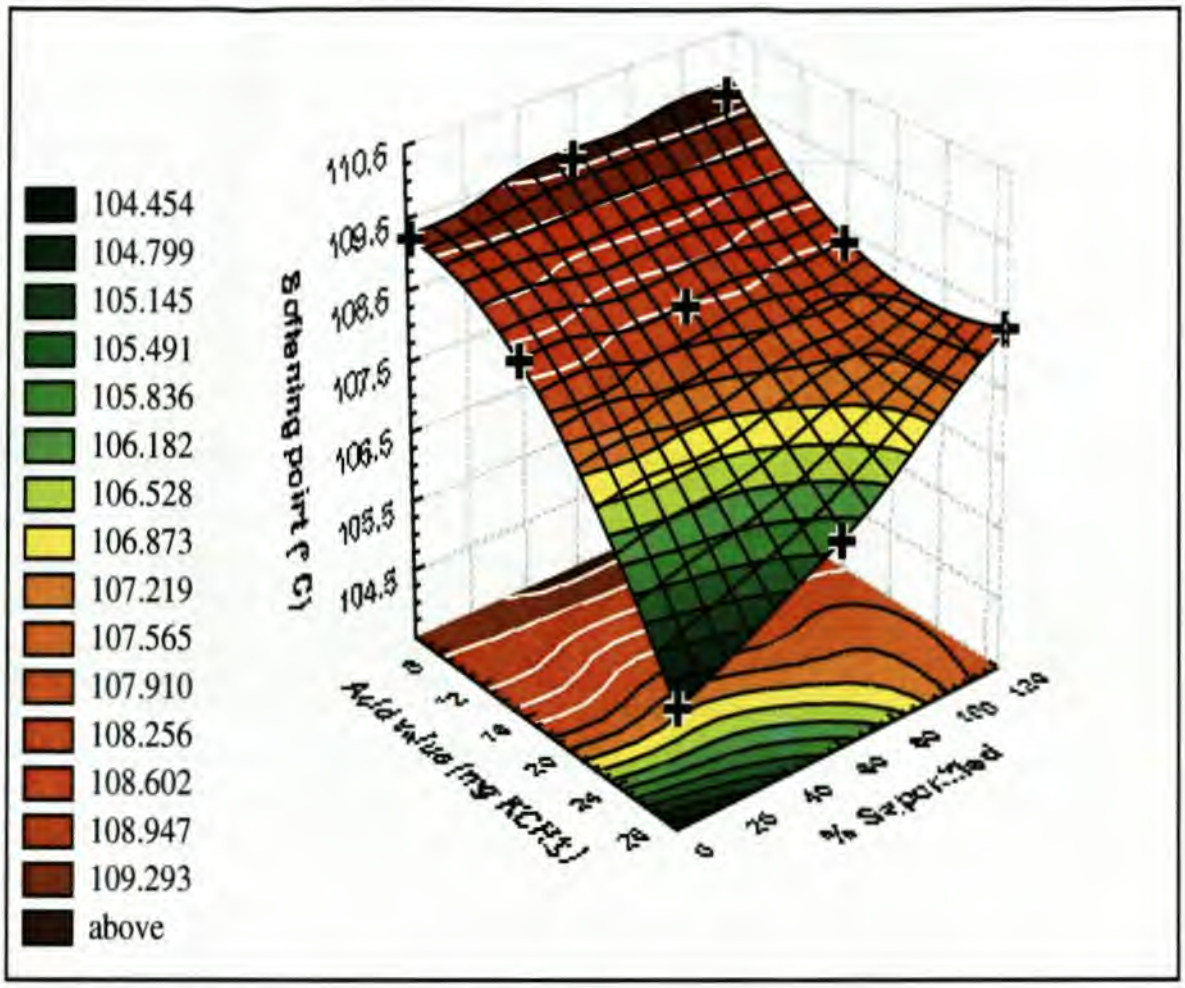

FIGURE 5.12 : Ca cation : Acid value vs. % Saponified vs. Softening point

For this graph I had to rotate the axis so that the graph was more visible and easier to read. The acid value and % saponified are thus not on the same axis as in the previous three graphs.

The above graph for the calcium cation shows that:

1. For both the ca. 50 % saponified samples and the ca. 100 % saponified samples, the softening points essentially stay the same, within experimental error. This is true but for WAX 28 samples, which show an increase in softening point value with an increase in saponification value.

2. This differs from results for the monovalent cations, where the ca. 100 % saponified samples show an increase in softening point with an increase in acid value. Although multiplet formation is possible, it is not more predominant than the

possible disruption of the crystallinity, so that the net result is the lowering of the softening point.

3. It is also noted that even for WAX 28 (high acid value), saponified at ca. 100 %, the softening point is still lower than for the non-saponified WAX 6 and WAX 16.
4. From the above graph one can thus deduce that only the WAX 28 ca. 50 % and 100 % saponified samples were forming multiplets.

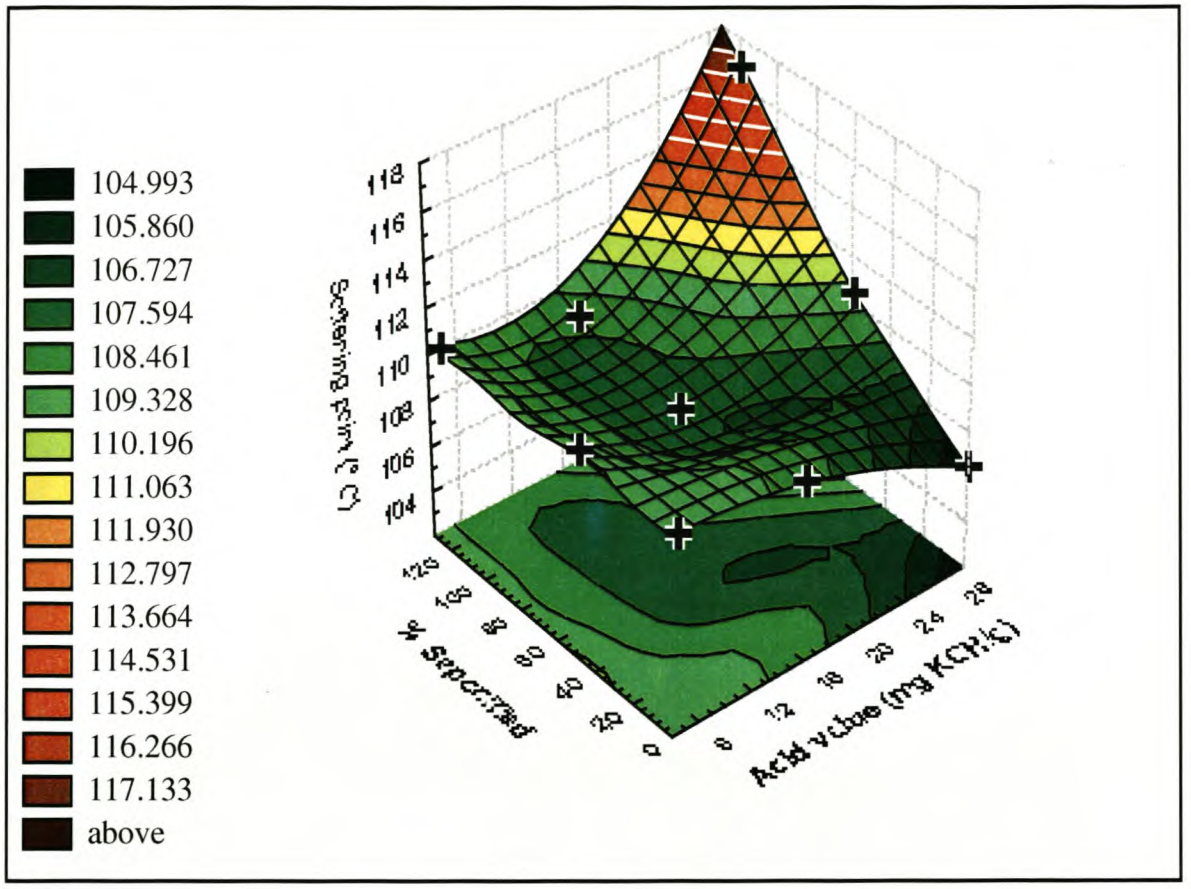

FIGURE 5.13 : Ba cation : Acid value vs. % Saponified vs. Softening point

The above graph for barium cation shows that:

1. Barium cation results are more similar to the sodium cation results at ca. 50 % saponification and to the lithium and potassium cation results at ca. 100 % saponification than to the calcium cation results. The results at 100 % saponification are less pronounced than the lithium cation and potassium cation results, so that I cannot conclude that possible cluster/multiplet formation is predominant.

2. The above graph shows that, as in the Ca samples, only WAX 28 samples seem to have

formed multiplets on saponification. The fact that there is not a dramatic increase in softening point value from the WAX 28 ca. 50 % saponified sample to the ca. 100 % saponified samples (as was the case for Li, Na and K samples) leads me to conclude that cluster formation has not taken place.

I have not included the grafted wax samples in the above graphs, as I wanted to compare the grafted results in another set of graphs shown below in FIGURE 5.14.

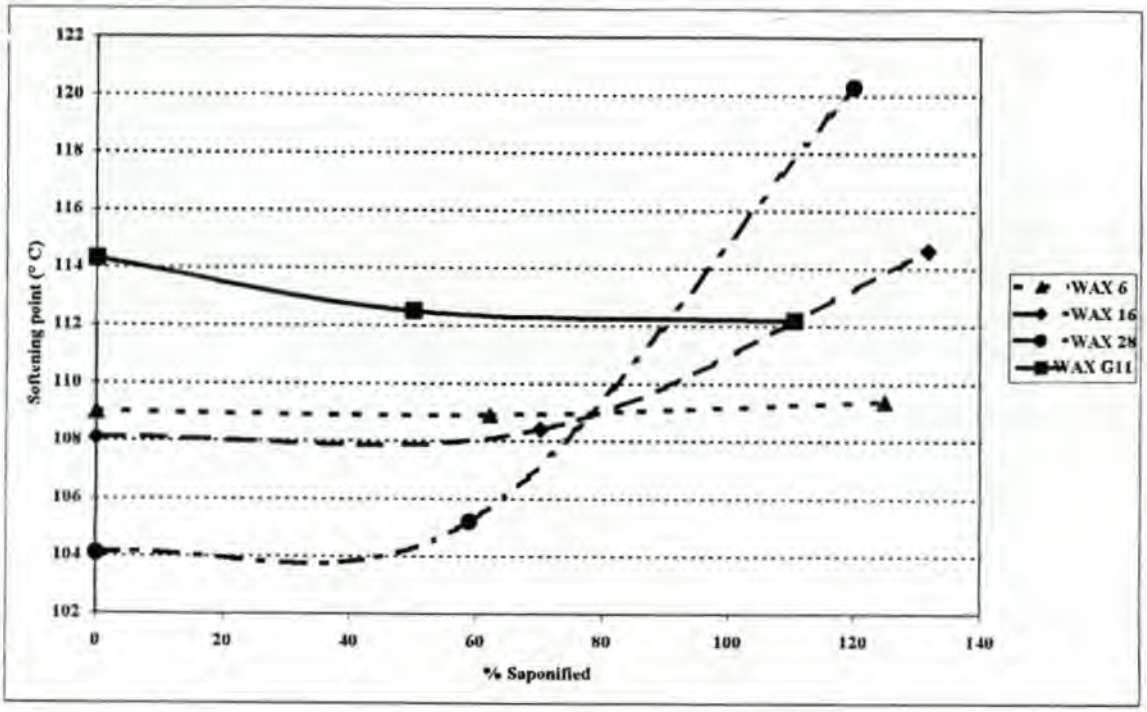

FIGURE 5.14 : K cation: % Saponified vs. Softening point.

The most important fact shown in the above graph is that the softening point of WAX G11, 0 % saponified is ca. 114 °C. This is ca. 1 °C lower than the non-grafted starting wax, C105, which has a softening point of ca. 115 °C. The grafting process thus does not disrupt the crystallinity to such a degree that the softening point drops dramatically. It is further noted that the ca. 50 % saponified and ca. 100 % saponified WAX G11 samples show a slight decrease in softening point, which could imply that although the crystallinity is decreased with increasing percentage saponification, the possible formation of multiplets counteracts the softening effect to a large extent. It is also noticeable that the grafted wax does not show the same trends as the oxidised wax on saponification, which would be expected. The grafted wax has only the maleic acid groups grafted onto the wax backbone, while the oxidised wax has many other functional groups present, all of which could have an influence on the tests that were carried out on the waxes. WAX G11 seems to behave more like WAX 6 than WAX 16. This is understandable as WAX G11 has a saponification value

of ca. 12 mg KOH/g close to the ca. 10 mg KOH/g of WAX 6. It would also appear that the more polar character of the oxidised waxes causes them to form possible multiplets and possible clusters to a greater degree than the corresponding grafted wax, if the acid values are equal.

Graphs of the oxidised and grafted calcium saponified waxes are shown below.

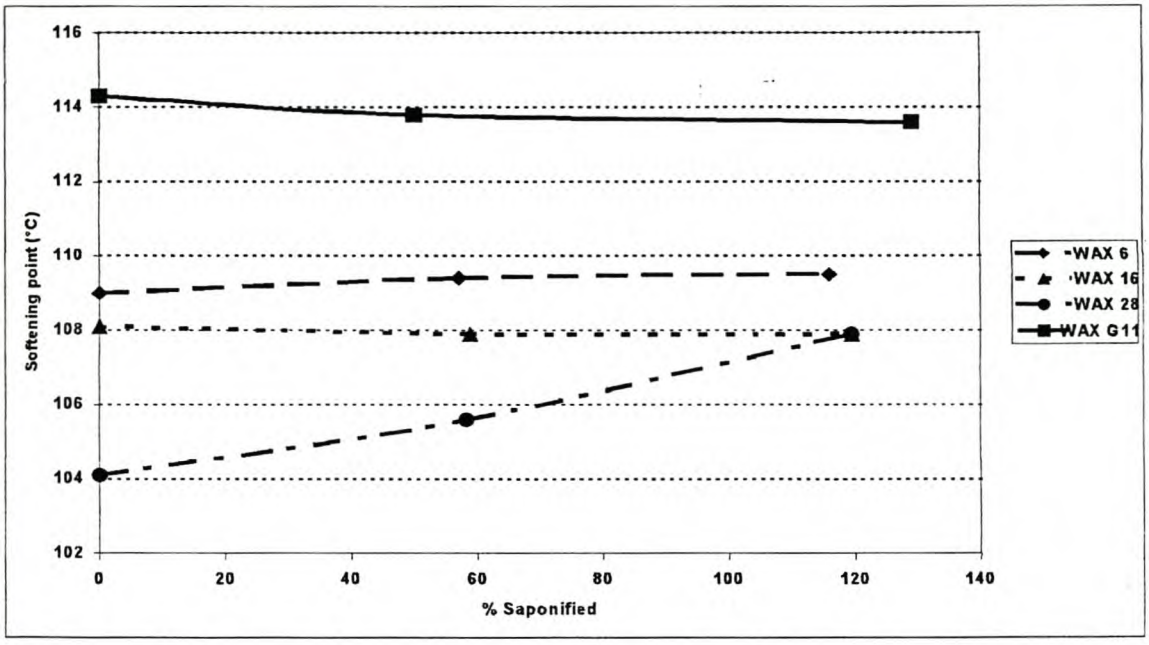

FIGURE 5.15 : Ca cation: % Saponified vs. Softening point.

In FIGURE 5.15 one can see that, except for WAX 28, the waxes do not seem to form significant quantities of multiplets to influence the softening point dramatically. The results shown in this graph agree with both the penetration results and the impact results (see sections 5.2 and 5.3), where the saponification with calcium cations does not provide large changes in results. It appears that the saponification only makes the original oxidised waxes relatively harder.

In TABLE 2.6 [20], the effect of ionomerisation on various polymers has been shown. This table compares the effect of ionomerisation versus melting point and the degree of crystallinity. The various polymers had molar percentage acid groups of up to about 6 mole percentage and, for the polymers tested, it was found that the melting point dropped for all the polymers, except for the magnesium ionised samples where some of the samples became non-fusible.

Firstly, there should be a comparison between the melting point and the softening point as both are related to heating the sample to a specific temperature. The softening point

however also incorporates the use of gravitational force to induce viscous flow to determine the softening point. Correlations might therefore be found between the polymer results and the wax results. There is however no direct comparison between the results of the oxidised waxes tested and the polymer results in TABLE 2.6. I presume that oxidation of the waxes disrupts the crystallinity to such a degree that other effects such as multiplet and cluster formation become more pronounced in determining the softening point. The saponified grafted waxes (based on WAX G11) however show the same trend as shown by the polymers in TABLE 2.6. The crystallinity is probably not disrupted to such a degree when grafting the waxes, compared to oxidising the waxes. The saponification of the waxes, when grafting the waxes, thus only lowers the degree of crystallinity, hence lowering the softening point while the formation of multiplets and clusters is not sufficient enough to counteract the decrease in the softening point.

5.5 Mechanical analysis

The waxes were moulded into dumbbells and the samples were analysed for their mechanical properties to see whether there are any trends that could be correlated to the starting oxidation value, the percentage saponified or the cation used.

Using the argument I used to explain the inappropriateness of the impact test (section 5.3), one would conclude that if you test the waxes on a tensile tester at a very slow rate, say 0.5 mm/min crosshead speed, then trends may possibly be identified by this method of testing. Whether the test would be sensitive enough to show real structural changes is difficult to predict. The test results stated in literature [14,15,21-27] were all done on polymers with very high molecular masses (relative to waxes). Waxes are however very rigid, due to their crystallinity, and I was not sure of the influence of multiplets/clusters formation on the tensile strength and elongation.

5.5.1 Dumbbell preparations

The waxes were heated to a molten state and cast in dumbbell mould, specially designed for waxes. The waxes were allowed to cool down in an oven; the oven temperature was lowered in stages, 10 °C/30 minute, to room temperature. The dumbbell samples were kept in a desiccator until the mechanical tests were done.

5.5.2 Mechanical analysis results and discussions

The test conditions were as follows:

Crosshead speed : 0.5 mm/min
Temperature : 23 °C
Humidity : 50 %

The mechanical analysis results can be seen in TABLE 5.5, and a summary of the raw data can be seen in Appendices 5.1 to 5.4.

TABLE 5.5
Mechanical test results of the Fisher-Tropsch ionomeric waxes

Oxidised wax	Cation	% Saponified	Max. Tensile strength (MPa)	Max. Elongation (%)	Modulus (MPa)	Toughness (KPa)
WAX 6	Li	0	3.0	8.6	35.8	161
		50.0	2.4	7.6	32.0	134
		100.0	2.1	7.1	29.3	115
	Na	0	3.0	8.6	35.8	161
		59.3	2.6	8.0	33.4	137
		115.0	3.2	8.6	37.5	167
	K	0	3.0	8.6	35.8	161
		62.3	3.4	9.2	37.4	211
		125.0	4.4	11.0	46.1	277
	Ca	0	3.0	8.6	35.8	161
		57.0	1.4	8.4	17.4	95
		115.8	2.7	8.6	31.8	144
	Ba	0	3.0	8.6	35.8	161
		50.0	3.5	8.7	40.9	184
		126.0	1.5	5.7	25.8	58
WAX 16	Li	0	2.6	10.3	25.7	165
		58.7	3.9	9.1	42.9	195
		100.0	3.3	9.6	34.9	202
	Na	0	2.6	10.3	25.7	165
		59.9	3.5	9.1	39.3	190
		100.0	2.1	7.2	29.5	119
	K	0	2.6	10.3	25.7	165
		70.2	1.7	7.5	22.9	101
		131.9	1.7	6.1	27.3	71
	Ca	0	2.6	10.3	25.7	165
		58.8	1.3	5.0	27.8	49
		119.4	3.4	9.4	36.5	190
	Ba	0	2.6	10.3	25.7	165
		63.3	1.8	7.0	25.7	97
		117.9	1.1	5.3	21.6	59

TABLE 5.5 (continued)
Mechanical test results of the Fisher-Tropsch ionomeric waxes

Oxidised wax	Cation	% Saponified	Max. Tensile strength (MPa)	Max. Elongation (%)	Modulus (MPa)	Toughness (KPa)
WAX 28	Li	0	1.9	12.0	15.8	134
		50.0	2.5	7.4	33.7	108
		72.5	2.5	8.5	30.1	165
	Na	0	1.9	12.0	15.8	134
		51.4	3.4	9.8	34.8	195
		100.0	1.4	4.5	30.3	37
	K	0	1.9	12.0	15.8	134
		59.0	2.3	8.5	27.3	125
		119.9	2.2	6.4	34.7	86
	Ca	0	1.9	12.0	15.8	134
		58.2	1.2	5.9	215	60
		119.3	0.6	6.5	9.1	32
	Ba	0	1.9	12.0	15.8	134
		58.8	2.3	8.6	26.8	115
		118.8	1.8	5.5	32.0	62
WAX G11	K	0	2.9	7.9	37.3	165
		50.0	4.2	10.6	40.0	266
		110.7	4.0	10.8	37.1	283
	Ca	0	2.9	7.9	37.3	165
		50.0	2.4	6.0	40.3	102
		129.1	5.4	9.5	56.2	300

FIGURES 5.16 to 5.19 show the mechanical results of the mechanical tests for lithium, sodium, potassium, calcium and barium cation samples for all the types of waxes.

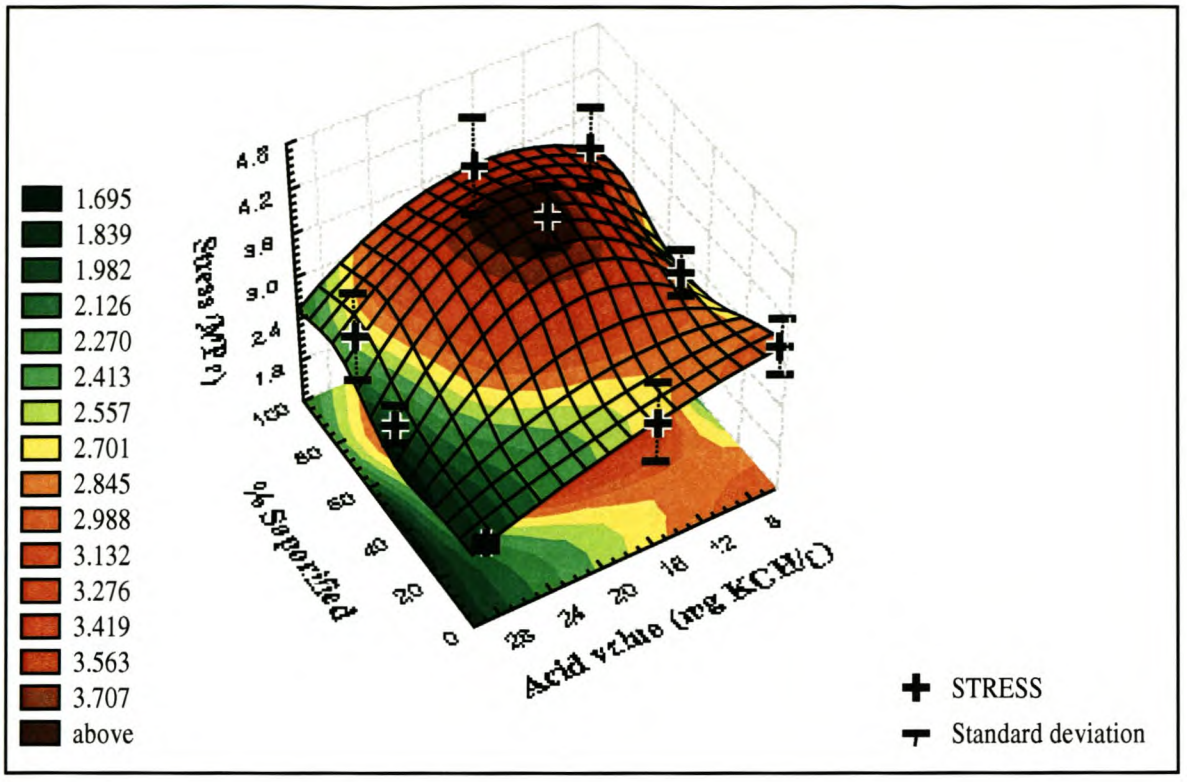

FIGURE 5.16 : Li cation: Stress vs. % Saponified vs. Acid value

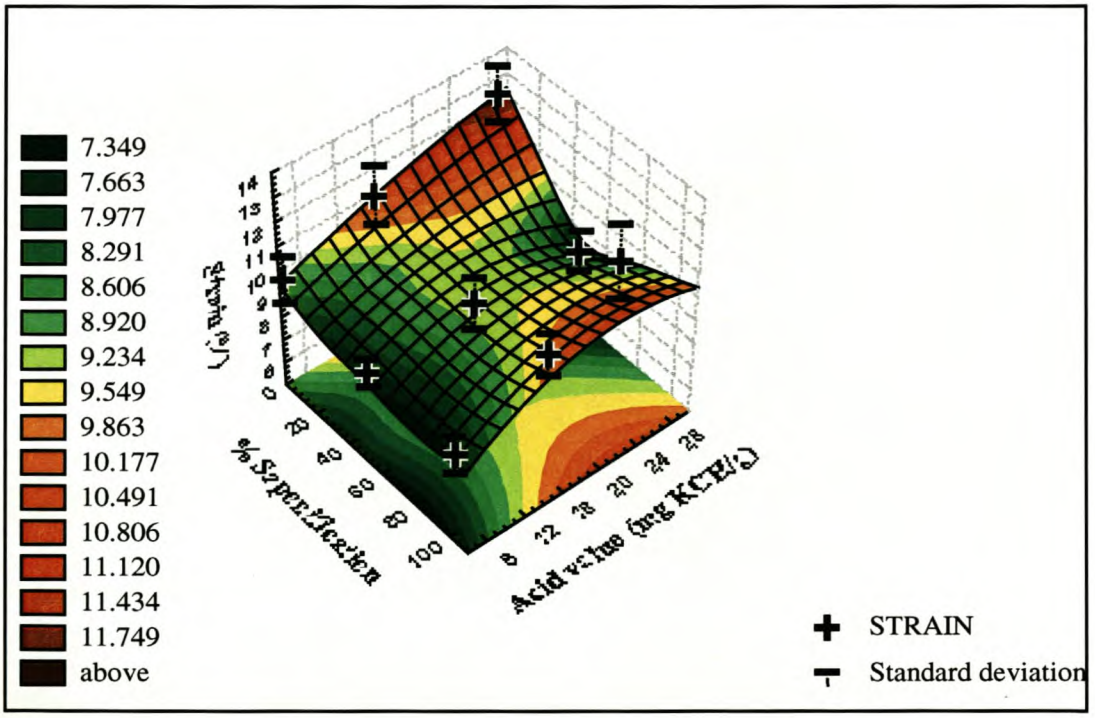

FIGURE 5.17 : Li cation: Strain vs. % Saponified vs. Acid value

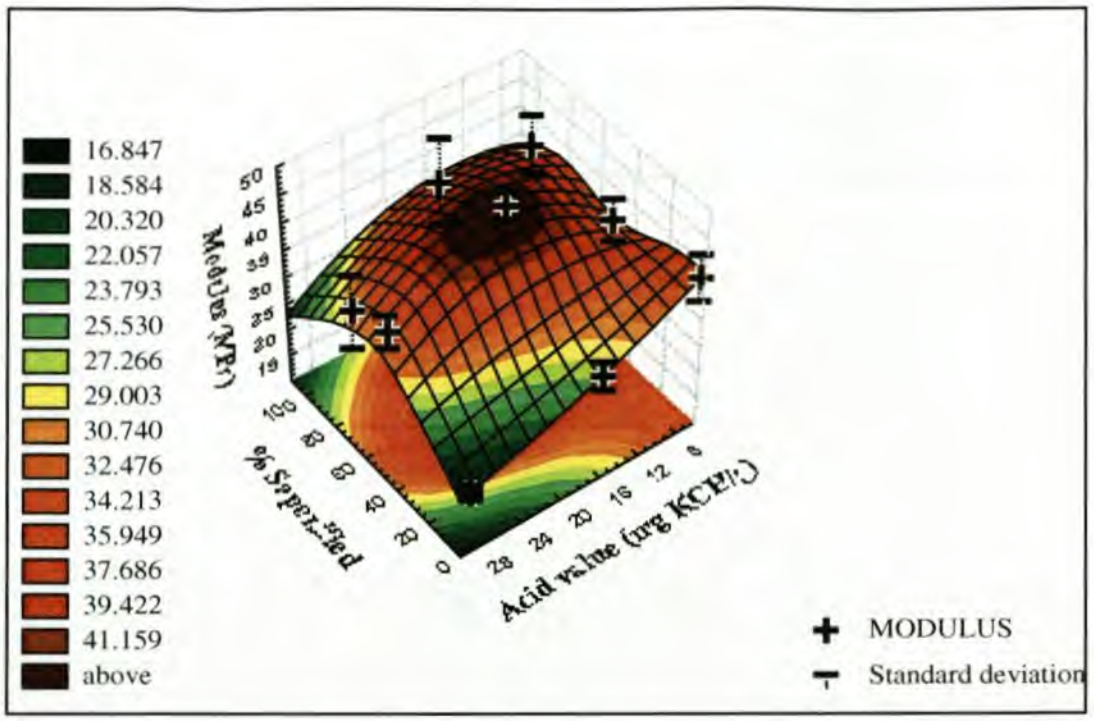

FIGURE 5.18 : Li cation: Modulus vs. % Saponified vs. Acid value

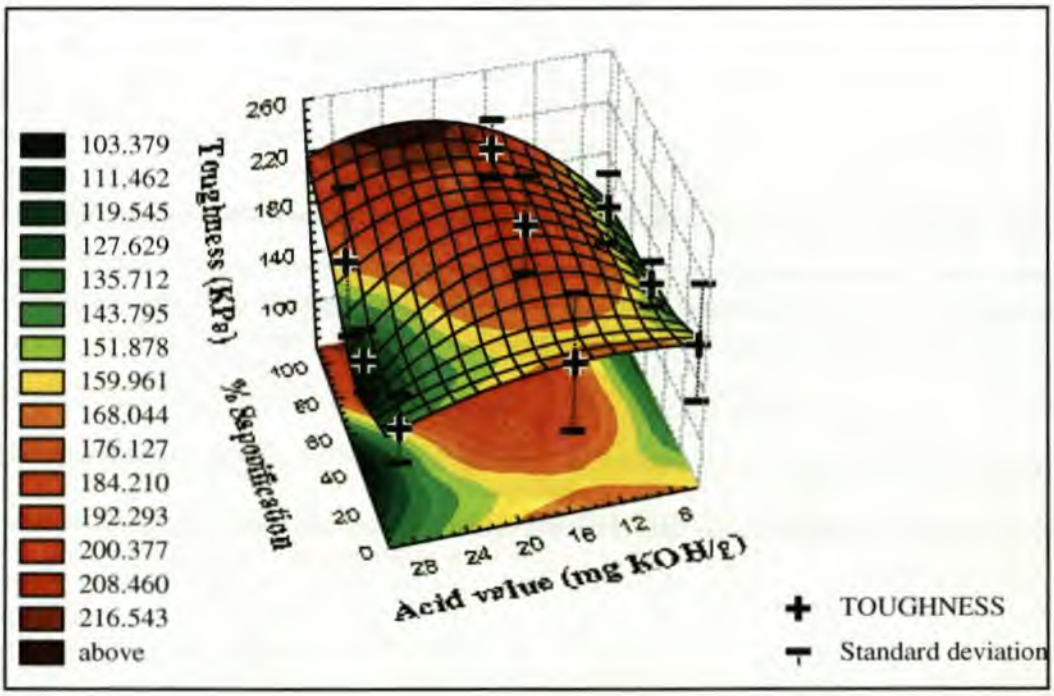

FIGURE 5.19 : Li cation: Toughness vs. % Saponified vs. Acid value

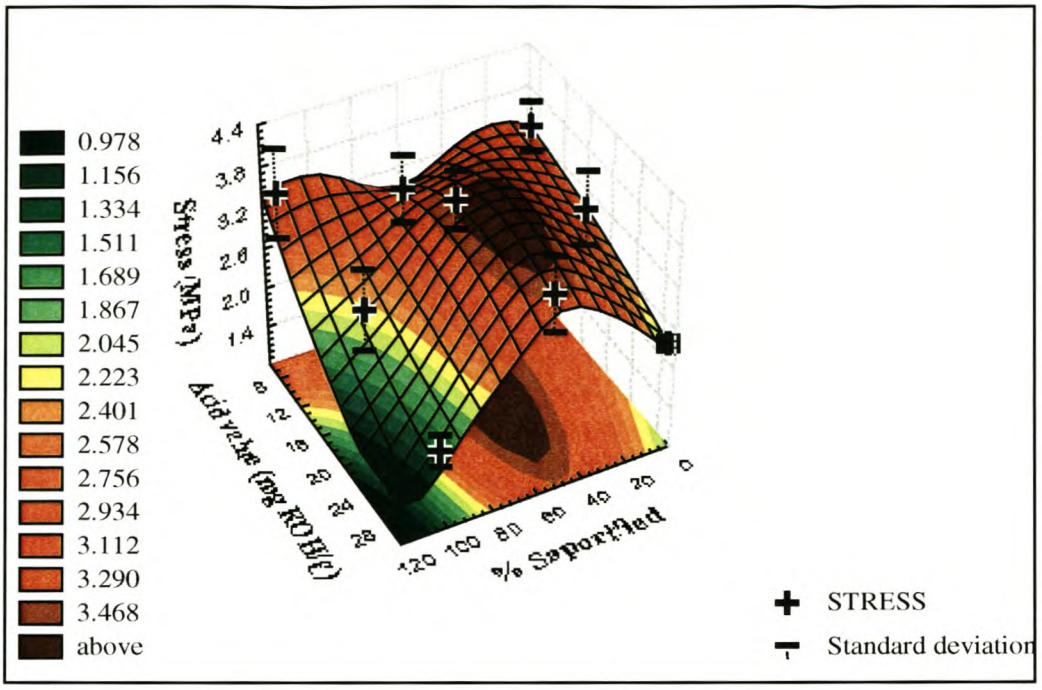

FIGURE 5.20 : Na cation: Stress vs. % Saponified vs. Acid value

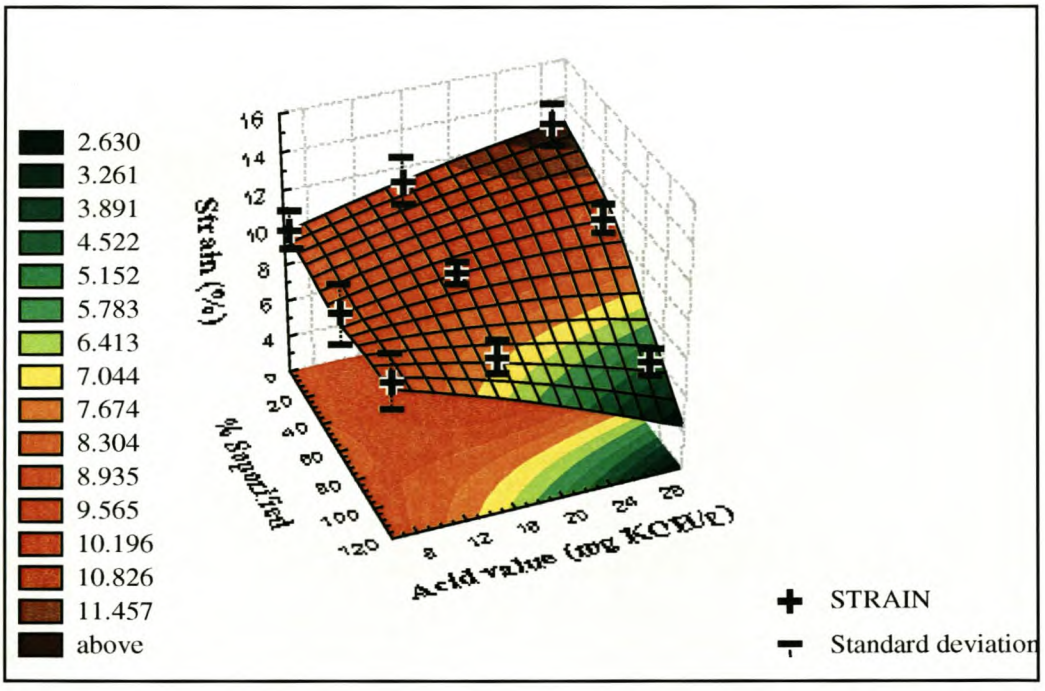

FIGURE 5.21 : Na cation: Strain vs. % Saponified vs. Acid value

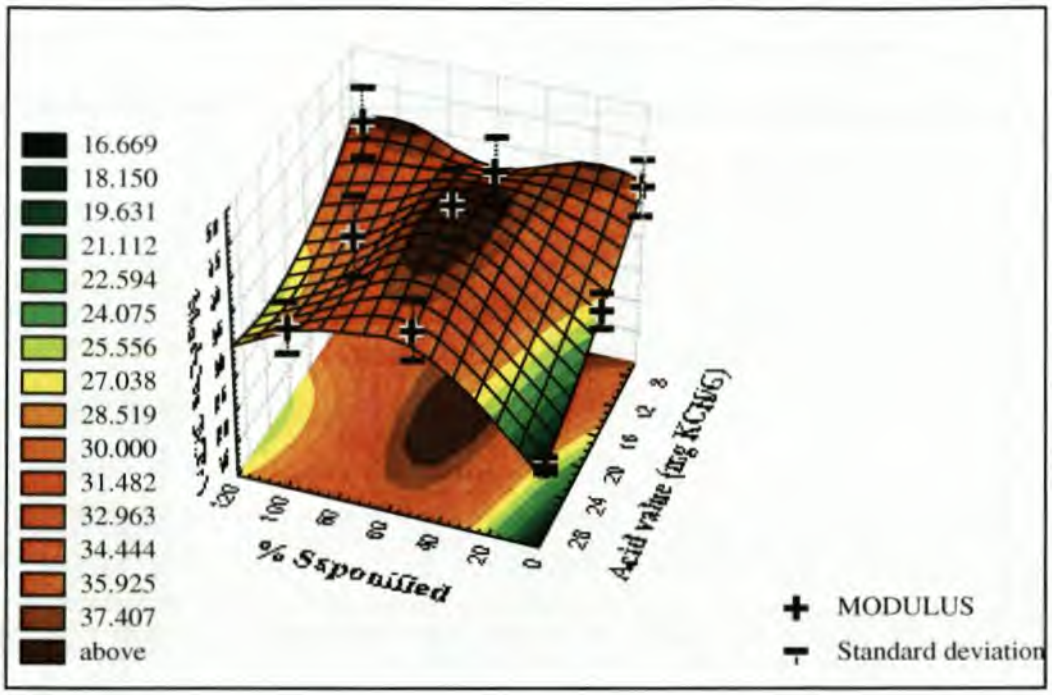

FIGURE 5.22 : Na cation: Modulus vs. % Saponified vs. Acid value

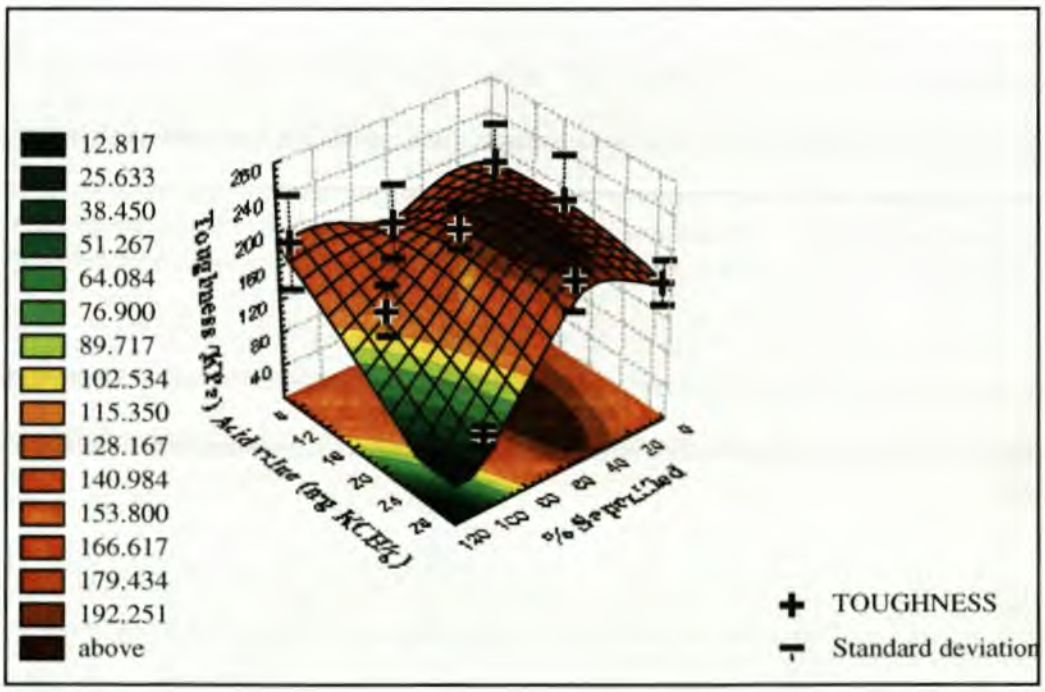

FIGURE 5.23 : Na cation: Toughness vs. % Saponified vs. Acid value

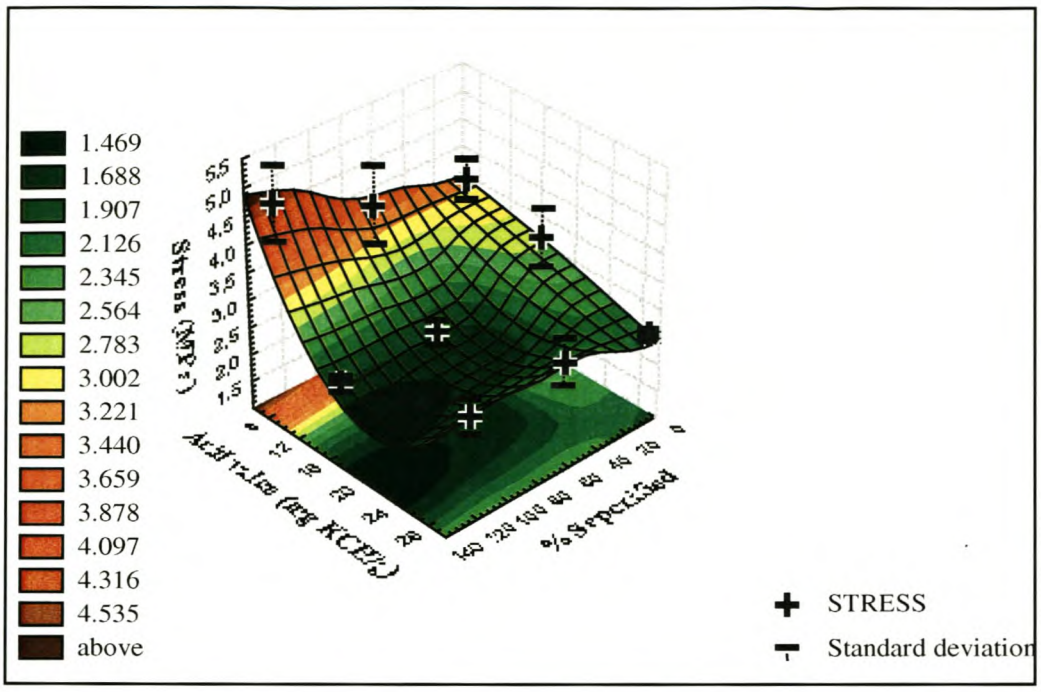

FIGURE 5.24 : K cation: Stress vs. % Saponified vs. Acid value

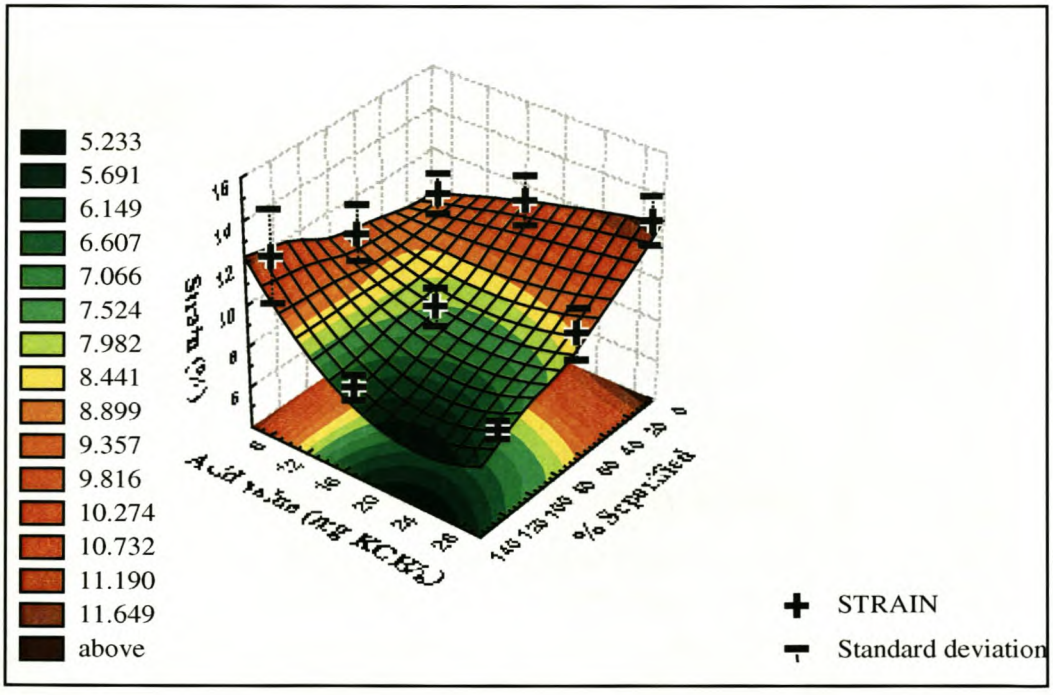

FIGURE 5.25 : K cation: Strain vs. % Saponified vs. Acid value

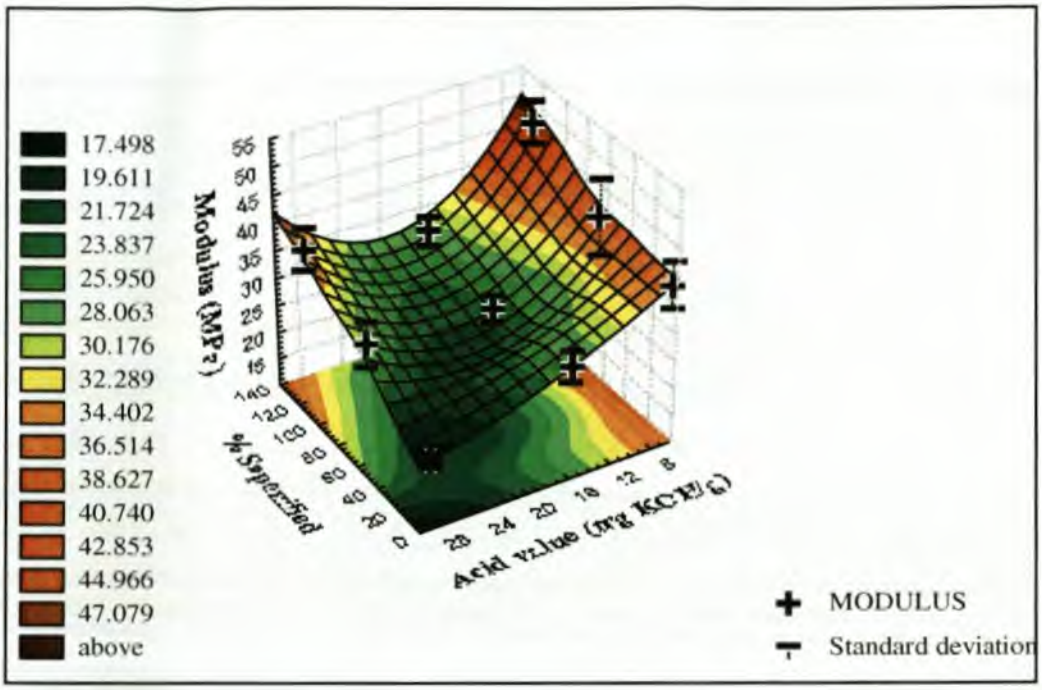

FIGURE 5.26 : K cation: Modulus vs. % Saponified vs. Acid value

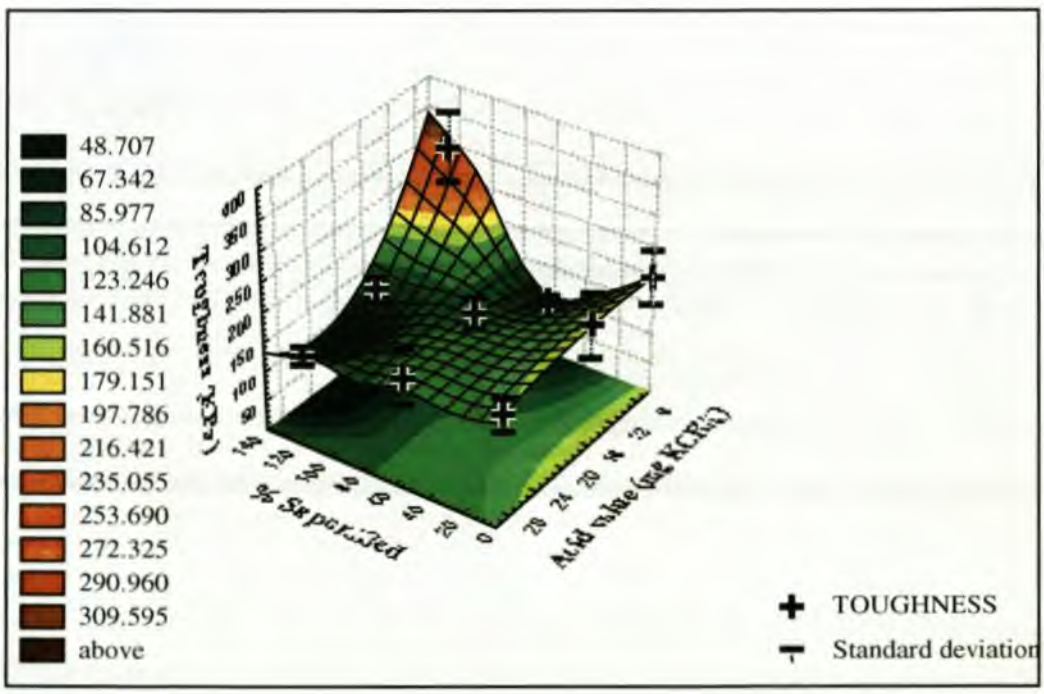

FIGURE 5.27 : K cation: Toughness vs. % Saponified vs. Acid value

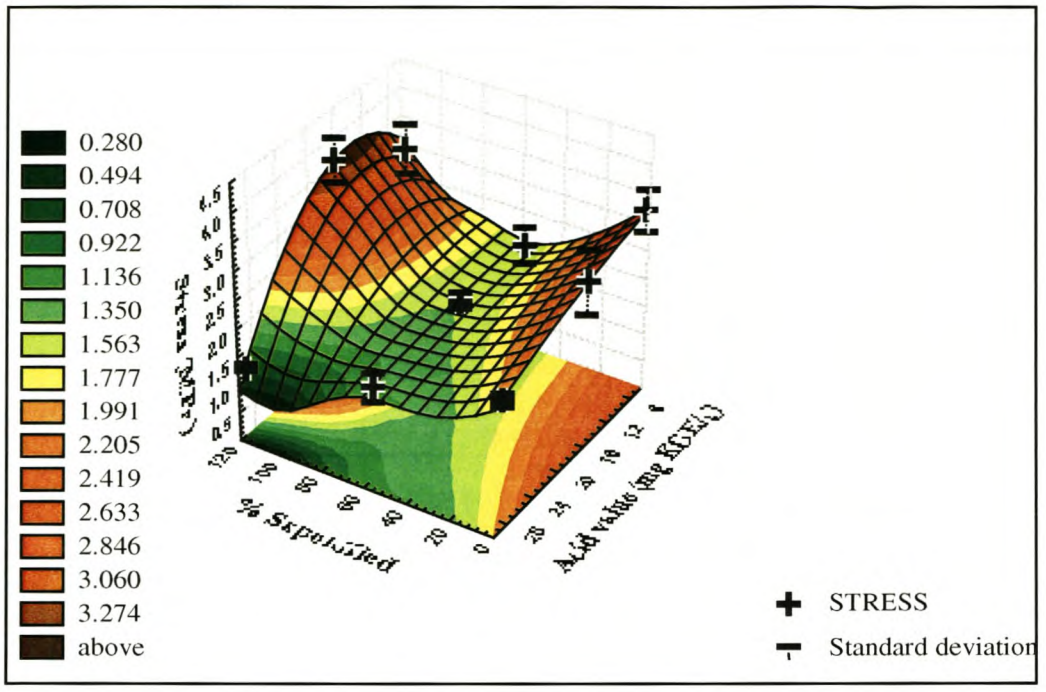

FIGURE 5.28 : Ca cation: Stress vs. % Saponified vs. Acid value

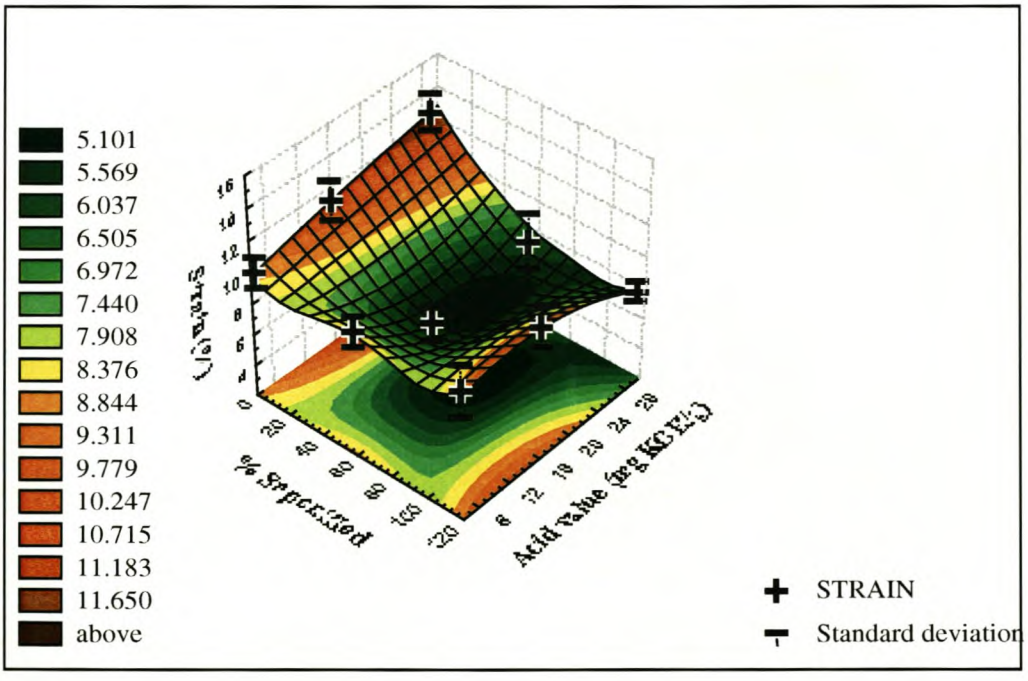

FIGURE 5.29 : Ca cation: Strain vs. % Saponified vs. Acid value

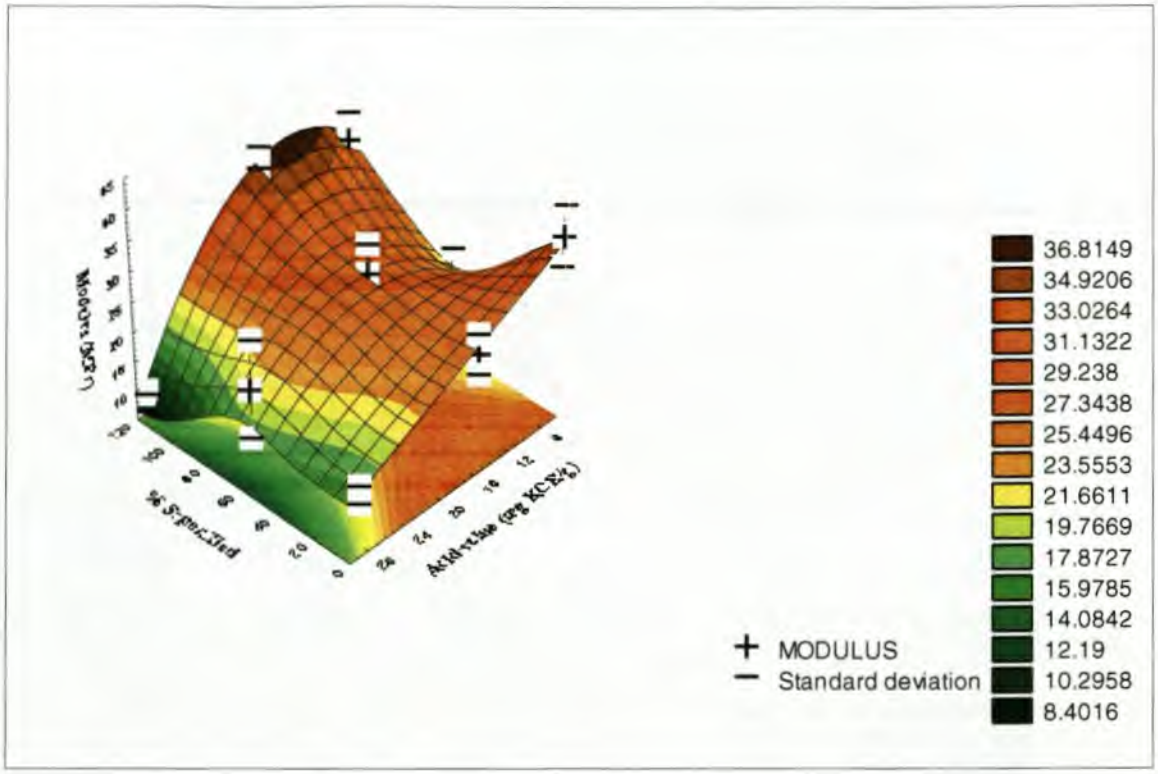

FIGURE 5.30 : Ca cation: Modulus vs. % Saponified vs. Acid value

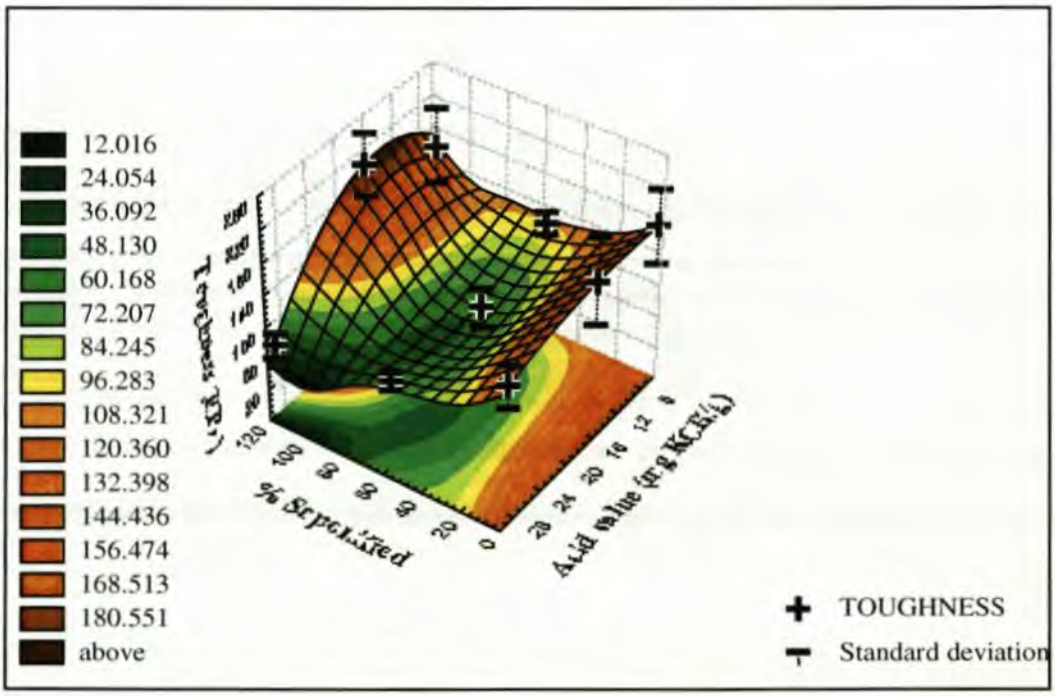

FIGURE 5.31 : Ca cation: toughness vs. % Saponified vs. Acid value

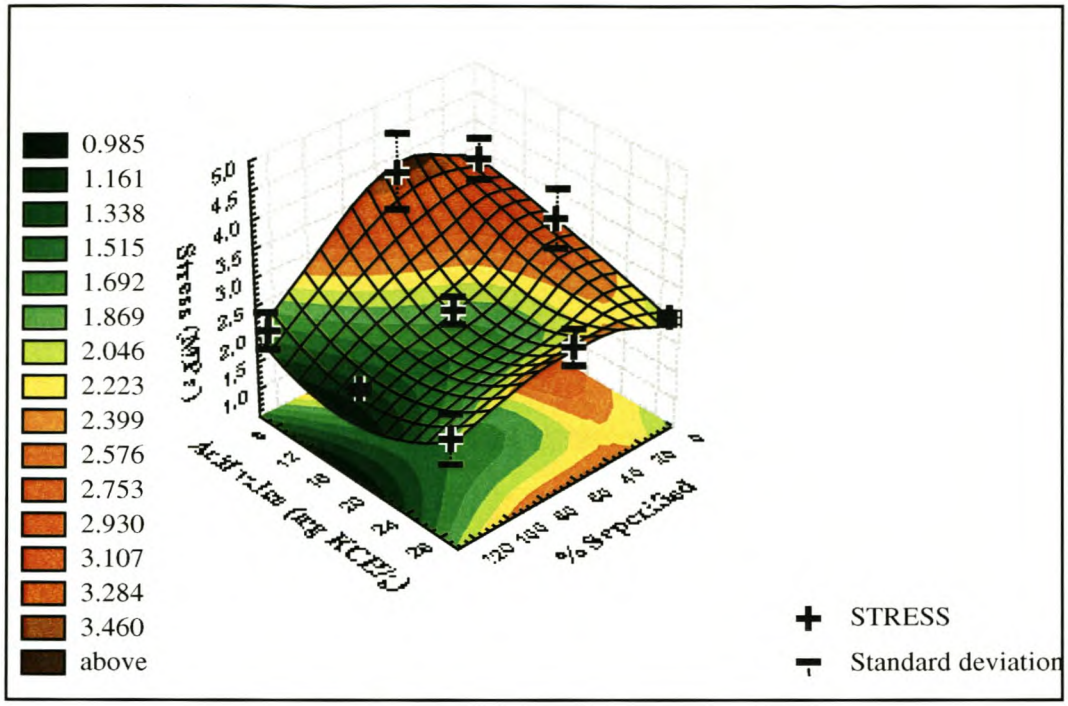

FIGURE 5.32 : Ba cation: Stress vs. % Saponified vs. Acid value

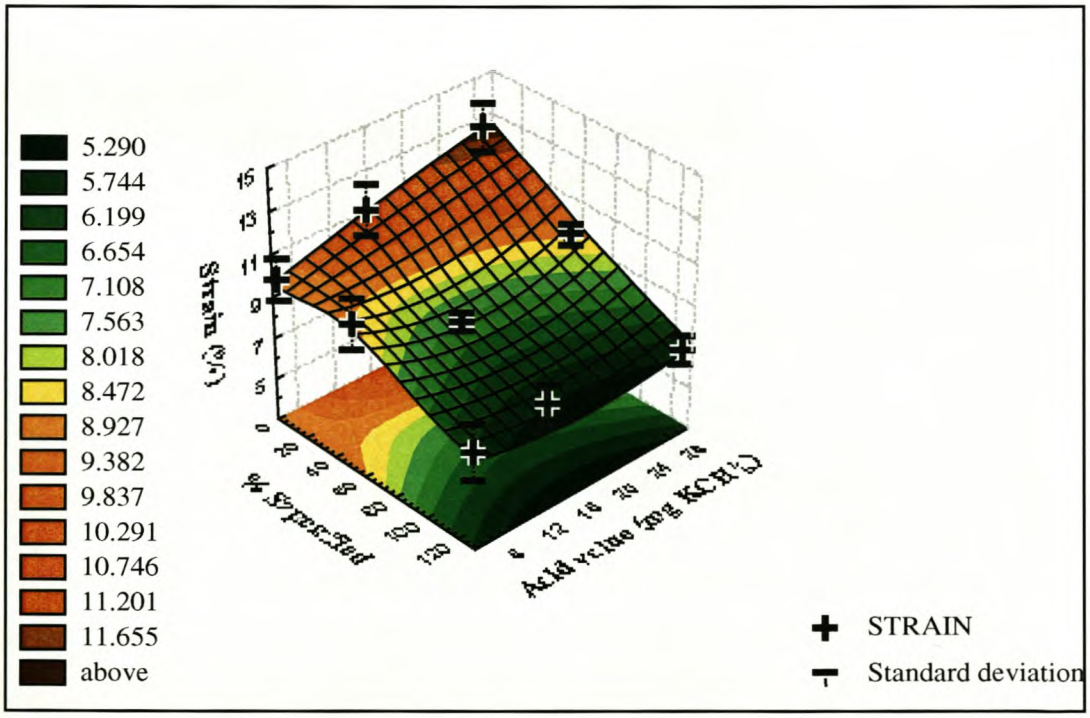

FIGURE 5.33 : Ba cation: Strain vs. % Saponified vs. Acid value

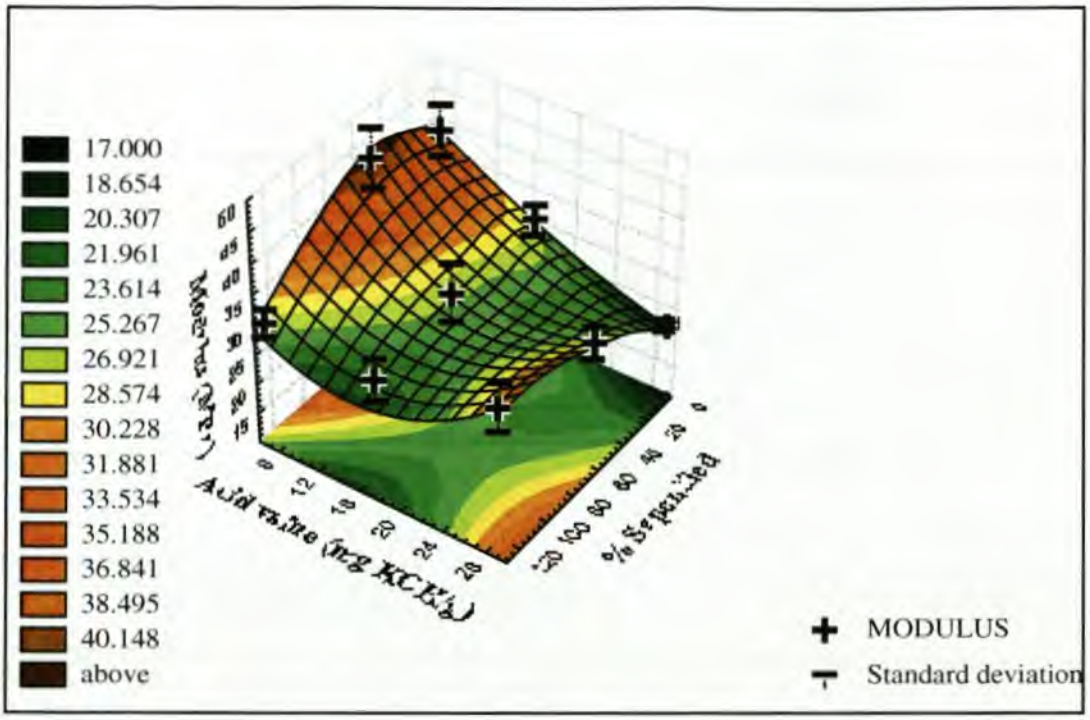

FIGURE 5.34 : Ba cation: Modulus vs. % Saponified vs. Acid value

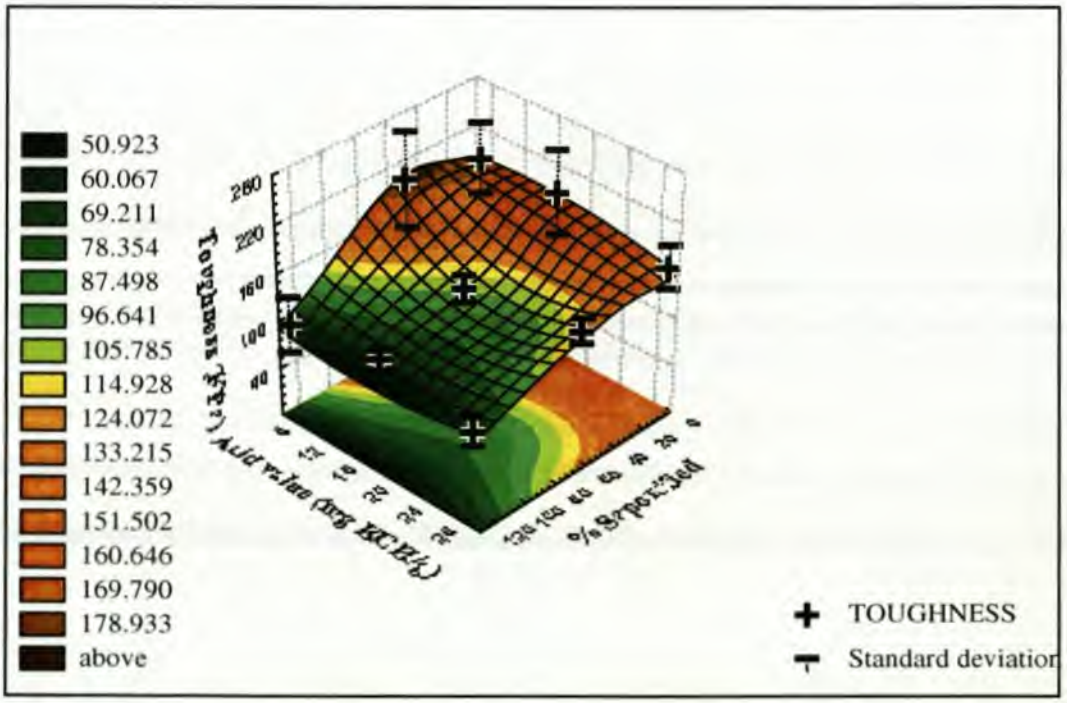

FIGURE 5.35 : Ba cation: Toughness vs. % Saponified vs. Acid value

TABLE 5.6 summarises the observations made from the above graph FIGURES 5.16 to 5.35).

TABLE 5.6
Summary of observations of the mechanical test results for the Fisher-Tropsch ionomeric waxes

CATION	OBSERVATIONS
Li cation	1. For the 0 % saponified samples; looking along the acid value axis, the tensile strength decreases, the strain increases and the modulus decreases with increasing acid value. The toughness remains more or less the same. This could be expected, as the crystallinity is likely to decrease with higher acid values, resulting in the above observations. 2. WAX 6 (6.5 mg KOH/g acid value) does not show significant changes with saponification. The tensile strength, strain, modulus and toughness all remain more or less the same. 3. WAX 16 (16.0 mg KOH/g acid value) at ca. 50 % saponification shows a decrease in strain and an increase in tensile strength, modulus and toughness. The ca. 100 % saponified sample shows a levelling off of changes when compared to the ca. 50 % saponified sample, except for the toughness, which seems to increase further. This is most likely due to the formation of multiplets. Cluster formation does not appear to be taking place. 4. Saponified WAX 28 samples seem to show the same trend as the WAX 16 samples.
Na cation	1. WAX 6 saponified samples do not show significant changes for any of the four mechanical test responses. This could possibly imply that the decrease in crystallinity with the increased degree of saponification is more or less compensated for by the formation of multiplets, causing the mechanical test responses to be more or less the same. 2. WAX 16 saponified samples show an increase in tensile stress, modulus and toughness for the ca. 50 % saponified sample while the ca. 100 % sample shows a decrease in tensile strength, modulus and toughness. The WAX 16 strain samples show a decrease in strain, going from the WAX 16, 0 % saponified sample to the ca. 100 % saponified sample. The above responses to the mechanical stresses applied could be explained by the assumption that for the ca. 50 % saponified sample, there is formation of multiplets in the sample, counteracting the decrease in crystallinity of the sample and increasing the "strength" of the sample. For the ca. 100 % saponified sample, however cluster formation is possible, with much more clearly defined boundaries between the clusters than when multiplets are formed. The areas between the clusters can however then be seen as weaker areas than the clusters themselves, acting as stress points and causing the samples to fail more quickly on stress induction. The assumption that there is cluster formation taking place in the ca. 100 % saponified sample is corroborated by the softening point results. 3. WAX 28 samples show the same trend as the WAX 16 samples, but the decrease in tensile strength, modulus and toughness for the ca. 100 % saponified versus the ca. 50 % saponified sample is more pronounced.

TABLE 5.6 (continue)
Summary of observations of the mechanical test results for the Fisher-Tropsch ionomeric waxes

CATION	OBSERVATIONS
K cation	1. WAX 6 samples show increases in tensile stress, strain, modulus and toughness with an increase in saponification value. This is most probably due to the formation of multiplets, which counteracts the decrease in crystallinity with an increase in saponification value. 2. WAX 16 samples, show a decrease in stress, modulus and toughness for the ca. 50 % saponified sample, which then flattens out for the ca. 100 % saponified sample. The strain results show a linear decrease with an increase in % saponified. The above results imply that the ca. 50 % saponified sample is already in the cluster phase and that the increased % saponification does not drastically change the morphology of the sample. This is not in total agreement with the softening point results, where it seems that cluster formation is prominent only for the ca. 100 % saponified sample. 3. There must therefore be other influences, such as test speed, playing an important part in the test results. 4. WAX 28 shows an increase in stress and modulus and a decrease in strain and toughness with increasing % saponification. From the above results, it is very difficult to say whether cluster formation is dominant or not.
Ca cation	1. WAX 6 shows an initial decrease in stress, modulus and toughness (for the ca. 50 % saponified sample) after which there is an increase in the stress, modulus and toughness values with increasing saponification values. The strain values stay more or less constant with increasing saponification values. This could possibly be due to an initial decrease in the crystallinity, after which the formation of multiplets results in the higher "strength" values. 2. WAX 16 shows an initial decrease in the stress, strain and toughness values (for the ca. 50 % saponified sample) after which there is an increase in the stress, strain and toughness values with increasing saponification values. The modulus values initially stay more or less constant with increasing saponification values. Subsequently there is an increase in modulus value (for the ca. 100 % saponified sample). The behaviour of WAX 16 samples is slightly different to that of WAX 6. I suspect that for WAX 16 the samples are initially weakened due to saponification, but that with further saponification, multiplets are formed which results in higher stress, strain and toughness values. In theory, the strain should decrease when the stress increases, but while multiplets are formed, crystallisation would be decreased which could cause the increase in strain with higher saponification values. 3. WAX 28 shows a decreasing trend for the stress, strain, modulus and toughness results with increasing saponification value. The only logical explanation for these results is that there is perhaps some multiplet formation taking place, but not to such an extent that the decrease in crystallinity (to produce a "weaker" wax) is overcome. Cluster formation must be non-existent.

TABLE 5.6 (continue)
Summary of observations of the mechanical test results for the Fisher-Tropsch ionomeric waxes

CATION	OBSERVATIONS
Ba cation	1. WAX 6 samples show an initial increase in stress, modulus and toughness with increasing saponification values (for the ca. 50 % saponified sample) after which the stress, modulus and toughness decrease in value. The strain shows a continued decrease in value with an increase in saponification value. These results are exactly opposite to the calcium cation results. The fact that the strain decreases implies that the sample must become more brittle. This would also imply a lower stress and modulus. It would thus appear that although multiplet formation must be prominent, the multiplets resist molecular movement to such an extent that the samples fail more quickly with mechanical testing. 2. WAX 16 samples show decreases in stress, strain and toughness with increasing saponification values. The modulus values remain essentially constant. The explanation for this is similar to that for WAX 6, ca. 100 % saponified sample. The multiplets formed resist movement to such a degree that the samples appear "weaker" on mechanical testing. 3. WAX 28 samples show no apparent change in stress up to ca. 50 % saponified sample, after which there is a decrease in stress to the ca. 100 % saponified sample. The strain and toughness, decrease with increasing saponification value. The modulus increases with increasing saponification value. The above is explained by the fact that there is multiplet formation, but that the multiplets are more pronounced than for WAX 16 samples, resulting in an increased modulus, but yet still giving lower stress results due to brittleness.

The graphs for the grafted waxes showing mechanical tests results vs. % saponified are shown below in FIGURE 5.36 to FIGURE 5.43.

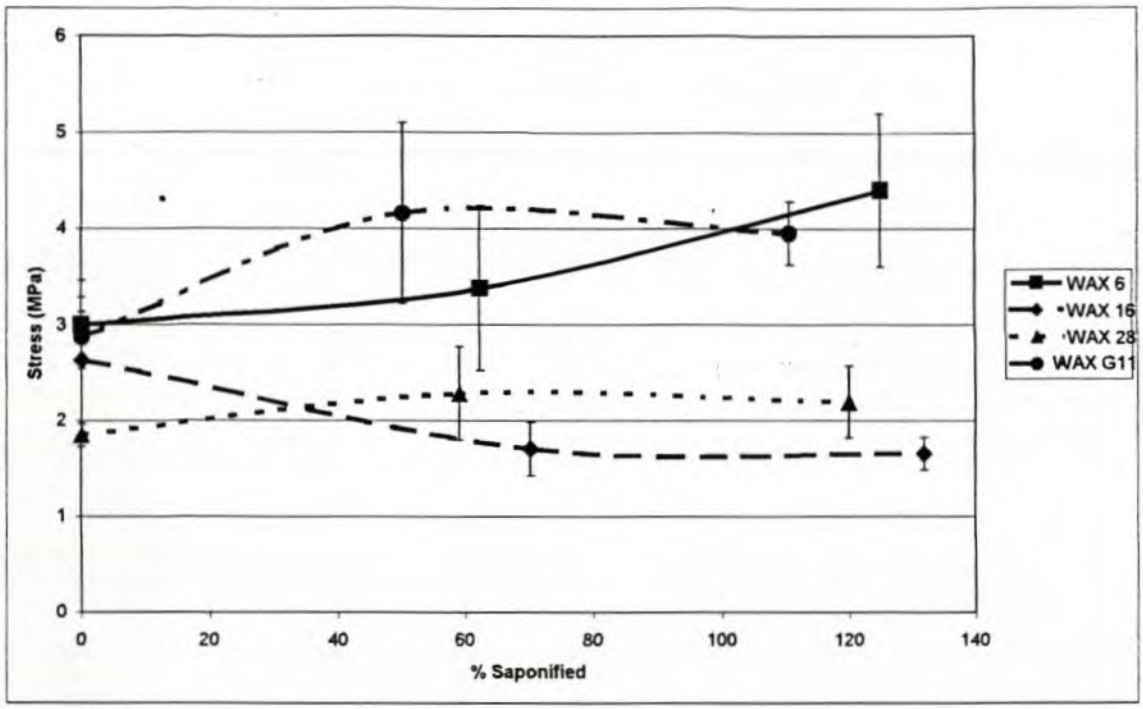

FIGURE 5.36 : K cation: Stress vs. % Saponified

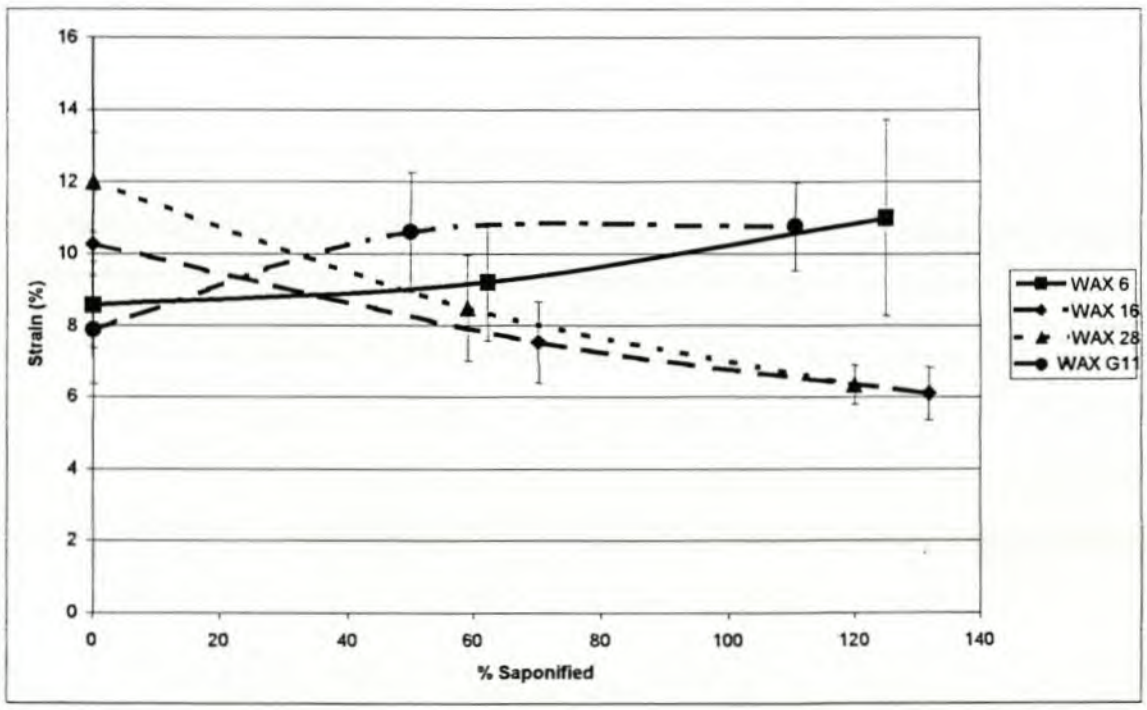

FIGURE 5.37 : K cation: Strain vs. % Saponified

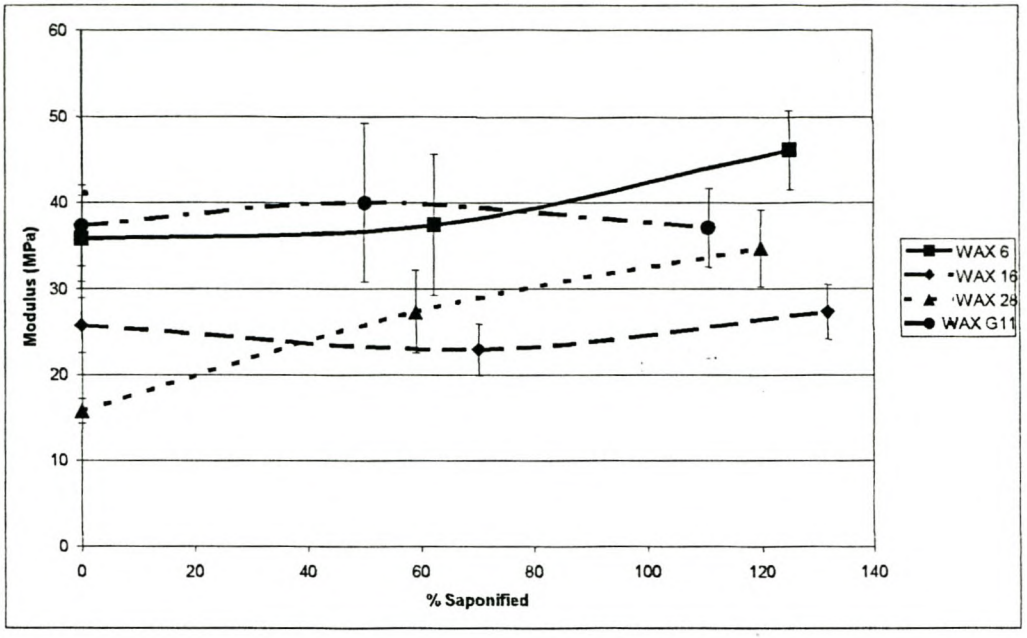

FIGURE 5.38 : K cation: Modulus vs. % saponified

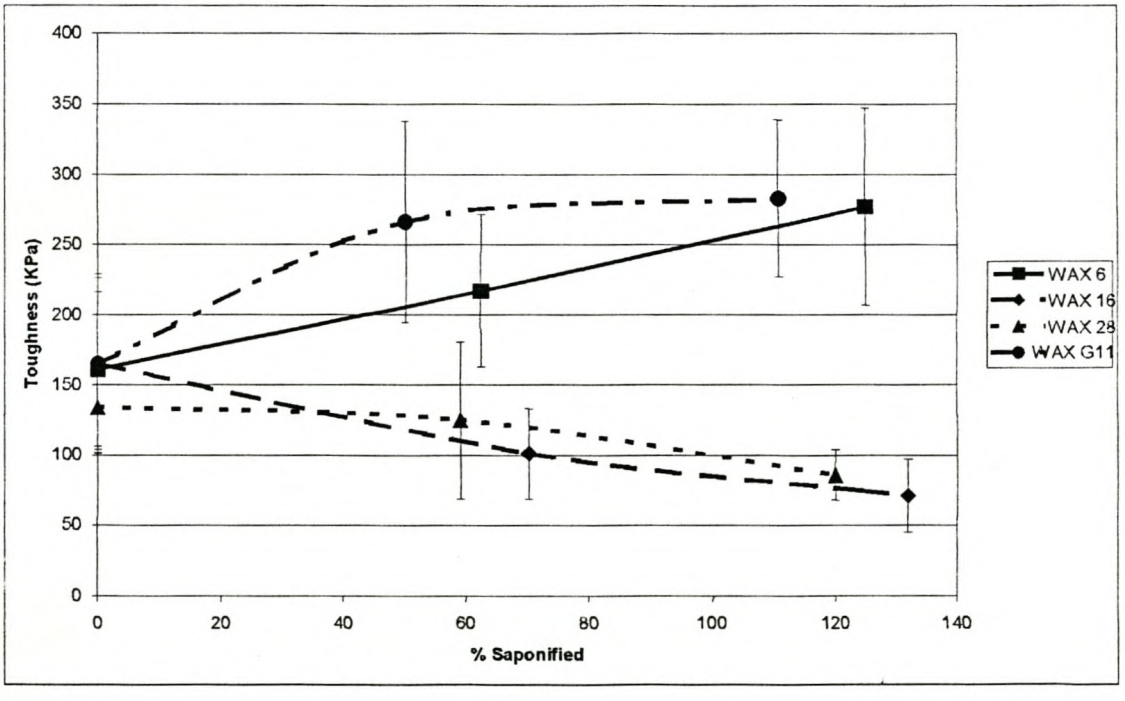

FIGURE 5.39 : K cation: Toughness vs. % saponified

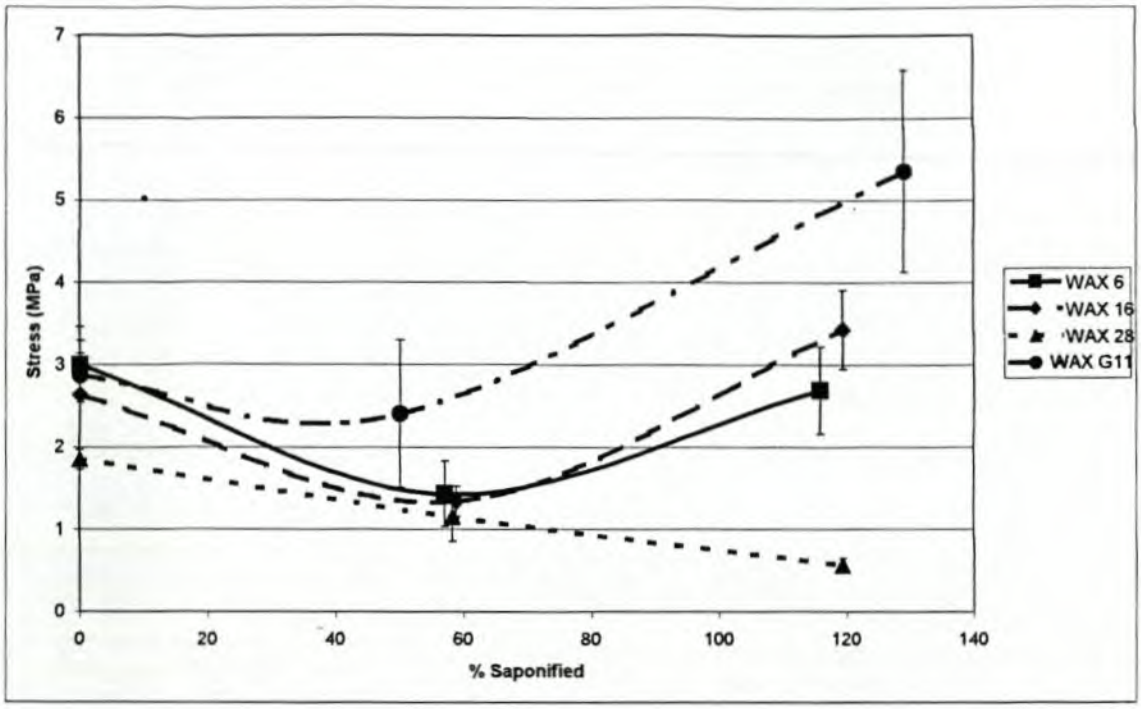

FIGURE 5.40 : Ca cation: Stress vs. % saponified

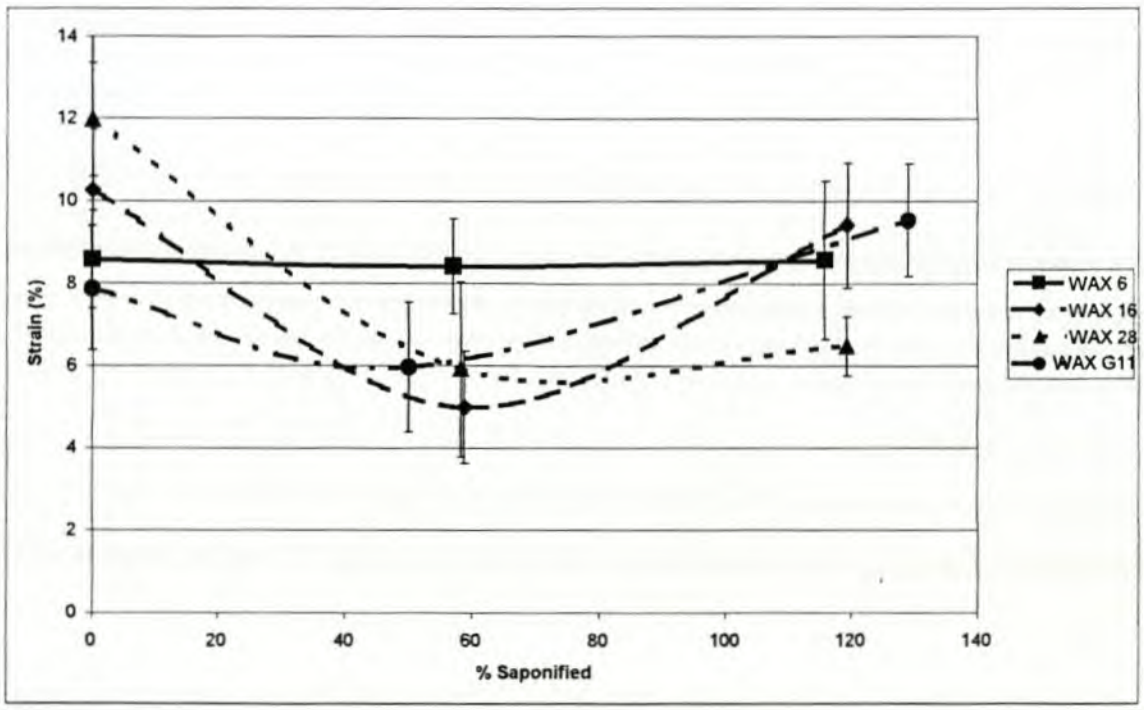

Figure 5.41 : Ca cation: Strain vs. % saponified

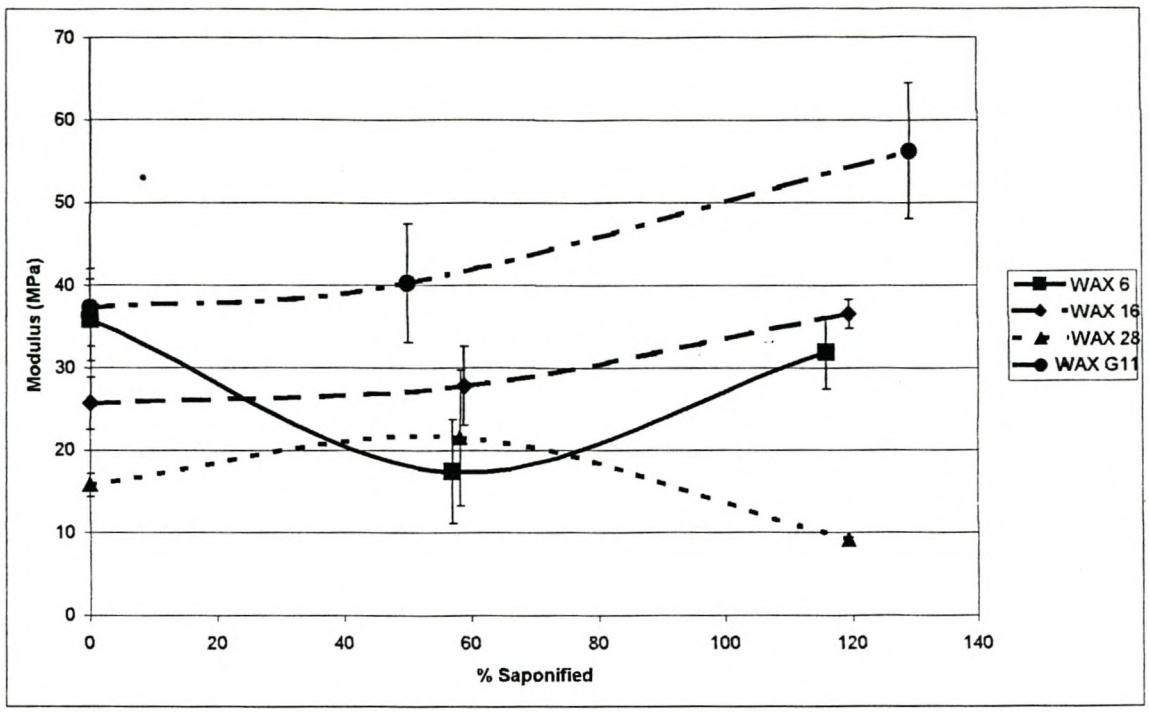

FIGURE 5.42 : Ca cation: Modulus vs. % saponified

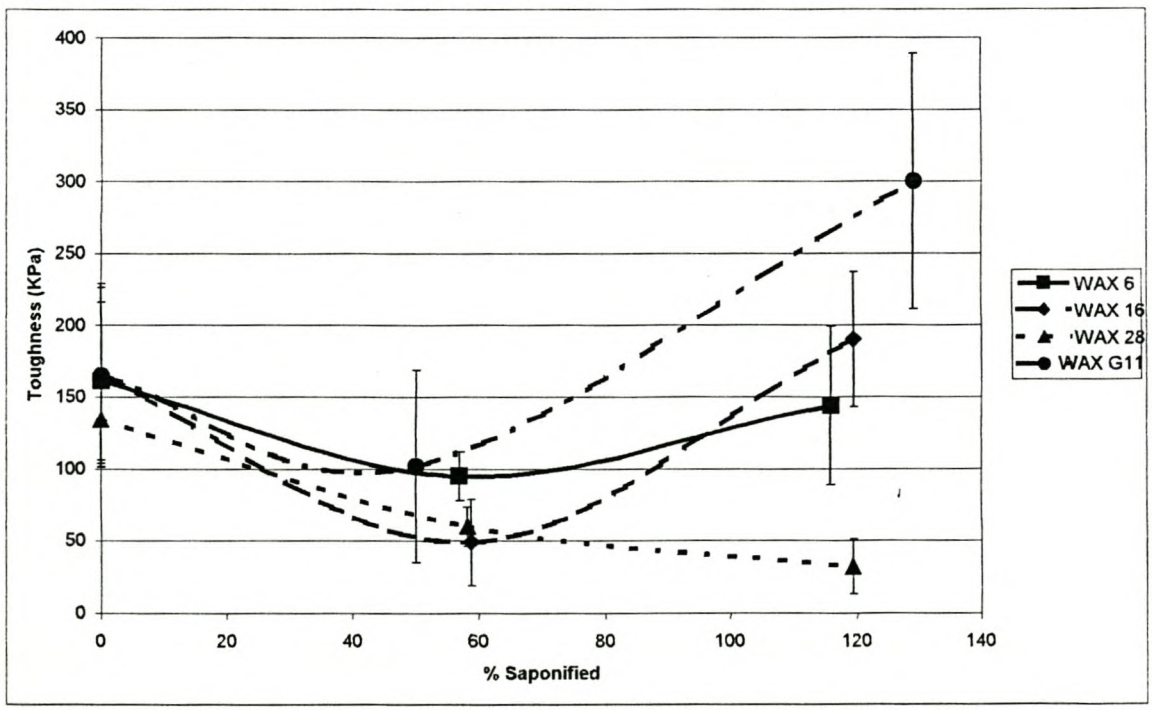

FIGURE 5.43 : Ca cation: Toughness vs. % saponified

A summary of the observations that can be made from the above graphs (FIGURES 5.36 to 5.43), is given in TABLE 5.7.

TABLE 5.7
Summary of observations of the mechanical test results for the Fisher-Tropsch ionomeric waxes

CATION	OBSERVATIONS
K cation	1. FIGURE 5.36 is very interesting because there does not seem to be any trend in the wax sample results. WAX 6 shows an increase in stress values as the % saponification increases. WAX 16 shows a decrease in stress values, flattening out from the ca. 50 % saponified sample to the ca. 100 % saponified sample. WAX 28 samples show very little change with an increase in saponification percentage, staying essentially horizontally unchanged. WAX G11 shows an increase in stress value with increasing saponification value up to the ca. 50 % saponified sample, after which the stress value essentially flattens out towards the ca. 100 % saponified sample. 2. FIGURE 5.37 shows that WAX 6 samples show increasing strain values with increasing saponification percentage values. WAX 16 and WAX 28 show decreasing strain values with increasing saponification values and WAX G11 shows an increase in strain value with increasing saponification value up to the ca. 50 % saponified sample, after which the strain value essentially flattens out towards the ca. 100 % saponified sample. 3. In FIGURE 5.38, WAX 6 and WAX 28 show increases in modulus with increasing saponification values, while WAX 16 and WAX G11 modulus values remain essentially unchanged with increasing saponification values. 4. FIGURE 5.39 shows that WAX 6 and WAX G11 show an increase in toughness values for an increase in saponification value, while WAX 16 and WAX 28 show a decrease in toughness values for an increase in saponification values. 5. What can one conclude from the above observations? It would appear that the mechanical test responses above show a trend as to the molar % acid available and the molar % cation with which saponification takes place. The higher the molar % cation, the more the sample is inclined to show brittleness, which gives lower stress and strain results. This would imply that the spread of multiplets and clusters throughout the sample is important for the response to mechanical testing.

TABLE 5.7 (continue)
Summary of observations of the mechanical test results for the Fisher-Tropsch ionomeric waxes

CATION	OBSERVATIONS
Ca cation	1. FIGURE 5.40 shows the same trend for WAX 6, WAX 16 and WAX G11. All these waxes show an initial decrease in stress up to the ca. 50 % saponified sample, after which the stress increases with an increasing saponification value up to the ca. 100 % saponified sample. WAX G11 shows a marked increase from the ca. 50 % saponified sample to the ca. 100 % saponified sample. WAX 28 shows a continuous decrease in stress with an increasing saponification value. 2. In FIGURE 5.41, WAX 6 shows no change in strain with an increasing saponification value. WAX 16 and WAX G11 show the same pattern in strain that was seen for the stress results (FIGURE 5.40). WAX 28 shows a decrease in strain with an increasing saponification value, flattening from the ca. 50 % saponified sample to the ca. 100 % saponified sample. 3. For the modulus graph (FIGURE 5.42) WAX 16 and WAX G11 show the same trend: an increase in modulus with an increasing saponification value. WAX 6 initially shows a decrease in modulus with an increasing saponification value after which the modulus increases to the ca. 100 % saponified sample. WAX 28 is just the opposite of WAX 6. Initially an increase in modulus is seen, after which a decrease in modulus follows with increasing saponification values. 4. FIGURE 5.43 shows that for WAX 6, WAX 16 and WAX G11, the pattern is the same. An initial decrease in toughness is followed by an increase in the toughness with an increasing saponification value. WAX 28 shows a continuous decrease in toughness with increasing saponification value. 5. For the calcium saponified samples, the trend seems to be that the samples, for low molar % cation concentration show a decrease in "strength" after which the samples show an increase in stress and toughness values. WAX 28, which starts out with a high molar % cation value for the ca. 50 % saponified sample is "brittle" and thus gives lower values for stress, strain, modulus and toughness. This trend then continues for the ca. 100 % saponified sample. WAX G11 shows more or less the same trend in mechanical tests that was shown by WAX 6.

I did one more analysis of the mechanical test results. I assumed that the initial oxidation value has an influence on the mechanical response. If one then takes the initial acid groups and their corresponding mole percentage acid value and adds the mole percentage cation, creating a shift effect on the corresponding graph, would one more clearly understand the mechanical analysis results? The graphs for the shifted modulus results are shown below in FIGURES 5.44 to 5.47.

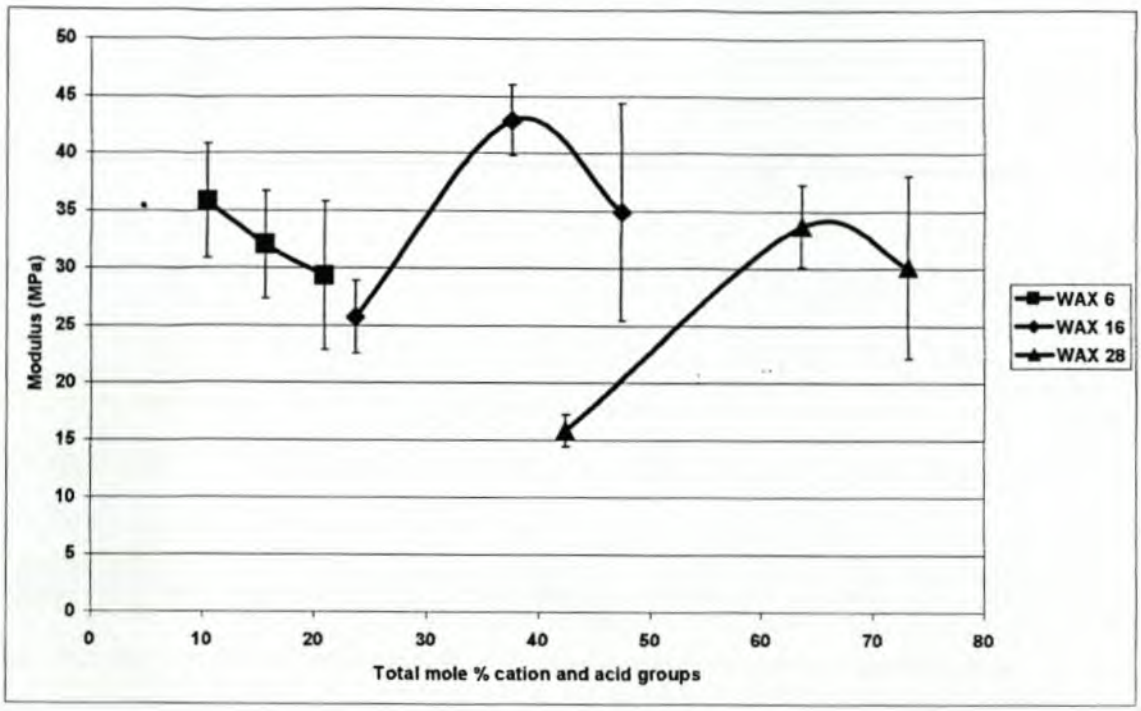

FIGURE 5.44 : Li cation: Modulus vs. Total mole percentage cation and acid groups

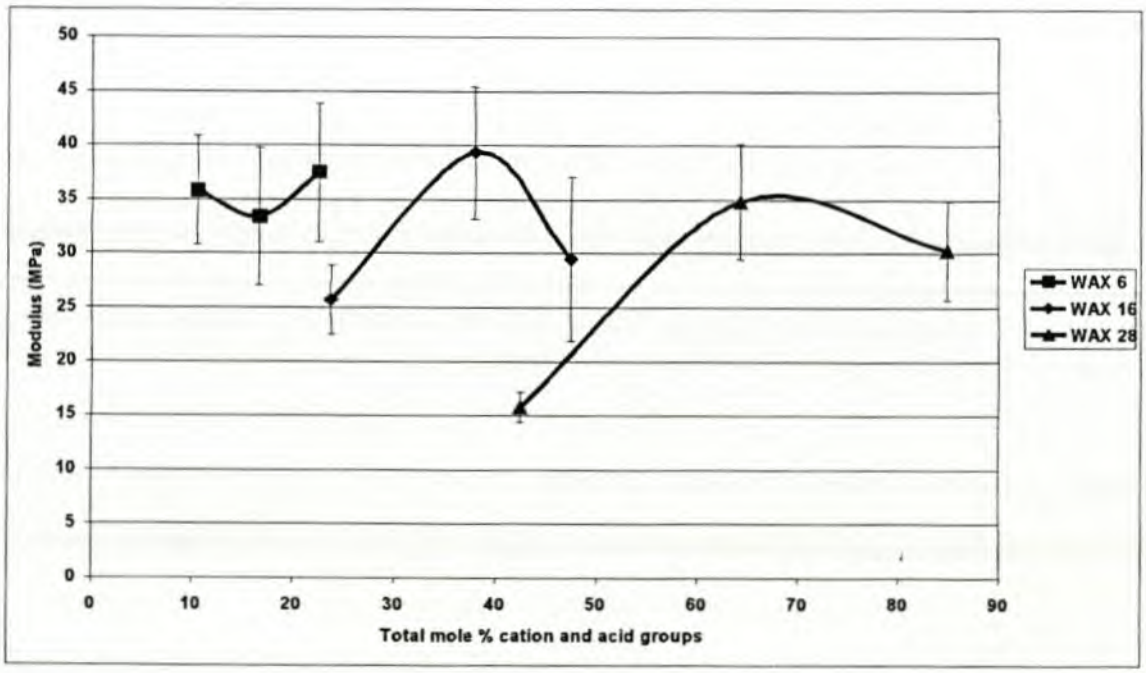

FIGURE 5.45 : Na cation: Modulus vs. Total mole percentage cation and acid groups

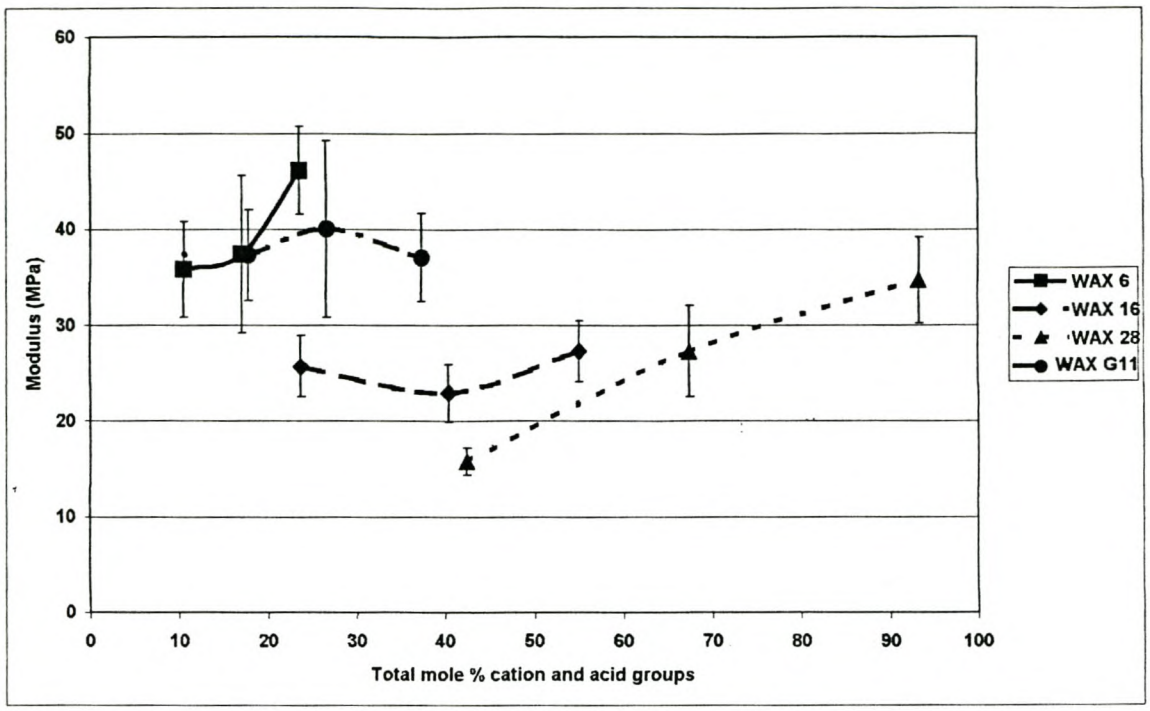

FIGURE 5.46 : K cation: Modulus vs. Total mole percentage cation and acid groups

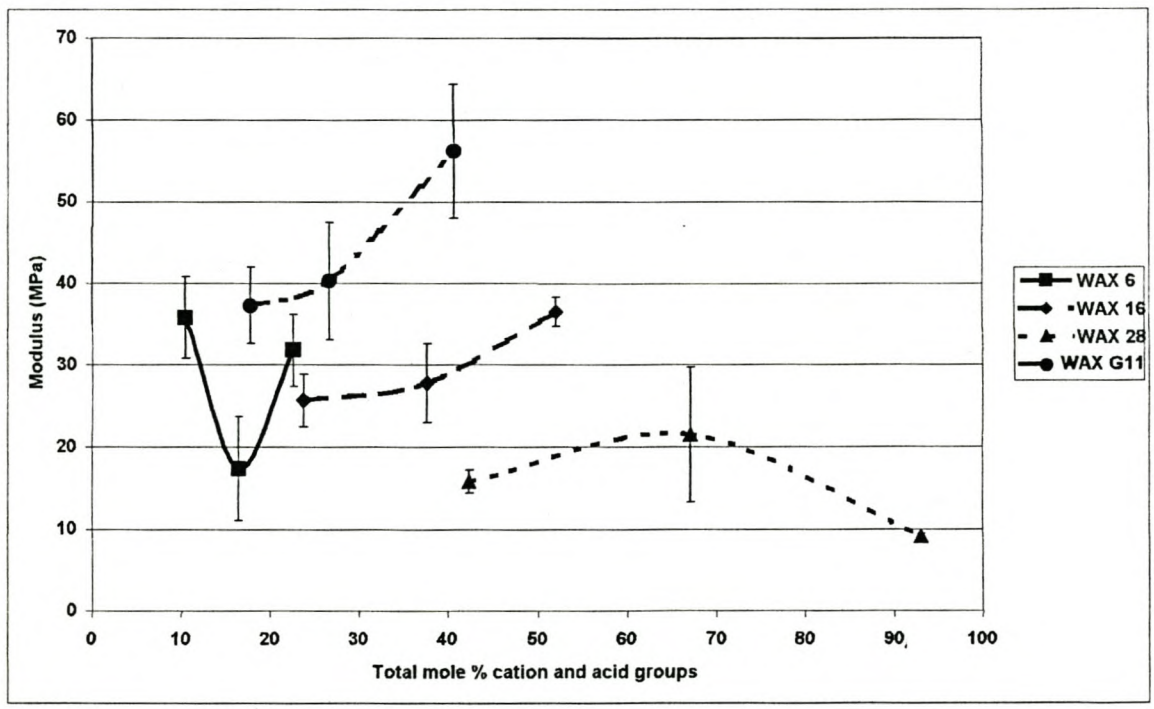

FIGURE 5.47 : Ca cation: Modulus vs. Total mole percentage cation and acid groups

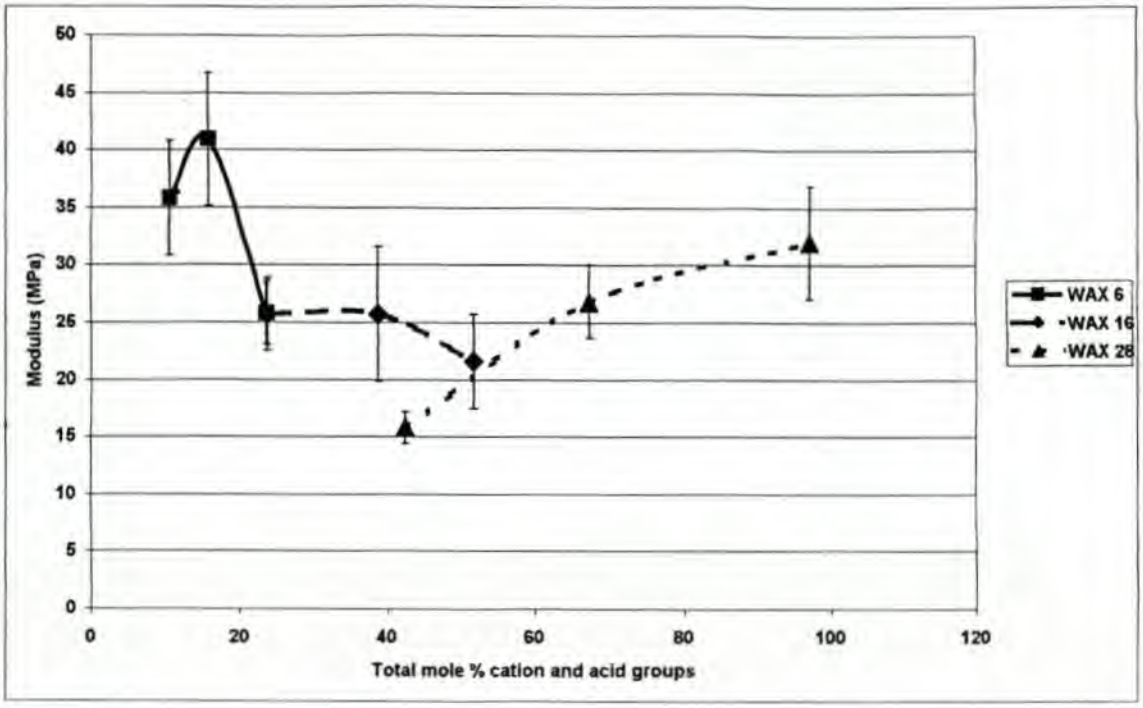

FIGURE 5.48 : Ba cation: Modulus vs. Total mole percentage cation and acid groups

The above graphs show that the effect of each cation is different w.r.t. the mechanical test results. None of the graphs above show exactly the same pattern for the various cations. The literature quoted in Chapter 2 with respect to mechanical properties (references 29, 76, 124 and 163) also concludes that each cation has a different effect on the ionomers tested. In the above references, polymers were used which were relatively simple and not as complex as the waxes that I used for this thesis, which makes it even more difficult to draw conclusions.

5.5.3 Summary of mechanical test results

The above results for the mechanical tensile tests seem inconclusive as to whether multiplet formation or cluster formation is dominant, if seen in isolation. If one looks at relative changes however, then there are patterns to observe.

First of all if one looks at the oxidised wax samples (WAX 6, WAX 16 and WAX 28), then from the values in Table 5.5, it can be seen that as the acid value increase, so the elongation increases, the maximum tensile strength decreases and the modulus decreases. The only significant change in these samples was the increase in oxidative groups, the decrease in

crystallinity and the increase in amorphous regions. The above relative changes thus make sense.

For the saponified samples, the picture is however more complex. As the wax samples increase in acid value and % saponified, there will be a decrease in crystallinity, an increase in amorphous regions, the formation of multiplets and clusters. The way to correlate the above changes as to the mechanical results is to look initially at the elongation in isolation. As the crystallisation decrease and the amorphous regions increase, the elongation increase for a sample. If this sample were to be saponified, the amorphous regions would first be filled with multiplets, causing a decrease in elongation values. If one had to still continue saponifying the sample, the multiplets would start growing in number and in size. This would then disrupt the crystalline regions, giving more amorphous regions and increasing the elongation. If you still kept on saponifying the sample, the multiplets would grow too significant amounts and cluster formation would take place. At this stage, the clusters would cause the sample elongation to decrease. In conjunction with the elongation results, the tensile strength results must also be considered. As a sample is saponified and the amorphous regions with acid and ester groups are saponified, the tensile strength will increase. As the sample is further saponified, the tensile strength can decrease or increase due to crystalline regions decreasing and multiplet formation increasing. As the sample is further saponified and the elongation decreases, the sample becomes brittle and tensile strength decreases. At this stage, cluster formation is predominant. Table 5.8 tabulates, for each sample, based on above principle of analysis, whether multiplet formation is predominant or whether cluster formation is predominant. In this table, in the maximum tensile strength and maximum elongation columns, the letters I (for increase in value versus the previous value), L (for more or less similar values relative to the previous value) and D (for decrease in value relative to the previous value) are used. Taking the values in Table 5.5, I compared the values in sequence in a column. Thus as an example, for WAX 6, Li cation, the maximum elongation column, the WAX 6 value for maximum elongation is 8.6 %. The next value in the column, 7.6 % is lower than the value 8.6 % and the last value for Li, 7.4 % is more or less similar to the previous value if you take the standard deviation in Appendix 5.2 into account. The rest of the table works on the same principle. Now for the last column, I have taken the analysis principle explained above and deduced whether multiplet of cluster formation is predominant. All the cation ca. 50 % saponified samples were relatively compared to the WAX 6, WAX 16, WAX 28 and WAX G11 samples. For the table below, I also looked at, relatively speaking, the changes taking place between the

different wax groups (WAX 6, etc.) for the same cation. Where the symbol M/C is shown, it means that I am not sure whether multiplet or cluster formation is predominant.

TABLE 5.8
Summary of the mechanical test results showing whether multiplet or cluster formation is predominant

Oxidised wax	Cation	% Saponified	Max. Tensile strength	Max. Elongation	Predominantly multiplet or cluster formation
WAX 6		0	***	***	***
	Li	50.0	D	D	M
		100.0	I	L	M
	Na	59.3	D	L	M
		115.0	I	L	M
	K	62.3	I	L	M
		125.0	I	I	M
	Ca	57.0	D	L	M
		115.8	I	L	M
	Ba	50.0	I	L	M
		126.0	D	D	C
WAX 16		0	***	***	***
	Li	58.7	I	L	M
		100.0	D	L	M
	Na	59.9	I	D	M
		100.0	D	D	C
	K	70.2	D	D	M/C
		131.9	L	D	C
	Ca	58.8	D	D	M
		119.4	I	I	M
	Ba	63.3	D	D	C
		117.9	D	D	C
WAX 28		0	***	***	***
	Li	50.0	L	D	M
		72.5	I	I	M/C
	Na	51.4	I	D	M
		100.0	D	D	C
WAX 28	K	59.0	I	D	M
		119.9	L	D	C
	Ca	58.2	D	D	M
		119.3	D	I	M
	Ba	58.8	I	D	M
		118.8	D	D	C
WAX G11		0	***	***	***
	K	50.0	D	D	M
		110.7	L	L	M/C
	Ca	50.0	D	D	M
		129.1	I	I	M

To test the above results, I have, in this chapter's summary, compared the other test results from the penetration tests, the impact tests and softening point tests in one table to summarise whether multiplet formation or cluster formation is predominant.

One last thought is that if one did stress relaxation tests at constant stress, instead of tensile tests, one could possibly have learnt more. I think that the test speed of 0.5 mm/min is still too high to really show the morphological changes taking place in the wax. If one also had an idea at where multiplet formation and cluster formation took place, one could zoom into a smaller experimental area and choose the samples to give responses where the possible transitions take place.

5.6 Chapter 5 summary

A summary of all the results of this chapter is given in Table 5.9, shown below. In this table I show all the results with respect to whether the individual samples have formed predominantly multiplets or predominantly clusters. Where I am uncertain, a M/C symbol is shown meaning that cluster formation is possible. The symbol ND implies that this sample was not tested.

TABLE 5.9

Summary of Chapter 5 results with respect to multiplet or cluster predominance

Oxidised wax	Cation	% Saponified	Penetration test results	Impact test results	Softening point results	Tensile test results
WAX 6	-	0	***	***	***	***
	Li	50.0	ND	ND	M	M
		100.0	ND	ND	M	M
	Na	59.3	ND	ND	M	M
		115.0	ND	ND	M	M
	K	62.3	ND	ND	M	M
		125.0	ND	ND	M	M
	Ca	57.0	ND	ND	M	M
		115.8	ND	ND	M	M
	Ba	50.0	ND	ND	M	M
		126.0	ND	ND	M	C
WAX 16		0	***	***	***	***
	Li	58.7	M/C	ND	M	M
		100.0	M/C	ND	M	M
	Na	59.9	M/C	ND	M	M
		100.0	M/C	ND	C	C
	K	70.2	M/C	ND	M	M/C
		131.9	M/C	ND	C	C
	Ca	58.8	M/C	ND	M	M
		119.4	M/C	ND	M	M
	Ba	63.3	M/C	M/C	M	C
		117.9	M/C	M/C	M	C
WAX 28		0	***	***	***	***
	Li	50.0	M/C	M/C	M	M
		72.5	M/C	M/C	C	M/C
	Na	51.4	M/C	M/C	M	M
		100.0	M/C	ND	C	C
	K	59.0	M/C	M/C	M	M
		119.9	ND	ND	C	C
	Ca	58.2	M/C	M/C	M	M
		119.3	M/C	M/C	M	M
	Ba	58.8	M/C	M/C	M	M
		118.8	M/C	ND	M/C	C
WAX G11		0	***	***	***	***
	K	50.0	ND	ND	M	M
		110.7	ND	ND	M	M/C
	Ca	50.0	ND	ND	M	M
		129.1	ND	ND	M	M

The above results as a whole correlate each other, but for the Ba cation results where the softening point and mechanical analysis results are not in agreement for a few samples. This could be due to many factors, but the rheological results of the next chapter will be used to

correlate the results of Table 5.9 and thus define in which morphological state the samples are.

5.7 References

1. Macknight W J, Earnest JR T R, **J. Polym. Sci. Macromol. Rev.**, 16, pp44, 1981
2. Longworth R, **Developments in Ionic Polymers I**, Applied Science Publishers Ltd, Chapter 2, pp154, 1983
3. Macknight W J, Lundberg R D, **Rubber Chem. Technol.**, 57(3), pp 652, 1984
4. Makowski H S, Lundberg R D, Westerman L, Bock J, **Advances in Chemistry**, 187, pp3, 1980
5. **Encyclopaedia of Polymer Science and Technology**, Interscience Publishers, John Wiley and Sons inc., New York, 6, pp426, 1964
6. Zhulina E B, Birshtein T M, **Macromolecules**, 28, pp1491, 1995
7. Plante M, Bazuin C G, Jerome R, **Macromolecules**, 28, pp 1567, 1995
8. Eisenberg A, Hird B, Moore R B, **Macromolecules**, 23, pp4098, 1990
9. Broze G, Jerome R, Teyssié P, Gallot G, **J. Polym. Sci. Polym. Lett. Ed.**, 19 pp415, 1981
10. Shohamy E, Eisenberg A, **J. Polym. Sci. Polym. Phys.**, 14 pp1211, 1976
11. Xie H, Ao Z, Guo J, J. **Macromol. Sci. Phys.**, B34(3), pp249, 1995
12. Bagrodia S, Pisipati R, Wilkes G L, Storey R F, Kennedy J P, **J. Appl. Polym. Sci.**, 29, pp3065, 1984
13. Takahashi T, Watanabe J, Minagawa K, Takimoto J, Iwakura K, Koyama K, **Rheol. Acta**, 34, pp163, 1995
14. Eisenberg A, **J. Polym. Sci. Polym. Symp.**, 45, pp99, 1974
15. Rees R W, Vaughn D J, **Polym. Prepr. Am. Chem. Soc. Div. Polym. Chem.**, 6, pp296, 1965
16. Fitzgerald J J, Weiss R A, **J. Macromol. Sci. Rev. Macromol. Chem. Phys.**, c28, pp99, 1988
17. Eisenberg A, **Inorg. Macr. Rev.**, 1, pp75, 1970
18. Kim Y, Ha C, Cho W, **Pollimo**, 18(5), pp737, 1994
19. Nishida M, Eisenberg A, **Macromolecules**, 29, pp1507, 1996
20. Otocka E P, Kwei T K, **Macromolecules**, 1, pp244, 1968
21. Rees R W, **USA Patent 3404134**, 1968
22. Rees R W, **USA Patent 3264272**, 1966
24. Tachino H, Hara H, Hirasawa E, Kutsumizu S, Yano S, **J. Appl. Polym. Sci.**, 55 (1), pp 134, 1995
25. Makowski H S, Lundberg R D, Westerman L, Bock J, **Advances in Chemistry Series, American Chemical Soc.**, 187, pp12, 1980

26. Mohajer Y, Bagrodia S, Wilkes G L, **J. Appl. Polym. Sci.**, 29, pp 1946, 1984

27. Bagrodia S, Tant M R, Wilkes G L, Kennedy J P, **Polymer**, 28, pp2212, 1987

CHAPTER 6: Ionomeric Fischer-Tropsch wax : Rheological properties

6.1 Introduction

Rheometry has been one of the more successful methods used to analyse ionomeric polymers in order to see cluster and multiplet formations [1-25] and it is a very sensitive method of analysis with respect to morphological changes [26-28]. The onset of multiplets and clusters has been deduced from rheometry results. I wanted to see in this chapter if I could deduce more about the morphology of ionomeric F-T waxes when studied through rheometry. This rheometry chapter was done in an attempt to verify the results of the previous chapters.

6.2 Background

There are many mathematical models describing the viscoelastic behaviour of polymers under stress, such as the Maxwell and Voigt models [29,30]. These models describe polymer response to stress as a spring and dashpot response. In the spring response, the polymer can store the energy exerted on it and then release the stored energy when the stress is removed. Hence the description as storage modulus (G'). The second component to induced stress, acts as a dashpot. This element acts as a damping resistance to the establishment of equilibrium of the spring element. The dashpot element is described as the loss modulus (G"). When a polymer, or in the case of this thesis an ionomeric wax, is subjected to a stress over a certain temperature range, the results are given as the storage modulus G', loss modulus G" and the loss tangent (Tan δ). The implication of the tests is to show that if one were to saponify a wax increasingly, the morphological structure of the wax would change and thus the transition associated with these structural changes would also be seen at different temperatures. One would thus be able to follow changes in the structure of the wax with increased saponification or oxidation, or with combinations of both. The effect of the types of cations should also be visible.

6.3 Experimentation and results

A Rheometrics ARES was used to analyse the ionomeric wax samples. The samples were cast in a rubber mould, 50 mm long, 3 mm thick and 10 mm wide. These samples were placed in a desiccator with silica gel to make sure that moisture did not play a role in the analysis of the samples. The temperature of analysis ranged from – 50 °C to about 80 °C

and the frequency of testing was kept constant at 1 Hz. The samples were analysed in duplicate and in triplicate if the results were not close enough in duplicate analysis. The average results are given in Appendix 6.1.

In analysing the experimental results, I took the G' peak temperature and value results, the G" first transition peak temperature and its values and the Tan δ transition temperature and value. The results of all the analyses are shown Appendix 6.1. I initially only worked with the Tan δ peak for this thesis (see Table 6.1 below), as this region is where multiplet and cluster transitions would most probably be seen. I also only looked at the oxidized wax samples in this part of the thesis, as there was not enough sample left of the grafted waxes by the time the rheometric experimentation was done.

The rheometric results for the tan δ values for the individual cations are shown in TABLE 6.1.

TABLE 6.1
Rheometric experimental results

Wax type	Cation type	% Saponified	Tan δ peak temperature (°C)	Tan δ peak value
WAX 6		0.0	13.8	0.088
	Li	50.0	7.5	0.086
		100.0	9.0	0.074
	Na	59.3	9.2	0.063
		115.0	7.2	0.072
	K	62.3	0.5	0.091
		125.0	7.5	0.072
	Ca	57.0	6.2	0.080
		115.8	6.6	0.091
	Ba	50.0	9.6	0.077
		126.0	7.9	0.091
WAX 16		0.0	9.2	0.105
	Li	58.7	9.6	0.084
		100.0	8.9	0.075
	Na	59.9	5.9	0.072
		100.0	6.3	0.055
	K	70.2	7.0	0.084
		131.9	7.0	0.071
	Ca	58.8	4.0	0.077
		119.4	8.0	0.075
	Ba	63.3	7.3	0.084
		117.9	9.6	0.078
WAX 28		0.0	-12.1	0.094
	Li	50.0	-3.0	0.071
		72.5	0.6	0.067
	Na	51.4	-3.7	0.068
		100.0	4.2	0.057
	K	59.0	-0.7	0.089
		119.9	-0.4	0.069
	Ca	58.2	-8.4	0.067
		119.3	1.0	0.063
	Ba	58.8	-10.1	0.068
		129.1	6.9	0.078

The results in TABLE 6.1 are shown graphically for the tan δ peak temperature values in FIGURES 6.1 to 6.5

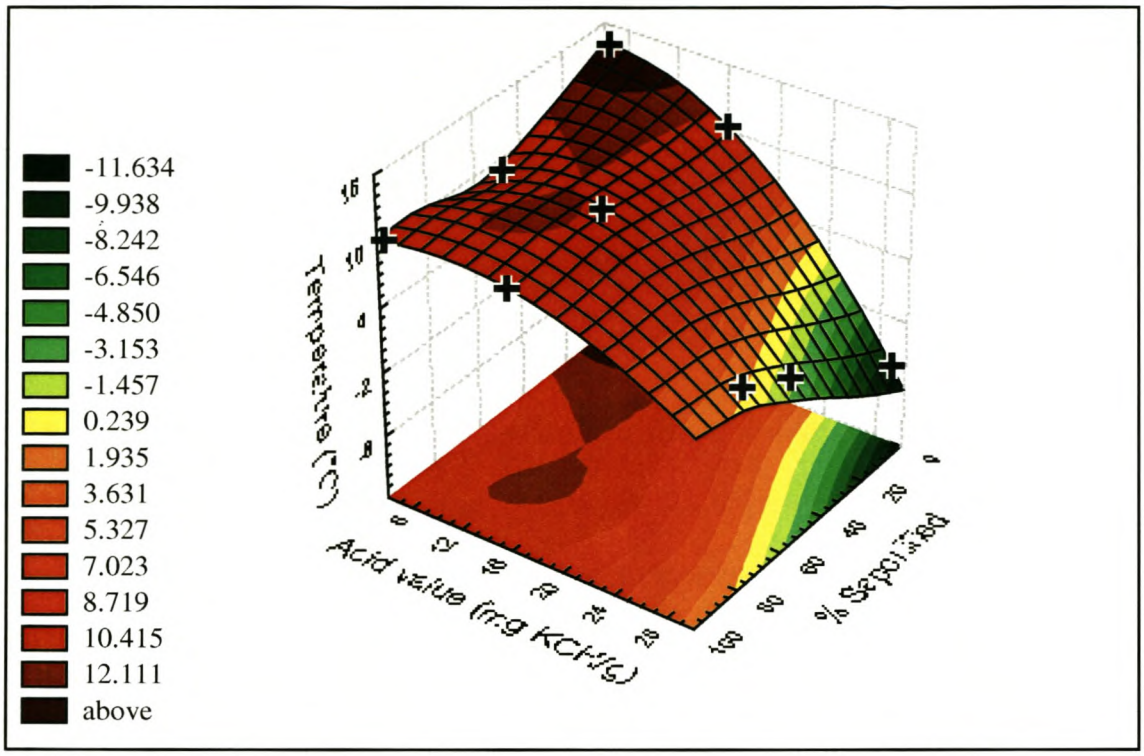

FIGURE 6.1 : Li cation : Tan δ transition temperature vs. Acid value vs. % Saponified

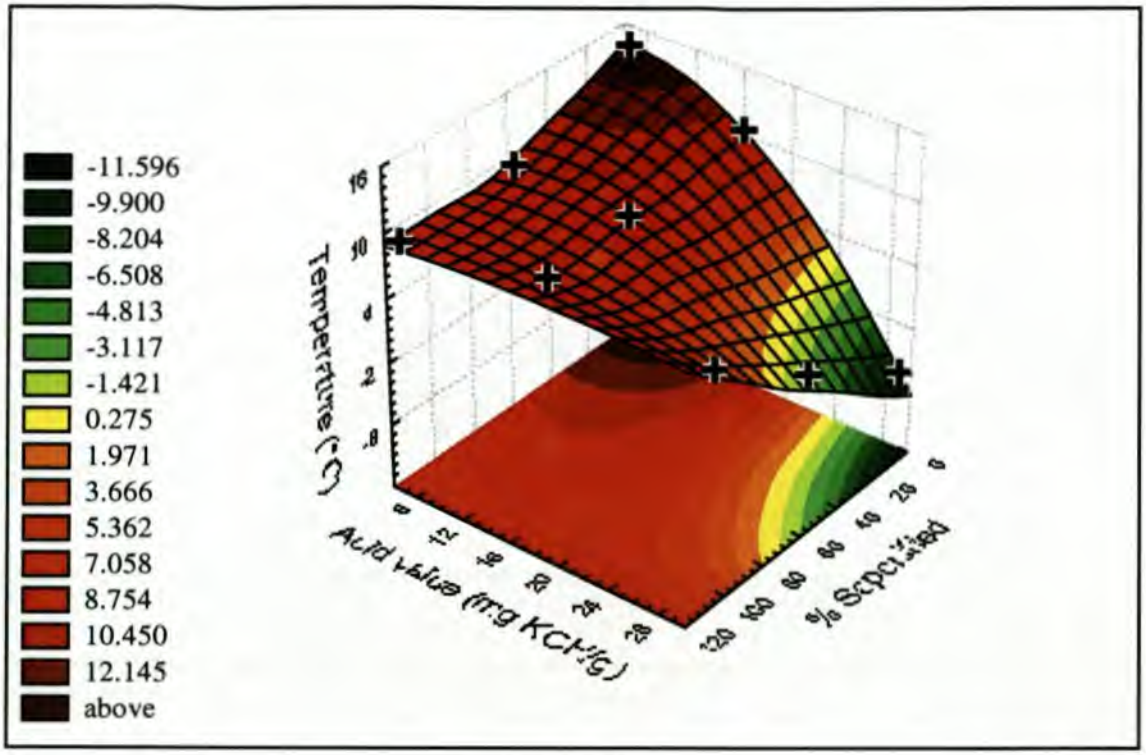

FIGURE 6.2 : Na cation : Tan δ transition temperature vs. Acid value vs. % Saponified

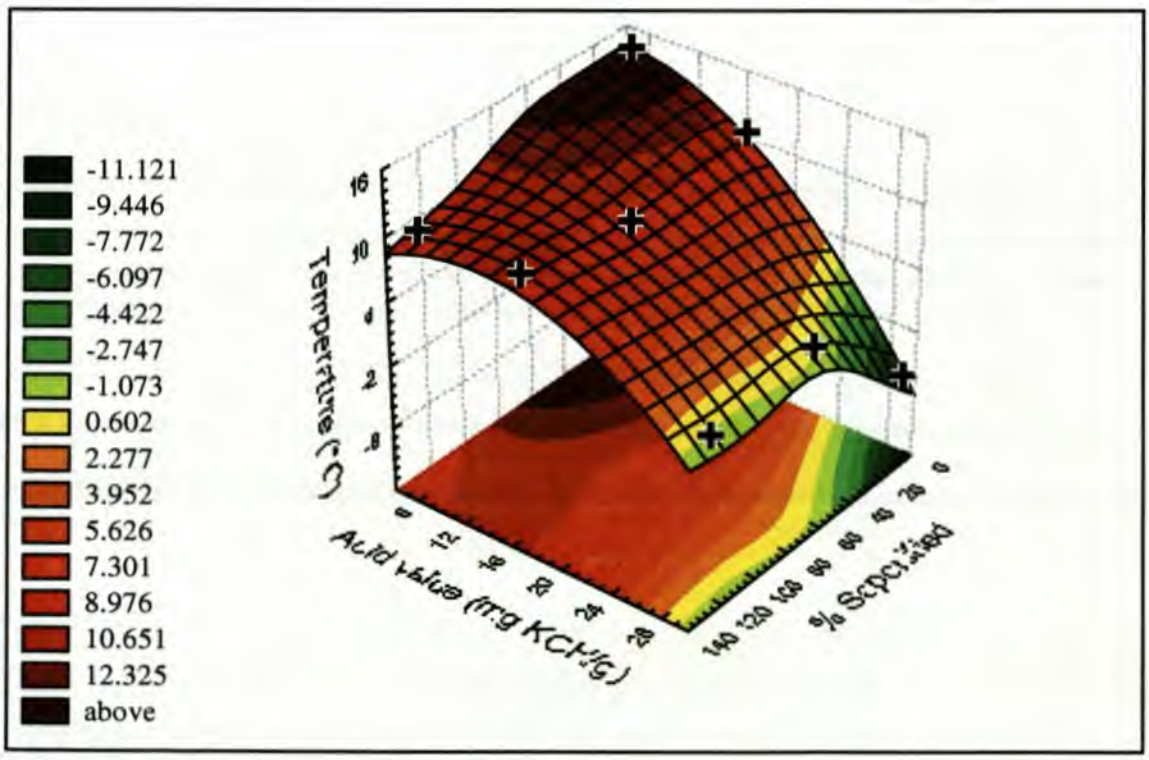

FIGURE 6.3 : K cation : Tan δ transition temperature vs. Acid value vs. % Saponified

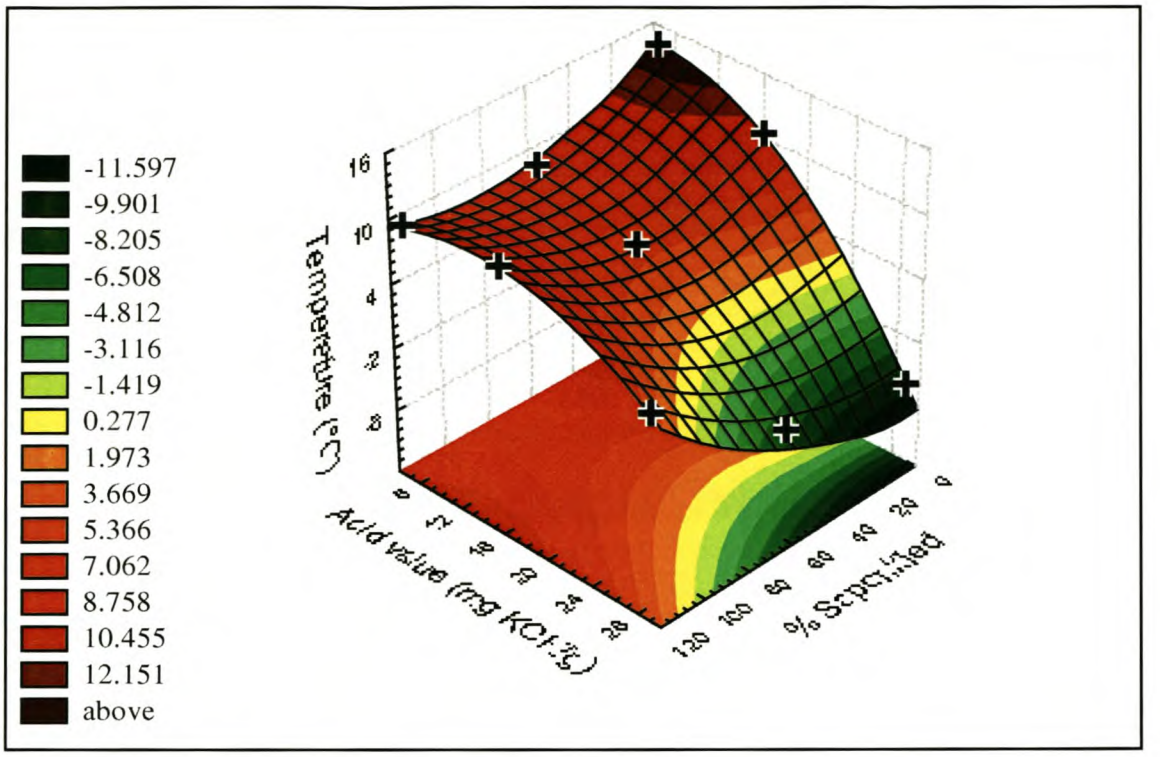

FIGURE 6.4 : Ca cation : Tan δ transition temperature vs. Acid value vs. % Saponified

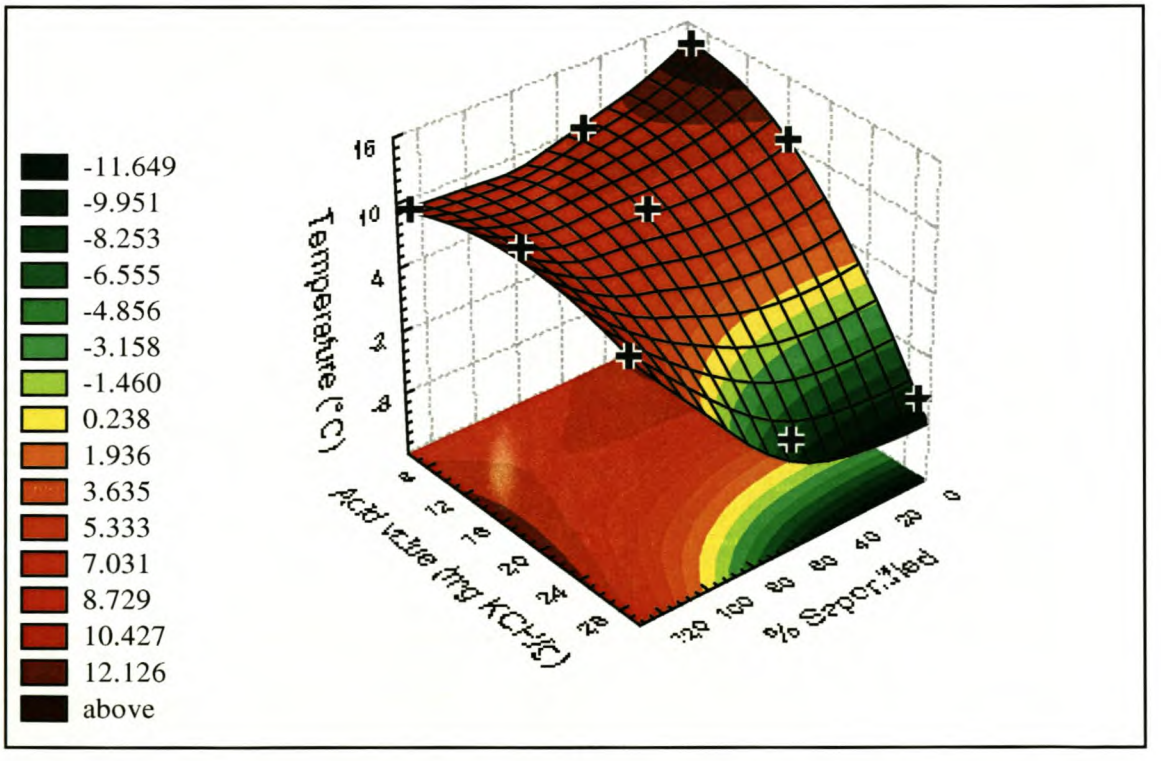

FIGURE 6.5 : Ba cation : Tan δ transition temperature vs. Acid value vs. % Saponified

These graphs show the following:

1 When one looks at the oxidised waxes, progressing from WAX 6 through to WAX 28, then the tan δ transition temperatures decreases in value. This is understandable, as the tan δ peak is associated with the crystallinity of the wax samples and there is a crystallinity decrease in the waxes as the acid number increases.

2. If one looks along the acid value axis for the Li cation graph, for WAX 6 and WAX 16, the tan δ peak temperature values are essentially linear. For WAX 28 however, there is a definite increase in temperature value.

3. For the Na cation graph, there is a slight drop in tan δ peak temperature values for WAX 6 and WAX 16, whereafter, for WAX 28 there is a definite increase in temperature value as seen along the acid value axis. The Li cation and Na cation graphs thus show the same trends.

4. The K cation graph shows the same trends as the Li and Na graphs, when looking along the acid value axis. For WAX 6 and WAX 16, essentially linear responses for the tan δ peak temperature values and for WAX 28, an increase in tan δ peak temperature values. It does however appear that for the K cation, WAX 28 results, that there is an initial increase in Tan δ peak temperature value, followed by a flattening out effect.

5. For both the Ca and Ba cation graphs, the trend is slightly different to the monovalent cations, when looking along the acid value axis. For WAX 6 and WAX 16, there is an initial drop in tan δ peak temperature values, whereafter the tan δ peak temperature values increase. WAX 28 for both the divalent cations shows an increase in tan δ peak temperature values.

6.4 Discussion

It appears that the rheometric analysis results show that this method of analysis for tan δ alone does not give enough results to conclusively state that a sample is either in multiplet or cluster formation. The lowering of crystallinity and the increased formation of multiplets and clusters were seen as a combined peak in the tan δ peak temperature values, for the sets of samples tested. There are thus two types of transitions that must be accounted for. For WAX 6 and WAX 16, as the crystallinity decreases and the multiplets increase, they counteract each other, giving an essentially linear response on the tan δ peak temperature

values. For WAX 28, the increase in multiplets and clusters are predominant and hence the rise in the tan δ peak temperature values. Unfortunately, one cannot see from the above graphs where multiplet formation is predominant and where cluster formation is predominant.

To try and understand the tan δ peak temperature value results more fully, I used the same reasoning that I used in the mechanical analysis chapter (Chapter 5). I assumed that the initial oxidation value has an influence on the morphology for the tan δ peak temperature value response. If one then took the initial acid groups and their corresponding mole percentage acid value and added the mole percentage cation added, creating a shift effect on the corresponding graph, one could more clearly understand the results of the rheological analysis. The graphs for the five cations are shown below in FIGURES 6.6 to 6.10.

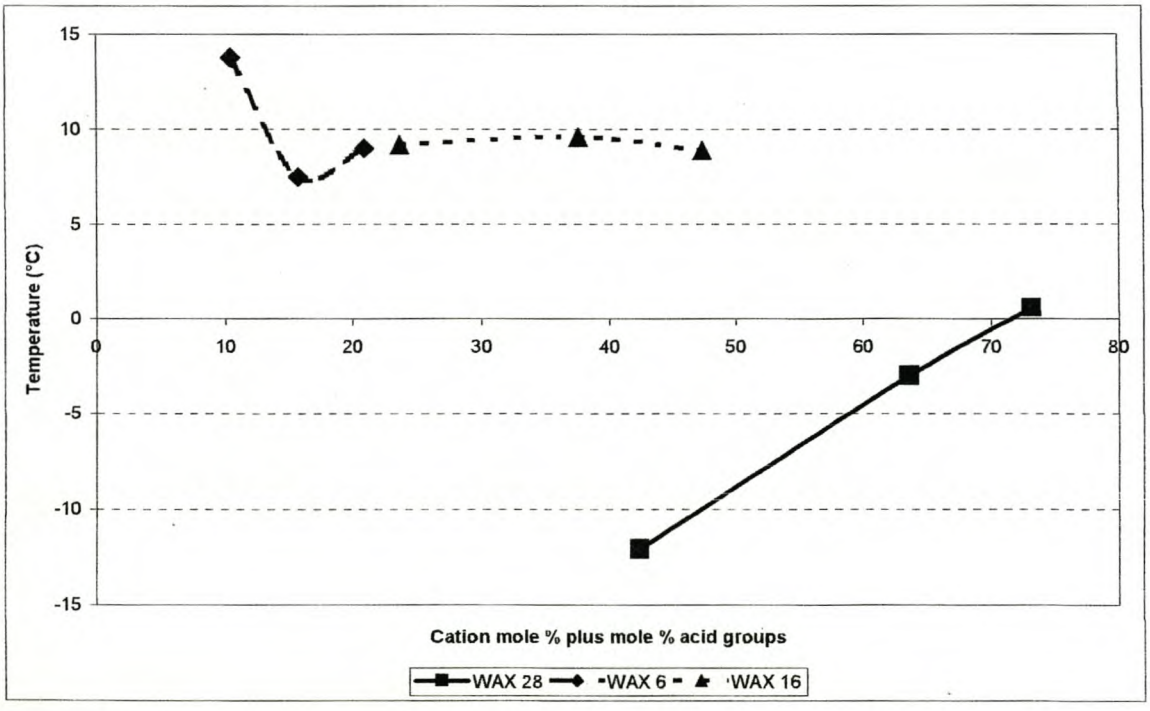

FIGURE 6.6 : Li cation: Graph of cation mole % plus mole % acid groups vs. Tan δ peak temperature value

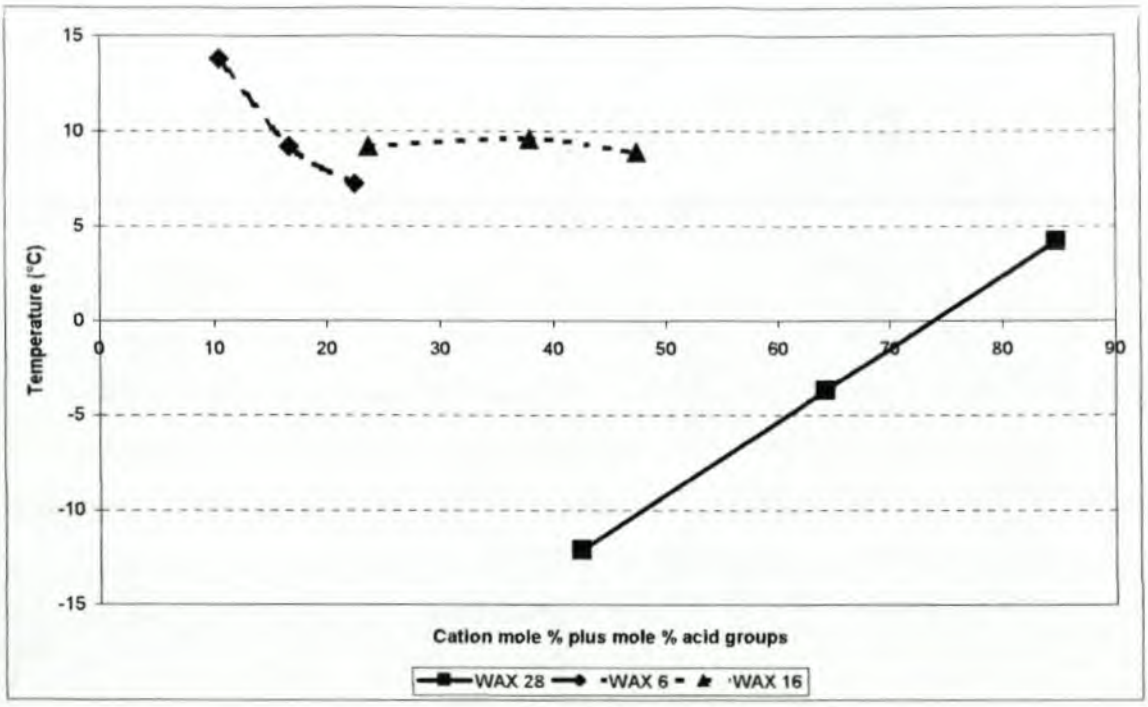

FIGURE 6.7 : Na cation: Graph of cation mole % plus mole % acid groups vs. Tan δ peak temperature value

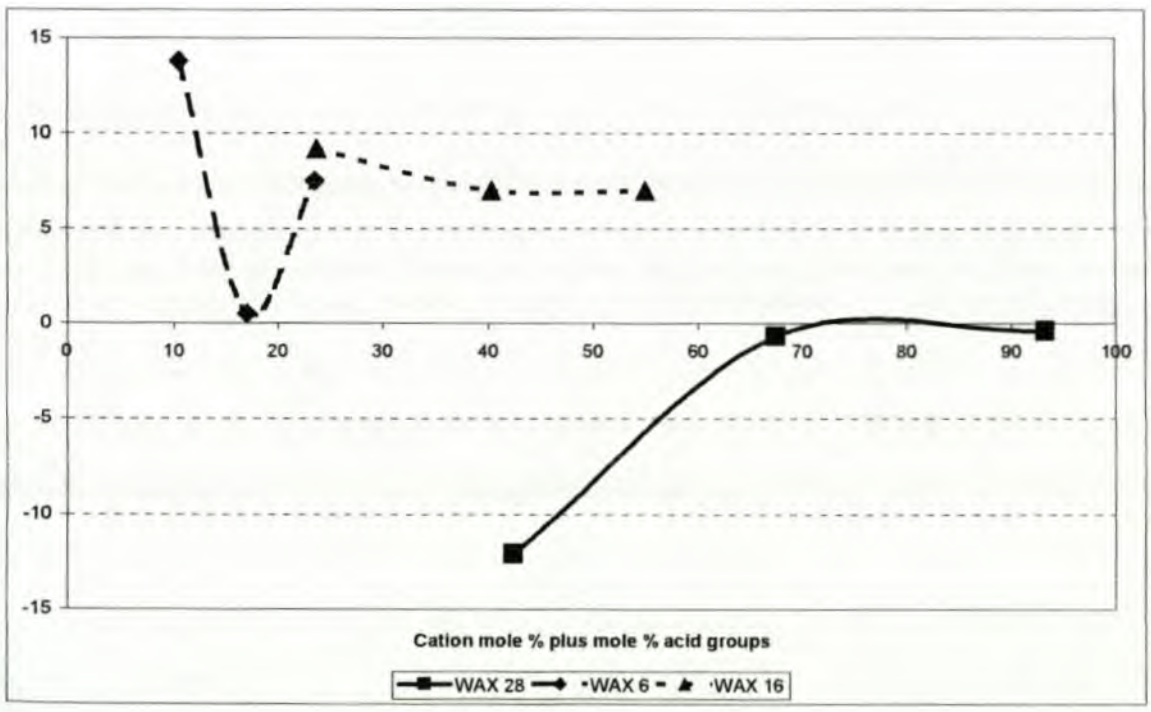

FIGURE 6.8 : K cation: Graph of cation mole % plus mole % acid groups vs. Tan δ peak temperature value

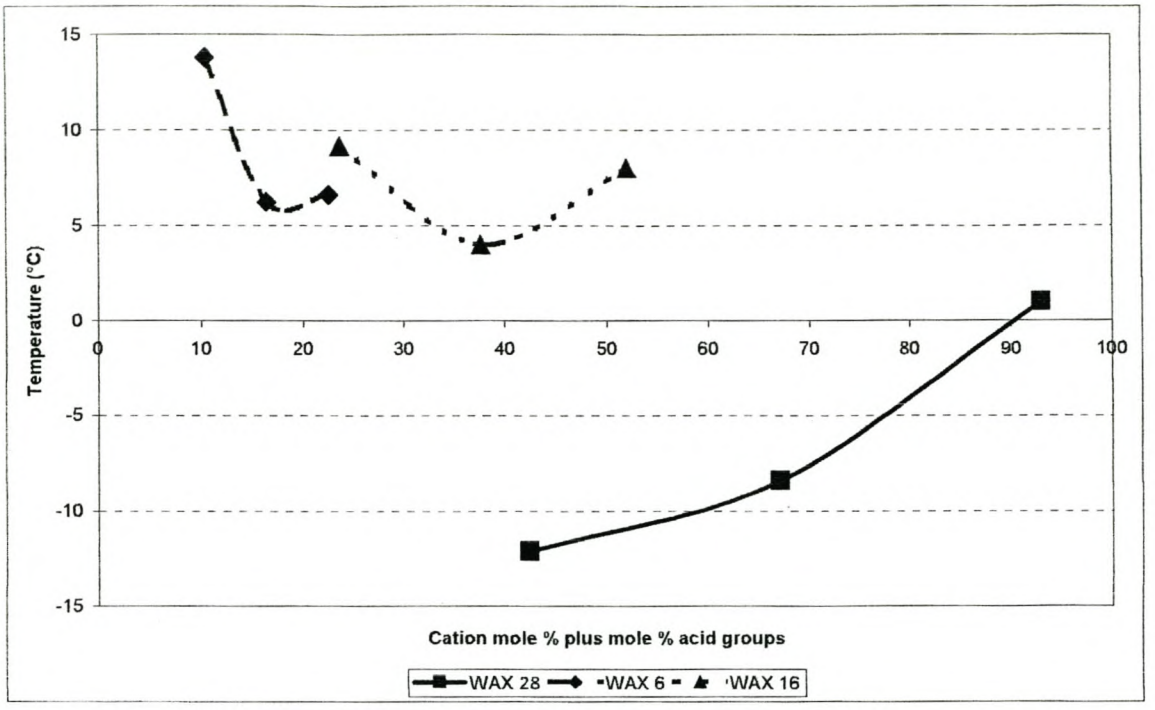

FIGURE 6.9 : Ca cation: Graph of cation mole % plus mole % acid groups vs. Tan δ peak temperature value

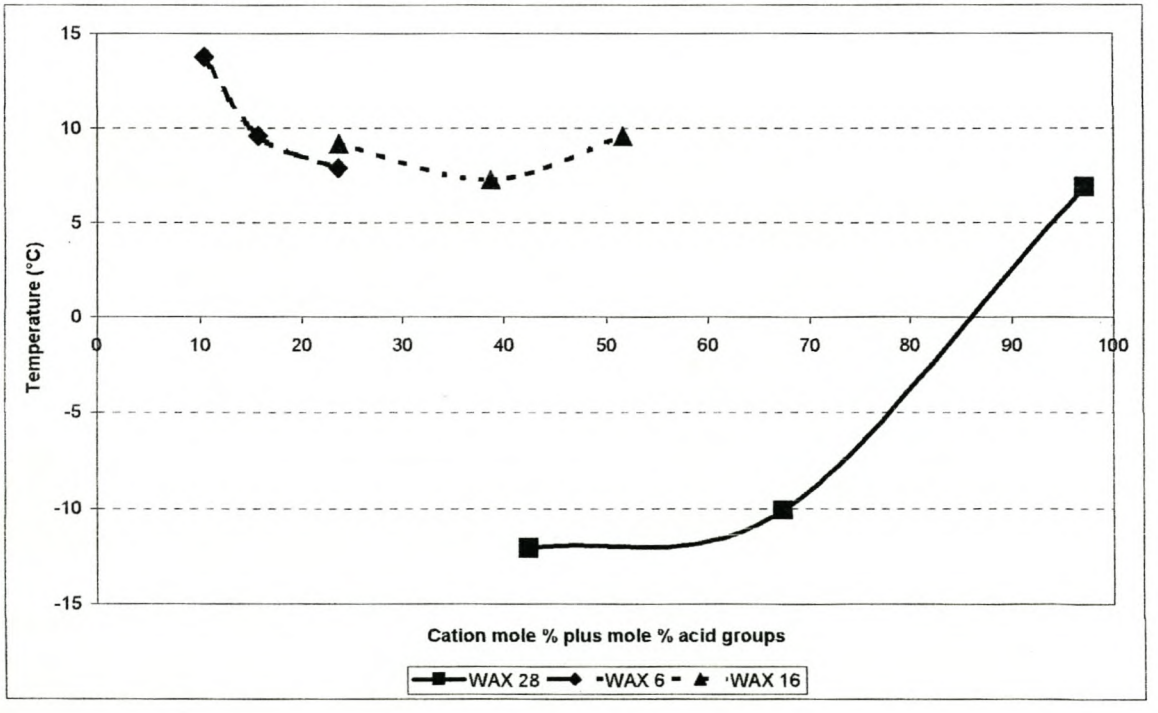

FIGURE 6.10 : Ba cation: Graph of cation mole % plus mole % acid groups vs. Tan δ peak temperature value

The above graphs (FIGURES 6.6 to 6.10) gives one a clearer understanding of the morphological changes taking place. For both the Li and Na cation graphs, WAX 6 and WAX 16 show that there is a lowering degree in crystallinity, but the formation of multiplets counteract the lowering degree in crystallinity. For WAX 28 Li and Na cation samples, the linear increase for the tan δ peak temperature values indicates that multiplet or cluster formation must be taking place. For the K graph, the trend is the same as for the Li and Na cation graphs. But for the WAX 28 K graph, there is an increase in the Tan δ peak temperature values up to the ca. 50 % saponified sample, where the graph flattens out. This may indicate that cluster formation is complete and the excess K cation added now acts as a filler, found in the cluster surroundings [31].

The divalent cations react differently and the graphs for Ca and Ba cations show that up to about 50 % saponification for WAX 28, only multiplet formation can be dominant. The steep rise in the Tan δ peak temperature values after about 50 % saponification for WAX 28 samples indicate that formation of clusters could be predominant. Again, if more data points were shown between the ca. 50 % saponified and ca. 100 % saponified samples, the exact point of multiplet and cluster formation may be seen.

The above analysis was not conclusive enough to state whether a sample is in multiplet or cluster formation so I did one last analysis. I initially looked at the relative percentage change in values taking place in the three oxidized waxes. What is shown in Table 6.2, is the peak temperature values of WAX 16 and deducting this value from the corresponding sample for WAX 6. This is then expressed in percentage form. This then gives me a relative value as to whether WAX 16 has increased or decreased in value from WAX 6 for a specific parameter and by how much.

TABLE 6.2
Percentage difference in the rheometric test results

Wax type	% Difference in G' (peak temp.)	% Difference in G' (peak value)	% Difference in G" (peak temp.)	% Difference in G" (peak value)	% Difference in tan δ (peak temp.)	% Difference in tan δ (peak value)
WAX 6	0.0	0.0	0.0	0.0	0.0	0.0
WAX 16	-7.8	-35.3	-223.2	1.3	-33.4	19.0
WAX 28	-11.0	-38.8	-185.5	-15.0	-231.5	-10.5

The above table shows that the most significant changes take place with the temperature values of G" and Tan δ. This would be due to the decrease in the crystallinity and associated increase in amorphous material. Table 6.3 below, now shows the rest of the wax samples with the percentage change given, where each set of samples, that is for the oxidised wax, the ca. 50 % and ca. 100 % samples, are then compared relative to one another and the increase or decrease in values are compared relatively speaking. The above values in Table 6.2 are also duplicated from above into Table 6.3.

TABLE 6.3

Percentage difference in results and a column with multiplet of cluster predominance indication

Wax Type	% Saponified	Cation type	% Difference in G' (Temp.)	% Difference in G' (Values)	% Difference in G" (Temp.)	% Difference in G" (Values)	% Difference in Tan delta (Temp.)	% Difference in Tan delta (Values)	Multiplet or Cluster formation (M/C)
6	0.0		***	***	***	***	***	***	***
	50.0	Li	-10.8	-19.6	-72.4	-16.3	-45.7	-2.3	M
	100.0		12.4	14.2	52.9	-0.7	20.0	-14.1	M
	59.3	Na	0.7	-17.1	-28.7	-41.3	-33.4	-28.6	M
	115.0		-1.1	2.6	-104.5	34.6	-21.7	14.3	M
	62.3	K	-18.0	-62.4	-258.8	-43.9	-96.4	3.1	M
	125.0		-9.6	67.3	106.1	-13.1	1,400.0	-20.9	C
	57.0	Ca	-10.4	-25.1	-124.3	664.7	-55.1	-8.8	M
	115.8		-12.3	4.3	140.0	-88.8	6.5	13.1	M
	50.0	Ba	3.8	-13.5	-57.9	-18.4	-30.5	-12.9	M
	126.0		-24.0	-13.8	-69.2	3.2	-17.7	18.7	M
16	0.0		-7.8	-35.3	-223.2	1.3	-33.4	19.0	***
	58.7	Li	-6.8	17.4	111.8	-23.1	4.3	-19.8	M
	100.0		8.8	-22.1	-33.3	-24.5	-7.3	-10.7	M
	59.9	Na	-5.0	-86.9	73.3	-92.6	-35.9	-31.4	M
	100.0		-4.5	-19.3	147.7	-47.0	6.8	-23.7	C
	70.2	K	9.0	-90.7	85.5	-92.8	-23.9	-20.0	M
	131.9		-27.3	49.3	489.0	-21.5	0.0	-15.5	C
	58.8	Ca	-13.8	25.9	5.3	-23.2	-56.5	-26.6	M
	119.4		8.1	-92.7	90.3	-93.2	100.0	-2.6	C
	63.3	Ba	-6.8	10.5	55.3	-25.4	-20.7	-20.3	M
	117.9		8.6	-24.4	244.1	-30.2	32.1	-7.0	C
28	0.0		-11.0	-38.8	-185.5	-15.0	-231.5	-10.5	***
	50.0	Li	-10.7	80.6	36.4	-13.4	75.2	-24.0	C
	72.5		48.4	-95.3	65.9	-92.6	120.0	-6.5	C
	51.4	Na	7.6	-87.2	55.3	-94.8	69.4	-27.4	C
	100.0		-12.3	1,371.8	57.7	956.6	213.5	-17.2	C
	59.0	K	-4.8	0.5	59.0	-35.1	94.2	-5.3	C
	119.9		-8.8	-85.1	13.5	-90.7	42.9	-22.5	C
	58.2	Ca	-4.8	105.4	14.7	-7.9	30.6	-28.7	C
	119.3		3.2	-92.6	69.2	-94.3	111.9	-5.3	C
	58.8	Ba	-16.9	55.9	4.6	-24.3	16.5	-27.7	M
	129.1		51.0	-41.0	86.5	-37.2	168.3	14.7	C

If one looks at specifically the temperature values for G" and Tan δ, then a pattern becomes evident. Where both the G" and Tan δ values changes positive, it would imply that the decrease in crystallinity has been overshadowed by the formation of initially multiplets and if there are significant increase in relative values, by cluster formation. The above table includes the column to show what is the most likely dominant formation, multiplet or cluster.

6.5 Summary

The above data showed that:

1. For the monovalent cation samples, multiplet formation is predominant for WAX 6 and WAX 16 saponified samples. For WAX 28 saponified samples, cluster formation is predominant.
2. For the divalent samples, multiplet formation is predominant for WAX 6 and WAX 16 samples. For the WAX 28 samples, multiplet is predominant around the ca. 50 % saponified samples and cluster formation is predominant for the ca. 100 % saponified samples.

If one had included a larger set of samples, that is for 10 % saponification, 20 % saponification, etc., then the exact point of transition for multiplet and cluster formation would be seen.

6.6 References

1. Takahashi T, Watanabe J, Minagawa K, Koyama K, **Polymers**, V 35, 26, pp 5722, 1994
2. Kim Y, Ha C, Cho W, **Polymer (Korea)**, V 18, 5, pp 737, 1994
3. Eisenberg A, **J. Polym. Sci. Polym. Symp.**, 45, pp 99, 1974
4. Fan X, Bazuin C G, **Macromolecules**, 28, pp 8216, 1995
5. Visser S A, Cooper S L, **Polymer**, 33, pp 920, 1992
6. Alice Ng C W, MacKnight W J, **Macromolecules**, 29, pp 2421, 1996
7. Ma X, Sauer J A, Hara M, **Macromolecules**, 28, pp 3953, 1995
8. Shohamy E, Eisenberg A, **J. Polym. Sci. Polym. Phys.**, 14, pp 1211, 1976
9. Earnest T R, Higgins J S, MacKnight W J, **J. Polym. Sci. Polym. Phys.**, 16, pp 143, 1978
10. Earnest T R, MacKnight W J, **J. Polym. Sci. Macrom. Rev.**, 16, pp 41, 1981
11. Plante M, Bazuin C G, Jerome R, **Macromolecules**, 28, pp1567, 1995
12. Kim J, Roberts S B, Eisenberg A, Moore R B, **Macromolecules**, 26, pp 5256, 1993
13. Bazuin C G, Eisenberg A, **J. Polym. Sci. Part B Polym. Phys.**, 24, pp 1137, 1986
14. Tong X, Bazuin C G, **J. Polym. Sci. Part B Polym. Phys.**, 30, pp 389, 1992
15. Tsagaropoulos G, Eisenberg A, **Macromolecules**, 28, pp 396, 1995
16. Villeneuve S, Bazuin C G, **Polymer**, 32, pp 2811, 1991
17. Kim J, Eisenberg A, **J. Polym. Sci. Part B Polym. Phys.**, 33, pp 197, 1995
18. Weiss R A, Fitzgerald J J, Kim D, **Macromolecules**, 24, pp 1064, 1991
19. Fitzgerald J J, Weiss R A, **J. Macromol. Sci. Rev. Macromol. Chem. Phys.**, C28, pp 99, 1988
20. Bagrodia S, Pisipati R, Wilkes G L, Storey R F, Kennedy J P, **J. Appl. Polym. Sci.**, 29, pp 3065, 1984
21. Ma X, Sauer J A, Hara M, **Macromolecules**, 28, pp 3953, 1995
22. Ma X, Sauer J A, Hara M, **Macromolecules**, 28, pp 5526, 1995
23. Takahashi T, Watanabe J, Minagawa K, Takimoto J, Iwakura K, Koyama K, **Rheol. Acta**, 34, pp163, 1995
24. Weiss R A, **ASTM Spec. Tech Publ. STP 1249**, pp 214, 1994
25. Lefelar J A, Weiss R A, **Macromolecules**, 17, pp1145, 1984
26. Eisenberg A, **Polym. Prep.**, 14, pp 871, 1973
27. Yoshikawa K, Desjardins A, Dealy J M, Eisenberg A, **Macromolecules**, 29, pp 1235, 1996
28. Nishida M, Eisenberg A, **Macromolecules**, 29, pp 1507, 1996
29. Billmeyer F W, **Textbook of Polymer Science,** New York, John Wiley and Sons, CH 6, pp 203, 1971

30. Ward I M, **Mechanical properties of solid polymers,** second edition, New York, John Wiley and Sons, CH 5, pp 89, 1971

31. Tsagaropoulos G, Eisenberg A, **Macromolecules**, 28, pp 396, 1995

CHAPTER 7 : Ionomeric Fischer-Tropsch wax : Water sorption and diffusion properties

7.1 Introduction

The water absorption of F-T ionomeric waxes is investigated in this chapter. The waxes were exposed to water vapour, to see what the influence of type of cation versus type of wax would be on moisture absorption. The percentage moisture absorption was used versus time and the Margolin [1] empirical formula used to determine the concentration percentage of the water in the wax at time infinity.

The Margolin formula is given as:

$$M(t) = t/(a + bt) + c \qquad \textbf{Equation 1}$$

Where : a, b and c are constants for a particular polymer and

$$M(\infty) = 1/b \qquad \textbf{Equation 2}$$

This gives one an idea of the maximum water absorption for a particular wax at time infinity. Next, the average diffusion coefficient was determined from the initial gradient of the sorption curve when plotted against the square root of time [2-10]. The equation is given as:

$$M(t)/M(\infty) = 4/\pi^{1/2}(Dt/L^2)^{1/2} \qquad \textbf{Equation 3}$$

Where $M(t)$ = mass increase at time t

$M(\infty)$ = mass increase at time infinity (maximum mass increase)

D = average diffusion coefficient

L = thickness of sample.

t = time in seconds

For my thesis, I assumed that the increase in L is small and used it as a constant of 1 cm. If the initial gradient I is observed in a sorption experiment where D is concentration independent, then the average diffusion coefficient **Đ** is given by:

$$\text{Đ} = (\pi\, l^2)/16 \qquad \textbf{Equation 4}$$

7.2. Experimental

Disks of wax were cast with a ca. 55 mm diameter and ca. 10 mm thickness. These disks were placed in a desiccator, with a pan of water in the bottom of the desiccator so that the samples could absorb the moisture. The mass increase of the samples was monitored versus time, while the temperature was kept constant at 23 °C.

7.3. Sorption results and discussion

The results of the test can be seen in APPENDICES 7.1 to 7.4. The results in APPENDICES 7.1 to 7.4 are shown graphically in APPENDICES 7.5 to 7.8.and the values for the constants a, b and M(∞) is shown below in TABLE 7.1.

TABLE 7.1
Sorption experimental results for the Fisher-Tropsch ionomeric waxes

	Cation type	% Saponified	Constant a	Constant b	M(∞) = 1/b (%)
WAX 6		0.0	2000.0	19.00	0.053
	Li	50.0	550.0	3.70	0.270
		100.0	350.0	2.35	0.426
	Na	59.3	250.0	1.45	0.690
		115.0	78.0	0.32	3.175
	K	62.3	150.0	0.87	1.149
		125.0	29.0	0.10	10.000
	Ca	57.0	455.0	6.30	0.159
		115.8	190.0	4.88	0.205
	Ba	50.0	330.0	8.61	0.116
		126.0	125.0	9.80	0.102
WAX 16		0.0	85.0	17.50	0.057
	Li	58.7	125.0	2.65	0.377
		100.0	85.0	1.80	0.556
	Na	59.9	45.0	0.38	2.660
		100.0	23.5	0.02	50.000
	K	70.2	5.0	0.14	7.143
		131.9	0.8	0.09	11.111
	Ca	58.8	125.0	3.60	0.278
		119.4	100.0	2.43	0.412
	Ba	63.3	125.0	4.00	0.250
	Ba	117.9	100.0	2.25	0.444
WAX 28		0.0	100.0	7.00	0.143
	Li	50.0	70.0	0.93	1.081
		72.5	60.0	0.63	1.587
	Na	51.4	4.5	0.10	10.526
		100.0	1.3	0.05	20.000
	K	59.0	0.8	0.09	11.111
		119.9	0.5	0.01	100.000
	Ca	58.2	90.0	1.70	0.588
		119.3	80.0	1.40	0.714
	Ba	58.8	80.0	1.75	0.571
		129.1	90.0	1.69	0.592
WAX G11		0.0	2000.0	16.50	0.061
	K	50.0	200.0	1.45	0.690
		110.7	190.0	0.94	1.062
	Ca	50.0	950.0	7.50	0.133
		129.1	800.0	6.91	0.145

The results of TABLE 7.1 are shown below in Figures 7.1 to 7.5.

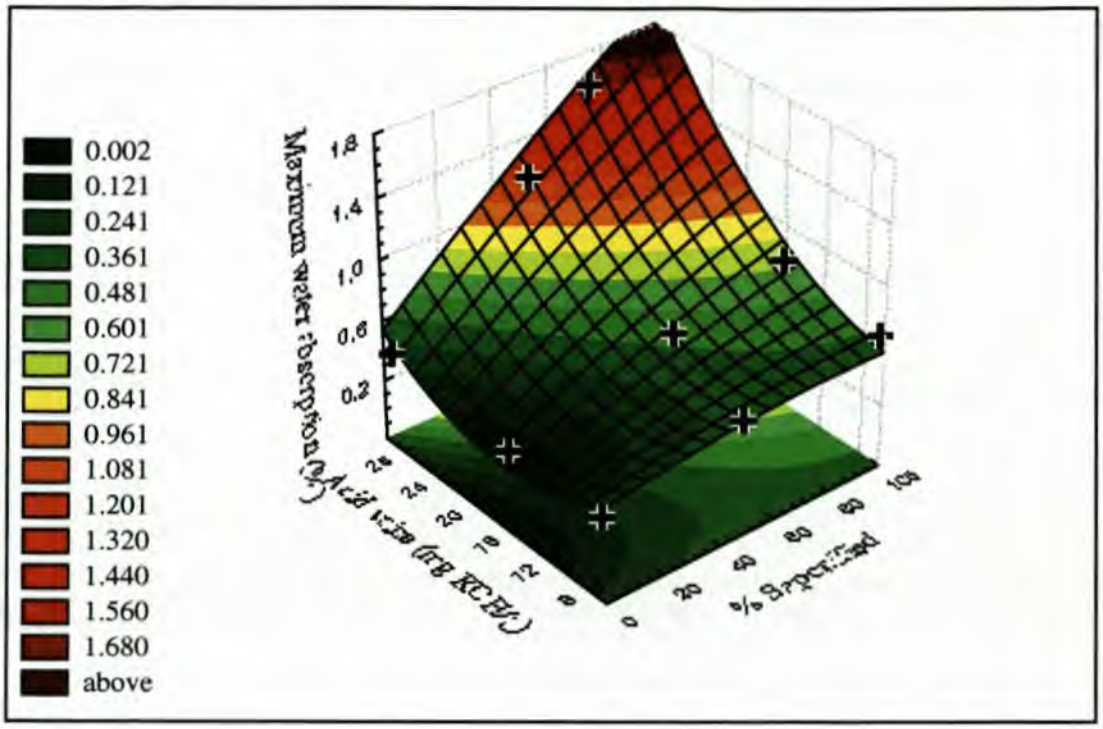

FIGURE 7.1 : Li cation: % Saponified vs. Acid value vs. Maximum water absorption (%)

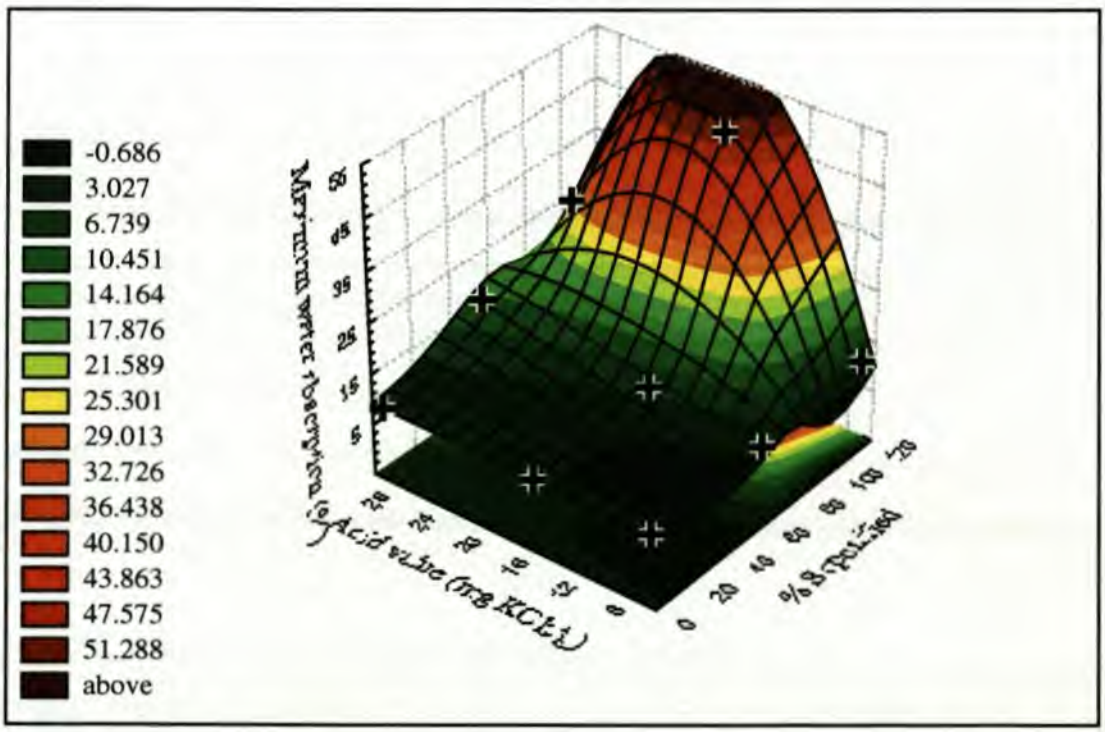

FIGURE 7.2 : Na cation: % Saponified vs. Acid value vs. Maximum water absorption (%)

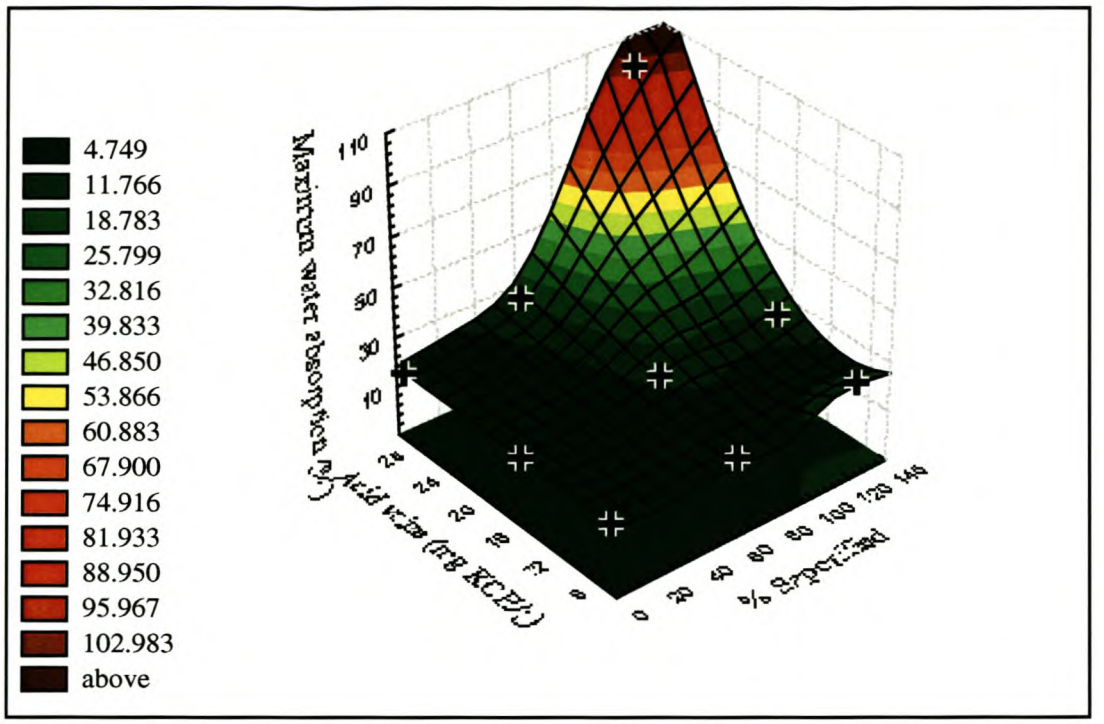

FIGURE 7.3 : K cation: % Saponified vs. Acid value vs. Maximum water absorption (%)

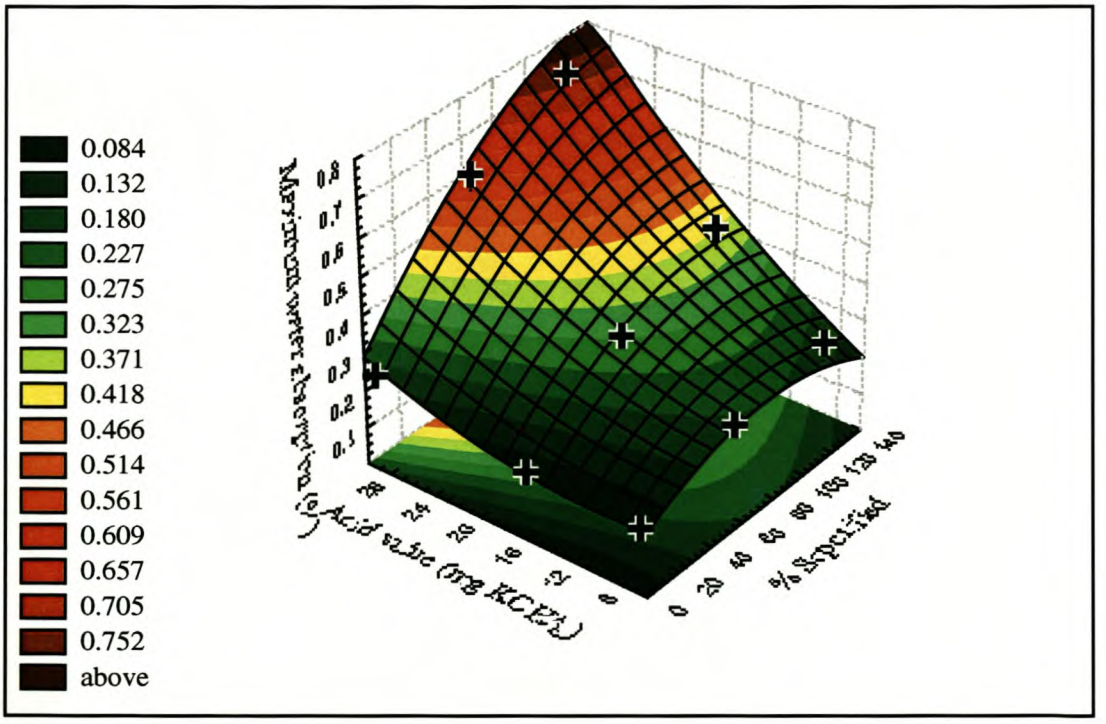

FIGURE 7.4 : Ca cation: % Saponified vs. Acid value vs. Maximum water absorption (%)

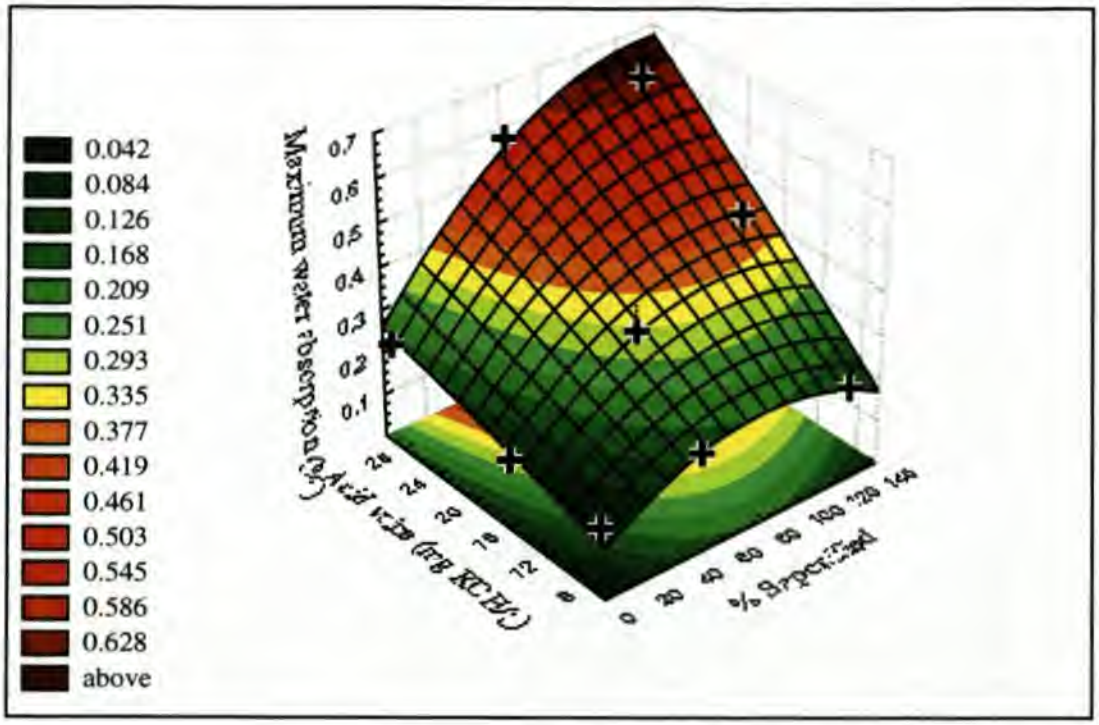

FIGURE 7.5 : Ba cation: % Saponified vs. Acid value vs. Maximum water absorption (%)

Figures 7.1 to 7.5 all show the trend that the higher the percentage saponified and the higher the acid value, the greater the maximum water absorbed. An exception to the above rule is the ca. 50 % saponified sodium cation sample where there was not enough data to give an accurate reading. What is totally different for all the cations is the total percentage water absorption. Lithium cation samples go to a maximum absorption of about 1.6 %, sodium cation samples to a maximum of about 20 %, potassium cation samples to about 100 %, calcium cation samples to about 0.7 % and barium cation samples to about 0.6 %. The divalent samples thus have much lower water absorption than the monovalent cations. One cannot deduce from the above graphs where possible multiplets and clusters start or end and there does not seem to be a distinction between the maximum water absorption of a sample with possible predominant multiplet formation versus a sample with possible predominant cluster formation.

The results do not agree with the results depicted in FIGURE 2.14, CHAPTER 2. In the case of FIGURE 2.14 (Makowski, et al. [11]), barium cation shows the highest water absorption and magnesium is of the same order as sodium. I cannot explain the difference in my results to that of Makowski, et al. [11], but divalent cations normally do not absorb water as monovalent cations do. My results agree more with those of Villeneuve, et al. [12]

and Tachino, et al. [13] as well as Bagrodia, et al. [14], where the monovalent cation absorb more water than the divalent cations.

With respect to the grafted waxes, in theory I would expect the grafted wax to absorb less water than WAX 6, as WAX 6 has more or less the same saponification value as WAX G11, but WAX 6 has a greater number of other polar groups (alcohols, ketones, etc.) than WAX G11. Also, WAX G11 should in theory have a higher crystallinity value than WAX 6. In this case the theory fits the practical results. The results in Table 7.1 show that for WAX G11, K and Ca samples, the maximum water absorbed is less than the maximum water absorbed for WAX 6, K and Ca samples.

7.4. Diffusion results and discussions

The diffusion results were calculated utilising formula 7.2. The diffusion data is tabulated in Appendix 7.9 and shown graphically in Appendices 7.10. to 7.13. The average diffusion slope results are shown in TABLE 7.2.

TABLE 7.2
Diffusion experimental results for the F-T ionomeric waxes

Type of wax	Cation type	% Saponified	Slope from graph, I (cm/seconds^{½}) (/10^4)	Đ (cm^2/second) (/10^9)
WAX 6		0.0	1.067	2.24
	Li	50.0	1.100	2.38
		100.0	1.175	2.71
	Na	59.3	1.029	2.08
		115.0	0.649	0.83
	K	62.3	1.016	2.03
		125.0	0.458	0.41
	Ca	57.0	1.517	4.52
		115.8	2.544	12.71
	Ba	50.0	2.092	8.59
		126.0	4.239	35.28
WAX 16		0.0	4.841	46.02
	Li	58.7	1.928	7.30
		100.0	1.921	7.25
	Na	59.9	0.870	1.49
		100.0	0.077	0.01
	K	70.2	2.278	10.19
		131.9	4.555	40.74
	Ca	58.8	2.175	9.29
		119.4	2.082	8.51
	Ba	63.3	1.393	3.81
		117.9	1.989	7.77
WAX 28		0.0	2.941	16.98
	Li	50.0	1.337	3.51
		72.5	1.519	4.53
	Na	51.4	1.891	7.02
		100.0	0.792	1.23
	K	59.0	4.251	35.48
		119.9	1.202	2.84
	Ca	58.2	1.849	6.71
		119.3	1.805	6.40
	Ba	58.8	2.022	8.03
	Ba	129.1	1.768	6.14
WAX G11		0.0	1.160	2.64
	K	50.0	1.184	2.75
		110.7	0.940	1.73
	Ca	50.0	1.136	2.53
		129.1	1.201	2.83

The above data show some trends, but for a few anomalies, which I will discuss first. The first anomaly to be seen is that the WAX 16 average diffusion coefficient is too high. The value should most likely be about 7 cm^2/second to 8 cm^2/second. If one looks at all the other wax samples, then the values for the lithium cation samples are very close to the value of the unsaponified starting wax. This is most likely due to inaccurate data readings or too little data, which makes the slope determination inaccurate. Secondly, the average diffusion value for the WAX 16, K 131.9 % saponified sample value is too high and it should be at a lower value. The most likely reason for this anomaly is probably due to human error or

again due to too few data points on the diffusion graph to determine the slope accurately. The average diffusion sample value for the ca. 100 % potassium sample seems to always be lower than the ca. 50 % samples for the monovalent cations. All the other waxes show the same pattern, but for the above anomalies, the basic trends are shown above as:

- Lithium samples have the same order of average diffusion coefficient as the original starting wax.
- Sodium and potassium samples show a decrease in average diffusion value as the saponification value increases.
- Calcium and barium samples show an increase in average diffusion value versus percentage saponified, except for WAX 28 samples, which do not show the same trend. I suspect however that within experimental deviations, the trend could possibly be the same.

I hypothesize that the reason that the lithium samples stay more or less constant in average diffusion rate is that the samples do not absorb a large amount of water, and the path that the water molecules must follow stays more or less constant with very little swelling of the sample disks. In the case of the sodium and potassium samples, the samples may be relatively saturated so that the water diffusion rate decreases with an increase in saponification value. The calcium and barium samples increases in diffusion rates could be due to the samples increasing in actual dimensions and thus creating a "larger" path through which the water molecules can diffuse. Remember that the absorption values for the divalent cations are much lower than the monovalent cations (see section 7.3). In hindsight, it would thus be a good idea to include the increase in dimensions (L), which I assumed to be a constant, in the calculations of the average diffusion constant.

As in the sorption results, there is no clear distinction between possible predominantly multiplet formation samples and possible predominantly cluster samples. It is thus clear that the diffusion of water into the samples is not reliant on the ionomeric morphology of the waxes, but only on the type of cation used and on the original oxidised wax.

The grafted wax samples show the same trend as the oxidised wax samples with respect to average diffusion coefficients. That is, the K samples show a decrease in diffusion rate going from the ca. 50 % saponified sample to the ca. 100 % saponified sample, while the Ca samples show an increase in diffusion rate as the saponification value increases.

There was no literature available which looked at diffusion of water in ionomeric polymers so I could draw no comparative conclusions.

7.5 References

1. Margolin E D, Indian Head, MD: **US Naval powder factory report no. AD 9032**, 1953
2. Crank J, Park G S, eds., **Diffusion in Polymers,** Academic press, London, Chapter 1, 1968
3. Crank J, **The Mathematics of Diffusion,** Claredon Press, Oxford, Second edition, Chapter 10, 1975.
4. Davis B K, **Proc. Nat. Acad. Sci. USA,** Vol 71, No. 8, pp 3129-3123, 1974
5. Flory P J, Rehner J, **J. Chem. Phys.,** Vol 11, No.11, pp 58, 1943
6. Flory J, **J. Chem. Phys.**, Vol 18, No. 1, pp 108, 1950
7. Fujita H, **Fortschr Hochpolym-Forsch**, BD. 3, pp 1, 1961
8. Berens A R, **J. Memb. Sci.**, Vol. 10, pp 283, 1982
9. Reinhart C T, Peppas N A, **J. Membr. Sci.**, Vol. 18, pp 227, 1984
10. Barrer R M, eds., **Diffusion In and Through Solids,** Cambridge Press, pp 443, 1951
11. Makowski H S, Lundberg R D, Westerman L, Bock J, **Adv. Chem. Ser.**, 187(1), pp17, 1980
12. Villeneuve S, Bazuin C G, **Polymer**, 32, pp2811, 1991
13. Tachino H, Hara H, Hirasawa E, Kutsumizu S, Yano S, **J. Appl. Polym. Sci.**, 55(1), pp136, 1995
14. Bagrodia S, Tant M R, Wilkes G L, Kennedy J P, **Polymer**, 28, pp2223, 1987

CHAPTER 8 : Conclusions and recommendations for further research

8.1 Thesis conclusions

In this thesis, the following were determined:

1. When a F-T wax is oxidised, alkanes can be formed from the original starting material or be left unoxidised, that will have a carbon distribution ranging from C2 to the carbon number equal to that of the original starting material. Ketones and aldehydes will be formed with carbon numbers ranging up to the carbon number equal to the highest parent hydrocarbon. Lactones ranging from C6 to two carbons less than the highest carbon number of the starting material will be formed. Acids having carbon numbers ranging from C2 to two carbons less than the highest carbon number from the starting material will be formed. Long chain esters will also be formed. Alcohols will be present. A myriad of oxidised products will thus be present, of which the acid groups, the ester groups and lactones will be utilised for the formation of the ionomeric waxes.

2. The amount of ester consumed during saponification shows no pattern for the different acid value waxes. One can see from CHAPTER 4 results that there are samples that showed excess salt content and others that showed no extra salt content, but that the ester value had then dropped. There is also a correlation between the samples gelling up (needing a higher temperature to get the sample to flow) and the lack of excess salt.

3. The penetration test results on the ionomeric waxes show that the monovalent cations react differently from the calcium cation samples. From a morphological viewpoint, it appears that the monovalent cations have already formed clusters or multiplets at about 50 % saponification values. This could be deduced from the fact that the wax does not become harder and seems to flatten out in hardness. The calcium samples show a definite decrease in penetration value from the oxidised wax to the 100 % saponified samples. As the penetration type of test is not very sensitive to morphological changes, it is difficult to state whether the 100 % saponified calcium samples are indeed in a cluster or multiplet stage and whether the possible decrease in crystallinity with an increase in saponification values are responsible for the samples becoming "softer" with an increase in saponification value. The barium samples reacted to a large extent in the same way as the monovalent cation reacted.

4. The impact test results generally show no significant trend.

5. The softening point test results show that there is no direct comparison between the oxidised waxes tested and CHAPTER 2, TABLE 2.6 polymer results. The oxidation of the waxes had disrupted the crystallinity to such a degree that other effects such as multiplets and clusters become more pronounced in determining the softening point. The saponified grafted waxes (based on WAX G11) however showed more of the same trend as that shown by the polymers in TABLE 2.6.

6. The mechanical test results were much more complex to interpret than anticipated. Factors such as crystallinity, the acid value (and corresponding oxidised groups in the oxidised samples), the molar % cations present (% saponified), the amount of excess salt, sample preparation and the type of cation may all have played an important role in the mechanical analysis results. The multiplet or cluster predominance was determined by stepwise comparison of the individual samples relative to each other.

7. The mechanical and physical test results as a whole correlate each other, but for the Ba cation results where the softening point and mechanical analysis results are not in agreement for a few samples.

8. The rheological test results show that for the monovalent cation samples, multiplet formation is predominant for WAX 6 and WAX 16 saponified samples. For WAX 28 saponified samples, cluster formation is predominant. For the divalent cation samples, multiplet formation is predominant for WAX 6 and WAX 16 samples. For the WAX 28 divalent cation samples, multiplet is predominant around the ca. 50 % saponified samples and cluster formation is predominant for the ca. 100 % saponified samples.

9. For the water sorption and diffusion tests, lithium samples had the same order of average diffusion coefficient as the original starting wax. Sodium and potassium samples showed a decrease in average diffusion value as the saponification value increased. Calcium and barium samples showed an increase in average diffusion value versus the percentage saponified. As in the sorption results, there was not a clear distinction between multiplet formed samples and cluster samples. The diffusion of water into the samples is not reliant on the ionomeric morphology of the waxes.

10. Table 8.1 below shows the individual tests and the conclusion as to whether the individual samples are in a state of multiplet of cluster formation. The last column shows a summary as to what is the most likely morphological state the samples are in,

based on the individual tests. The designations M,C, ND mean multiplet formation, cluster formation and not determined, respectively.

TABLE 8.1

Summary of thesis results with respect to multiplet or cluster predominance

Oxidised wax	Cation	% Saponified	Mole % cation	Penetration test results	Impact test results	Softening point results	Tensile test results	Rheological test results	Thesis summary results
WAX 6		0	0	***	***	***	***	***	***
	Li	50.0	5.2	**ND**	**ND**	**M**	**M**	**M**	**M**
		100.0	10.5	**ND**	**ND**	**M**	**M**	**M**	**M**
	Na	59.3	6.2	**ND**	**ND**	**M**	**M**	**M**	**M**
		115.0	12.0	**ND**	**ND**	**M**	**M**	**M**	**M**
	K	62.3	6.5	**ND**	**ND**	**M**	**M**	**M**	**M**
		125.0	13.1	**ND**	**ND**	**M**	**M**	**C**	**M/C**
	Ca	57.0	6.0	**ND**	**ND**	**M**	**M**	**M**	**M**
		115.8	12.1	**ND**	**ND**	**M**	**M**	**M**	**M**
	Ba	50.0	5.2	**ND**	**ND**	**M**	**M**	**M**	**M**
		126.0	13.2	**ND**	**ND**	**M**	**C**	**M**	**M**
WAX 16		0	0	***	***	***	***	***	***
	Li	58.7	13.9	**M/C**	**ND**	**M**	**M**	**M**	**M**
		100.0	23.7	**M/C**	**ND**	**M**	**M**	**M**	**M**
	Na	59.9	14.2	**M/C**	**ND**	**M**	**M**	**M**	**M**
		100.0	23.7	**M/C**	**ND**	**C**	**C**	**C**	**C**
	K	70.2	16.7	**M/C**	**ND**	**M**	**M/C**	**M**	**M**
		131.9	31.3	**M/C**	**ND**	**C**	**C**	**C**	**C**
	Ca	58.8	14.0	**M/C**	**ND**	**M**	**M**	**M**	**M**
		119.4	28.3	**M/C**	**ND**	**M**	**M**	**C**	**C**
	Ba	63.3	15.0	**M/C**	**M/C**	**M**	**C**	**M**	**M**
		117.9	28.0	**M/C**	**M/C**	**M**	**C**	**C**	**C**

TABLE 8.1 (continued)

Summary of thesis results with respect to multiplet or cluster predominance

Oxidised wax	Cation	% Saponified	Mole % cation	Penetration test results	Impact test results	Softening point results	Tensile test results	Rheological test results	Thesis summary results
WAX		0	0	***	***	***	***	***	***
28	Li	50.0	21.2	**M/C**	**M/C**	**M**	**M**	**C**	**C**
		72.5	30.8	**M/C**	**M/C**	**C**	**M/C**	**C**	**C**
	Na	51.4	21.8	**M/C**	**M/C**	**M**	**M**	**C**	**C**
		100.0	42.4	**M/C**	**ND**	**C**	**C**	**C**	**C**
	K	59.0	25.0	**M/C**	**M/C**	**M**	**M**	**C**	**C**
		119.9	50.9	**ND**	**ND**	**C**	**C**	**C**	**C**
	Ca	58.2	24.7	**M/C**	**M/C**	**M**	**M**	**C**	**C**
		119.3	50.6	**M/C**	**M/C**	**M**	**M**	**C**	**C**
	Ba	58.8	25.0	**M/C**	**M/C**	**M**	**M**	**M**	**M**
		118.8	54.8	**M/C**	**ND**	**M/C**	**C**	**C**	**C**
WAX		0	0	***	***	***	***	***	***
G11	K	50.0	9.0	**ND**	**ND**	**M**	**M**	**ND**	**M**
		110.7	19.8	**ND**	**ND**	**M**	**M/C**	**ND**	**M/C**
	Ca	50.0	9.0	**ND**	**ND**	**M**	**M**	**ND**	**M**
		129.1	23.1	**ND**	**ND**	**M**	**M**	**ND**	**M**

The above table shows that cluster formation is evident for Li cation at ca. 21 mole %, for Na cation at 22 mole %, for K cation possibly at ca. 13 mole %, but definitely at 25 mole %, for Ca cation at 25 mole % and Ba cation at 28 mole %. If one compares the values given in Table 2.1, then the ionomeric waxes described in this thesis will have onset of clustering which could be in the region of the acrylic acid described, but with a mole % which is greater than the rest of the ionomeric polymers described.

8.2 Future research

The subject that I chose for this thesis was much more complex than I initially thought. I now understand why people such as A Eisenberg, M King, etc. worked on model ionomeric

polymers rather than complex polymers. The fact that there was no previous literature on Fisher-Tropsch ionomeric waxes to extract information from, made the analysis of the various test results very difficult. However, when you start a thesis, you have no idea what is in store for you. It appears, in hindsight, that if one rather focused on one oxidised wax versus one grafted wax and saponified more samples in a set (my three samples should have perhaps been five to seven samples in a set) the chances of seeing a multiplet or cluster transition would be easier to see. In this thesis, some questions arose which warrant further investigation. I would thus suggest for future research that:

1. The rheology of the different waxes should be investigated further to show at exactly which oxidation concentration versus which saponification multiplet to cluster transitions occur. I suggest that one should focus on only one oxidised wax type and compare it with a grafted wax. More samples for a wax should be prepared than the three I used. I would also suggest that the samples are prepared with oxidation values of about 15 mg KOH/g to 30 mg KOH/g. From my thesis results, the samples that I had tested, were already in cluster formation for WAX 28 samples tested (28 mg KOH/g acid value) and some of the WAX 16 samples had also already formed clusters (16 mg KOH/g acid value). These wax samples should show the exact transition from multiplet to cluster formation. It would also be possible to learn a lot more about ionomeric Fisher-Tropsch waxes if a frequency sweep versus temperature change for the specific wax samples chosen was carried out. It may be possible to fit to the WLF equation and then possibly see whether the equation also falters when cluster formation takes place, as previous researchers have found[1,2].

2. That relaxation at constant stress be conducted (mechanical test) on the ionomeric wax samples. This test is even slower in test speed than the tensile tests that I had done and with this type of test, changes in the morphological character of the samples will be exaggerated and easier to see. This recommendation also implies that one should use the same set of samples as are used as suggested in points 1 above.

8.3 References

1 Eisenberg A, King M, **Ion-Containing Polymers,** Academic Press Inc., New York, pp141, 1977

2 Broze G, Jerome R, Teyssié P, Marco C, **Polym. Bull. Berlin**, 4, pp243, 1981

APPENDIX 3.1
Typical analytical results for C14-C17 paraffins

	Units	METHOD	Typical results
Acidity	mg KOH/g	ASTM D 3242-79a	<0.01
Analine point	°C	ASTM D611-64/IP 2	112
Ash content	Mass %	ASTM D 482/IP 4	<0.01
Benzene content	mg/kg	ASTM D 2600-82	<1
Bromine index	mgBr/100g	ASTM2710-89/UOP304-59/D1159-84	<1
Colour	Saybolt	ASTM D 156	+30
Colour	ASTM	ASTM D 1500/ IP 196	0
Density @ :15.6°C(60°F)	g/cm^3	ANTON PAAR	0.775
:20 °C(68°F)	g/cm^3	ANTON PAAR	0.764
:26 °C(77°F)	g/cm^3	ANTON PAAR	0.758
Dist. at 101.325kPa: IBP	°C	ASTM D 1078/ IP 195	242
50%	°C	ASTM D 1078/ IP 195	252
DBP	°C	ASTM D 1078/ IP 195	279
Flash point (PM closed cup)	°C	ASTM D 93-85/IP 34-80	120
Kinematic viscosity @25°C(77°F)	mm^2/s	ASTM D 445	3.2
Kinematic viscosity @40°C(104°F)	mm^2/s	ASTM D 445	2.9
Kinematic viscosity @100°C(212°F)	mm^2/s	ASTM D 445	1.8
Average molecular mass	g/mol	HGPC	180
Pour point	°C	ASTM D 97/ IP 15	6
Residue on evaporation	Mass %	ASTM D 1353-86	<0.01
Total aromatic content	Mass %	ASTM D 1840-84/ UOP 495-75	<0.1
Total naphthenic content	Mass %	11.70/83	<0.1
	Units	METHOD	Typical results
Total i-paraffin content	Mass %	11.70/83	5.68
Total n-paraffin content	Mass %	11.70/83	94.32
Water content	mg/kg	ASTM E1064-92	<50
n-Paraffin/(i-Paraffin)		11.20/83	
C-distribution:(C13 + lower)			
(C13)	Mass %		0.94/(0.00)
(C14)	Mass %		23.22/(0.40)
(C15)	Mass %		39.74/(2.75)
(C16)	Mass %		24.24/(1.85)
(C17)	Mass %		5.69/(0.64)
(C18)	Mass %		0.46/(0.05)
(C19)	Mass %		0.03/(0.00)

INTERNAL STANDARD METHODS FOR SCHÜMANN SASOL

ANTON PAAR density instrument
BROOKFIELD = BROOKFIELD digital Viscometer, Model DV-1
11.20/83 Varian Aerograph's Autoprep A-700
11.70/83 Gas Chromatography

APPENDIX 3.2

Analytical results of C14-C17 paraffin oxidation

Oxidation time (minutes)	Oxidation temperature (°C)	Acid value (mg KOH/g)	Ester value (mg KOH/g)	Alcohol value (mg KOH/g)	Carbonyl value (mg KOH/g)	Peroxide value (mg KOH/g)
0	140	0	0	0	0	0
30		0.8	***	***	***	2.2
45		***	***	5.1	***	2.7
60		1.1	***	***	1.2	***
90		1.2	2.1	6.3	2.4	7.4
150		1.7	2.8	22.3	***	15.6
210		2.7	10.6	23.3	6.6	26.0
270		5.1	12.8	38.6	14.2	39.0
330		9.7	13.2	***	21.7	50.1
0	155	0	0	0	0	0
15		1.4	***	2.7	***	2.7
30		1.5	1.8	7.1	***	12.9
60		3.4	3.9	14.4	***	28.0
90		7.3	8.7	22.6	5.9	34.7
150		17.6	20.5	29.9	20.5	21.9
210		29.9	35.4	31.3	35.8	***
270		43.9	51.0	33.2	47.5	15.4
330		58.3	69.4	34.9	58.2	11.7
0	170	0	0	0	0	0
15		1.1	3.0	***	4.7	9.9
30		3.8	9.0	20.2	8.0	26.0
60		7.9	14.3	***	20.0	16.2
90		12.2	24.7	39.8	28.4	14.4
150		23.3	41.4	43.3	40.4	11.4
210		36.6	57.7	35.9	55.2	8.1
270		52.9	70.9	30.6	67.6	7.1
330		68.9	87.7	30.9	***	6.7

APPENDIX 3.3

Analytical results of C80 wax oxidation

Oxidation time (minutes)	Oxidation temperature (°C)	Acid value (mg KOH/g)	Ester value (mg KOH/g)	Alcohol value (mg KOH/g)	Peroxide value (mg KOH/g)
0	140	0	0	0	0
40		0.1	1.1	***	0.3
60		***	***	0.1	***
80		0.2	0.9	***	0.6
100		***	***	0.2	***
130		0.2	1.2	***	2.2
160		***	***	2.3	***
190		0.6	2.4	***	5.1
220		***	***	4.6	***
250		1.1	3.2	***	9.3
280		***	***	12.6	***
310		1.8	5.1	***	13.2
360		2.8	6.0	11.9	15.8
0	155	0	0	0	0
40		0.1	1.1	***	0.3
60		***	***	1.2	***
80		0.3	3.1	***	5.6
110		1.1	***	6.7	11.7
140		2.4	9.3	11.3	***
170		***	***	19.5	***
200		8.8	14.8	***	22.1
230		***	***	29.7	***
260		19.0	22.6	***	18.0
290		***	***	27.4	14.1
320		29.4	33.2	***	13.1
360		36.8	39.5	28.0	8.7
0	170	0	0	0	0
25		0.9	***	4.1	***
45		1.8	8.0	12.2	18.2
65		3.8	***	20.5	***
85		6.2	11.9	***	12.0
115		10.1	***	24.6	***
145		13.8	21.4	***	8.8
175		17.9	***	30.2	***
205		22.1	31.4	***	7.1
235		26.4	***	28.7	***
265		30.9	42.4	***	6.1
295		35.1	***	28.5	***
325		39.7	52.8	***	4.9
360		45.4	60.9	20.9	3.7

APPENDIX 4.1
Raw analysis data for acid values for Fischer-Tropsch ionomeric waxes

WAX TYPE	Cation	% Saponified	First acid value (mg KOH/g)	Second acid value (mg KOH/g)	Average values (mg KOH/g)	Standard deviation (mg KOH/g)
WAX 6		0	6.61	6.45	6.53	0.08
	Li	50.0	3.52	3.40	3.46	0.06
		100.0	0.51	0.62	0.57	0.06
	Na	59.3	3.23	3.44	3.34	0.11
		115.0	0.11	0.17	0.14	0.03
	K	62.3	3.33	3.54	3.44	0.11
		125.0	0.10	0.09	0.10	0.01
	Ca	57.0	3.23	3.31	3.27	0.04
		115.8	0.18	0.25	0.22	0.04
	Ba	50.0	3.65	3.59	3.62	0.03
		126.0	0.66	0.75	0.71	0.05
WAX 16		0	16.11	15.96	16.04	0.08
	Li	58.7	7.29	7.76	7.53	0.24
		100.0	1.22	1.34	1.28	0.06
	Na	59.9	7.90	7.45	7.68	0.23
		100.0	1.61	1.75	1.68	0.07
	K	70.2	7.37	7.88	7.63	0.26
		131.9	0.84	1.00	0.92	0.08
	Ca	58.8	8.23	8.74	8.49	0.26
		117.9	1.37	1.41	1.39	0.02
	Ba	63.3	8.53	7.87	8.20	0.31
		117.9	1.25	1.40	1.33	0.08
WAX 28		0	28.78	29.30	29.04	0.26
	Li	50	15.21	15.43	15.32	0.11
		72.5	7.70	7.14	7.42	0.28
	Na	51.4	14.83	15.25	15.04	0.21
		100.0	2.30	2.12	2.21	0.09
	K	59.9	14.64	15.37	15.01	0.37
		119.9	2.32	2.70	2.51	0.19
	Ca	58.2	17.50	16.30	16.90	0.60
		119.3	2.46	2.70	2.58	0.12
	Ba	58.8	16.13	16.81	16.47	0.34
		118.8	0.46	0.50	0.48	0.02
WAX G11		0	11.12	10.74	10.93	0.22
	K	50.0	5.03	5.17	5.10	0.07
		110.7	0.7	1.103	0.87	0.16
	Ca	50.0	5.50	5.06	5.28	0.22
		129.1	3.19	3.03	3.11	0.08

APPENDIX 4.2

Raw analysis data for saponification values of Fischer-Tropsch ionomeric waxes

Oxidised wax	Cation	% Saponified	First saponification value (mg KOH/g)	Second saponification value (mg KOH/g)	Average values (mg KOH/g)	Standard deviation (mg KOH/g)
WAX 6		0	10.01	11.61	10.81	0.8
	Li	50.0	7.42	7.84	7.63	0.2
		100.0	4.73	4.54	4.64	0.1
	Na	59.3	7.34	6.90	7.12	0.2
		115.0	4.12	3.59	3.86	0.2
	K	62.3	7.89	7.53	7.71	0.2
		125.0	3.73	4.15	3.94	0.2
	Ca	57.0	7.45	7.14	7.30	0.2
		115.8	4.31	4.09	4.20	0.1
	Ba	50.0	6.98	7.94	7.46	0.5
		126.0	4.89	4.38	4.64	0.3
WAX 16		0	30.11	31.35	30.73	0.9
	Li	58.7	19.50	19.68	19.59	0.1
		100.0	13.40	13.80	13.60	0.3
	Na	59.9	19.71	20.69	20.20	0.7
		100.0	12.15	13.79	12.97	1.2
	K	70.2	18.41	18.91	18.66	0.4
		131.9	8.67	9.68	9.18	0.7
	Ca	58.8	22.91	24.79	23.85	1.3
		117.9	16.85	15.23	16.04	1.6
	Ba	63.3	24.80	25.10	24.95	0.2
		117.9	17.22	16.21	16.72	0.7
WAX 28		0	50.71	50.32	50.52	0.3
	Li	50	41.25	39.07	40.20	1.1
		72.5	30.84	31.88	31.36	0.7
	Na	51.4	32.78	35.22	34.00	1.7
		100.0	22.08	20.63	21.36	1.0
	K	59.9	39.71	39.49	39.60	0.2
		119.9	19.59	19.90	19.75	0.2
	Ca	58.2	40.85	44.00	42.43	2.2
		119.3	25.81	22.90	24.36	2.1
	Ba	58.8	41.72	42.44	42.08	0.5
		118.8	15.65	15.63	15.64	0.0
WAX G11		0	12.90	12.54	12.72	0.3
	K	50.0	6.78	6.45	6.62	0.2
		110.7	2.19	2.76	2.48	0.3
	Ca	50.0	6.65	7.41	7.03	0.4
		129.1	4.74	4.51	4.63	0.1

APPENDIX 4.3

Graphs for the different cations showing acid and ester values for the different waxes after saponification

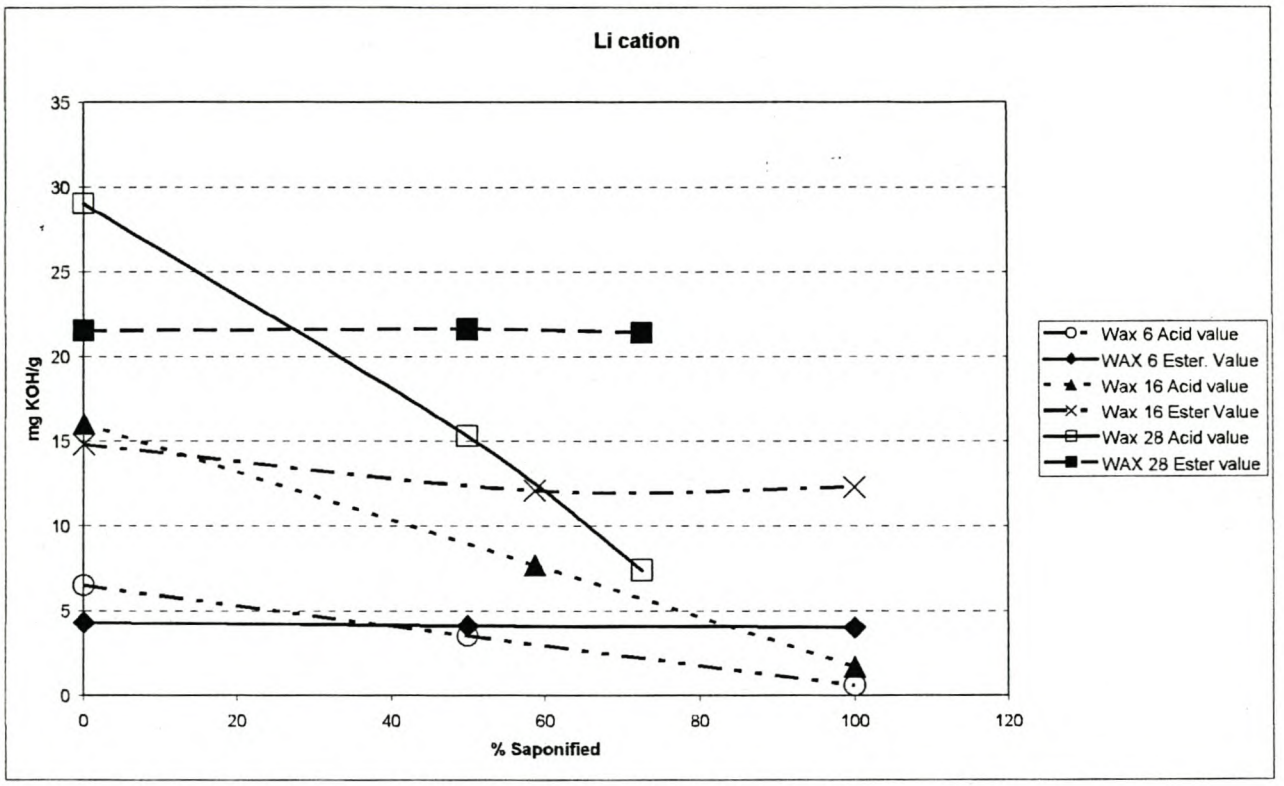

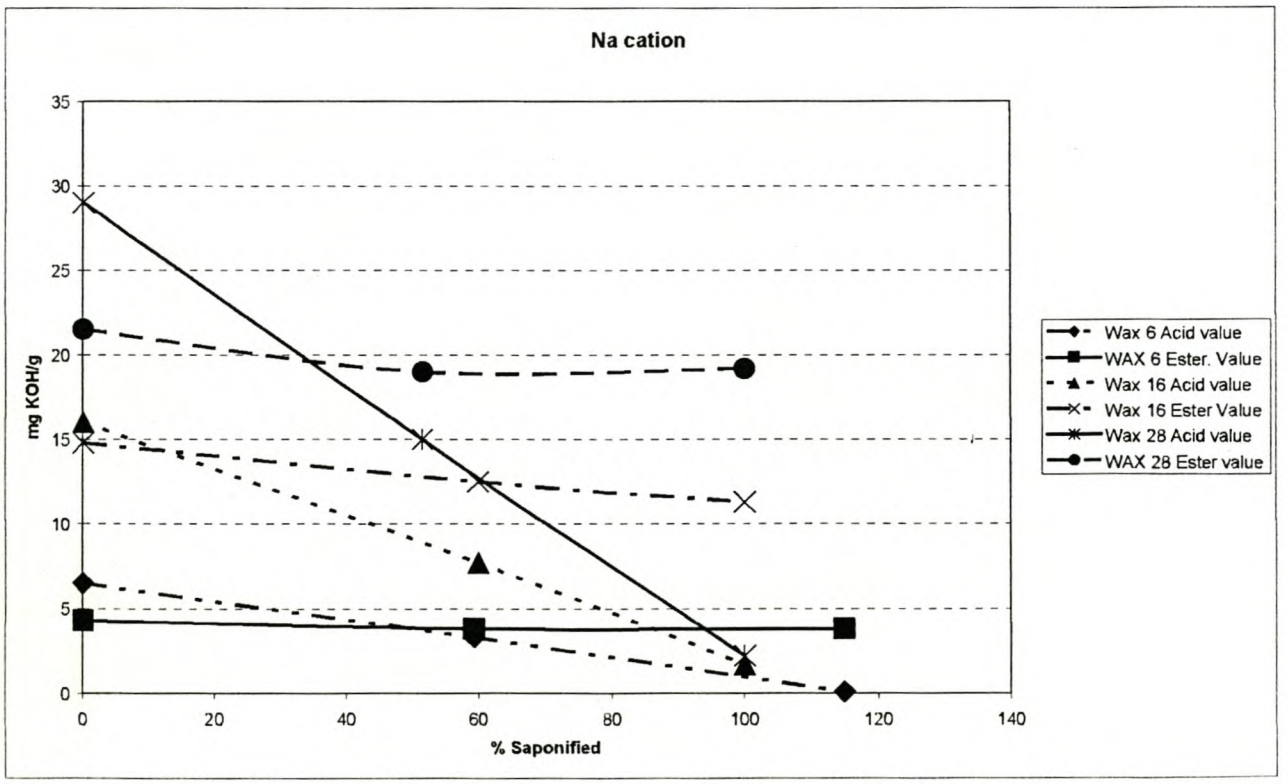

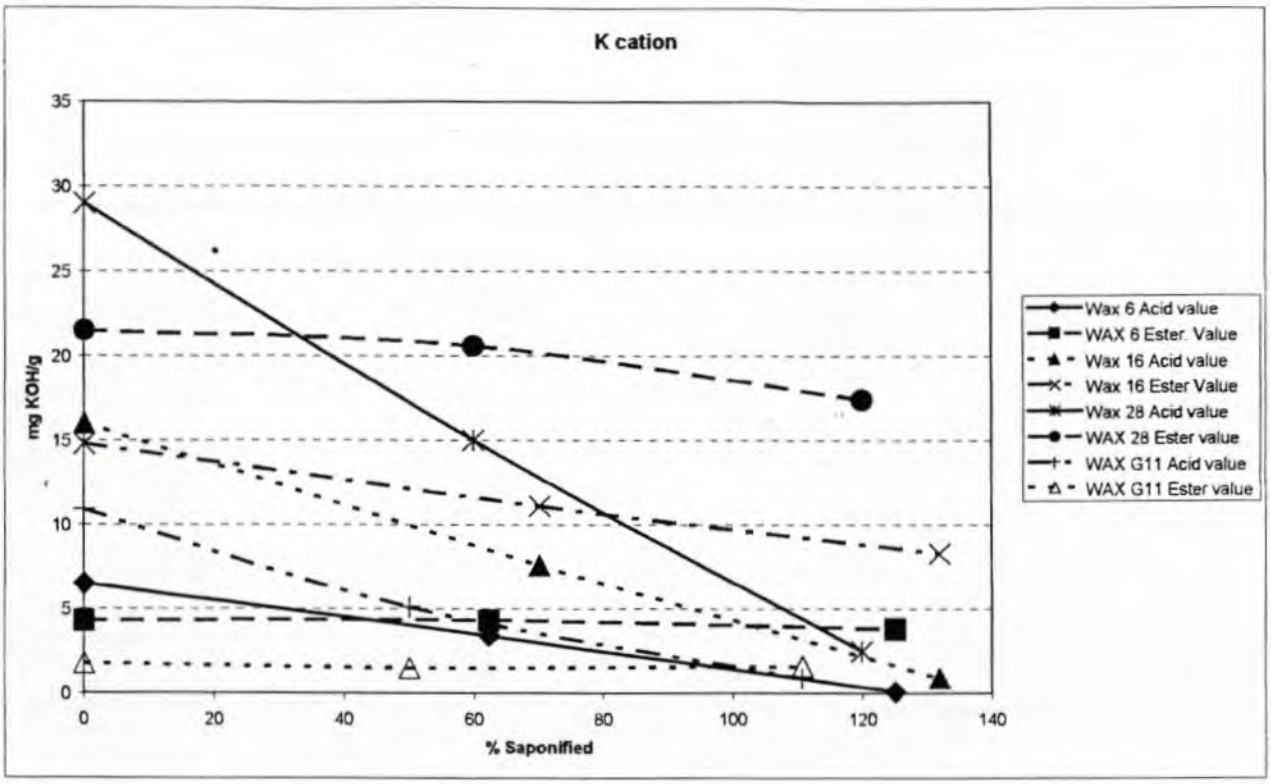

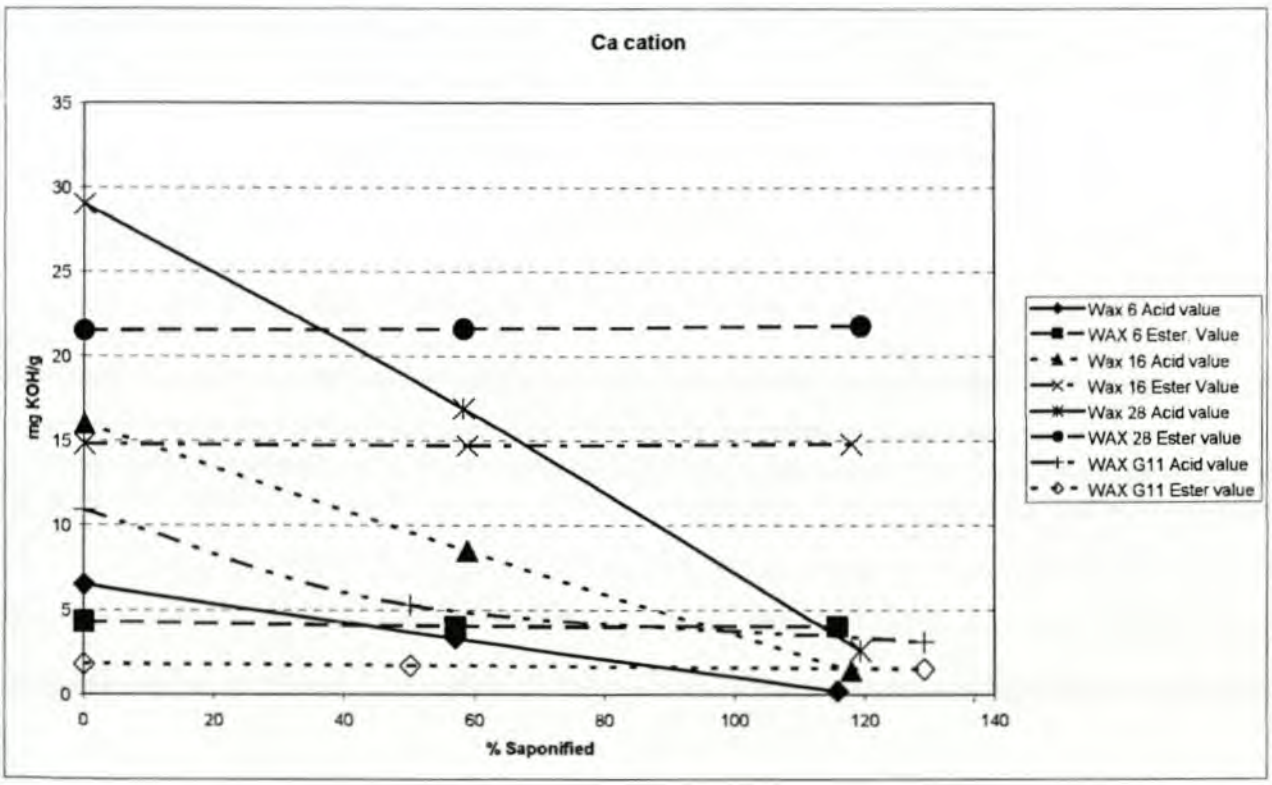

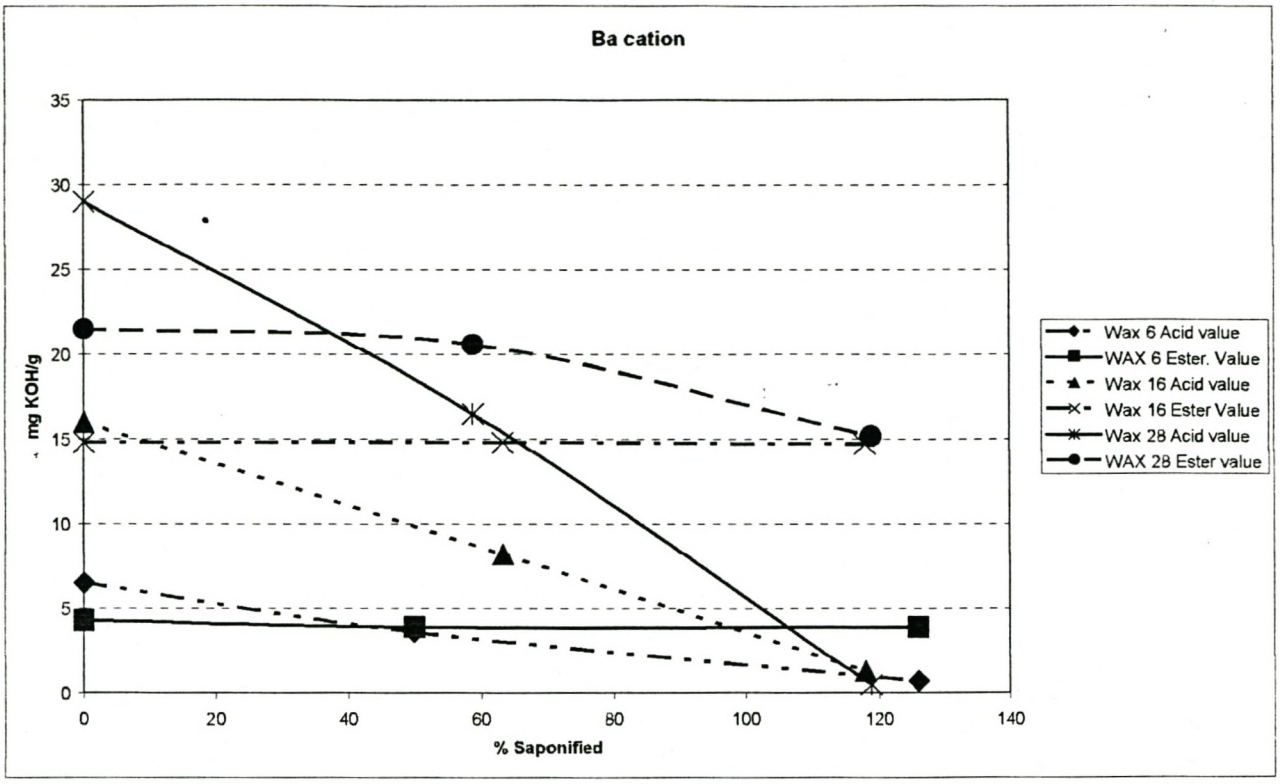

APPENDIX 5.1

Raw data for maximum stress results

Oxidised wax	Cation	% Saponified and (number of samples analysed)	Max. Tensile strength (MPa)	Standard deviation (MPa)	Coefficient of variance (%)
WAX 6*	Li	0 (6)	3.00	0.46	15.3
		50.0 (6)	2.42	0.38	15.6
		100.0 (7)	2.82	0.67	23.8
	Na	0 (6)	3.00	0.46	15.3
		59.3 (11)	2.59	0.61	23.7
		115.0 (9)	3.20	0.78	24.4
	K	0 (6)	3.00	0.46	15.3
		62.3 (6)	3.38	0.86	25.6
		125.0 (6)	4.40	0.80	18.1
	Ca	0 (6)	3.00	0.46	15.3
		57.0 (7)	1.43	0.40	28.0
		115.8 (5)	2.68	0.53	19.8
	Ba	0 (6)	3.00	0.46	15.3
		50.0 (7)	3.54	0.82	23.1
		126.0 (6)	1.46	0.41	28.4
WAX 16	Li	0 (6)	2.63	0.66	24.9
		58.7 (6)	3.87	0.49	12.8
		100 (7)	3.30	0.80	24.1
	Na	0 (6)	2.63	0.66	24.9
		59.9 (6)	3.53	0.51	14.5
		100 (5)	2.12	0.71	33.3
	K	0 (6)	2.63	0.66	24.9
		70.2 (6)	1.70	0.28	16.2
		131.9 (7)	1.65	0.17	10.1
	Ca	0 (6)	2.63	0.66	24.9
		58.8 (5)	1.34	0.18	13.1
		119.4 (5)	3.42	0.48	14.1
	Ba	0 (6)	2.63	0.66	24.9
		63.3 (6)	1.77	0.31	17.5

APPENDIX 5.1 (continued)

Raw data for maximum stress results

Oxidised wax	Cation	% Saponified and (number of samples analysed)	Max. Tensile strength (MPa)	Standard deviation (MPa)	Coefficient of variance (%)
WAX 16	Ba	117.9 (5)	1.11	0.08	7.2
WAX 28	Li	0 (5)	1.85	0.12	6.2
		50 (6)	2.48	0.33	13.4
		72.5 (7)	2.53	0.74	29.1
	Na	0 (5)	1.85	0.12	6.2
		51.4 (8)	3.40	0.65	19.2
		100 (6)	1.35	0.29	21.4
	K	0 (5)	1.85	0.12	6.2
		59 (6)	2.28	0.49	21.4
		119.9 (9)	2.19	0.38	17.4
	Ca	0 (5)	1.85	0.12	6.2
		58.2 (7)	1.15	0.30	25.6
		119.3 (5)	0.56	0.08	14.8
	Ba	0 (5)	1.85	0.12	6.24
		58.8 (5)	2.31	0.39	17.1
		118.8 (7)	1.77	0.51	28.5
WAX G11	K	0 (5)	2.87	0.26	9.0
		50.0 (6)	4.16	0.94	22.6
		110.7 (7)	3.95	0.33	8.5
	Ca	0 (5)	2.87	0.26	9.0
		50.0 (7)	2.40	0.89	37.0
		129.1 (9)	5.35	1.23	22.9

APPENDIX 5.2

Raw data for maximum strain results

Oxidised wax	Cation	% Saponified and (number of samples analysed)	Max. Elongation (%)	Standard deviation (%)	Coefficient of variance (%)
WAX 6	Li	0 (6)	8.58	1.19	13.9
		50.0 (6)	7.58	0.77	10.2
		100.0 (7)	7.42	0.97	13.1
	Na	0 (6)	8.58	1.19	13.9
		59.3 (11)	8.01	1.89	23.6
		115.0 (9)	8.58	1.72	20.0
	K	0 (6)	8.58	1.19	13.9
		62.3 (6)	9.22	1.64	17.8
		125.0 (6)	10.99	2.72	24.7
	Ca	0 (6)	8.58	1.19	13.9
		57.0 (7)	8.42	1.15	13.7
		115.8 (5)	8.56	1.93	22.5
	Ba	0 (6)	8.58	1.19	13.9
		50.0 (7)	8.72	1.49	17.1
		126.0 (6)	5.73	1.63	28.5
WAX 16	Li	0 (6)	10.26	1.48	14.5
		58.7 (6)	9.09	1.29	14.2
		100 (7)	9.61	1.07	11.1
	Na	0 (6)	10.26	1.48	14.5
		59.9 (6)	9.05	0.72	8.0
		100 (5)	7.16	1.10	15.3
	K	0 (6)	10.26	1.48	14.5
		70.2 (6)	7.53	1.14	15.2
		131.9 (7)	6.10	0.75	12.3
	Ca	0 (6)	10.26	1.48	14.45
		58.8 (5)	4.98	1.36	27.3
		119.4 (5)	9.41	1.52	16.1
	Ba	0 (6)	10.26	1.48	14.5
		63.3 (6)	6.99	0.53	7.6

APPENDIX 5.2 (continued)

Raw data for maximum strain results

Oxidised wax	Cation	% Saponified and (number of samples analysed)	Max. Elongation (%)	Standard deviation (%)	Coefficient of variance (%)
WAX 16	Ba	117.9 (5)	5.31	1.11	20.9
WAX 28	Li	0 (5)	11.98	1.38	11.5
		50 (6)	7.41	1.02	13.8
		72.5 (7)	8.54	1.87	21.9
	Na	0 (5)	11.98	1.38	11.5
		51.4 (8)	9.77	0.96	9.9
		100 (6)	4.50	0.88	19.4
	K	0 (5)	11.98	1.38	11.5
		59 (6)	8.49	1.47	17.3
		119.9 (9)	6.35	0.56	8.9
	Ca	0 (5)	11.98	1.38	11.5
		58.2 (7)	5.92	2.13	35.9
		119.3 (5)	6.47	0.72	11.1
	Ba	0 (5)	11.98	1.38	11.5
		58.8 (5)	8.58	0.65	7.6
		118.8 (7)	5.47	0.78	14.3
WAX G11	K	0 (5)	7.88	1.51	19.2
		50.0 (6)	10.59	1.66	15.7
		110.7 (7)	10.75	1.23	11.4
	Ca	0 (5)	7.88	1.51	19.2
		50.0 (7)	5.96	1.58	26.6
		129.1 (9)	9.53	1.37	14.4

APPENDIX 5.3

Raw data for modulus results

Oxidised wax	Cation	% Saponified and (number of samples analysed)	Modulus (MPa)	Standard deviation (MPa)	Coefficient of variance (%)
WAX 6	Li	0 (6)	35.8	5	13.9
		50.0 (6)	32.0	4.7	14.8
		100.0 (7)	32.8	6.5	19.8
	Na	0 (6)	35.8	5	13.9
		59.3 (11)	33.4	6.3	18.8
		115.0 (9)	37.5	6.4	16.9
	K	0 (6)	35.8	5	13.9
		62.3 (6)	37.4	8.2	21.9
		125.0 (6)	46.1	4.6	10.0
	Ca	0 (6)	35.8	5	13.9
		57.0 (7)	17.4	6.3	36.3
		115.8 (5)	31.8	4.4	13.7
	Ba	0 (6)	35.8	5	13.9
		50.0 (7)	40.9	5.8	14.2
		126.0 (6)	25.8	2.8	31.4
WAX 16	Li	0 (6)	25.7	3.2	12.5
		58.7 (6)	42.9	3.1	7.3
		100 (7)	34.9	9.5	27.2
	Na	0 (6)	25.7	3.2	12.5
		59.9 (6)	39.3	6.1	15.6
		100 (5)	29.5	7.6	26.0
	K	0 (6)	25.7	3.2	12.5
		70.2 (6)	22.9	3.0	13.0
		131.9 (7)	27.3	3.2	11.7
	Ca	0 (6)	25.7	3.2	12.5
		58.8 (5)	27.8	4.8	17.1
		119.4 (5)	36.5	1.8	4.8

APPENDIX 5.3 (continued)

Raw data for modulus results

Oxidised wax	Cation	% Saponified and (number of samples analysed)	Modulus (MPa)	Standard deviation (MPa)	Coefficient of variance (%)
WAX 16	Ba	0 (6)	25.7	3.2	12.5
		63.3 (6)	25.7	5.9	23.0
		117.9 (5)	21.6	4.1	19.1
WAX 28	Li	0 (5)	15.8	1.4	8.7
		50 (6)	33.7	3.6	10.8
		72.5 (7)	30.1	8.0	26.5
	Na	0 (5)	15.8	1.4	8.7
		51.4 (8)	34.8	5.3	15.1
		100 (6)	30.3	4.6	15.1
	K	0 (5)	15.8	1.4	8.7
		59 (6)	27.3	4.8	17.7
		119.9 (9)	34.7	4.5	13.0
	Ca	0 (5)	15.8	1.4	8.7
		58.2 (7)	21.5	8.2	38.3
		119.3 (5)	9.1	0.3	3.2
	Ba	0 (5)	15.8	1.4	8.7
		58.8 (5)	26.8	3.2	12.0
		118.8 (7)	32.0	4.9	15.3
WAX G11	K	0 (5)	37.3	4.7	12.5
		50.0 (6)	40.0	9.2	23.0
		110.7 (7)	37.1	4.6	12.4
	Ca	0 (5)	37.3	4.7	12.5
		50.0 (7)	40.3	7.2	17.9
		129.1 (9)	56.2	8.2	14.6

APPENDIX 5.4

Raw data for toughness results

Oxidised wax	Cation	% Saponified and (number of samples analysed)	Toughness (kPa)	Standard deviation (kPa)	Coefficient of variance (%)
WAX 6	Li	0 (6)	161	55	34
		50.0 (6)	134	22	16
		100.0 (7)	126	34	27
	Na	0 (6)	161	55	34
		59.3 (11)	137	53	39
		115.0 (9)	167	66	40
	K	0 (6)	161	55	34
		62.3 (6)	211	52	25
		125.0 (6)	277	70	25
	Ca	0 (6)	161	55	34
		57.0 (7)	95	17	18
		115.8 (5)	144	55	38
	Ba	0 (6)	161	55	34
		50.0 (7)	184	71	38
		126.0 (6)	58	42	72
WAX 16	Li	0 (6)	165	64	39
		58.7 (6)	195	45	23
		100 (7)	202	27	13
	Na	0 (6)	165	64	39
		59.9 (6)	190	29	15
		100 (5)	119	36	31
	K	0 (6)	165	64	39
		70.2 (6)	101	32	32
		131.9 (7)	71	26	37
	Ca	0 (6)	165	64	39
		58.8 (5)	49	30	61
		119.4 (5)	190	47	25
	Ba	0 (6)	165	64	39
		63.3 (6)	97	20	21
		117.9 (5)	59	15	26
WAX 28	Li	0 (5)	134	32	24
		50 (6)	108	31	29
		72.5 (7)	165	70	42

APPENDIX 5.4 (continued)

Raw data for toughness results

Oxidised wax	Cation	% Saponified and (number of samples analysed)	Toughness (kPa)	Standard deviation (kPa)	Coefficient of variance (%)
WAX 28	Na	0 (5)	134	32	24
		51.4 (8)	195	42	21
		100 (6)	37	14	64
	K	0 (5)	134	32	24
		59 (6)	125	56	45
		119.9 (9)	86	18	21
	Ca	0 (5)	134	32	24
		58.2 (7)	60	14	23
		119.3 (5)	32	19	58
	Ba	0 (5)	134	32	24
		58.8 (5)	115	19	17
		118.8 (7)	62	22	36
WAX G11	K	0 (5)	165	61	37
		50.0 (6)	266	72	27
		110.7 (7)	283	56	20
	Ca	0 (5)	165	61	37
		50.0 (7)	102	67	65
		129.1 (9)	300	89	30

APPENDIX 6.1
Rheometric experimental results

Wax Type	% Saponified	Cation type	G' Transition temperature (°C)	G' Transition value (Pa)	G" Transition temperature (°C)	G" Transition value (Pa)	Tan δ Temperature (°C)	Tan δ value
6	0.0		43.4	5.61E+09	6.2	8.33E+08	13.8	0.088
	50.0	Li	38.7	4.51E+09	1.7	6.97E+08	7.5	0.086
	100.0		43.5	5.15E+09	2.6	6.92E+08	9.0	0.074
	59.3	Na	43.7	4.65E+09	4.4	4.89E+08	9.2	0.063
	115.0		43.2	4.77E+09	-0.2	6.58E+08	7.2	0.072
	62.3	K	35.6	2.11E+09	-9.8	4.67E+08	0.5	0.091
	125.0		32.2	3.53E+09	0.6	4.06E+08	7.5	0.072
	57.0	Ca	38.9	4.20E+09	-1.5	6.37E+09	6.2	0.080
	115.8		34.1	4.38E+09	0.6	7.16E+08	6.6	0.091
	50.0	Ba	45.1	4.85E+09	2.6	6.80E+08	9.6	0.077
	126.0		34.2	4.18E+09	0.8	7.02E+08	7.9	0.091
16	0.0		40.0	3.63E+09	-7.6	8.44E+08	9.2	0.105
	58.7	Li	37.3	4.26E+09	0.9	6.49E+08	9.6	0.084
	100.0		40.6	3.32E+09	0.6	4.90E+08	8.9	0.075
	59.9	Na	38.0	4.77E+08	-2.0	6.24E+07	5.9	0.072
	100.0		36.3	3.85E+08	1.0	3.31E+07	6.3	0.055
	70.2	K	43.6	3.37E+08	-1.1	6.09E+07	7.0	0.084
	131.9		31.7	5.03E+08	4.3	4.78E+07	7.0	0.071
	58.8	Ca	34.5	4.57E+09	-7.2	6.48E+08	4.0	0.077
	119.4		37.3	3.33E+08	-0.7	4.42E+07	8.0	0.075
	63.3	Ba	37.3	4.01E+09	-3.4	6.30E+08	7.3	0.084
	117.9		40.5	3.03E+09	4.9	4.40E+08	9.6	0.078
28	0.0		35.6	2.22E+09	-21.7	7.17E+08	-12.1	0.094
	50.0	Li	31.8	4.01E+09	-13.8	6.21E+08	-3.0	0.071
	72.5		47.2	1.89E+08	-4.7	4.61E+07	0.6	0.067
	51.4	Na	38.3	2.84E+08	-9.7	3.71E+07	-3.7	0.068
	100.0		33.6	4.18E+09	-4.1	3.92E+08	4.2	0.057
	59.0	K	33.9	2.23E+09	-8.9	4.65E+08	-0.7	0.089
	119.9		30.9	3.33E+08	-7.7	4.32E+07	-0.4	0.069
	58.2	Ca	33.9	4.56E+09	-18.5	6.60E+08	-8.4	0.067
	119.3		35.0	3.36E+08	-5.7	3.73E+07	1.0	0.063
	58.8	Ba	29.6	3.46E+09	-20.7	5.43E+08	-10.1	0.068
	129.1		44.7	2.04E+09	-2.8	3.41E+08	6.9	0.078

APPENDIX 7.1

Original mass % increase results for WAX 6

TIME (DAYS)	% SAPONIFIED AND CATION TYPE (RESULTS BELOW ARE % INCREASE FROM ORIGINAL MASS)						
	0 %	Li, 50.0 %	Li, 100.0 %	Na, 59.3 %	Na, 100.0 %	K, 62.3 %	K, 125.0 %
7	0.0076	0.0277	0.0534	0.0732	0.1854	0.1466	0.4021
14	0.0101	0.0485	0.0757	0.1086	0.2879	0.1990	0.6245
22	0.0082	0.0510	0.0853	0.1275	0.3600	0.2262	0.8161
38	0.0158	0.0680	0.1139	0.1622	0.5049	0.2880	1.2062
53	0.0120	0.0787	0.1355	0.1913	0.6200	0.3272	1.5654
73	0.0171	0.0932	0.1527	0.2247	0.7523	0.3759	1.9851
95	0.0253	0.1070	0.1775	0.2557	0.8902	0.4151	2.4206
140	***	0.1291	0.2023	0.3081	1.1458	0.5098	***
193	***	0.1549	0.2341	0.3579	1.3672	0.5831	***
246	***	0.1668	0.2647	0.4047	1.5614	0.6627	***
310	***	0.1822	0.2876	0.4431	1.7645	0.7366	***

APPENDIX 7.1 (continued)

Original mass % increase results for WAX 6

TIME (DAYS)	% SAPONIFIED AND CATION TYPE (RESULTS BELOW ARE % INCREASE FROM ORIGINAL MASS)			
	Ca, 57.0 %	Ca, 115.8 %	Ba, 50.0 %	Ba, 126.0 %
7	0.0226	0.0515	0.2530	0.0444
14	0.0327	0.0711	***	0.0578
22	0.0402	0.0820	0.0411	0.0647
38	0.0571	0.1064	0.0549	0.0800
53	0.0653	0.1186	0.0619	0.0755
73	0.0753	0.1294	0.0726	0.0800
95	0.0873	0.1409	0.0789	0.0876
140	0.1030	0.1599	0.0935	0.0908
193	0.1080	0.1714	0.0966	0.0971
246	0.1212	0.1782	0.1042	0.0984
310	0.1300	0.1823	0.1035	0.0983

APPENDIX 7.2

Original mass % increase results for WAX 16

TIME (DAYS)	% SAPONIFIED AND CATION TYPE (RESULTS BELOW ARE % INCREASE FROM ORIGINAL MASS)						
	0 %	Li, 58.7 %	Li, 100.0 %	Na, 59.9 %	Na, 100.0 %	K, 70.2 %	K, 131.9 %
1	***	***	***	***	0.0880	***	***
2	***	***	***	0.1200	***	***	***
3	***	***	***	***	0.1650	0.9528	***
4	0.0205	0.0516	0.0700	***	***	***	3.6417
7	0.0285	0.0702	0.1000	0.2200	***	1.7571	5.0645
9	***	***	***	***	0.4460	***	***
10	***	***	***	0.2600	***	***	***
11	***	***	***	***	0.4820	***	***
12	0.0417	0.1006	0.1400	***	***	***	6.3754
15	***	***	***	0.3400	***	***	***
16	***	***	***	***	0.5920	***	***
17	***	***	***	***	***	2.2531	***
18	***	0.1145	0.1700	***	0.7300	***	***
21	***	***	***	***	0.8940	***	***
22	***	***	***	***	0.9270	***	***
28	***	***	***	***	1.2000	2.9867	***
29	0.0497	0.1443	0.2100	0.5200	***	***	***
30	***	***	***	***	1.1820	***	***
31	***	***	***	***	***	3.1575	***
32	0.0484	0.1502	0.2200	***	***	***	***
35	***	***	***	0.5800	1.3510	3.4284	***
36	0.0497	0.1575	0.2400	***	***	***	***
38	***	***	***	***	1.485	***	***
39	***	***	***	0.6300	***	***	***
42	***	***	***	***	***	3.9127	***
43	0.0523	0.1743	0.2700	***	1.7160	***	***
52	***	***	***	***	***	4.4886	***
53	0.0517	0.1946	0.2879	***	***	***	***
56	***	***	***	0.8374	***	***	***
60	***	***	***	***	***	4.8354	***
61	0.0523	0.2072	0.3017	***	***	***	***
63	***	***	***	***	2.5184	***	***
64	***	***	***	0.9231	***	***	***

APPENDIX 7.2 (continued)

Original mass % increase results for WAX 16

TIME (DAYS)	% SAPONIFIED AND CATION TYPE (RESULTS BELOW ARE % INCREASE FROM ORIGINAL MASS)						
67	***	***	***	***	2.6500	***	***
73	***	***	***	***	***	4.9859	***
74	0.0636	0.2323	0.3339	***	2.9157	***	***
77	***	***	***	1.0427	***	***	***
80	***	***	***	***	***	5.0317	***
81	0.0643	0.2409	0.3523	***	***	***	***
84	***	***	***	1.0963	3.4785	***	***
87	***	***	***	***	***	5.1626	***
88	0.0616	0.2495	0.3642	***	***	***	***
92	***	***	***	1.1133	3.8000	***	***
95	***	***	***	***	***	5.0971	***
96	0.0570	0.2502	0.3694	***	***	***	***
99	***	***	***	1.1754		***	***
105	***	***	***	***	4.2853	***	***
109	***	0.2528	0.3826	***	***	***	***
112	***	***	***	1.2974	4.4358	***	***
117	***	0.2621	0.3885	***	***	***	***
119	***	***	***	***	4.5547	***	***
120	***	***	***	1.3421	***	***	***
123	***	0.2687	0.3931	***	***	***	***
126	***	***	***	1.3761	***	***	***
127	***	***	***	***	4.7790	***	***
132	***	0.2747	0.4056	***	***	***	***
135	***	***	***	1.4199	***	***	***
145	***	0.2839	0.4207	***	***	***	***
148	***	***	***	1.4657	***	***	***

APPENDIX 7.2 (continued)
Original mass % increase results for WAX 16

TIME (DAYS)	% SAPONIFIED AND CATION TYPE (RESULTS BELOW ARE % INCREASE FROM ORIGINAL MASS)			
	Ca, 57.0 %	Ca, 115.8 %	Ba, 50.0 %	Ba, 126.0 %
2	0.0486	0.0653	***	0.0610
3	***	***	0.0415	***
6	***	***	0.0599	***
7	0.0617	0.0930	***	0.1092
10	0.0755	0.1095	***	***
11	***	***	0.0843	***
15	0.0971	0.1326	***	0.1320
17	***	***	0.0876	***
28	***	***	0.1165	***
29	0.1260	0.1795	***	0.1842
31	***	***	0.1185	***
35	0.1365	0.1907	0.1257	0.1942
39	0.1404	0.1960	***	0.2036
42	***	***	0.1323	***
46	0.1503	0.2138	***	0.223
52	***	***	0.1501	***
56	0.1641	0.2323	***	0.2420
60	***	***	0.1573	***
64	0.1719	0.2481	***	0.2550
73	***	***	0.1758	***
77	0.1936	0.2719	***	0.2850
80	***	***	0.1797	***
84	0.2008	0.2818	***	0.2974
87	***	***	0.1870	***
91	0.2041	0.2950	***	0.3041
95	***	***	0.1863	***
99	0.2041	0.2923	***	0.3054
112	***	0.2904	***	0.3061
115	***	***	0.1935	***
120	0.2107	0.3022	***	0.3195
122	***	***	0.1962	***
126	0.2146	0.3088	***	0.3262
131	***	***	0.2008	***
135	0.2205	0.3148	***	0.3322
145	***	***	0.2087	***

APPENDIX 7.3

Original mass % increase results for WAX 28

TIME (DAYS)	% SAPONIFIED AND CATION TYPE (RESULTS BELOW ARE % INCREASE FROM ORIGINAL MASS)						
	0 %	Li, 50.0 %	Li, 72.5 %	Na, 51.4 %	Na, 100.0 %	K, 59.0 %	K, 119.9 %
2	***	***	***	0.6950	1.6470	2.2430	5.1055
3	***	0.0938	***	***	***	***	***
4	0.0369	***	0.1244	***	***	***	***
5	***	***	***	1.2790	***	3.6690	***
6	***	0.1380	***	1.4430	***	4.1000	***
7	0.0519	***	0.1772	***	4.1490	***	12.2900
10	***	***	***	***	5.4550	***	***
11	***	0.1915	***	***	***	***	***
12	0.0674	***	0.2454	2.2030	***	6.3400	***
14	***	***	***	2.2790	***	***	***
15	***	***	***	***	***	7.4290	***
17	***	0.2325	***	***	***	***	***
18	***	***	0.2968	***	***	***	***
19	***	***	***	2.7290	***	***	***
22	***	***	***	3.0260	***	***	***
27	***	***	***	3.6300	***	***	***
28	***	0.3137	***	***	***	***	***
29	0.0817	***	0.3834	***	***	***	***
31	***	0.3210	***	***	***	***	***
32	0.0914	***	0.4070	***	***	***	***
35	***	0.3443	***	***	***	***	***
36	0.0959	***	0.4361	***	***	***	***
41	***	***	***	5.5250	***	***	***
42	***	0.3824	***	***	***	***	***
43	0.1043	***	0.4787	***	***	***	***
52	***	0.4379	***	***	***	***	***
53	0.1082	***	0.5551	***	***	***	***
58	***	***	***	5.8580	***	***	***
60	***	0.4795	***	***	***	***	***
61	0.1102	***	0.5970	***	***	***	***
68	***	***	***	6.2120	***	***	***
73	***	0.5323	***	***	***	***	***
74	0.1290	***	0.6789	***	***	***	***

APPENDIX 7.3 (continued)

Original mass % increase results for WAX 28

TIME (DAYS)	% SAPONIFIED AND CATION TYPE (RESULTS BELOW ARE % INCREASE FROM ORIGINAL MASS)						
75	***	***	***	6.4500	***	***	***
80	***	0.5594	***	***	***	***	***
81	0.1270	***	0.7133	***	***	***	***
87	***	0.5713	***	***	***	***	***
88	0.1290	***	0.7316	***	***	***	***
95	***	0.5937	***	***	***	***	***
96	0.1303	***	0.7728	***	***	***	***
108	***	0.6380	***	***	***	***	***
109	0.1186	***	0.8371	***	***	***	***
116	***	0.6426	***	***	***	***	***
117	0.1212	***	0.8628	***	***	***	***
122	***	0.6624	***	***	***	***	***
123	***	***	0.8878	***	***	***	***
131	***	0.6862	***	***	***	***	***
132	***	***	0.9141	***	***	***	***
144	***	0.7119	***	***	***	***	***
145	0.1082	***	0.9540	***	***	***	***

APPENDIX 7.3 (continued)

Original mass % increase results for WAX 28

TIME (DAYS)	% SAPONIFIED AND CATION TYPE (RESULTS BELOW ARE % INCREASE FROM ORIGINAL MASS)			
	Ca, 58.2 %	Ca, 119.3 %	Ba, 58.8 %	Ba, 119.1 %
2	***	***	***	0.0521
3	0.0812	***	0.0780	***
6	0.1102	***	0.1107	***
7	***	0.1359	***	***
10	***	0.1609	***	0.1143
11	0.1498	***	0.1528	***
14	***	0.1906	***	***
15	***	***	***	0.1457
17	0.1736	***	0.1808	***
28	0.2185	***	0.2308	***
29	***	0.2658	***	0.2166
31	0.2291	***	0.2382	***

APPENDIX 7.3 (continued)

Original mass % increase results for WAX 28

TIME (DAYS)	% SAPONIFIED AND CATION TYPE (RESULTS BELOW ARE % INCREASE FROM ORIGINAL MASS)			
	Ca, 58.2 %	Ca, 119.3 %	Ba, 58.8 %	Ba, 119.1 %
2	***	***	***	0.0521
3	0.0812	***	0.0780	***
6	0.1102	***	0.1107	***
7	***	0.1359	***	***
10	***	0.1609	***	0.1143
11	0.1498	***	0.1528	***
14	***	0.1906	***	***
15	***	***	***	0.1457
17	0.1736	***	0.1808	***
28	0.2185	***	0.2308	***
29	***	0.2658	***	0.2166
35	0.2370	0.2849	0.2535	0.2226
39	***	0.2922	***	0.2359
42	0.2608	***	0.2735	***
46	***	0.3166	***	0.2627
52	0.2883	***	0.3075	***
56	***	0.3570	***	0.2948
60	0.3056	***	0.3235	***
64	***	0.3720	***	0.3075
73	0.3360	***	0.3536	***
77	***	0.4116	***	0.3422
80	0.3479	***	***	***
81	***	***	0.3789	***
84	***	0.4347	***	0.3576
87	0.3651	***	***	***
88	***	***	0.3796	***
91	***	0.4436	***	0.3730
95	0.3670	***	***	***
96	***	***	0.3849	***
99	***	0.4492	***	0.3803
108	0.3779	***	***	***
109	***	***	0.3949	***
112	***	0.4617	***	0.3937
116	0.3941	***	***	***
117	***	***	0.4069	***

APPENDIX 7.3 (continued)

Original mass % increase results for WAX 28

TIME (DAYS)	% SAPONIFIED AND CATION TYPE (RESULTS BELOW ARE % INCREASE FROM ORIGINAL MASS)			
	Ca, 58.2 %	Ca, 119.3 %	Ba, 58.8 %	Ba, 119.1 %
2	***	***	***	0.0521
3	0.0812	***	0.0780	***
6	0.1102	***	0.1107	***
7	***	0.1359	***	***
10	***	0.1609	***	0.1143
11	0.1498	***	0.1528	***
14	***	0.1906	***	***
15	***	***	***	0.1457
17	0.1736	***	0.1808	***
28	0.2185	***	0.2308	***
29	***	0.2658	***	0.2166
120	***	0.4808	***	0.4077
122	0.4047	***	***	***
123	***	***	0.4163	***
126	***	0.4901	***	0.4144
131	0.4132	***	***	***
132	***	***	0.4243	***
136	***	0.5026	***	0.4264
144	0.4278	***	***	***
145	***	***	0.4343	***

APPENDIX 7.4

Original mass % increase results for WAX G11

TIME (DAYS)	% SAPONIFIED AND CATION TYPE (RESULTS BELOW ARE % INCREASE FROM ORIGINAL MASS)						
	0 %	K, 50.0 %	K, 110.7 %	Ca, 50.0 %	Ca, 129.1 %		
8	0.0026	0.0804	0.0894	0.0079	0.0111		
24	0.0150	0.1503	0.1736	0.0236	0.0281		
39	0.0131	0.1889	0.2231	0.0308	0.0366		
59	0.0170	0.2321	0.2766	0.0426	0.0497		
81	0.0235	0.2674	0.3269	0.0517	0.0595		
126	0.0281	0.3281	0.4143	0.0662	0.0733		
179	0.0366	0.3844	0.4926	0.0766	0.0857		
232	0.0431	0.4308	0.5650	0.0865	0.0981		
296	0.0425	0.4759	0.6316	0.0930	0.1040		

APPENDIX 7.5
WAX 6 and the different cation sorption graphs

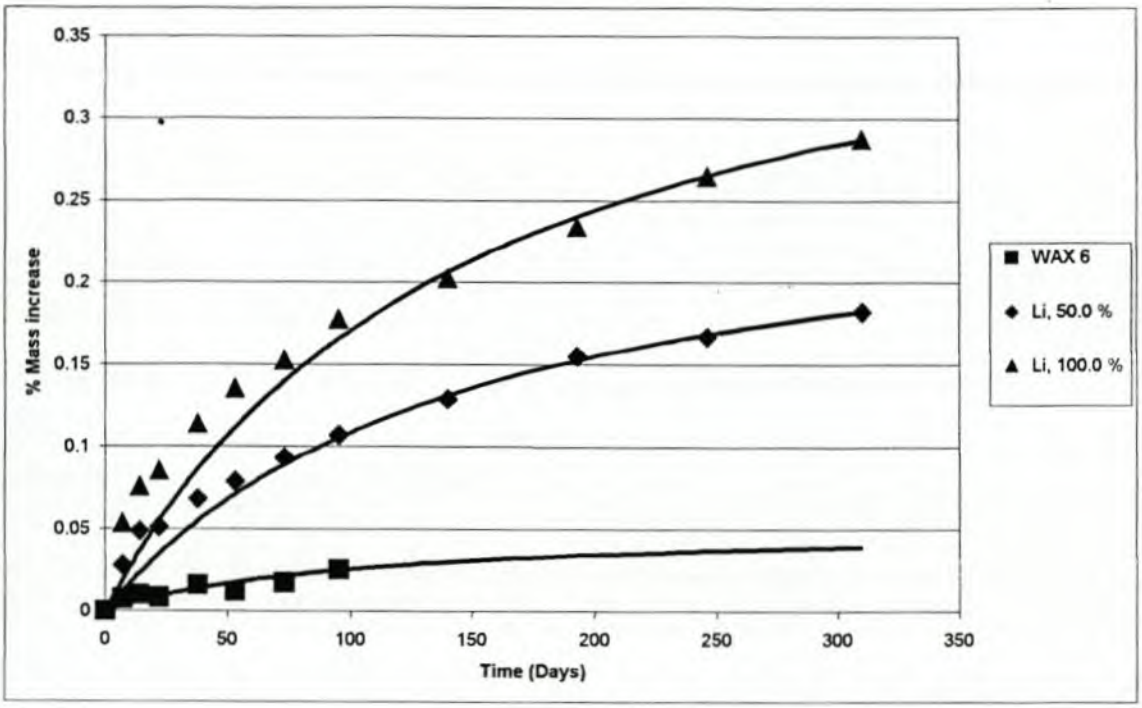

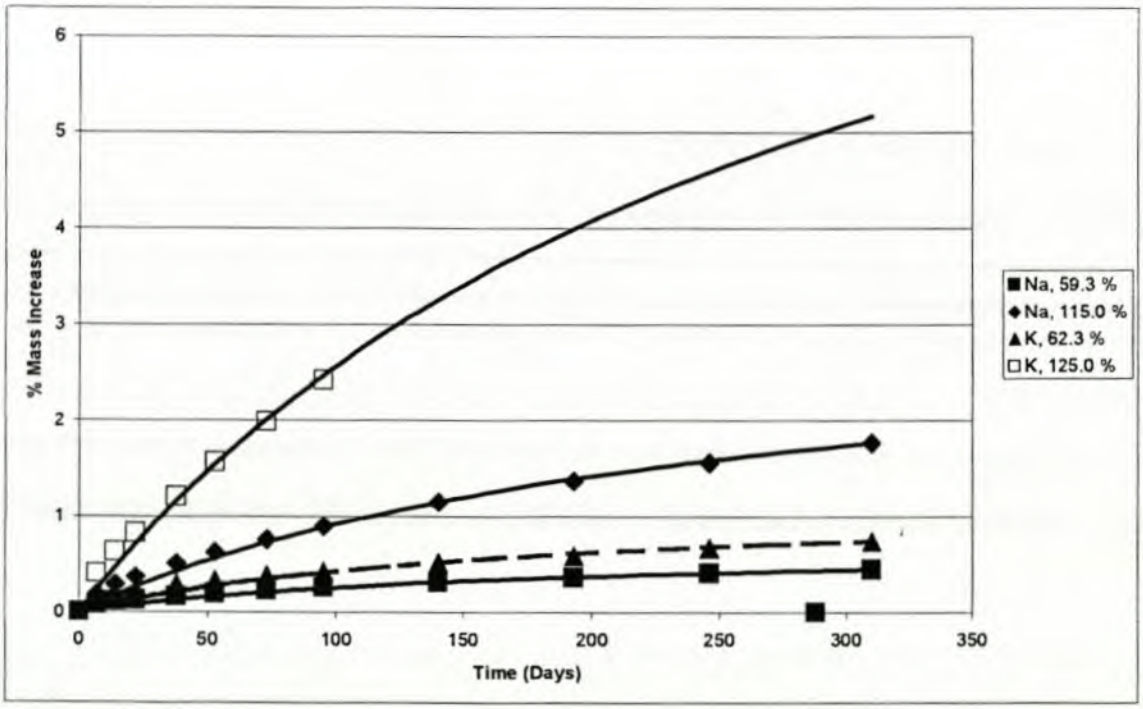

APPENDIX 7.5 (CONTINUED)

WAX 6 and the different cation sorption graphs

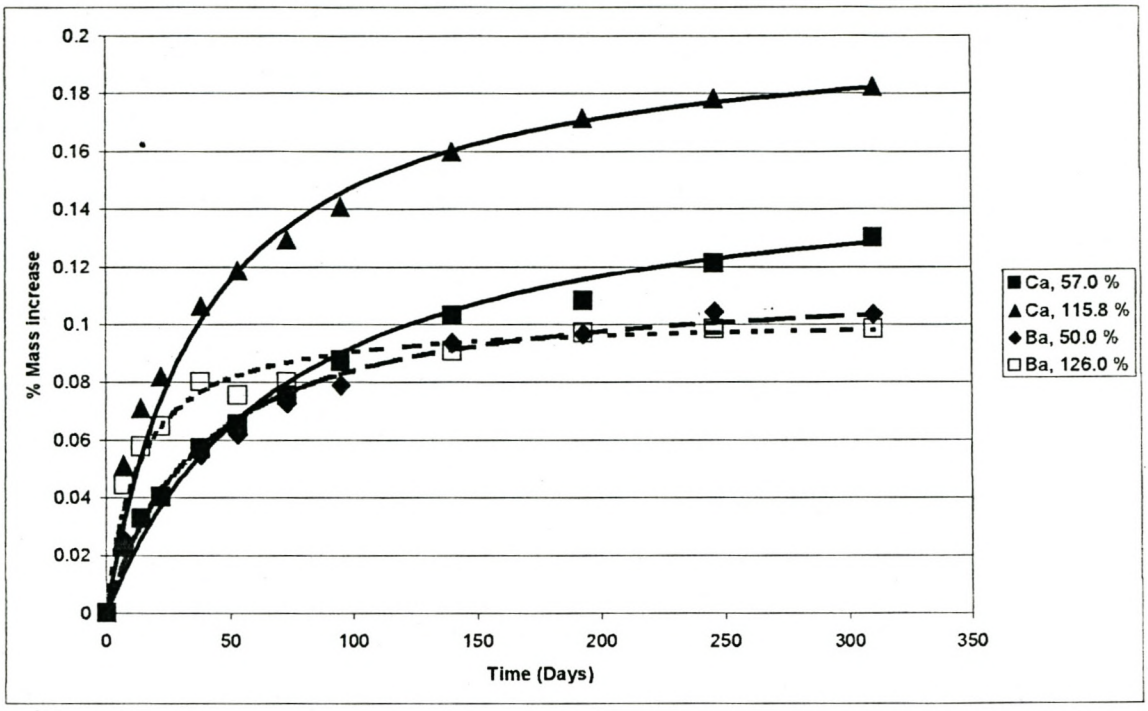

APPENDIX 7.6

WAX 16 and the different cation sorption graphs

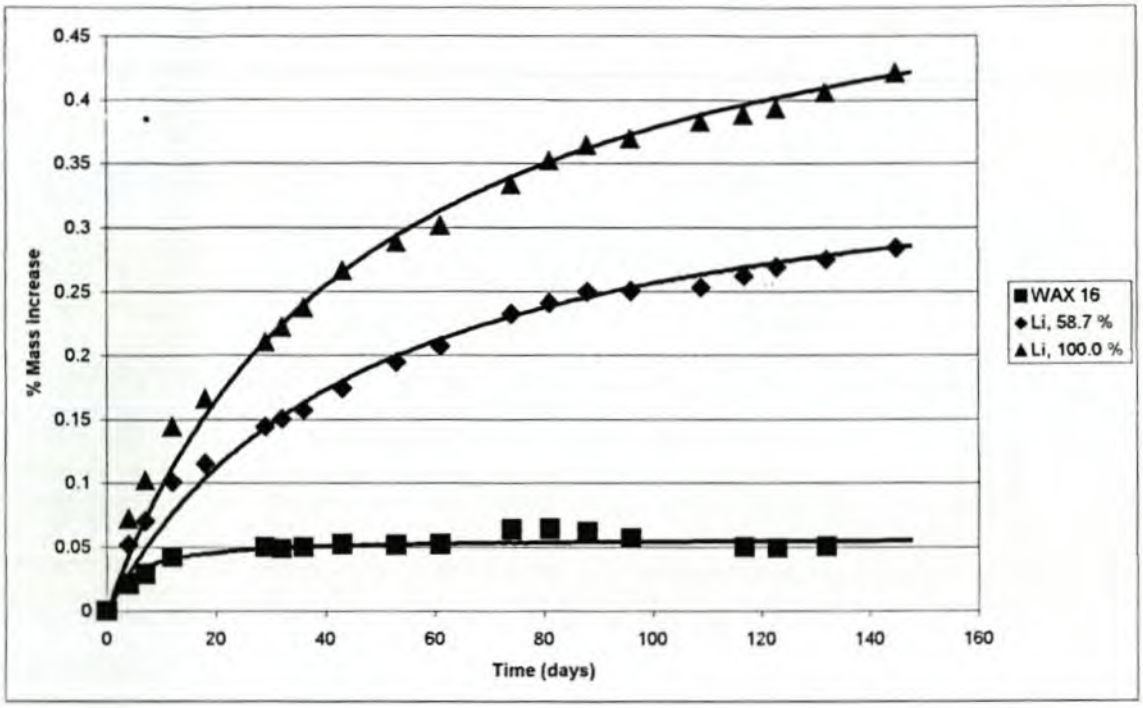

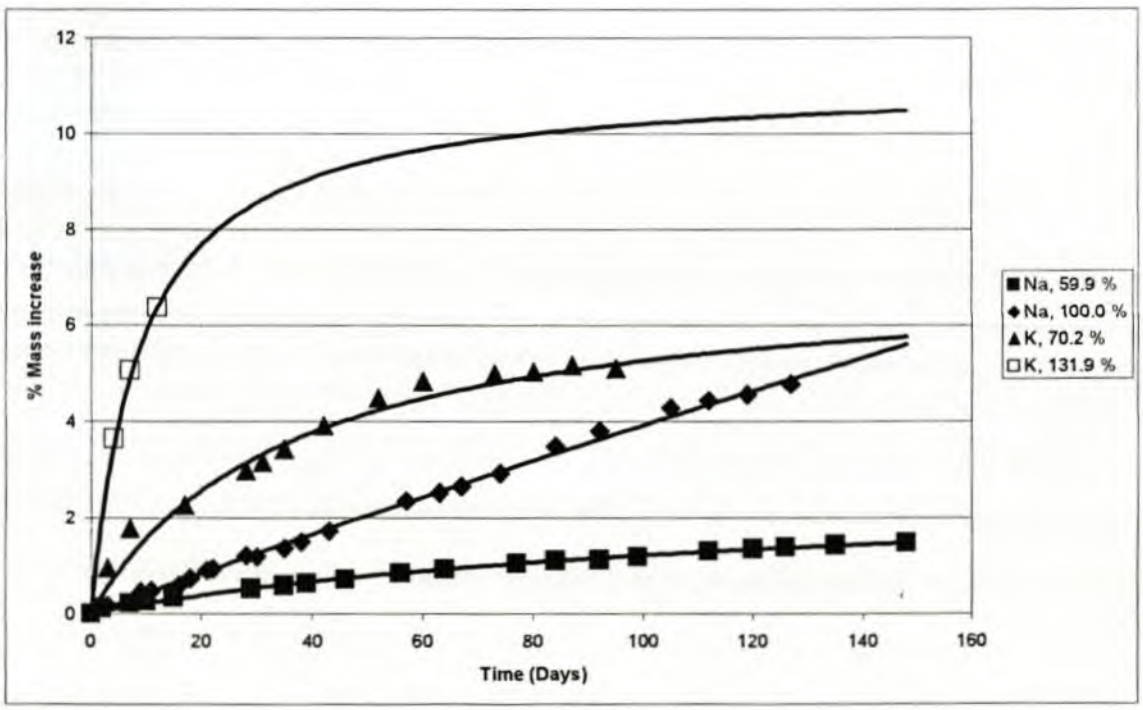

APPENDIX 7.6 (continued)

WAX 16 and the different cation sorption graphs

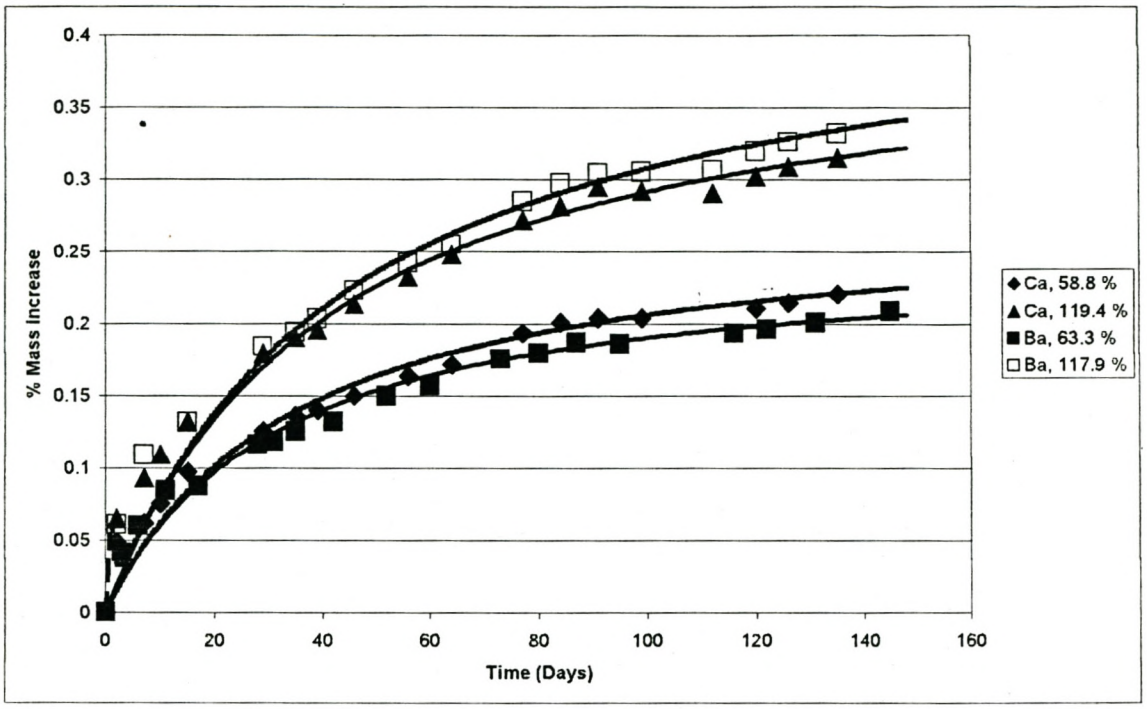

APPENDIX 7.7

WAX 28 and the different cation sorption graphs

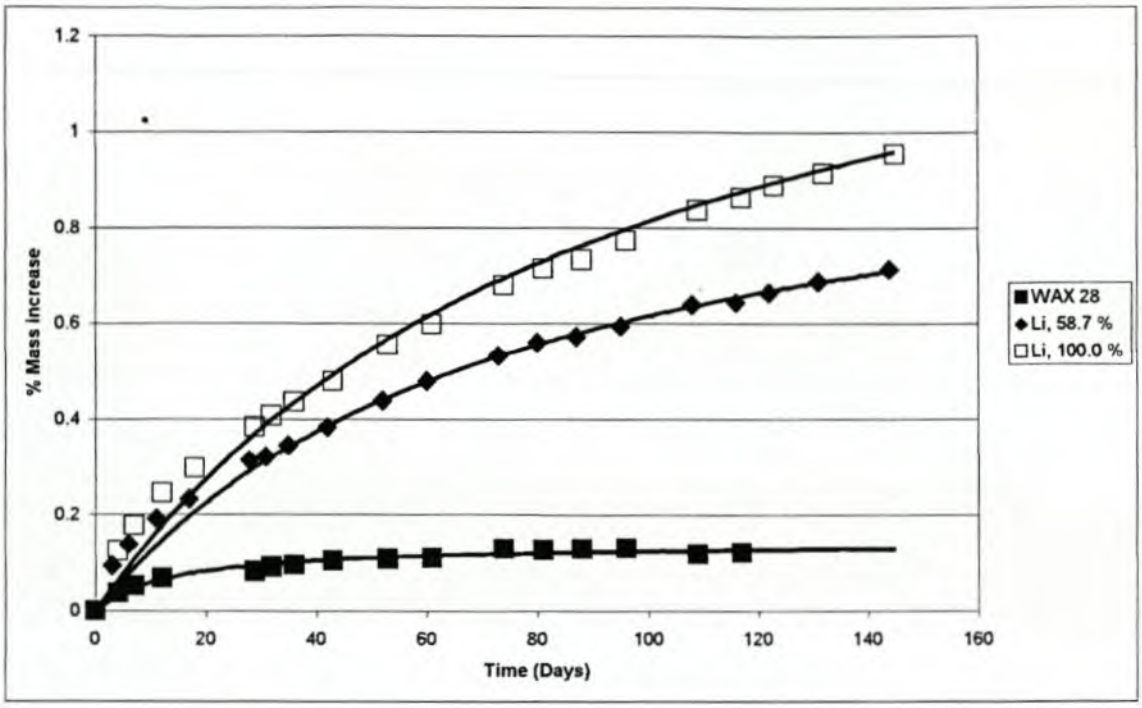

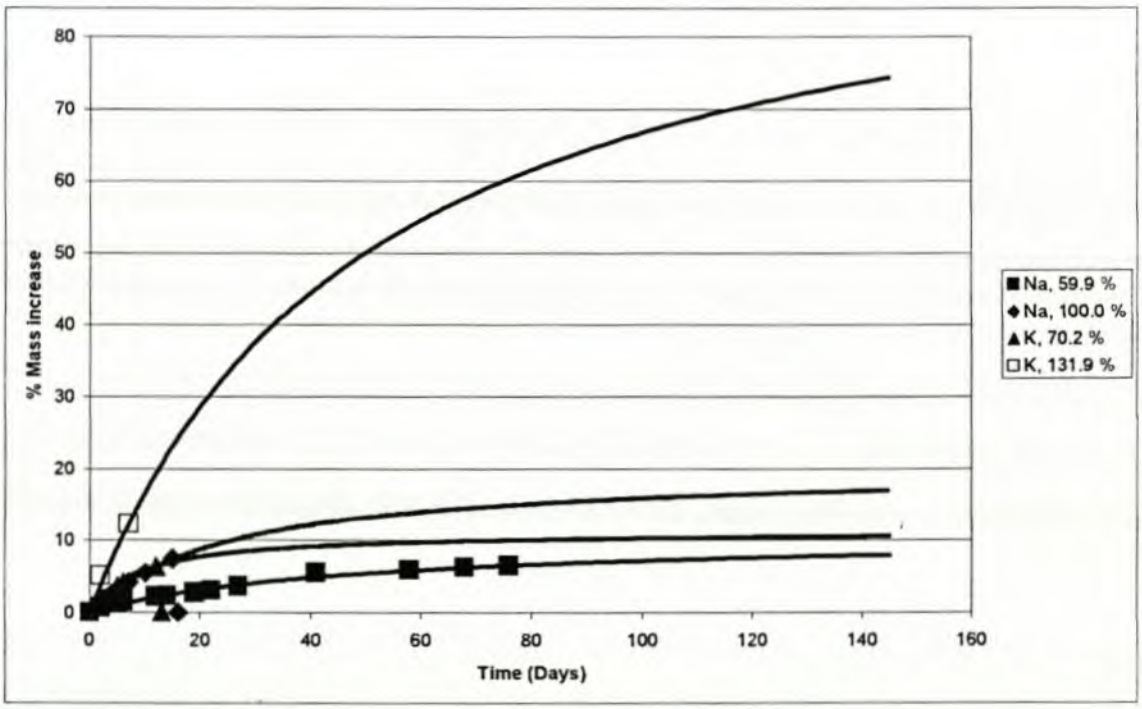

APPENDIX 7.7 (continued)

WAX 28 and the different cation sorption graphs

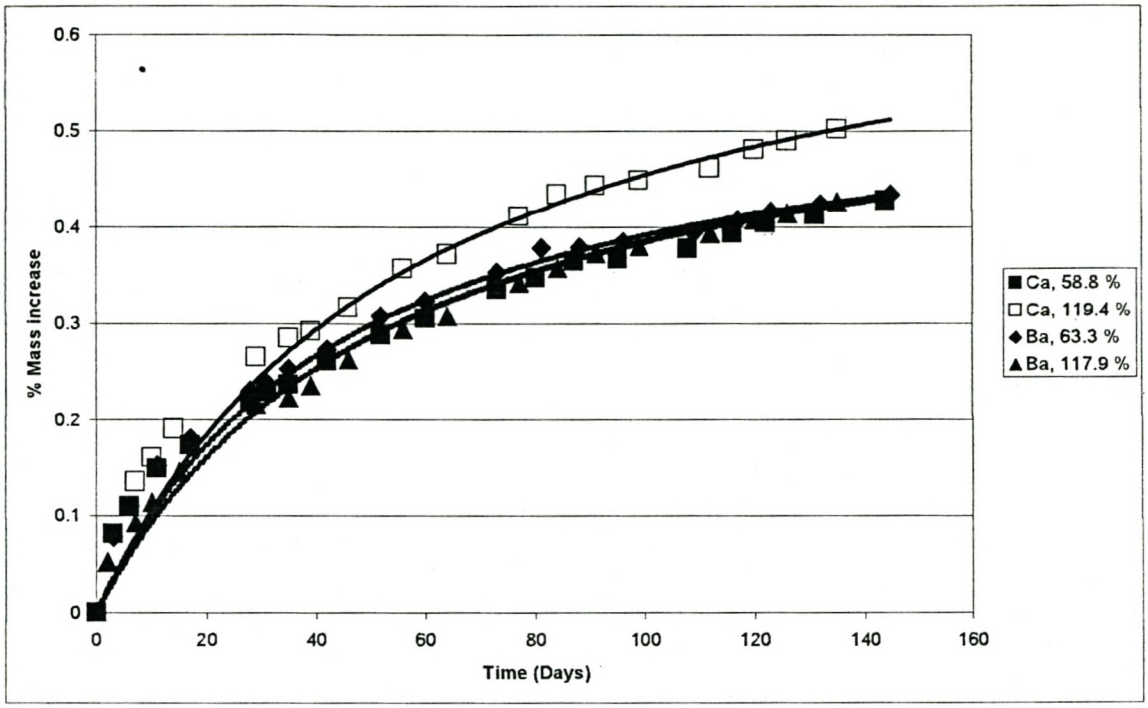

APPENDIX 7.8

WAX G11 and the different cation sorption graphs

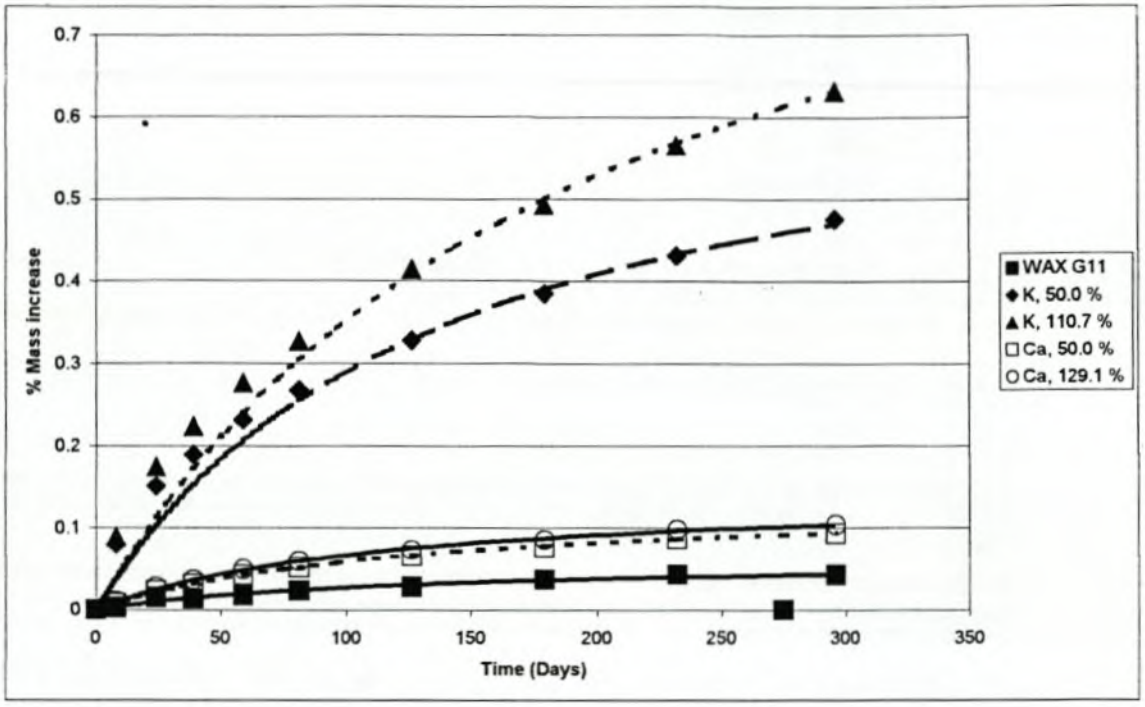

APPENDIX 7.9
DIFFUSION TEST RESULTS

SQRT t/L (sec.½/cm)	WAX 6	Li, 50.0 %	Li, 100.0 %	Na, 59.3 %	Na, 115.0 %	K, 62.3 %	K, 125.0 %	Ca, 57.0 %	Ca, 115.8 %	Ba, 50.0 %	Ba, 126.0 %
0	0.0000	0.0000	0.0000	0.0000	0.0000	0.0000	0.0000	0.0000	0.0000	0.0000	0.0000
972	0.1444	0.1025	0.1255	0.1061	0.0584	0.1275	0.0402	0.1424	0.2513	0.2178	0.4351
1,375	0.1919	0.1795	0.1779	0.1575	0.0907	0.1731	0.0625	0.2060	0.3470	0.0000	0.5664
1,723	0.1558	0.1887	0.2005	0.1849	0.1134	0.1968	0.0816	0.2533	0.4002	0.3539	0.6341
2,265	0.3002	0.2516	0.2677	0.2352	0.1590	0.2506	0.1206	0.3597	0.5192	0.4727	0.7840
2,675	0.2280	0.2912	0.3184	0.2774	0.1953	0.2847	0.1565	0.4114	0.5788	0.5330	0.7399
3,139	0.3249	0.3448	0.3588	0.3258	0.2370	0.3270	0.1985	0.4744	0.6315	0.6251	0.7840
3,581	0.4807	0.3959	0.4171	0.3708	0.2804	0.3611	0.2421	0.5500	0.6876	0.6793	0.8585
4,347	***	0.4777	0.4754	0.4467	0.3609	0.4435	0.0000	0.6489	0.7803	0.8050	0.8898
5,104	***	0.5731	0.5501	0.5190	0.4307	0.5073	0.0000	0.6804	0.8364	0.8317	0.9516
5,763	***	0.6172	0.6220	0.5868	0.4918	0.5765	0.0000	0.7636	0.8696	0.8972	0.9643
6,469	***	0.6741	0.6759	0.6425	0.5558	0.6408	0.0000	0.8190	0.8896	0.8911	0.9633
SQRT t/L (sec.½/cm)	WAX 16	Li, 58.7 %	Li, 100.0 %	Na, 59.9 %	Na, 100.0 %	K, 70.2 %	K, 131.9 %	Ca, 58.8 %	Ca, 119.4 %	Ba, 63.3 %	Ba, 117.9 %
0	0.0000	0.0000	0.0000	0.0000	0.0000	0.0000	0.0000	0.0000	0.0000	0.0000	0.0000
520	***	***	***	0.0455	***	***	***	0.1750	0.1587	***	***
636	***	***	***	***	0.0033	0.1334	***	***	***	0.1008	***
735	0.3588	0.1367	0.1301	***	***	***	0.3278	***	***	***	***
900	***	***	***	***	***	***	***	***	***	0.1456	***
972	0.4988	0.1860	0.1834	0.0811	***	0.2460	0.4558	0.2221	0.2260	***	0.2457
1,162	***	***	***	0.0988	***	***	***	0.2718	0.2661	***	***
1,219	***	***	***	***	0.0096	***	***	***	***	0.2048	***
1,273	0.7298	0.2666	0.2603	***	***	***	0.5738	***	***	***	***
1,423	***	***	***	0.1278	***	***	***	0.3496	0.3222	***	0.2970
1,515	***	***	***	***	***	0.3154	***	***	***	0.2129	***
1,559	***	0.3034	0.2993	***	0.0146		***	***	***	***	***
1,944	***	***	***	***	0.0240	0.4181	***	***	***	0.2831	***
1,979	0.8698	0.3824	0.3785	0.1949	***	***	***	0.4536	0.4362	***	0.4145
2,046	***	***	***	***	***	0.4421	***	***	***	0.2880	***
2,078	0.8470	0.3980	0.4000	***	***	***	***	***	***	***	***
2,174	***	***	***	0.2192	0.0270	0.4800	***	0.4914	0.4634	0.3055	0.4370
2,205	0.8698	0.4174	0.4271	***	***	***	***	***	***	***	***
2,295	***	***	***	0.2370	***	***	***	0.5054	0.4763	***	0.4581
2,381	***	***	***	***	***	0.5478	***	***	***	0.3215	***
2,409	0.9153	0.4619	0.4792	***	0.0343	***	***	***	***	***	***
2,492	***	***	***	0.2662	***	***	***	0.5411	0.5195	***	0.5018
2,650	***	***	***	***	***	0.6284	***	***	***	0.3647	***
2,675	0.9048	0.5157	0.5182	***	***	***	***	***	***	***	***
2,750	***	***	***	0.3149	***	***	***	0.5908	0.5645	***	0.5445
2,846	***	***	***	***	***	0.6770	***	***	***	0.3822	***
2,870	0.9153	0.5491	0.5431	***	***	***	***	***	***	***	***
2,939	***	***	***	0.3471	***	***	***	0.6188	0.6029	***	0.5738
3,139	***	***	***	***	***	0.6980	***	***	***	0.4272	***
3,161	1.1130	0.6156	0.6010	***	0.0583	***	***	***	***	***	***
3,224	***	***	***	0.3921	***	***	***	0.6970	0.6607	***	0.6413
3,286	***	***	***	***	***	0.7044	***	***	***	0.4367	***
3,307	1.1253	0.6384	0.6341	***	***	***	***	***	***	***	***
3,367	***	***	***	0.4122	0.0696	***	***	0.7229	0.6848	***	0.6692
3,427	***	***	***	***	***	0.7228	***	***	***	0.4544	***
3,447	1.0780	0.6612	0.6556	***	***	***	***	***	***	***	***
3,505	***	***	***	***	***	***	***	0.7348	0.7169	***	0.6842
3,581	***	***	***	***	***	0.7136	***	***	***	0.4527	***
3,600	0.9975	0.6630	0.6649	***	***	***	***	***	***	***	***
3,656	***	***	***	0.4420	***	***	***	0.7348	0.7103	***	0.6872
3,836	***	0.6699	0.6887	***	***	***	***	***	***	***	***
3,888	***	***	***	0.4878	0.0887	***	***	***	0.7057	***	0.6887
3,957	***	***	***	***	***	***	***	***	***	0.4702	***
3,974	0.8698	0.6946	0.6993	***	***	***	***	***	***	***	***

APPENDIX 7.9 (CONTINUED)
DIFFUSION TEST RESULTS

SQRT t/L (sec.½/cm)	WAX 28	Li, 50.0 %	Li, 72.5 %	Na, 51.4 %	Na, 100.0 %	K, 59.0 %	K, 119.9 %	Ca, 58.2 %	Ca, 118.3 %	Ba, 58.8 %	Ba, 129.1 %
0	0.0000	0.0000	0.0000	0.0000	0.0000	0.0000	0.0000	0.0000	0.0000	0.0000	0.0000
520	***	***	***	0.0660	0.0213	0.2019	0.0511	***	***	***	0.0880
636	***	0.0868	***	***	***	***	***	0.1380	***	0.1365	***
735	0.2583	***	0.0784	***	***	***	***	***	***	***	***
822	***	***	***	0.1215	***	0.3302	***	***	***	***	***
900	***	0.1277	***	0.1371	***	0.3690	***	0.1873	***	0.1937	***
972	0.3633	* ***	0.1116	***	0.0678	***	0.1229	***	0.1903	***	0.1570
1,162	***	***	***	***	0.0917	***	***	***	0.2253	***	0.1932
1,219	***	0.1771	***	***	***	***	***	0.2547	***	0.2674	***
1,273	0.4718	***	0.1546	0.2093	***	0.5706	***	***	***	***	***
1,375	***	***	***	0.2165	***	***	***	***	0.2668	***	***
1,423	***	***	***	***	0.1266	***	***	***	***	***	0.2462
1,515	***	0.2151	***	***	***	***	***	0.2951	***	0.3164	***
1,559	***	***	0.1870	***	***	***	***	***	***	***	***
1,602	***	***	***	0.2593	***	***	***	***	***	***	***
1,723	***	***	***	0.2875	***	***	***	***	***	***	***
1,909	***	***	***	0.3449	***	***	***	***	***	***	***
1,944	***	0.2902	***	***	***	***	***	0.3715	***	0.4039	***
1,979	0.5719	***	0.2415	***	***	***	***	***	0.3721	***	0.3661
2,046	***	0.2969	***	***	***	***	***	0.3895	***	0.4169	***
2,078	0.6398	***	0.2564	***	***	***	***	***	***	***	***
2,174	***	0.3185	***	***	***	***	***	0.4029	0.3989	0.4436	0.3762
2,205	0.6713	***	0.2747	***	***	***	***	***	***	***	***
2,295	***	***	***	***	***	***	***	***	0.4091	***	0.3987
2,353	***	***	***	0.5249	***	***	***	***	***	***	***
2,381	***	0.3537	***	***	***	***	***	0.4434	***	0.4786	***
2,409	0.7301	***	0.3016	***	***	***	***	***	***	***	***
2,492	***	***	***	***	***	***	***	***	0.4432	***	0.4440
2,650	***	0.4051	***	***	***	***	***	0.4901	***	0.5381	***
2,675	0.7574	***	0.3497	***	***	***	***	***	***	***	***
2,750	***	***	***	***	***	***	***	***	0.4998	***	0.4982
2,798	***	***	***	0.5565	***	***	***	***	***	***	***
2,846	***	0.4435	***	***	***	***	***	0.5195	***	0.5661	***
2,870	0.7714	***	0.3761	***	***	***	***	***	***	***	***
2,939	***	***	***	***	***	***	***	***	0.5208	***	0.5197
3,030	***	***	***	0.5901	***	***	***	***	***	***	***
3,139	***	0.4924	***	***	***	***	***	0.5712	***	0.6188	***
3,161	0.9030	***	0.4277	***	***	***	***	***	***	***	***
3,203	***	***	***	0.6128	***	***	***	***	***	***	***
3,224	***	***	***	***	***	***	***	***	0.5762	***	0.5783
3,286	***	0.5174	***	***	***	***	***	0.5914	***	***	***
3,307	0.8890	***	0.4494	***	***	***	***	***	***	0.6631	***
3,367	***	***	***	***	***	***	***	***	0.6086	***	0.6043
3,427	***	0.5285	***	***	***	***	***	0.6207	***	***	***
3,447	0.9030	***	0.4609	***	***	***	***	***	***	0.6643	***
3,505	***	***	***	***	***	***	***	***	0.6210	***	0.6304
3,581	***	0.5492	***	***	***	***	***	0.6239	***	***	***
3,600	0.9121	***	0.4869	***	***	***	***	***	***	0.6736	***
3,656	***	***	***	***	***	***	***	***	0.6289	***	0.6427
3,818	***	0.5902	***	***	***	***	***	0.6424	***	***	***
3,836	0.8302	***	0.5274	***	***	***	***	***	***	0.6911	***
3,888	***	***	***	***	***	***	***	***	0.6464	***	0.6654
3,957	***	0.5944	***	***	***	***	***	0.6700	***	***	***
3,974	0.8484	***	0.5436	***	***	***	***	***	***	0.7121	***
4,025	***	***	***	***	***	***	***	***	0.6731	***	0.6890
4,058	***	0.6127	***	***	***	***	***	0.6880	***	***	***
4,075	***	***	0.5593	***	***	***	***	***	***	0.7285	***
4,124	***	***	***	***	***	***	***	***	0.6861	***	0.7003
4,205	***	0.6347	***	***	***	***	***	0.7024	***	***	***
4,221	***	***	0.5759	***	***	***	***	***	***	0.7425	***
4,269	***	***	***	***	***	***	***	***	0.7036	***	0.7206
4,409	***	0.6585	***	***	***	***	***	0.7273	***	***	***
4,424	***	***	0.6010	***	***	***	***	***	***	0.7600	***

SQRT t/L (sec.½/cm)	WAX G11	K, 50.0 %	K, 110.7 %	Ca, 50.0 %	Ca, 129.1 %
0	0.0000	0.0000	0.0000	0.0000	0.0000
1,039	0.0429	0.1166	0.0842	0.0593	0.0767
1,800	0.2475	0.2179	0.1635	0.1770	0.1944
2,295	0.2162	0.2739	0.2102	0.2310	0.2529
2,822	0.2805	0.3365	0.2606	0.3195	0.3434
3,307	0.3878	0.3877	0.3079	0.3878	0.4111
4,124	0.4637	0.4757	0.3903	0.4965	0.5065
4,916	0.6037	0.5574	0.4640	0.5745	0.5922
5,596	0.7112	0.6247	0.5322	0.6488	0.6779
6,321	0.7013	0.6901	0.5950	0.6975	0.7186

APPENDIX 7.10

WAX 6 graphs to determine the average diffusion slope

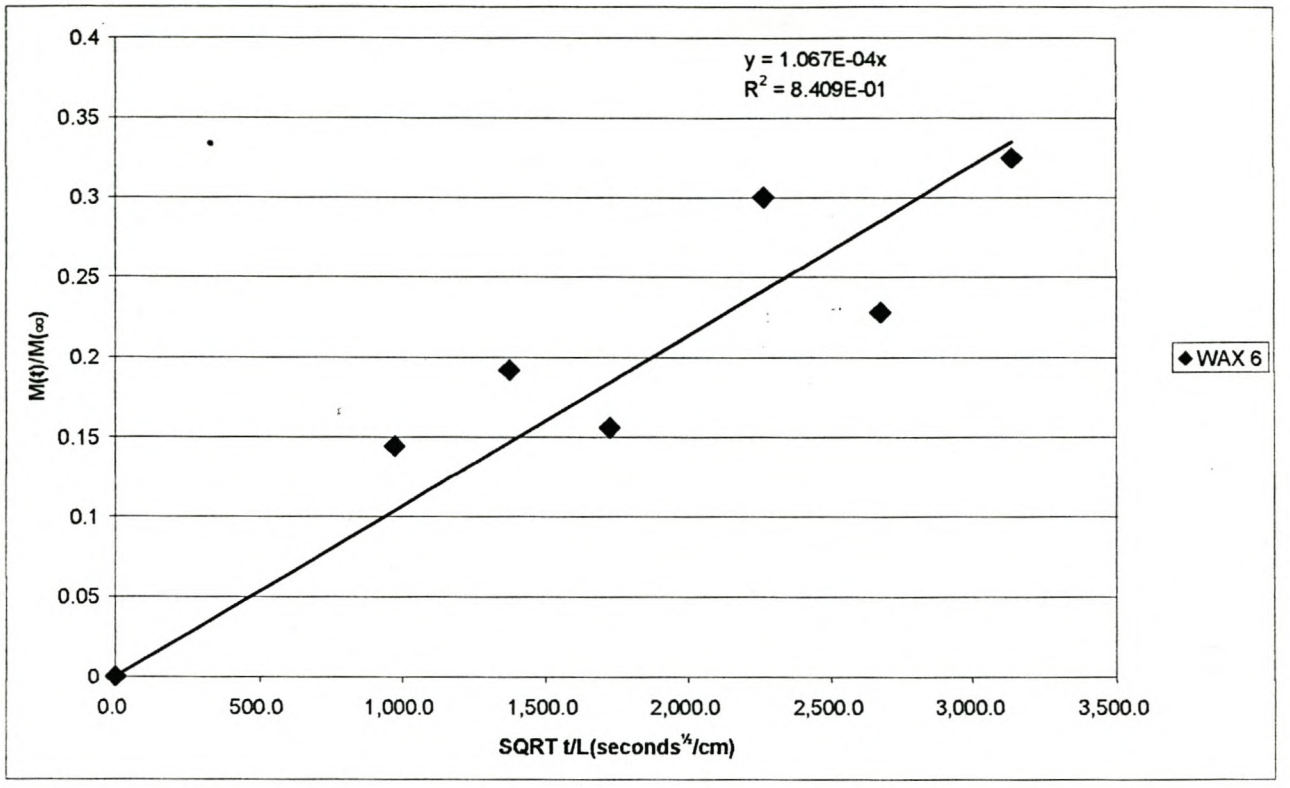

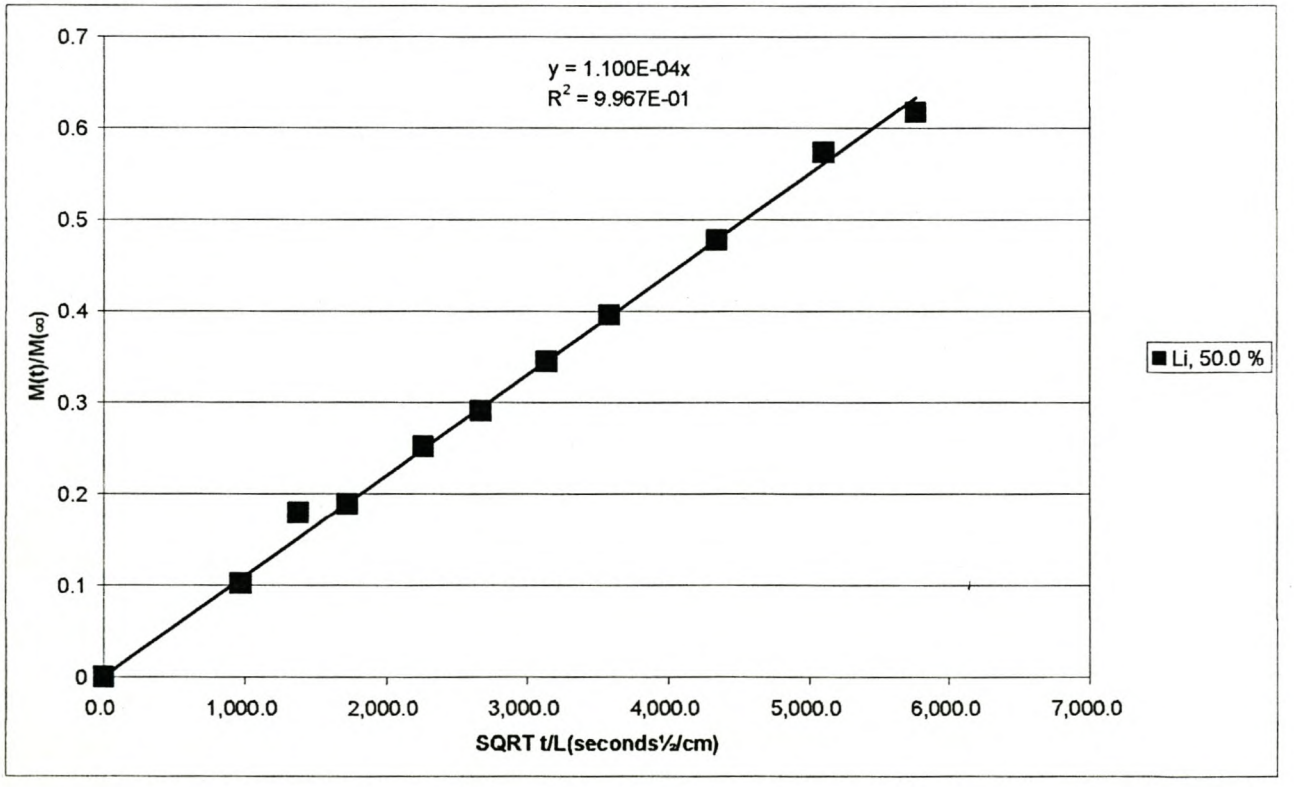

APPENDIX 7.10(continued)

WAX 6 graphs to determine the average diffusion slope

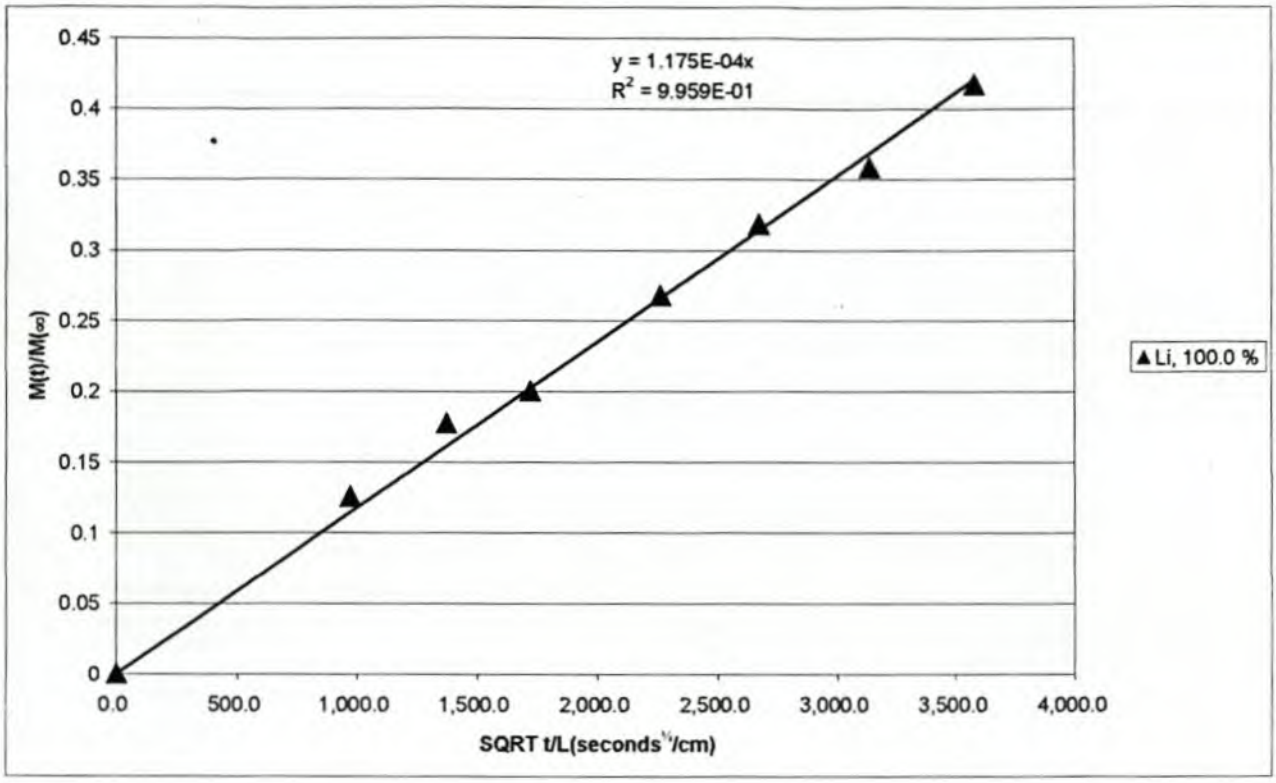

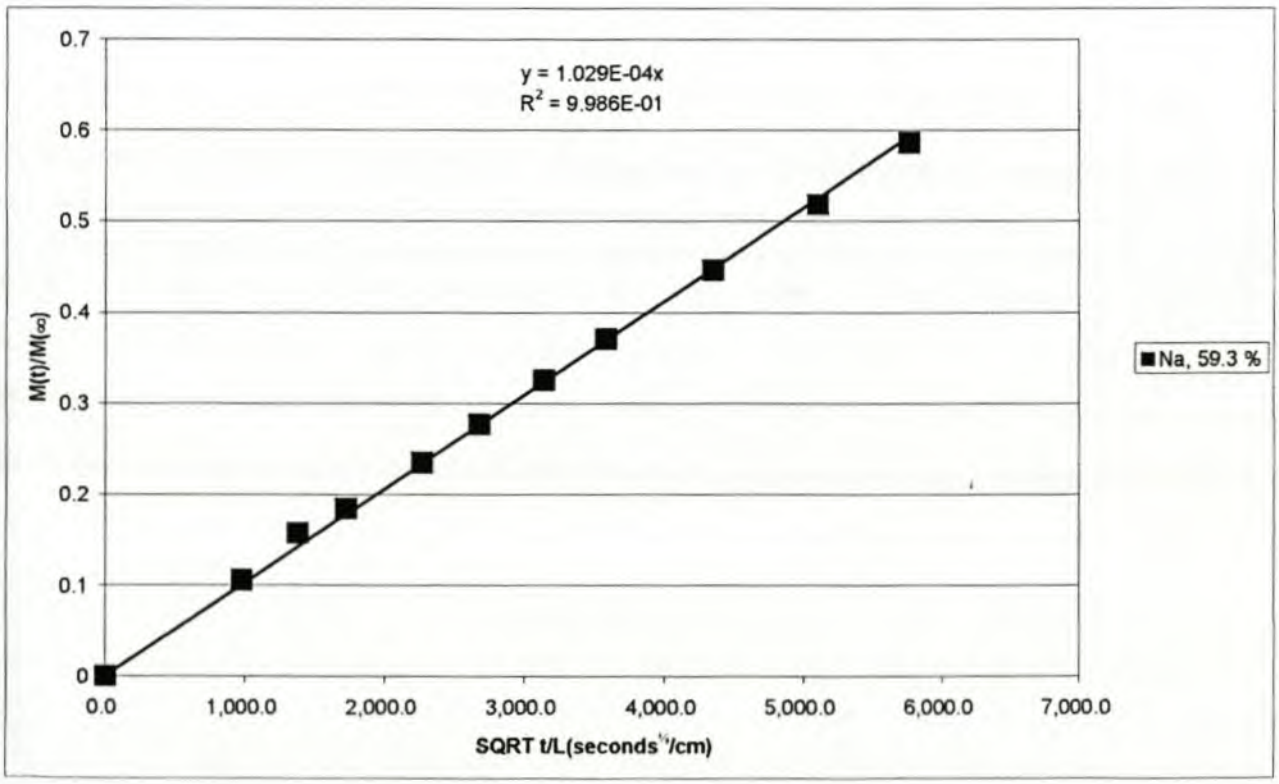

APPENDIX 7.10 (continued)

WAX 6 graphs to determine the average diffusion slope

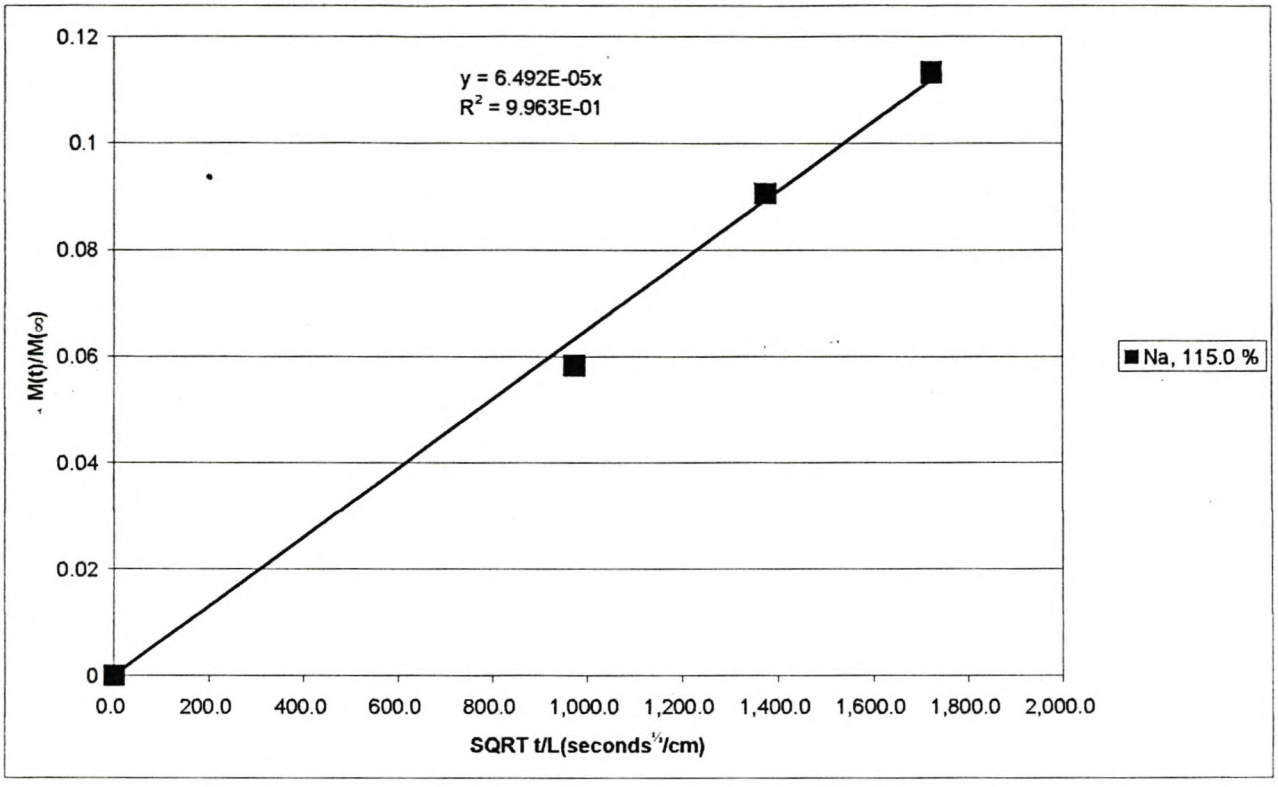

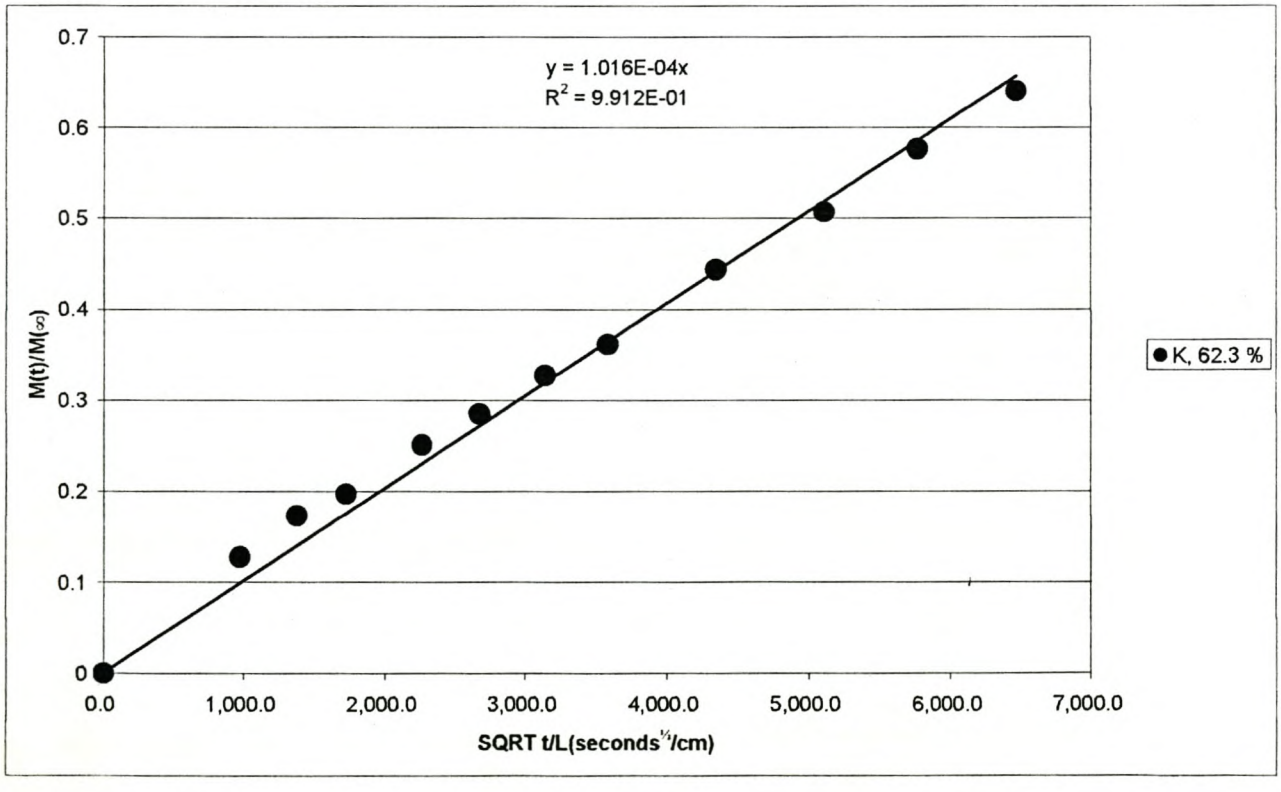

APPENDIX 7.10 (continued)

WAX 6 graphs to determine the average diffusion slope

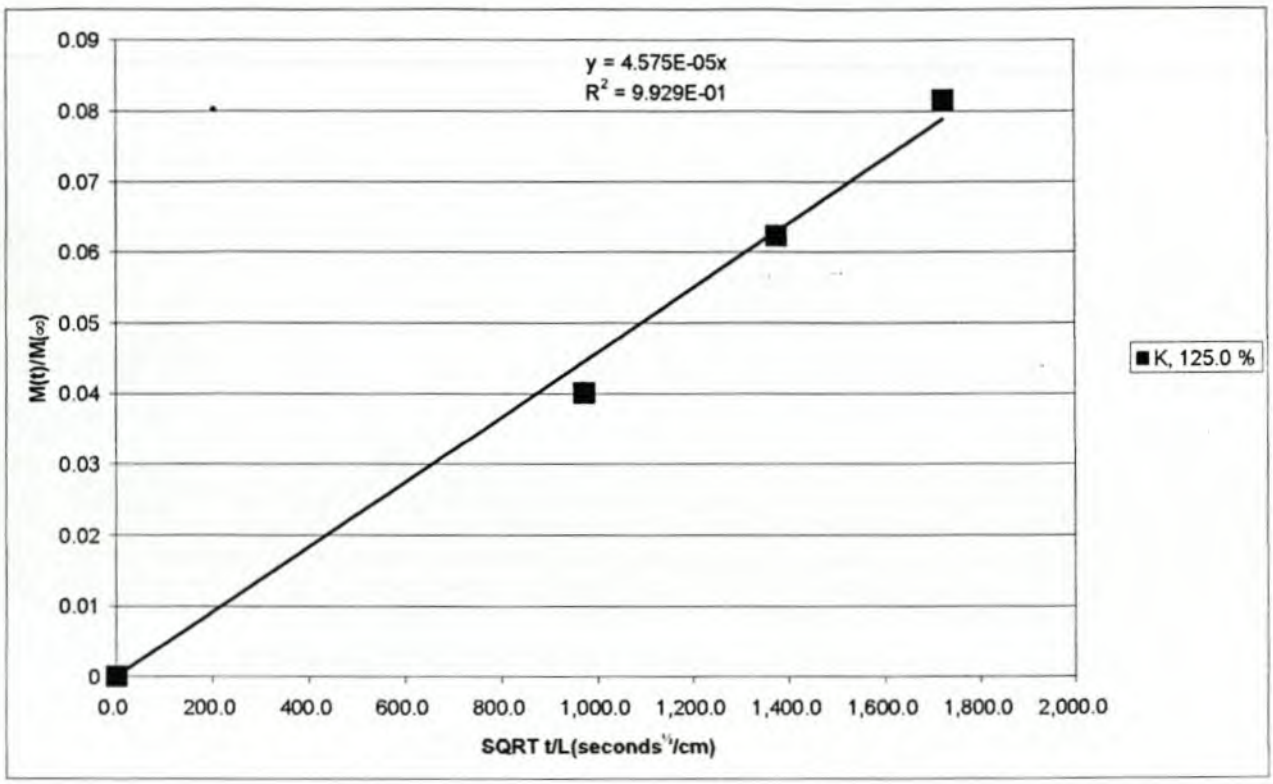

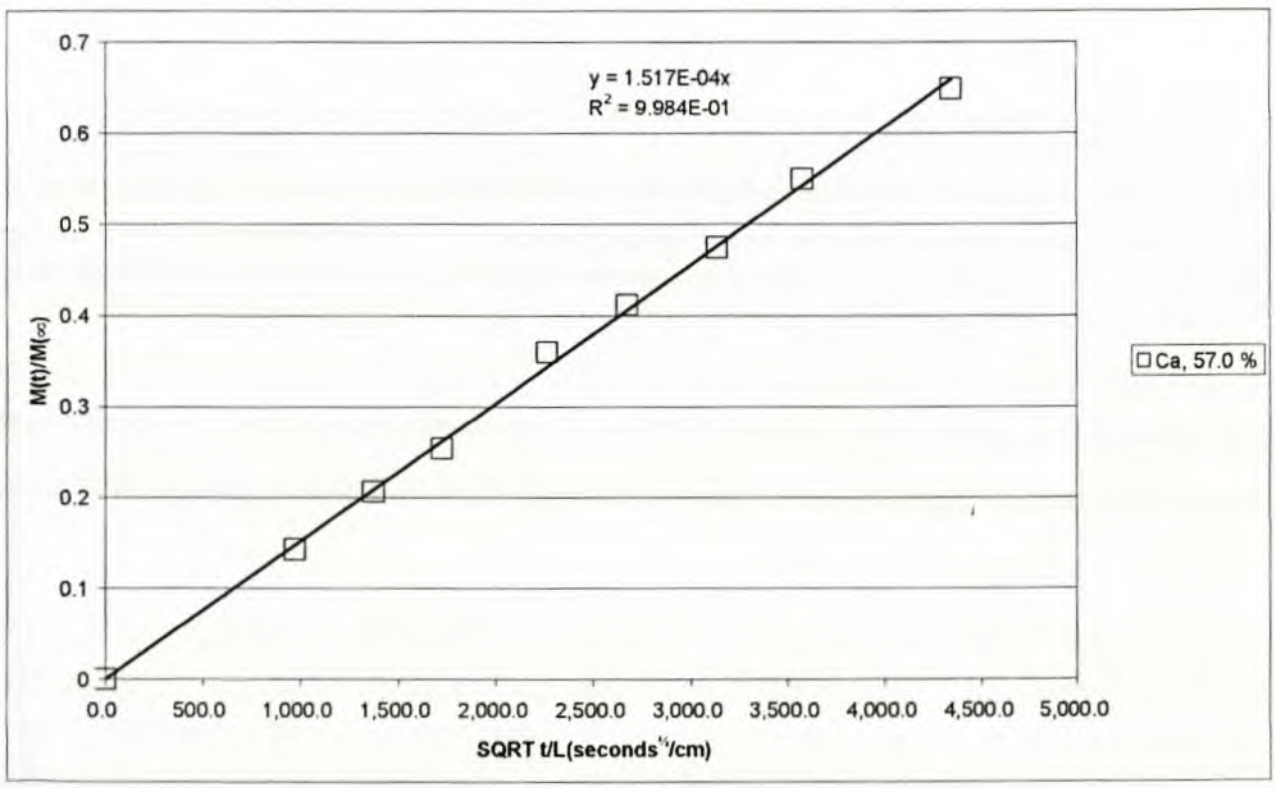

APPENDIX 7.10 (continued)

WAX 6 graphs to determine the average diffusion slope

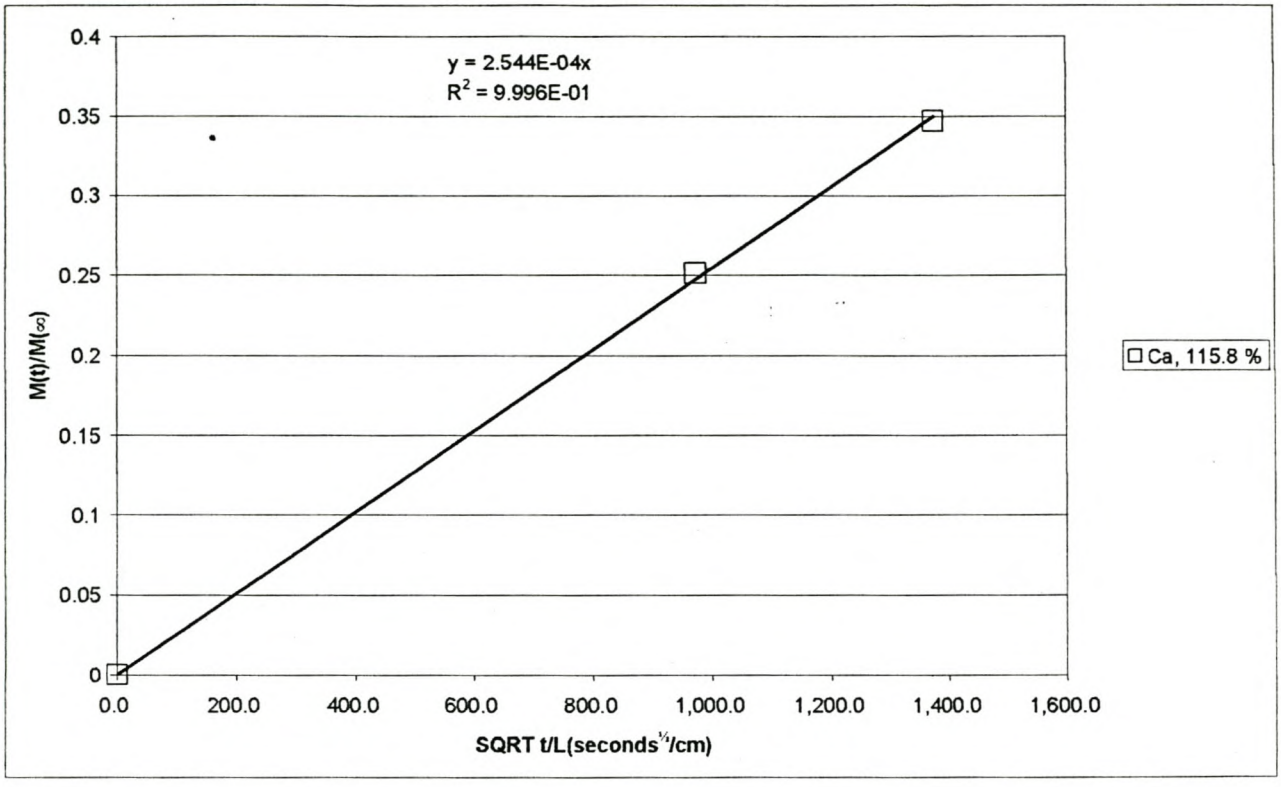

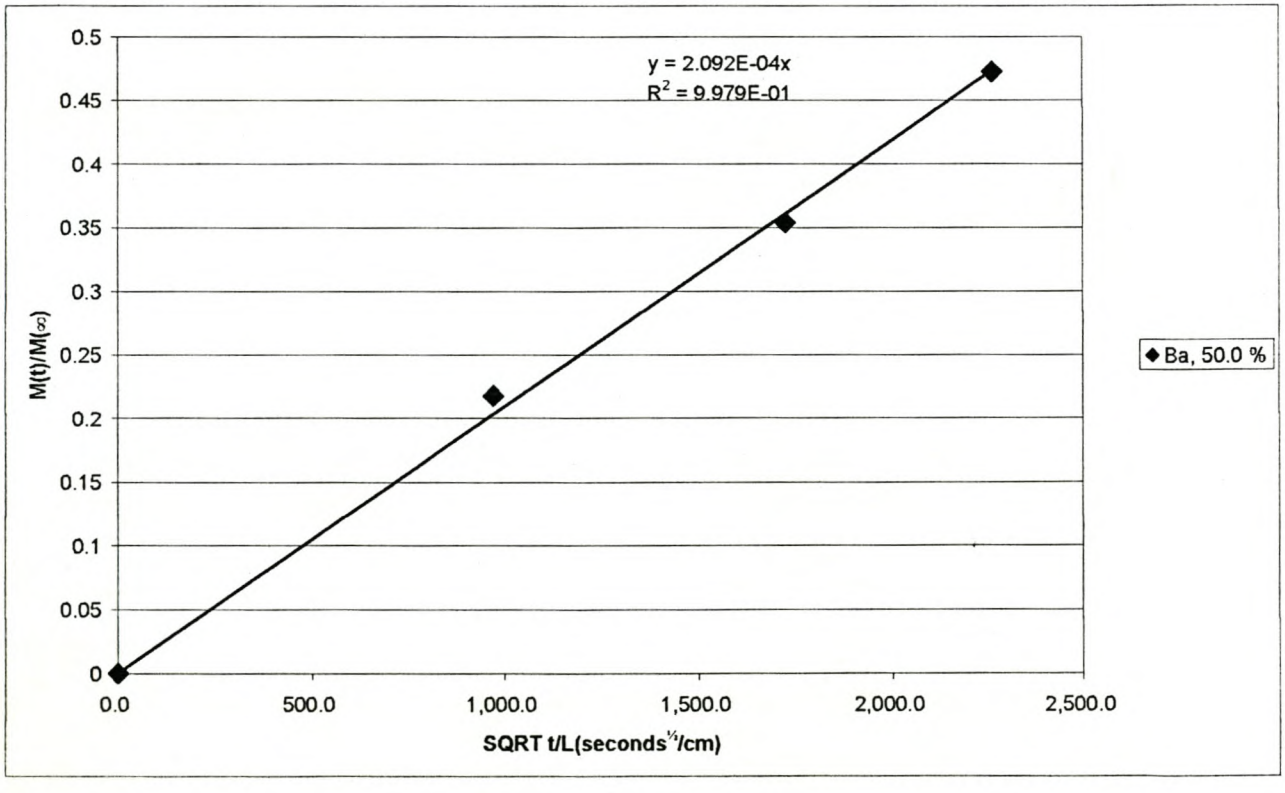

APPENDIX 7.10 (continued)

WAX 6 graphs to determine the average diffusion slope

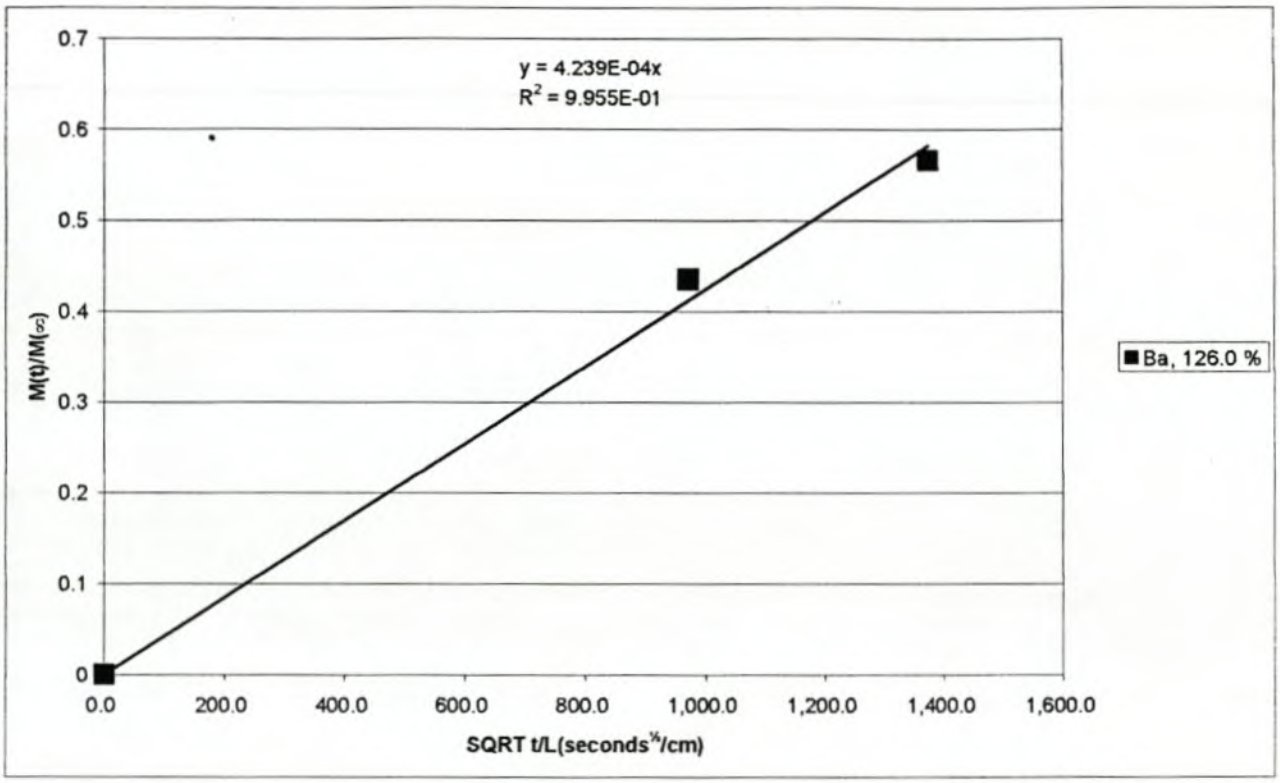

APPENDIX 7.11

WAX 16 graphs to determine the average diffusion slope

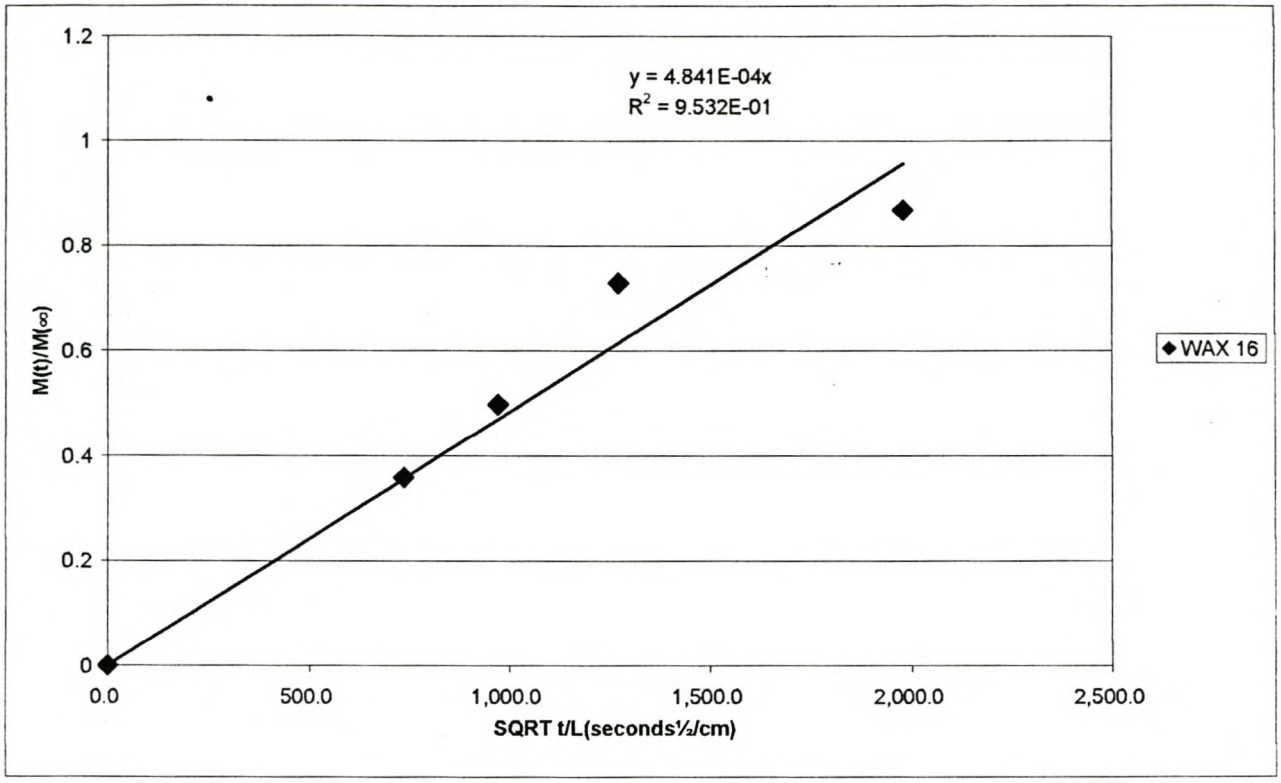

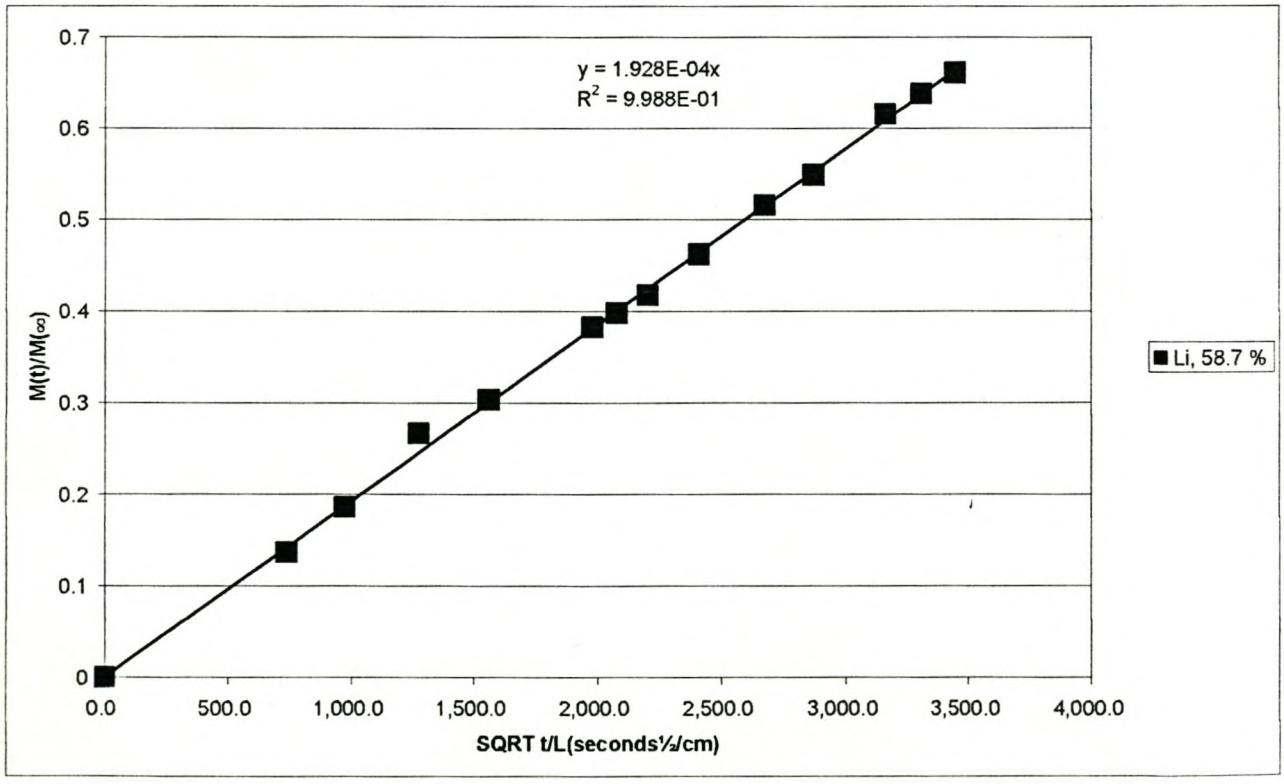

APPENDIX 7.11 (continued)

WAX 16 graphs to determine the average diffusion slope

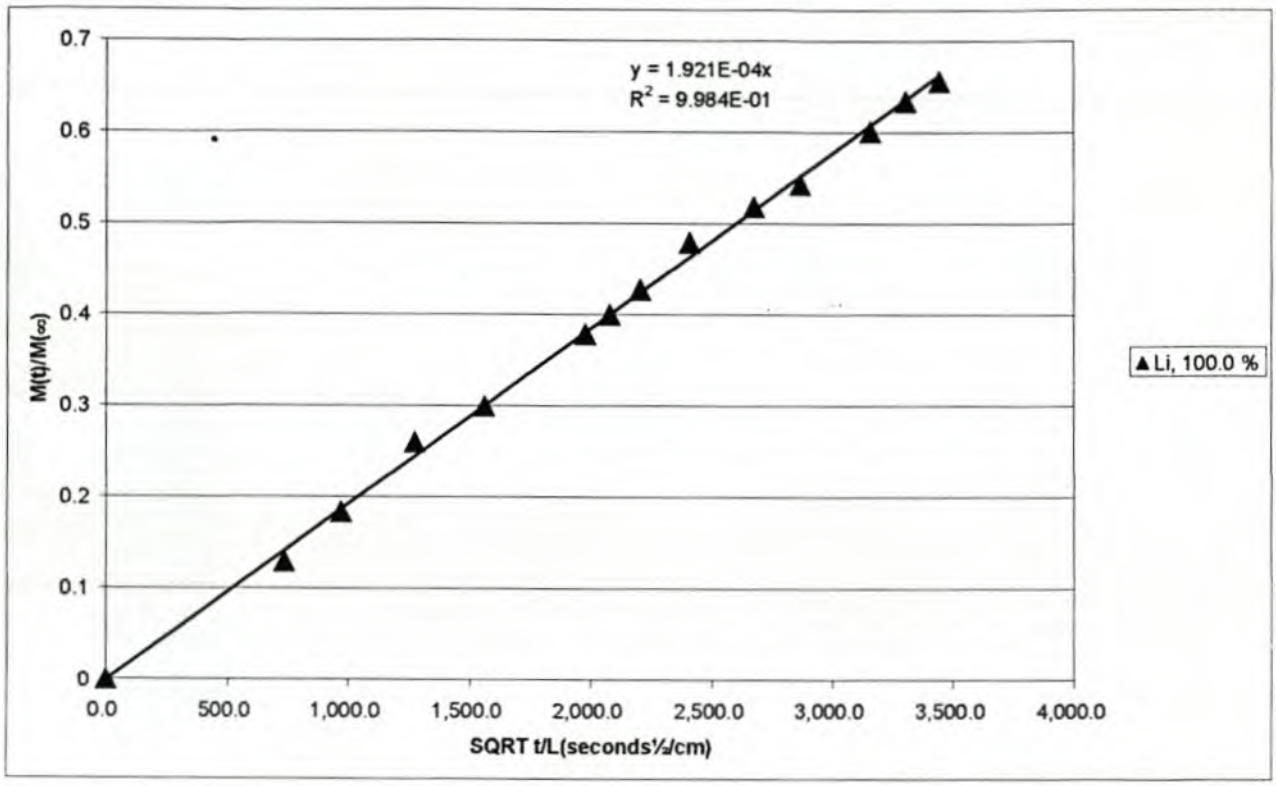

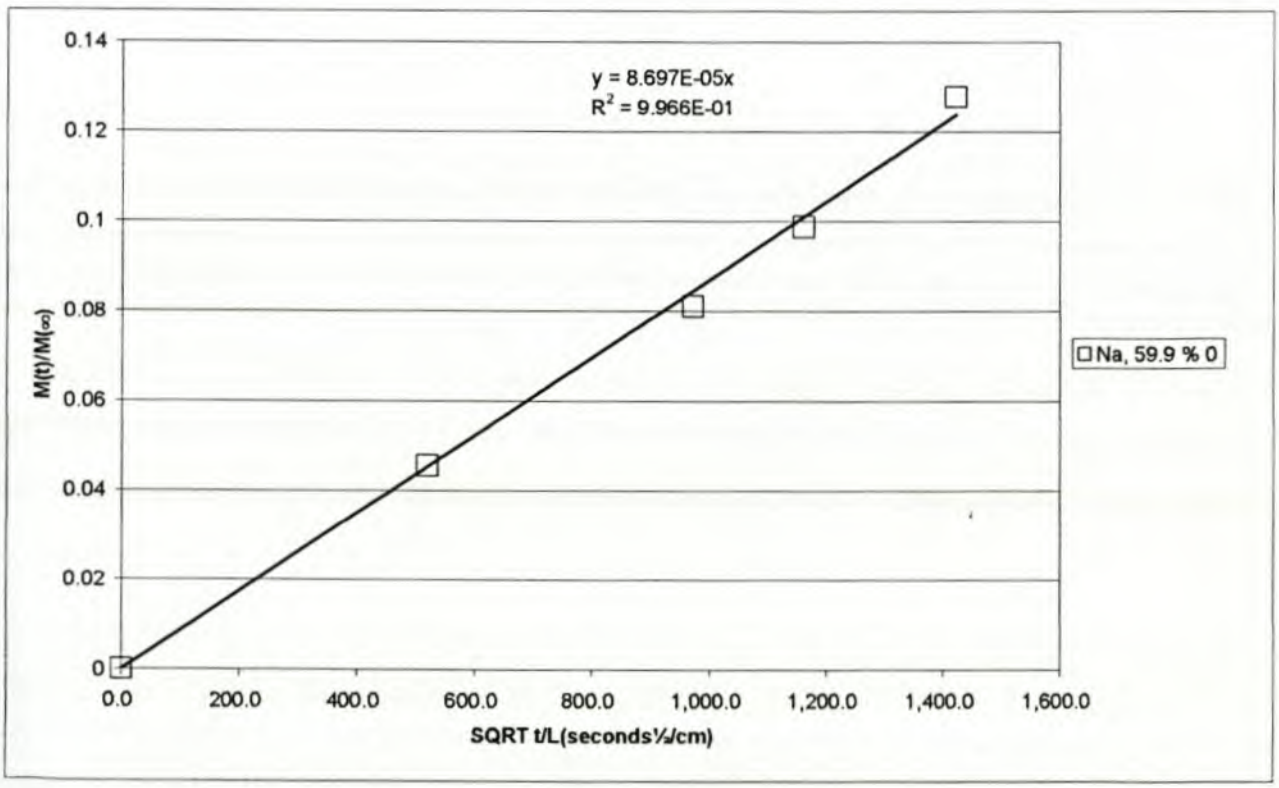

APPENDIX 7.11 (continued)

WAX 16 graphs to determine the average diffusion slope

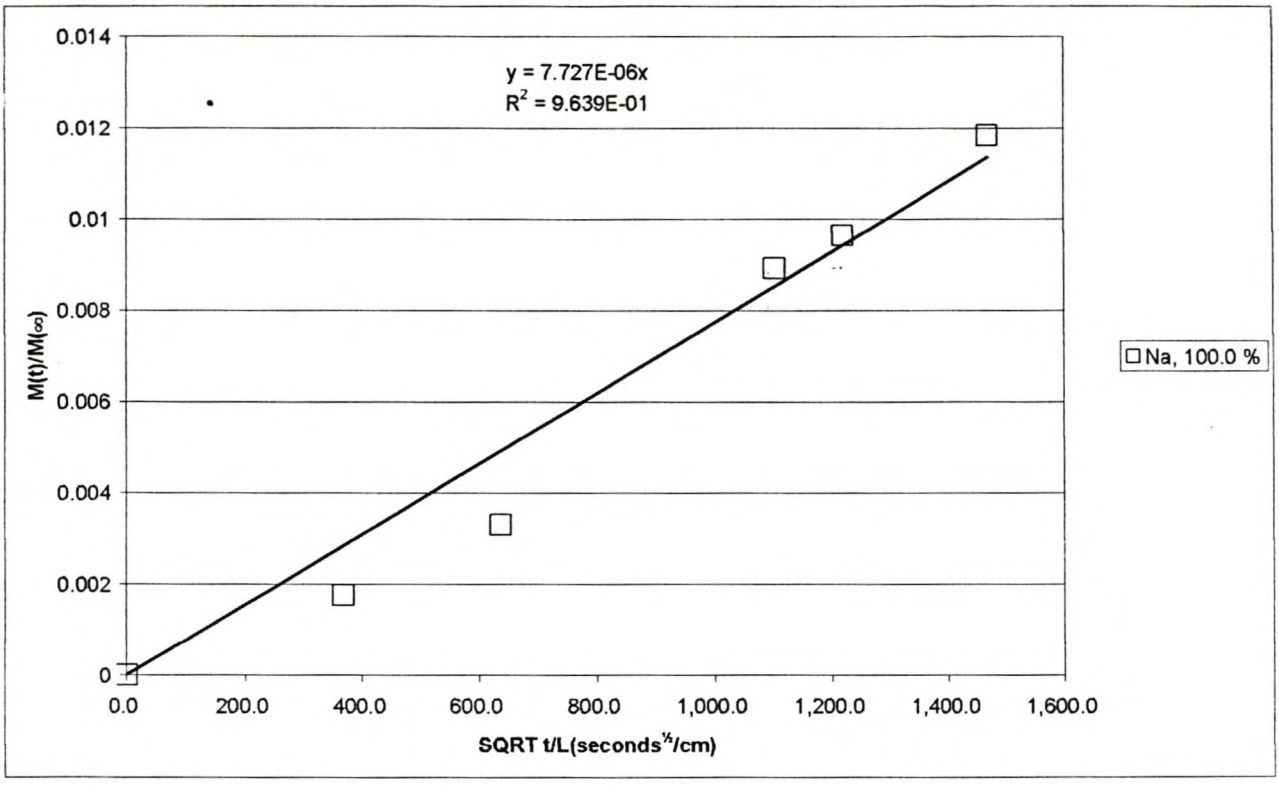

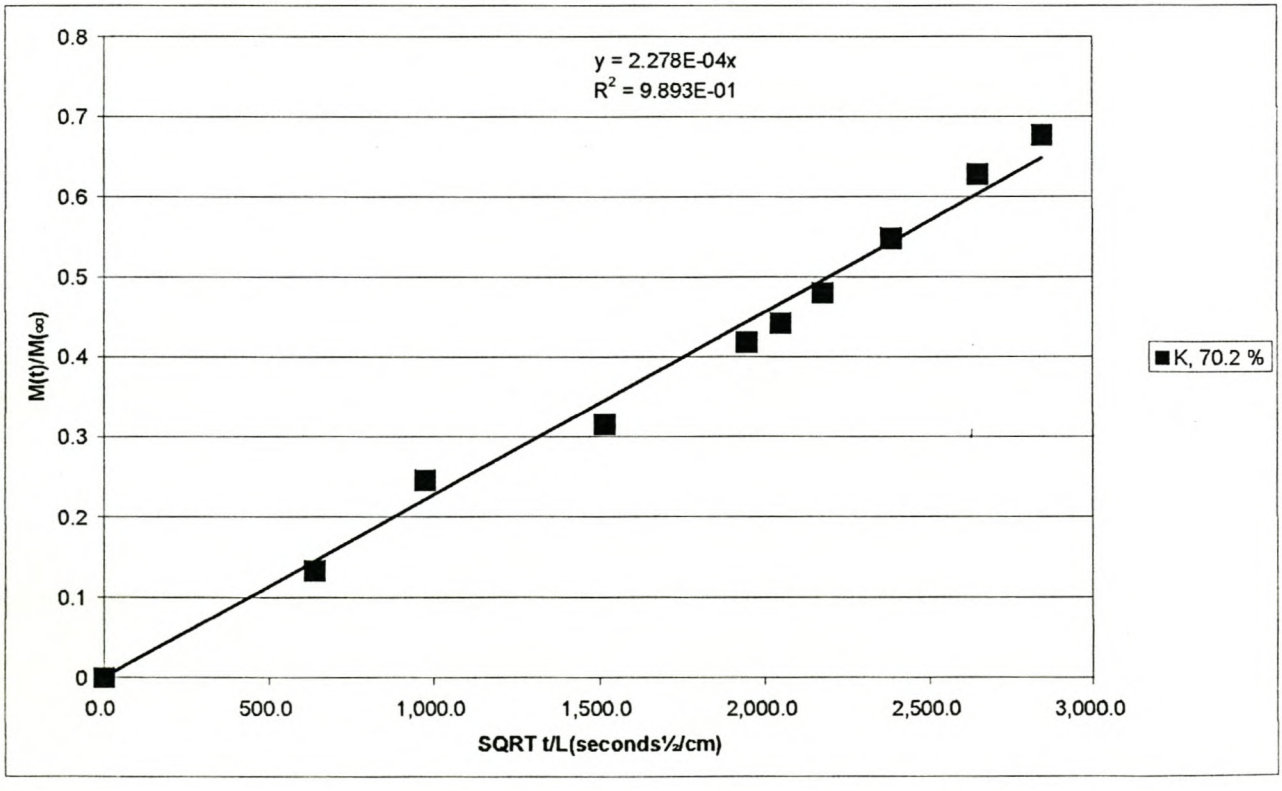

APPENDIX 7.11 (continued)

WAX 16 graphs to determine the average diffusion slope

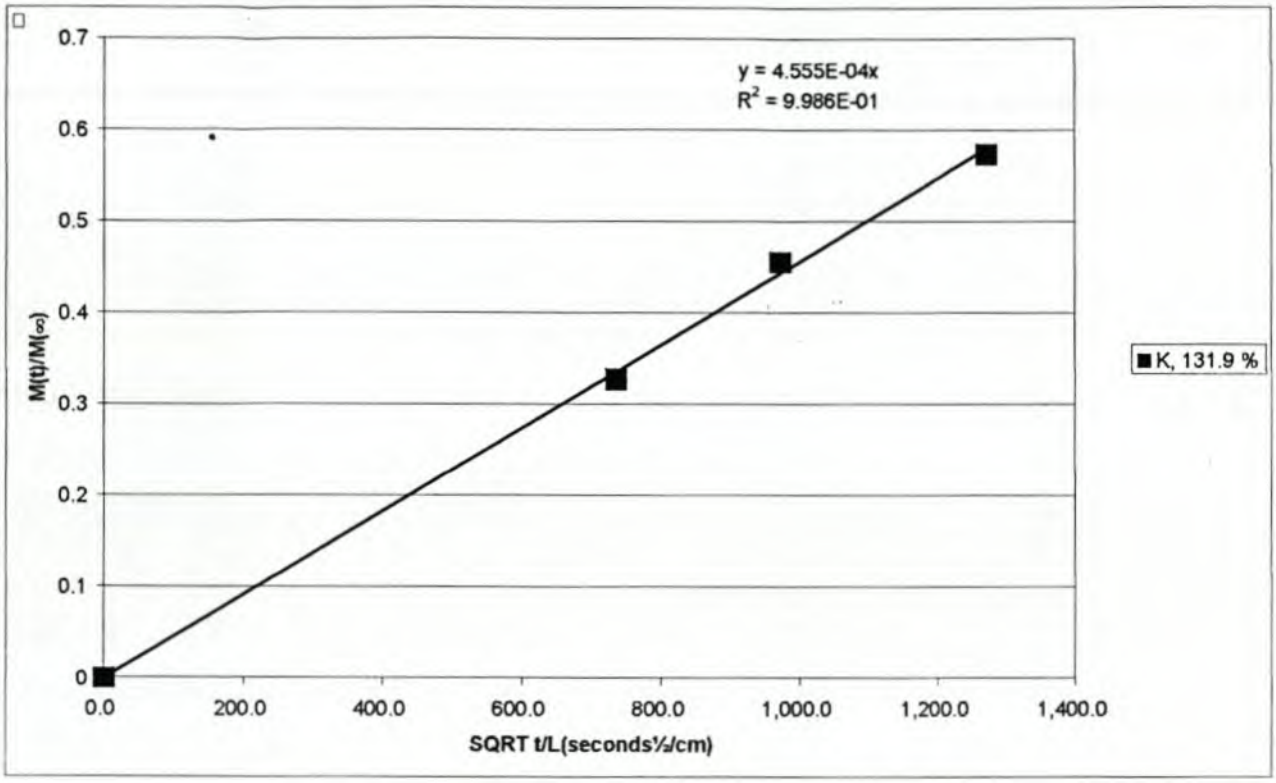

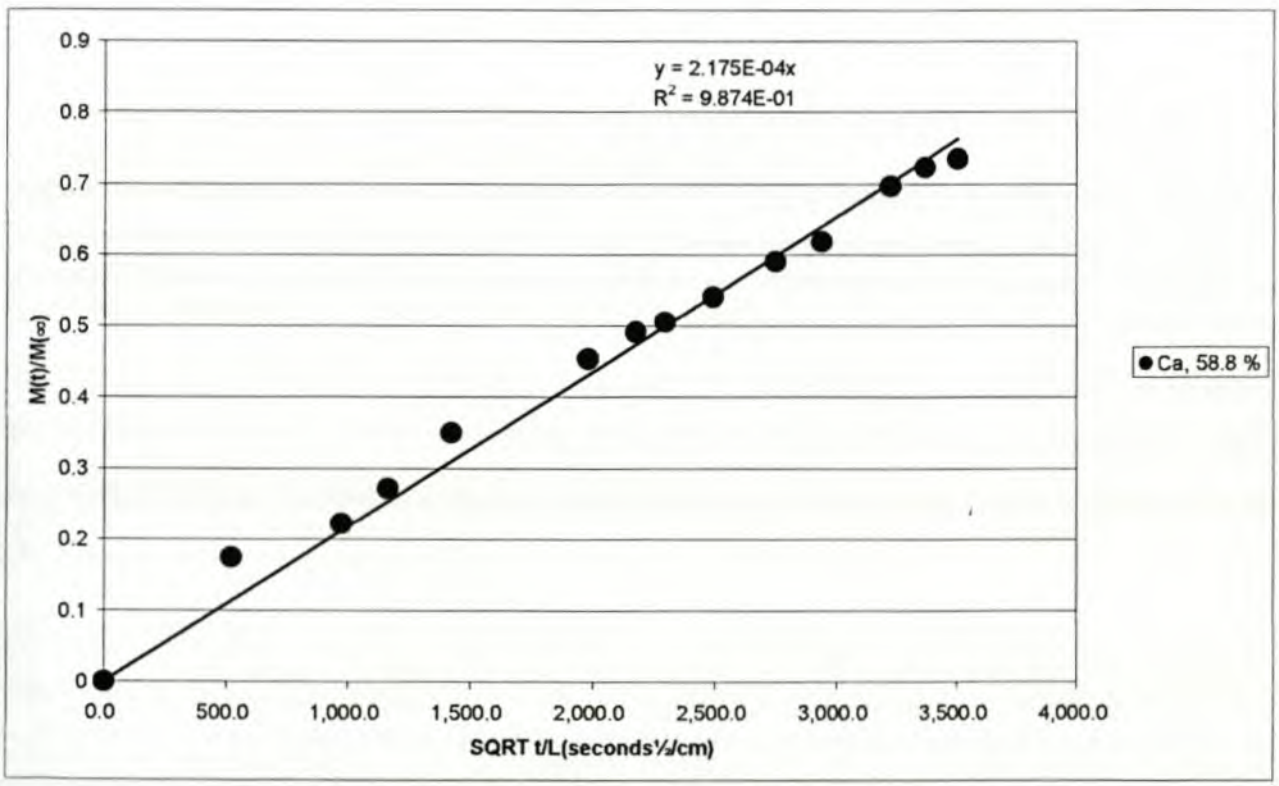

APPENDIX 7.11 (continued)

WAX 16 graphs to determine the average diffusion slope

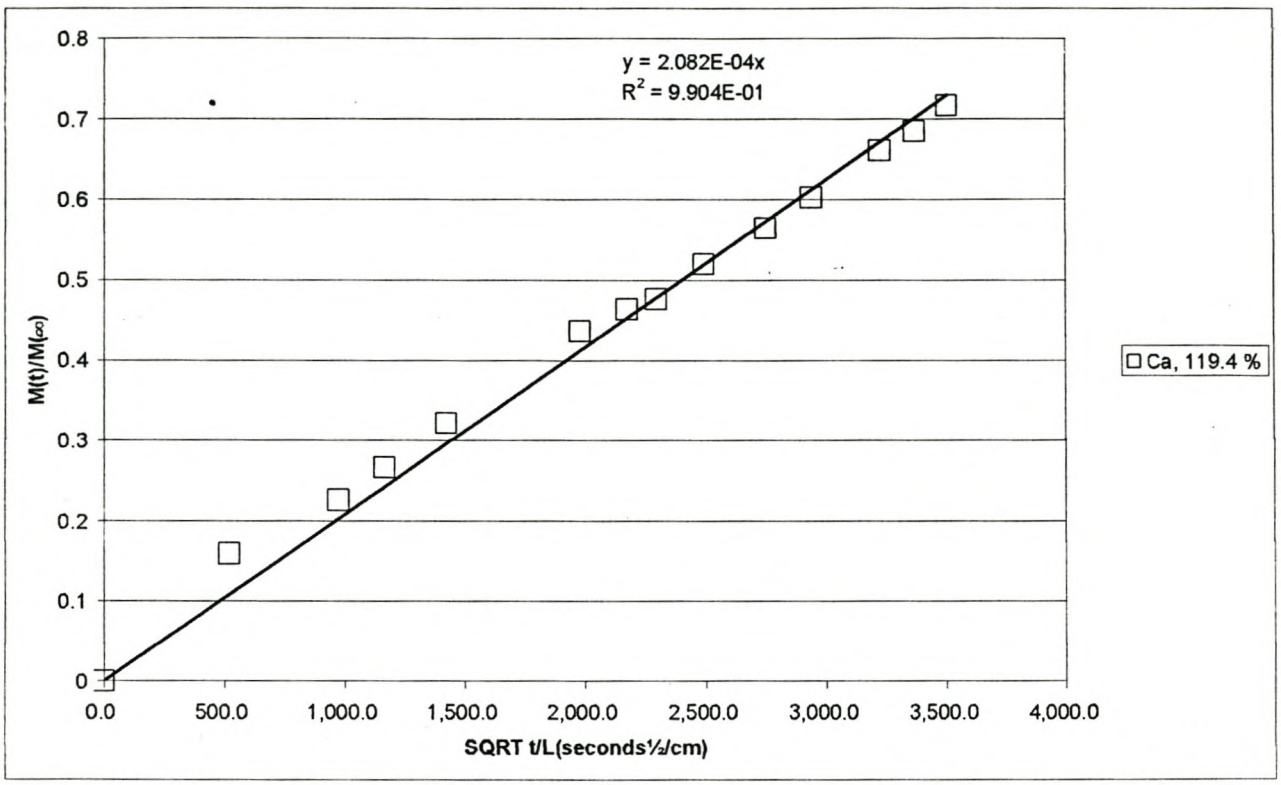

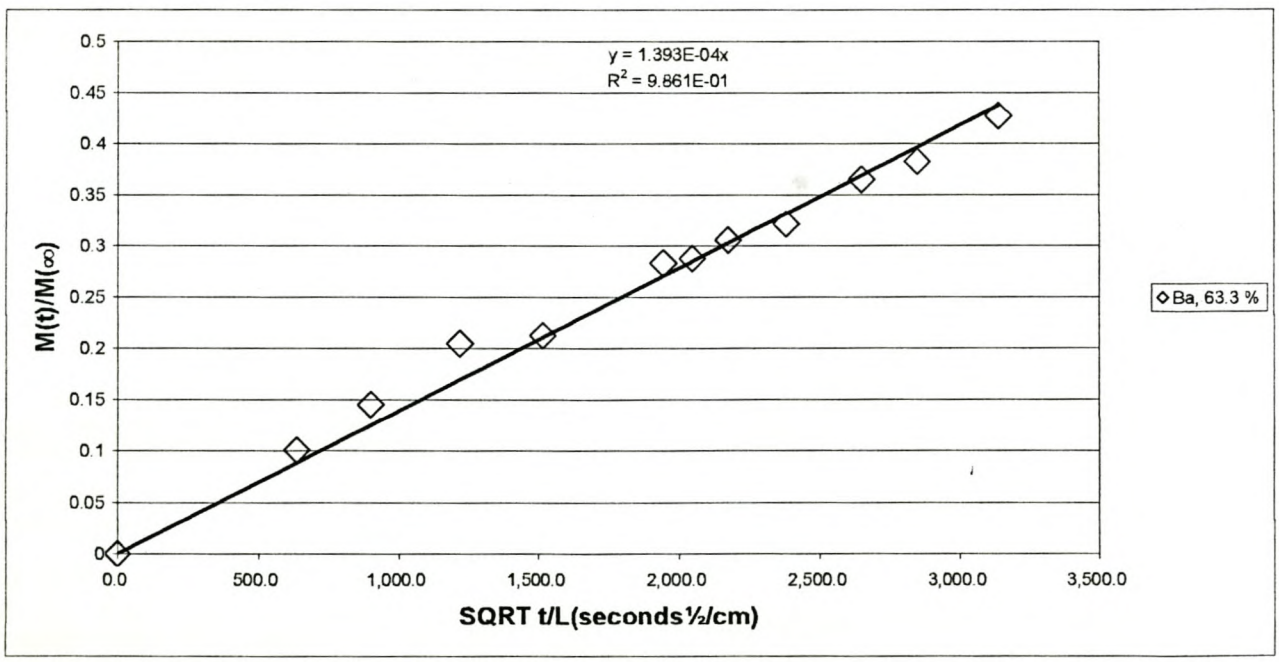

APPENDIX 7.11 (continued)

WAX 16 graphs to determine the average diffusion slope

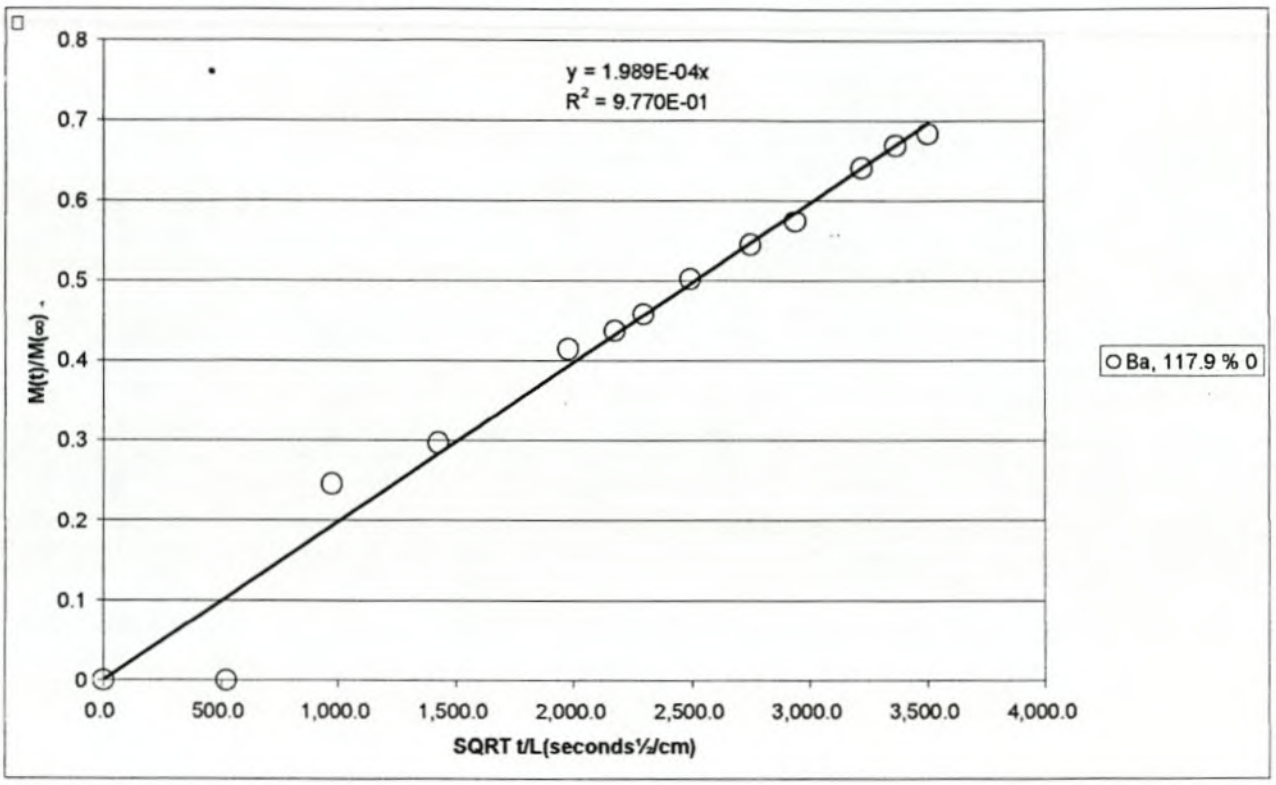

APPENDIX 7.12

WAX 28 graphs to determine the average diffusion slope

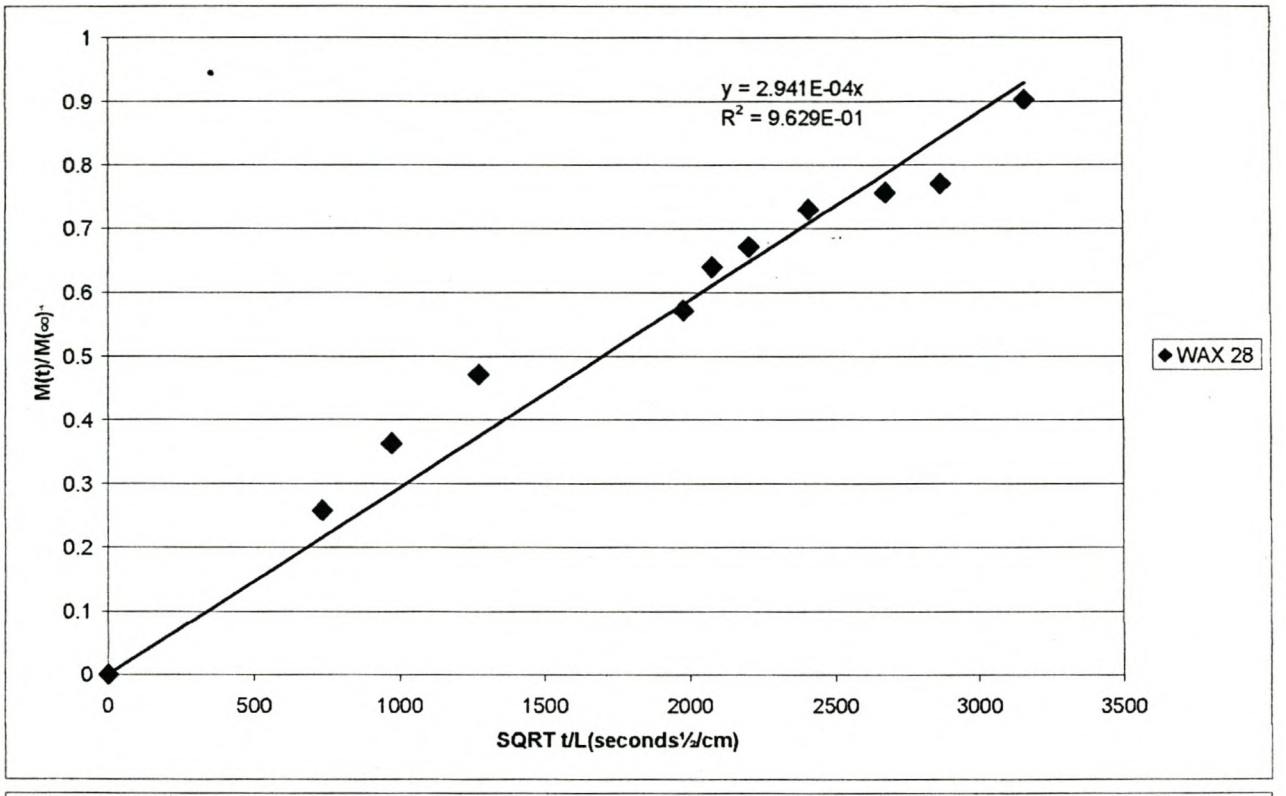

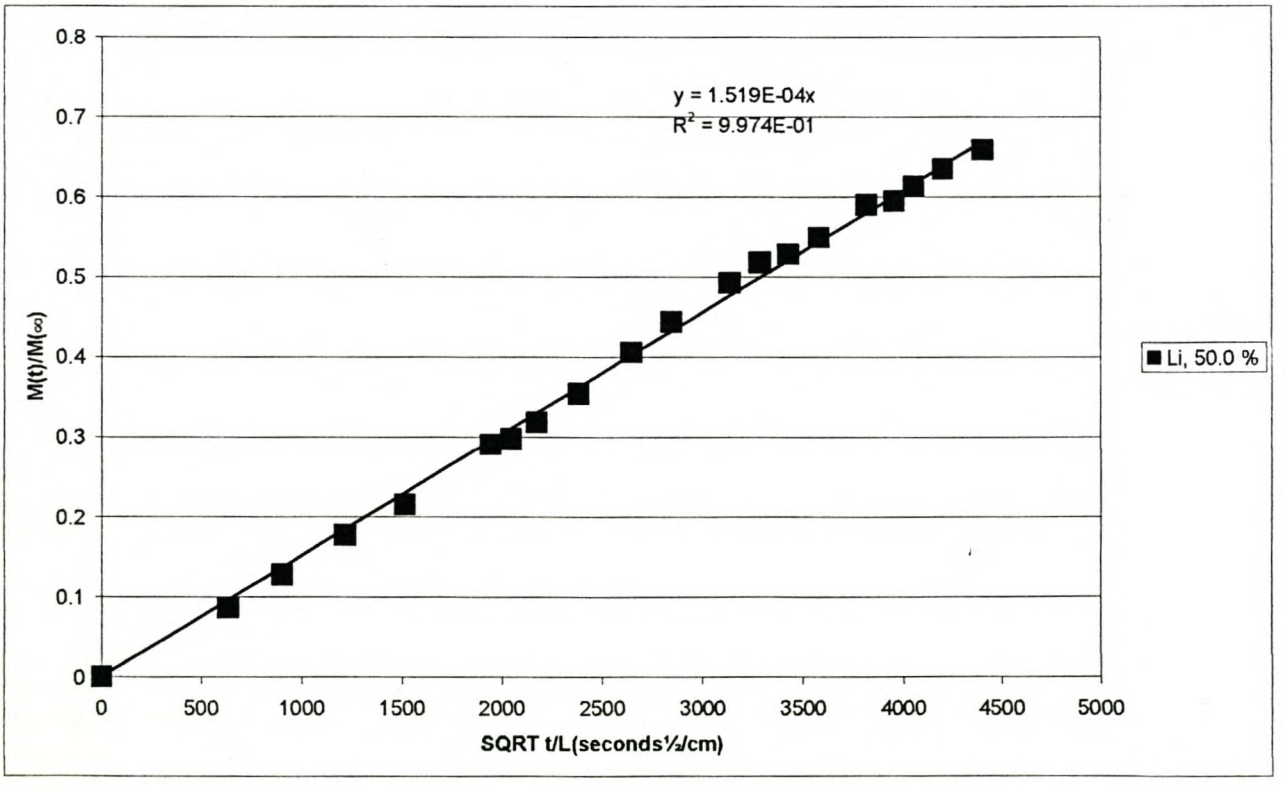

APPENDIX 7.12 (continued)

WAX 28 graphs to determine the average diffusion slope

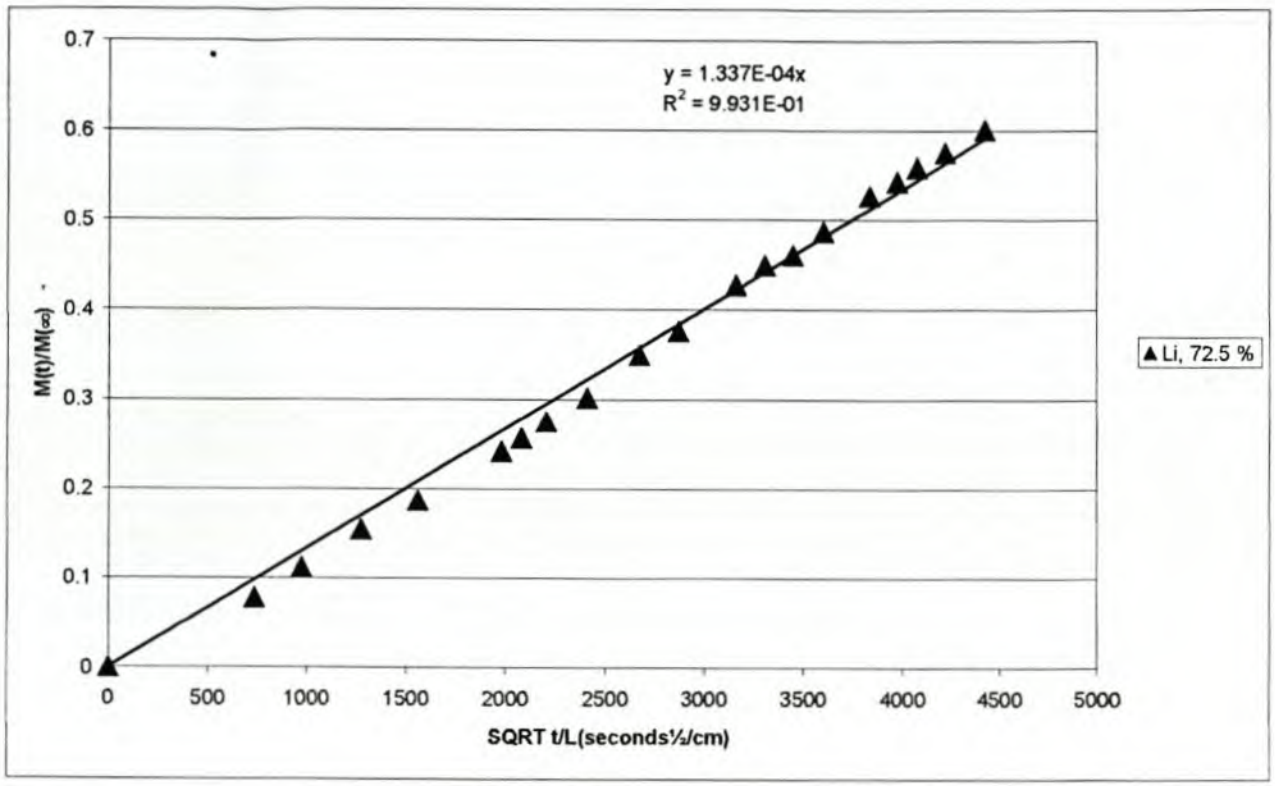

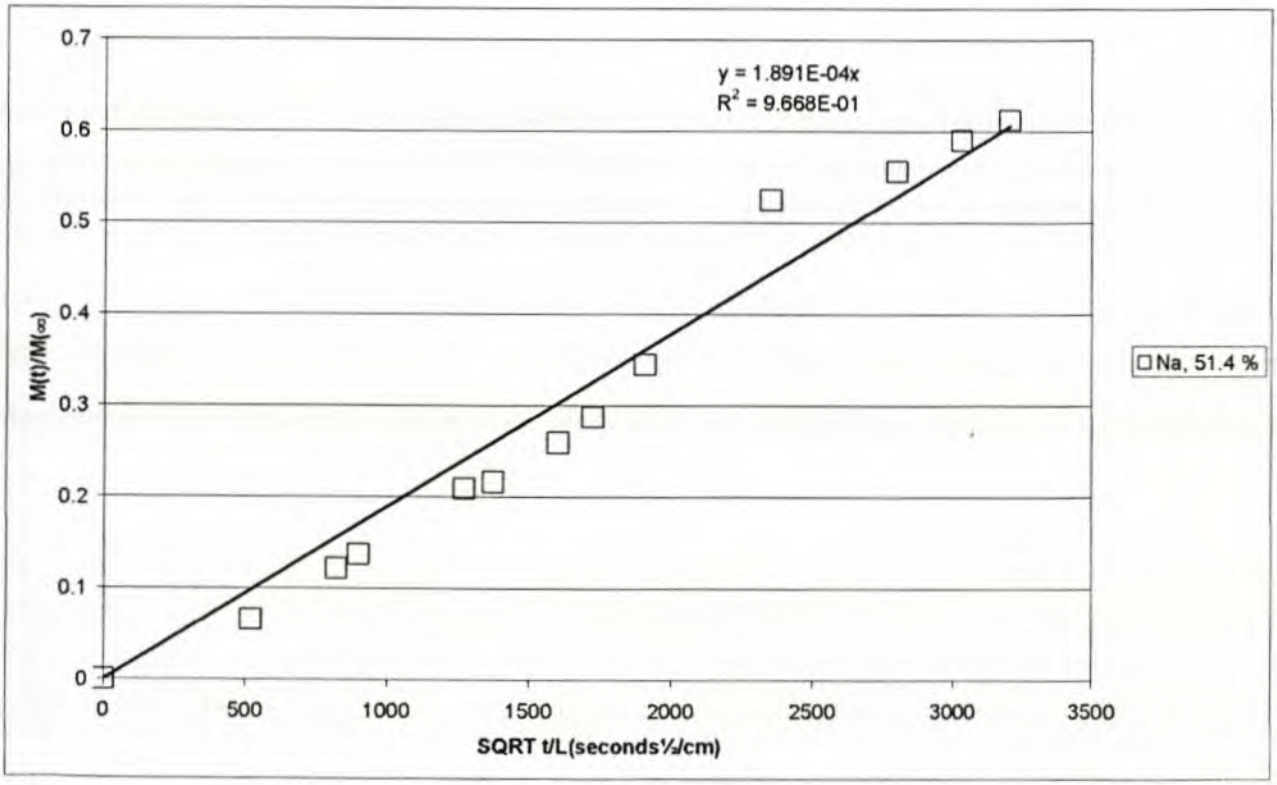

APPENDIX 7.12 (continued)

WAX 28 graphs to determine the average diffusion slope

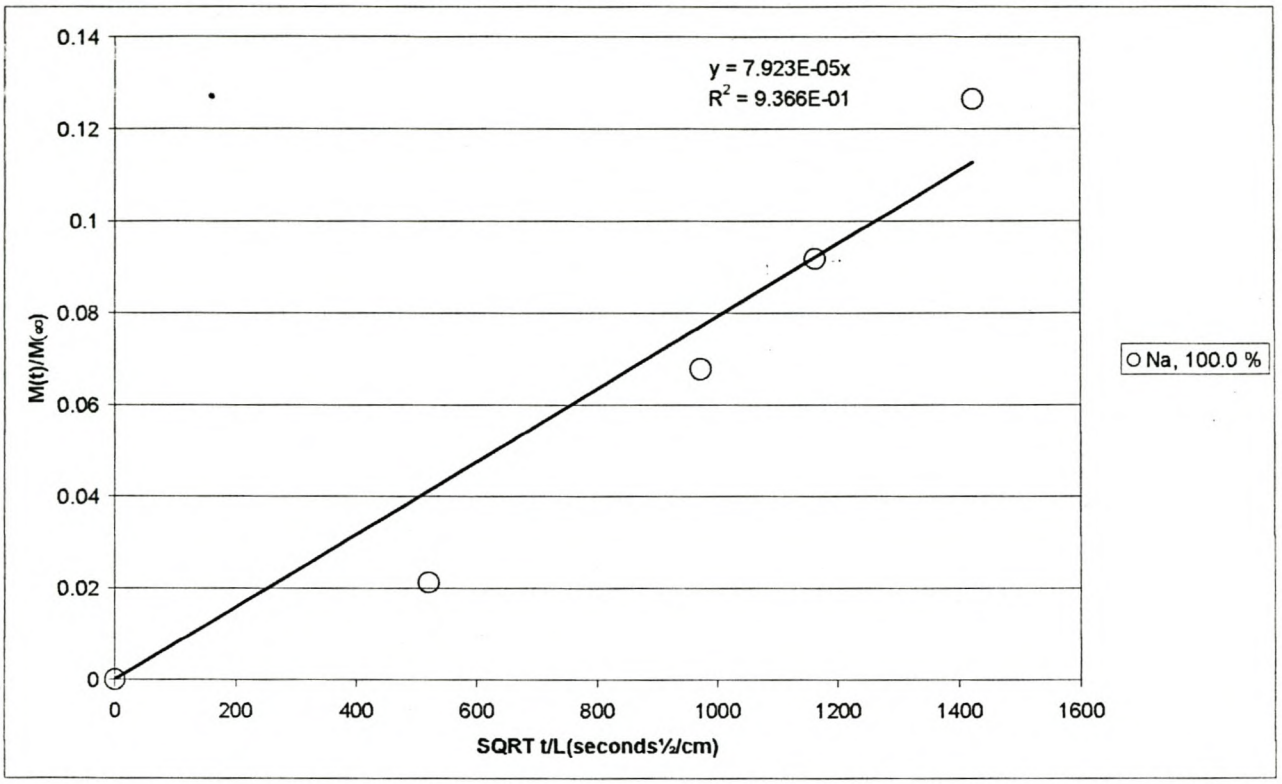

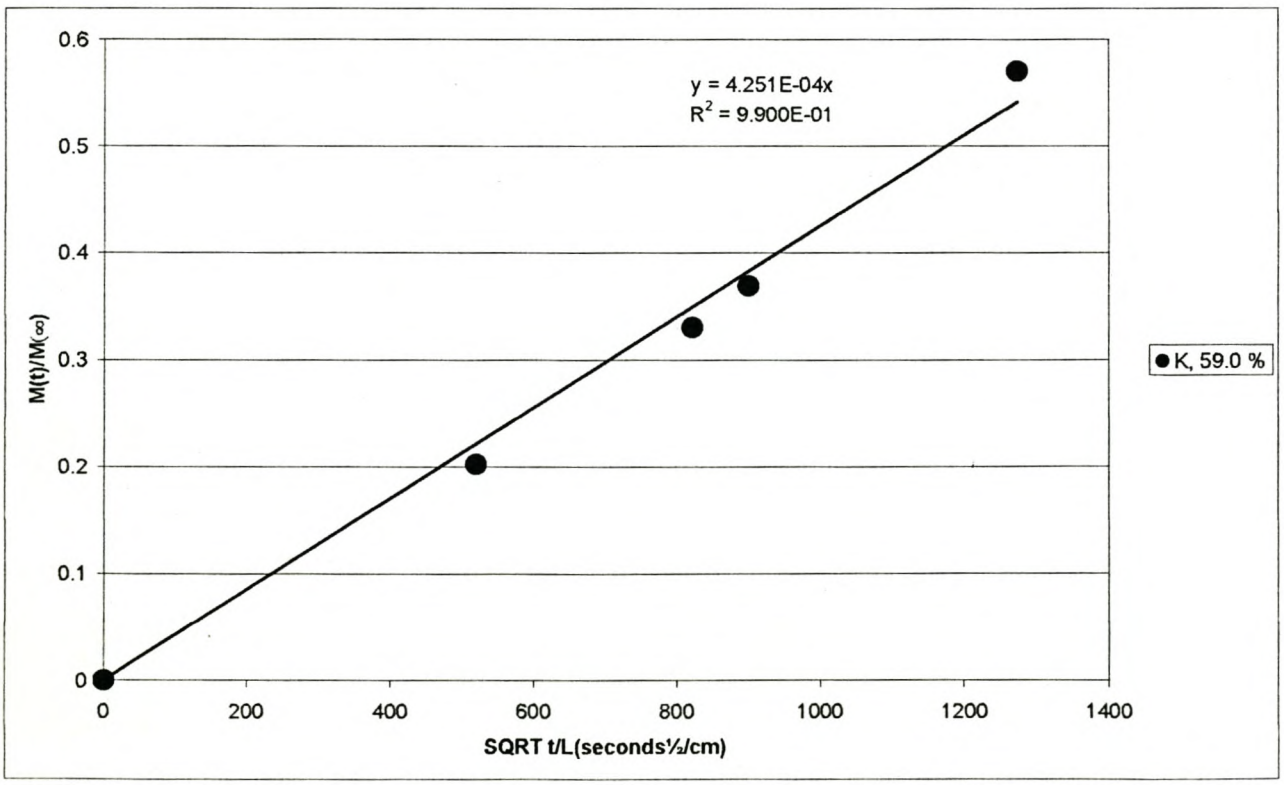

APPENDIX 7.12 (continued)

WAX 28 graphs to determine the average diffusion slope

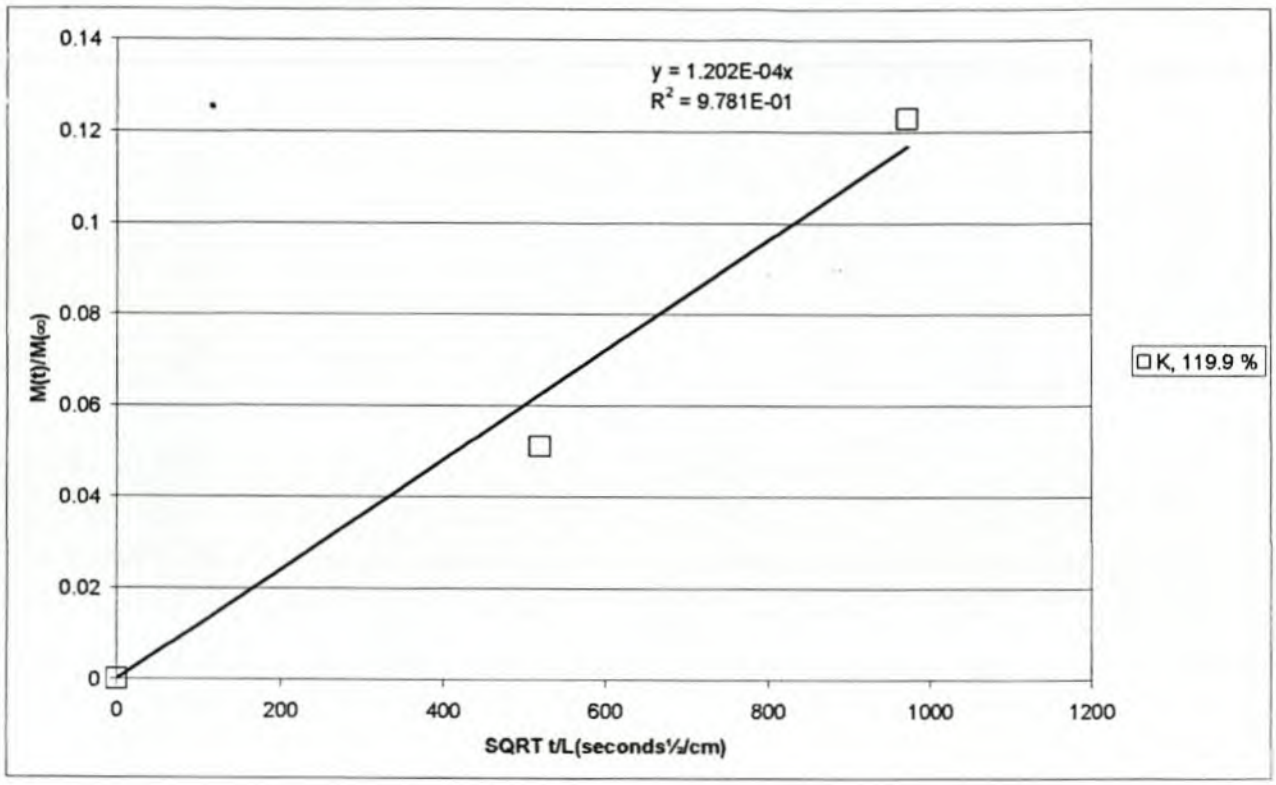

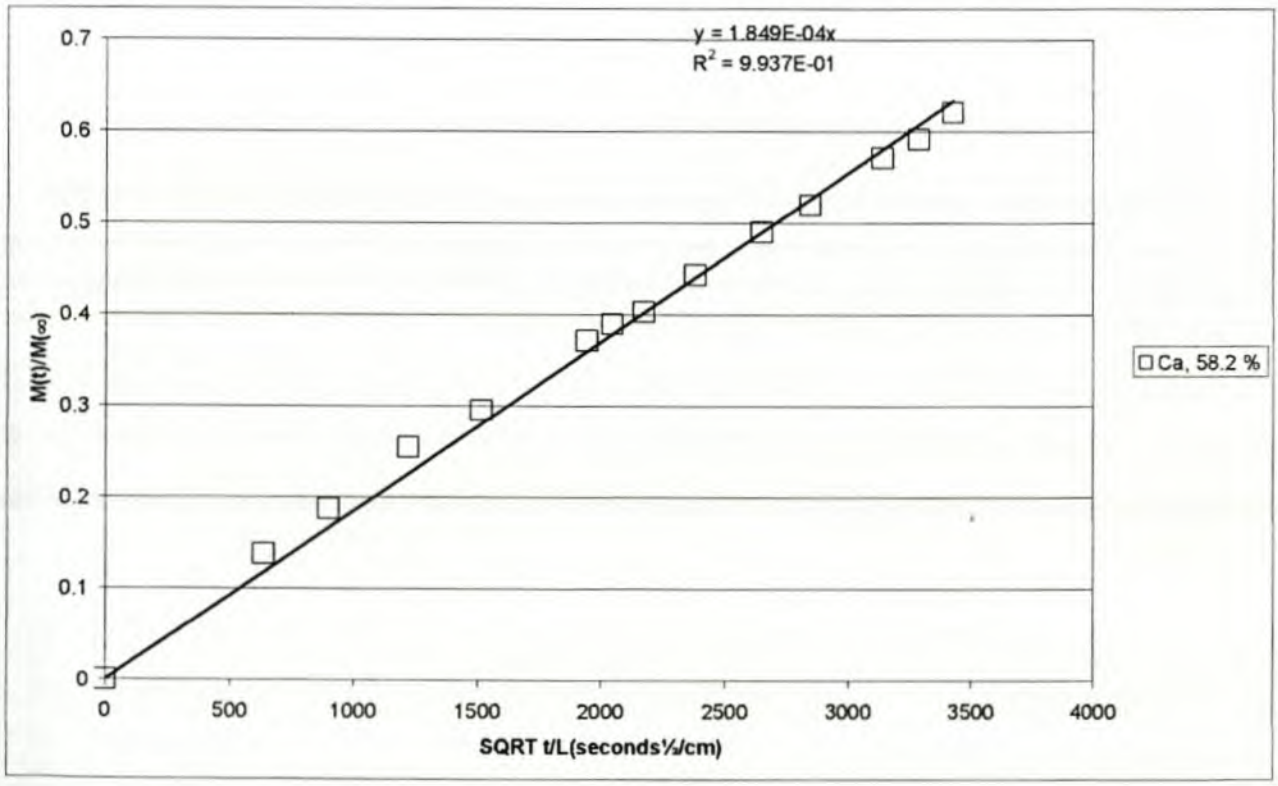

APPENDIX 7.12 (continued)

WAX 28 graphs to determine the average diffusion slope

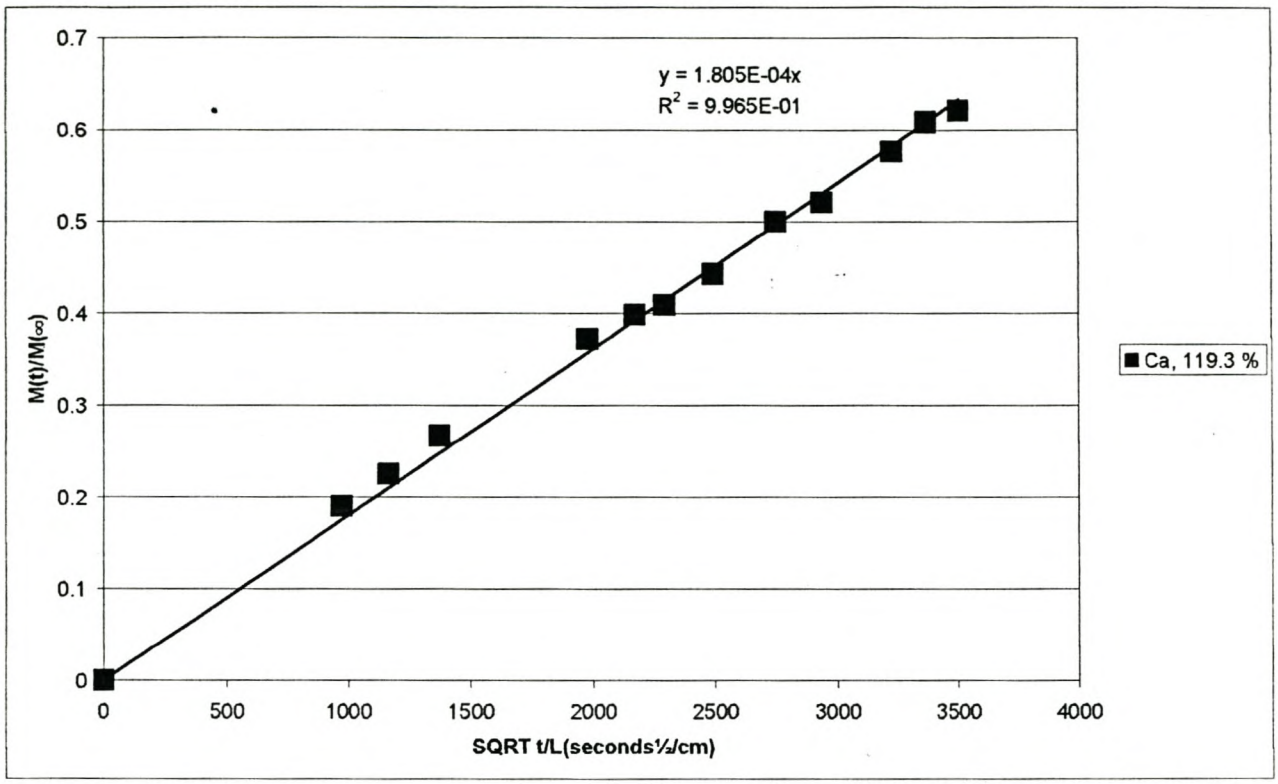

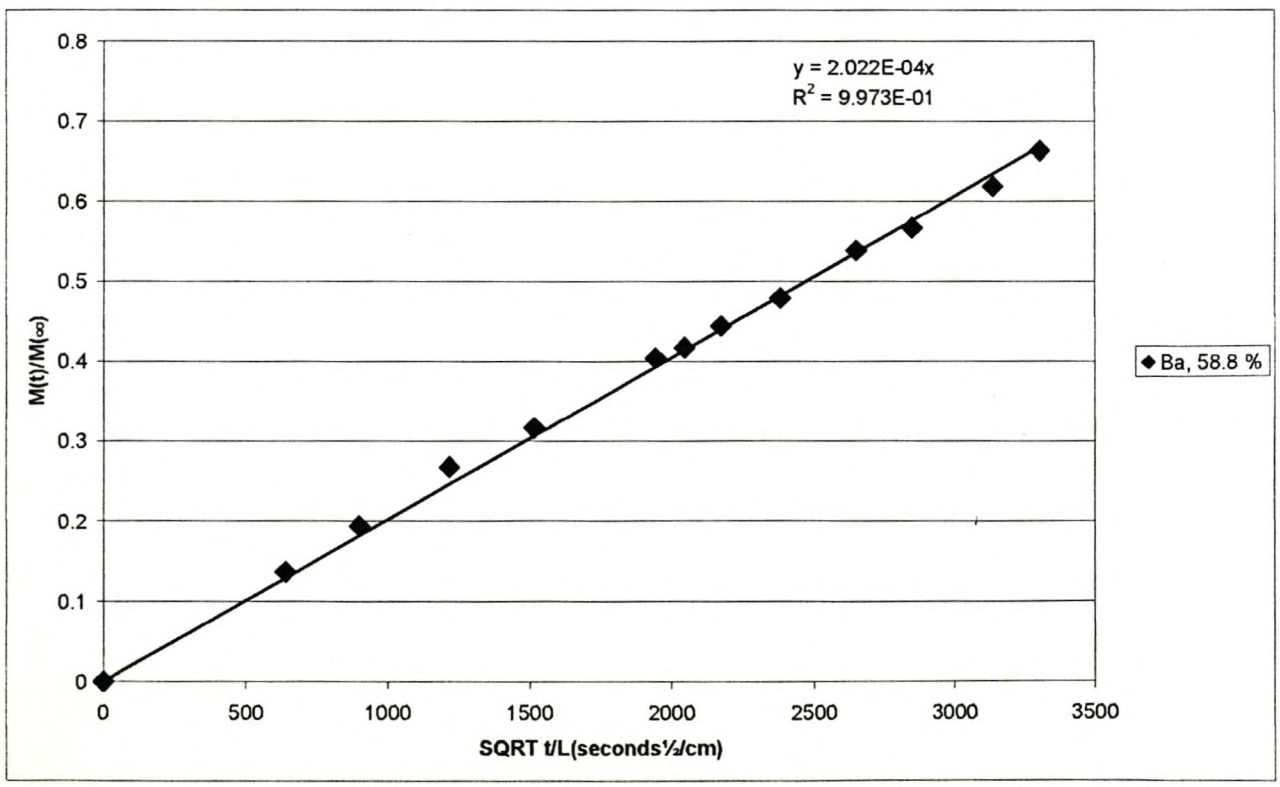

APPENDIX 7.12 (continued)

WAX 28 graphs to determine the average diffusion slope

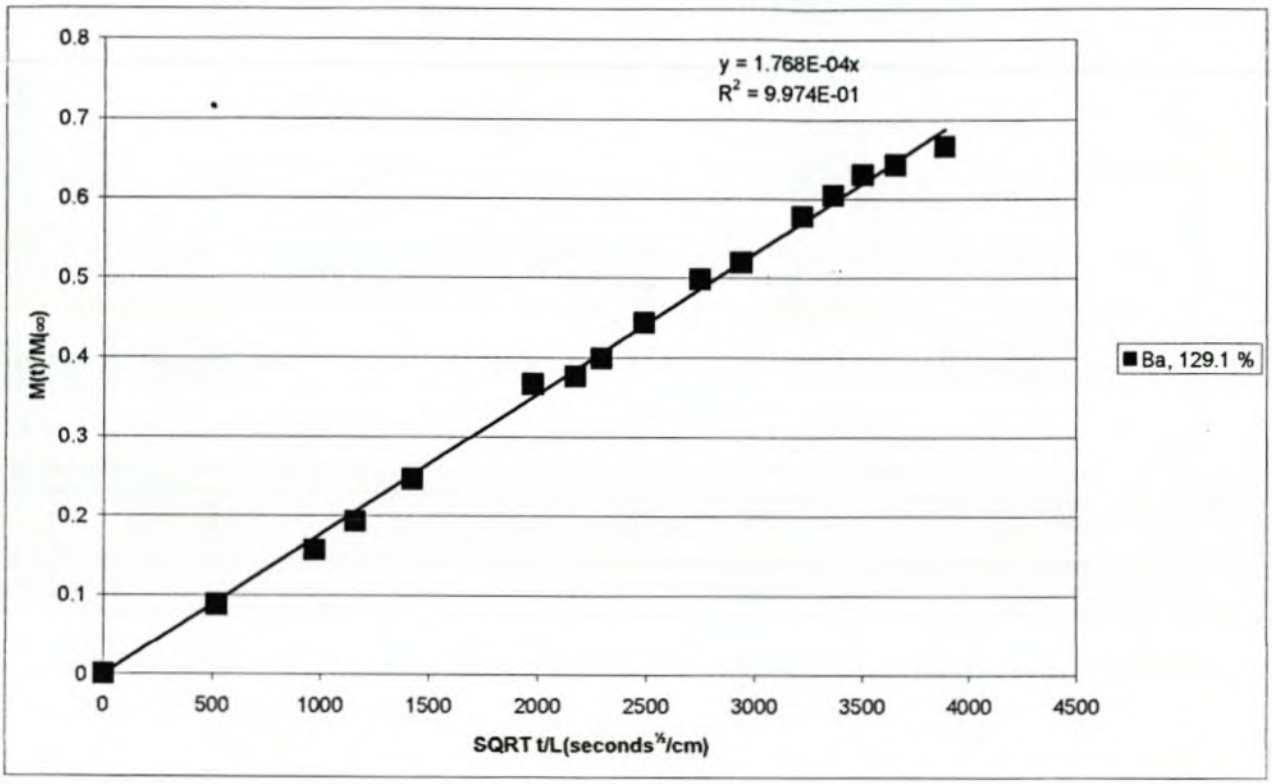

APPENDIX 7.13

WAX G11 graphs to determine the average diffusion slope

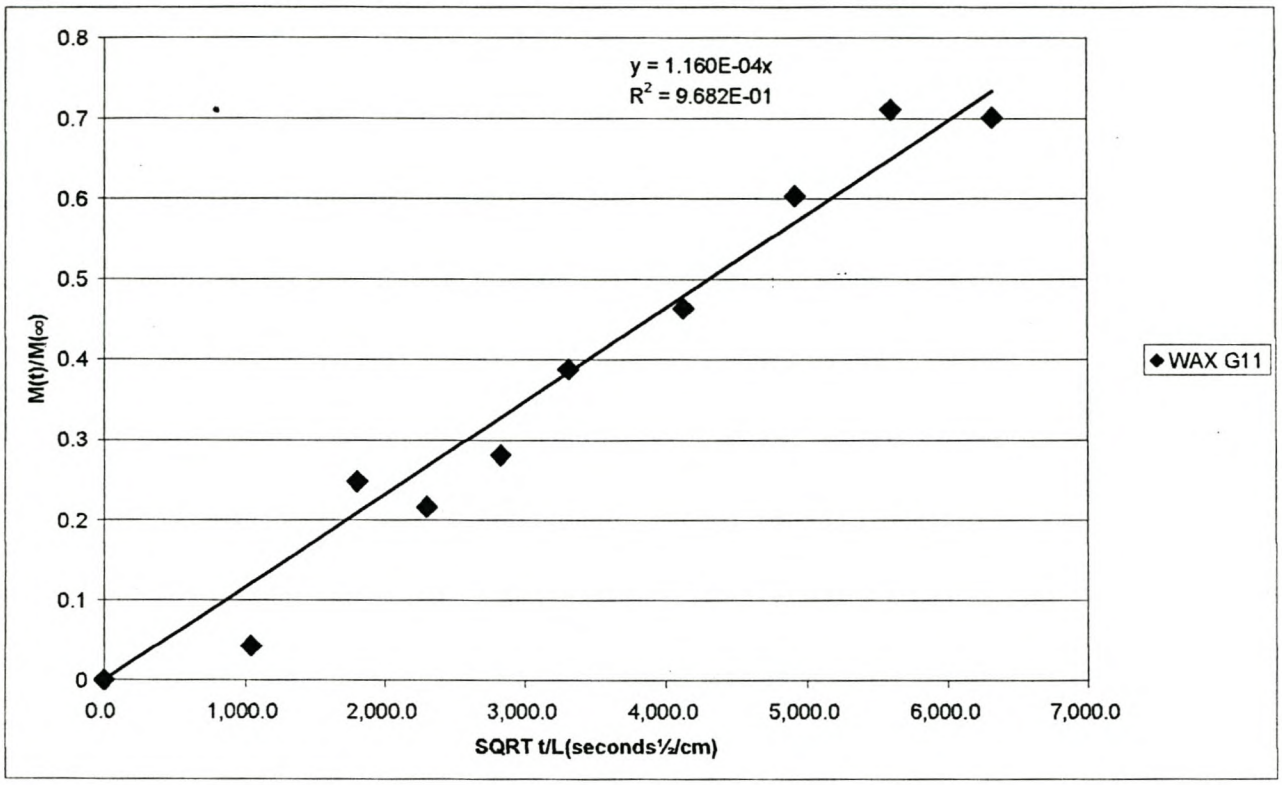

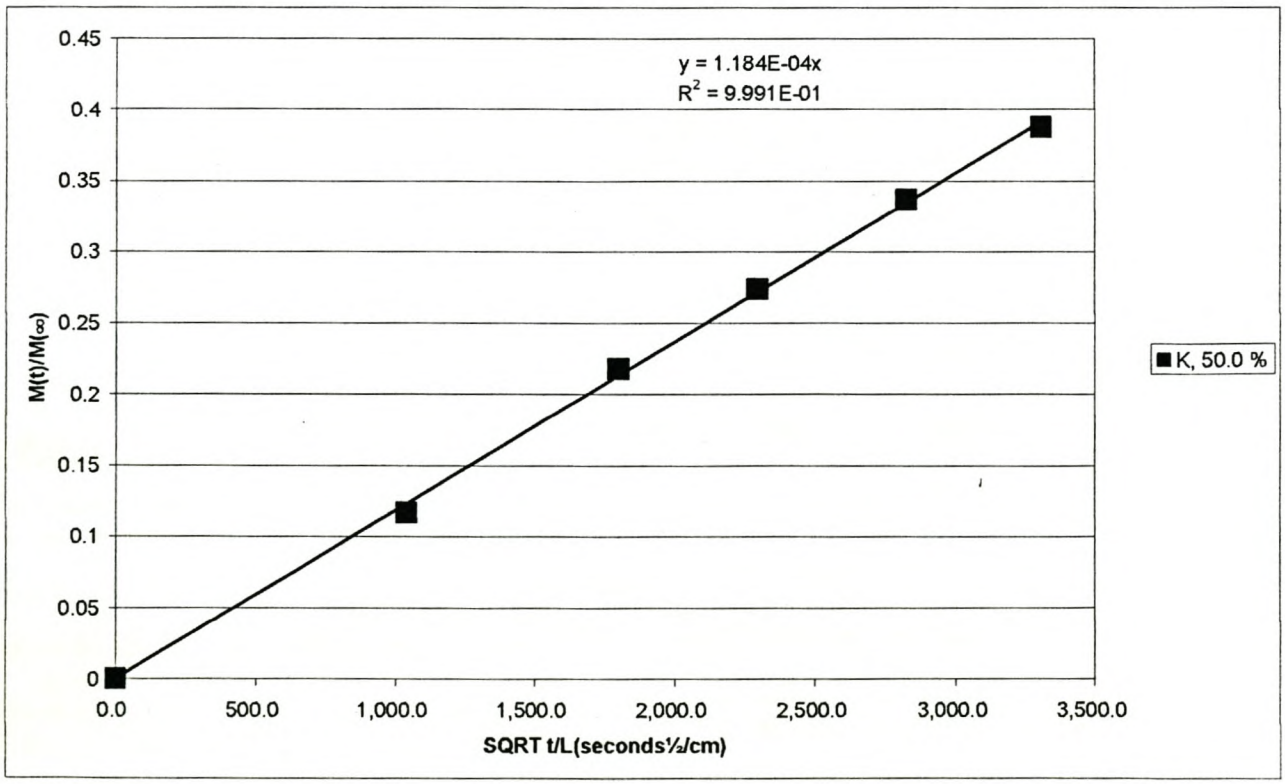

APPENDIX 7.13 (continue)

WAX G11 graphs to determine the average diffusion slope

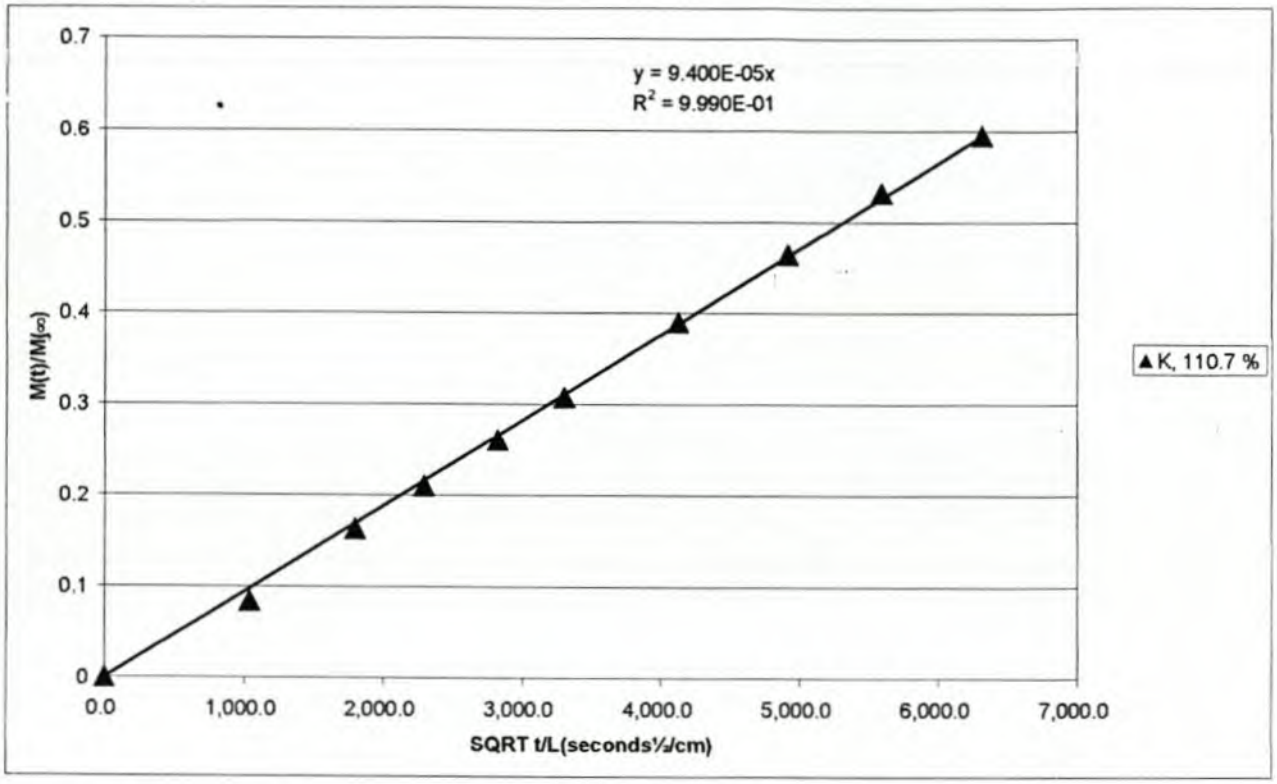

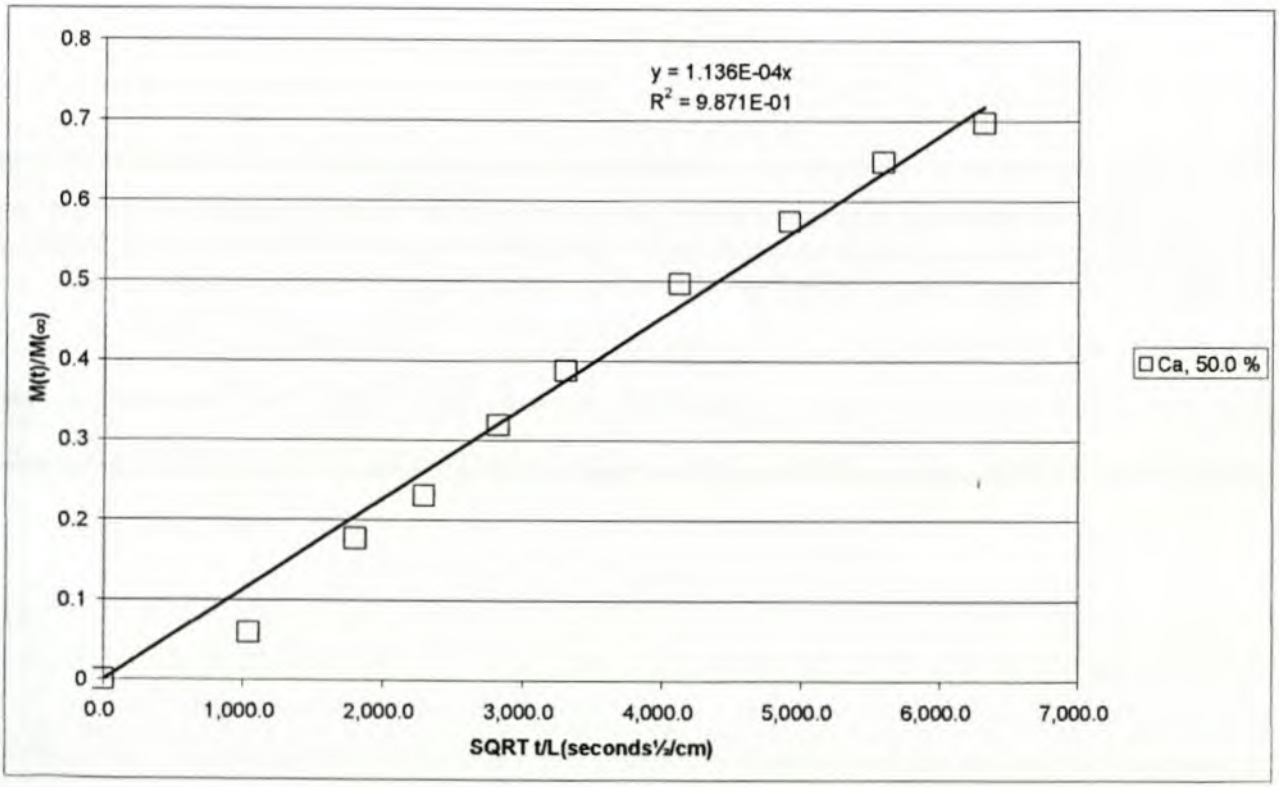

APPENDIX 7.13 (continue)

WAX G11 graphs to determine the average diffusion slope